MISCELLANEOUS PAPER GL-91-7

(2)

WAVE ANALYSIS OF MAT FOUNDATIONS TO RESIST DIFFERENTIAL SOIL MOVEMENTS

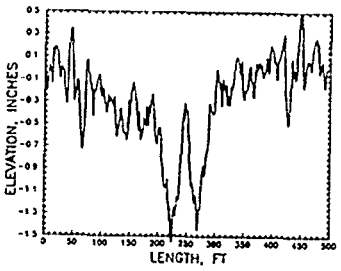

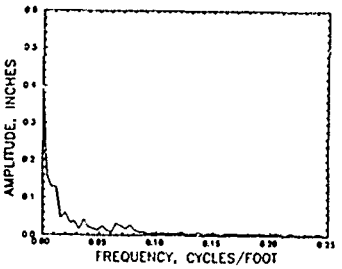

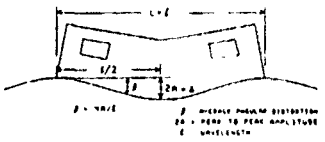

by

Lawrence D. Johnson

Geotechnical Laboratory

DEPARTMENT OF THE ARMY
Waterways Experiment Station, Corps of Engineers
3909 Halls Ferry Road, Vicksburg, Mississippi 39180-6199

March 1991
Final Report

Prepared for DEPARTMENT OF THE ARMY
US Army Corps of Engineers
Washington, DC 20314-1000

Under RDT&E Work Unit AT22/FR/001 and AT40/FR/001

91 4 29 010

Destroy this report when no longer needed. Do not return it to the originator.

The findings in this report are not to be construed as an official Department of the Army position unless so designated by other authorized documents.

The contents of this report are not to be used for advertising, publication, or promotional purposes. Citation of trade names does not constitute an official endorsement or approval of the use of such commercial products.

REPORT DOCUMENTATION PAGE

Form Approved
OMB No. 0704-0188

1. AGENCY USE ONLY (Leave blank)	2. REPORT DATE	3. REPORT TYPE AND DATES COVERED
	March 1991	Final report

4. TITLE AND SUBTITLE
Wave Analysis of Mat Foundations to Resist Differential Soil Movements

5. FUNDING NUMBERS
RDT&E WU AT22/FR/001 and AT40/FR/001

6. AUTHOR(S)
Lawrence D. Johnson

7. PERFORMING ORGANIZATION NAME(S) AND ADDRESS(ES)
USAE Waterways Experiment Station, Geotechnical Laboratory, 3909 Halls Ferry Road, Vicksburg, MS 39180-6199

8. PERFORMING ORGANIZATION REPORT NUMBER
Miscellaneous Paper GL-91-7

9. SPONSORING/MONITORING AGENCY NAME(S) AND ADDRESS(ES)
US Army Corps of Engineers, Washington, DC 20314-1000

10. SPONSORING/MONITORING AGENCY REPORT NUMBER

11. SUPPLEMENTARY NOTES
Available from National Technical Information Service, 5285 Port Royal Road, Springfield, VA 22161.

12a. DISTRIBUTION/AVAILABILITY STATEMENT
Approved for public release; distribution unlimited

12b. DISTRIBUTION CODE

13. ABSTRACT *(Maximum 200 words)*

Soil differential movement patterns are responsible for considerable damages to all types of structures and pavements such as military facilities, commercial buildings, housing, streets, highways, parking lots, and airfields. These differential movements occur from nonuniform soil volume changes, particularly in expansive clays and collapsible silty soils, attributed to a variety of mechanisms. Among the most important mechanisms leading to volume changes are those mechanisms that change the soil water content and stress. These mechanisms include desiccation from heavy vegetation, increased soil permeability from fissures, perimeter wetting and drying from climate changes, leakage from underground utilities, and many others.

This work develops a model for representing nonuniform volume changes by wave patterns of soil distortion underlying the foundation or at the ground surface. Soil-foundation distortion is measured in terms of angular distortion β which may be calculated as $4A/\ell$ where A is the amplitude and ℓ is the wavelength of the wave pattern. The wave pattern model leads to simple

(Continued)

14. SUBJECT TERMS		15. NUMBER OF PAGES
Angular distortion	Floor tolerance	248
Differential movement	Foundation performance	16. PRICE CODE
Expansive soil	Potential heave	

17. SECURITY CLASSIFICATION OF REPORT	18. SECURITY CLASSIFICATION OF THIS PAGE	19. SECURITY CLASSIFICATION OF ABSTRACT	20. LIMITATION OF ABSTRACT
Unclassified	Unclassified	Unclassified	

13. (Concluded).

methodology for rating the performance of structures subject to differential soil movement and can provide a tool to assist the design of foundations that reduce soil movement patterns. The model shows that some wavelengths are potentially more destructive than others depending on the magnitude of soil heave and the ability of the structure to tolerate soil-foundation distortion. This model may also be applicable to the analysis of pavements.

The model provides simple equations for calculating a relative thickness performance rating parameter D_{rel} and an equivalent thickness D_e of mat foundations required to reduce a given soil distortion. Elevation or level profile measurements of the first floors of a variety of structures subject to different degrees of soil distortion confirm that the maximum relative thickness D_{relm} in an elevation profile is a consistent performance rating index, although only total deformation profiles are available at this time. D_{relm} is a function of the most damaging distortion and can be used to indicate the location of the most damaging distortion in a soil profile. The wave index WI , a root mean squared summation of amplitudes in an elevation profile, was nearly as consistent an indicator for rating performance. These results appear to verify D_e as a potential design tool for foundations. Distortions leading to $D_{relm} > 40$ ft correlate with differential soil movements > 5 in. and crack widths > 0.5 in. and prevent economical design of mat foundations.

Field test sections are required to measure soil distortions for different climates and wetting conditions and for characterizing soil-foundation displacement patterns to be used for improving foundation design and construction methodology. Results of field studies will be used to confirm D_{relm} as a performance rating index, to confirm and calibrate D_e as a design tool, and to determine optimum soil improvement methods in preparation for foundation construction.

PREFACE

This report provides a new model for quantitatively describing soil distortion patterns that occur from a variety of different mechanisms. This report completes RDT&E Work Units AT22/FR/001 and AT40/FR/001, "Foundations in Unstable Soils," sponsored by the Headquarters, US Army Corps of Engineers (USACE). This work was begun in October 1988 and completed in September 1991. Mr. Wayne King and Mr. Greg Hughes were the USACE Technical Monitors.

This report was prepared by Dr. Lawrence D. Johnson, Research Group (RG), Soil & Rock Mechanics Division (S&RMD), Geotechnical Laboratory (GL), US Army Engineer Waterways Experiment Station (WES). Mr. A. L. Branch Jr. Foundation and Materials Branch, Fort Worth District, Southwestern Division (SWD) of the USACE assisted with field profilometer measurements in Fort Sam Houston, Texas, and Red River Army Depot.

Many helpful comments were provided by Dr. P. F. Hadala, Assistant Chief, GL, Mr. D. Earl Jones, Wright Water Engineers, Denver, Colorado, Mr. Joseph P. Hartman, SWD, and Dr. E. B. Perry, RG, S&RMD, GL.

The work was performed under the direct supervision of Mr. W. M. Myers, Chief, Engineering Branch, S&RMD, and Dr. D. C. Banks, Chief, S&RMD, GL. Dr. William F. Marcuson III was Chief, GL.

COL Larry B. Fulton, EN, was Commander and Director of WES. Dr. Robert W. Whalin was Technical Director.

CONTENTS

CONVERSION FACTORS, NON-SI TO SI (METRIC) UNITS OF MEASUREMENT

Non-SI units of measurement used in this report can be converted to SI (metric) units as follows:

Multiply	By	To Obtain
Fahrenheit degrees	5/9	Celsius degrees or Kelvins*
cubic yards	0.7645549	cubic metres
square yards	0.8361274	square metres
yards	0.9144	metres
cubic feet	0.02831685	cubic metres
square feet	0.09290304	square metres
feet	0.3048	metres
square inches	6.4516	square centimetres
inches	2.54	centimetres
miles (US statute)	1.609347	kilometres
kips (force)	4.448222	kilonewtons
pounds (force)	4.448222	newtons
pounds (force) per inch	175.1268	newtons per metre
pounds (force) per square foot	47.88026	pascals
pounds (force) per square inch	6.894757	kilopascals
pounds (mass) per cubic foot	16.01846	kilograms per cubic metre
pounds (mass) per cubic yard	0.593276	kilograms per cubic metre
tons (mass) per square foot	9,764.856	kilograms per square metre
tons (2,000 pounds, mass)	907.1847	kilograms
tons (force)	8.896444	kilonewtons

* To obtain Celsius (C) temperature readings from Fahrenheit (F) readings, use the following formula: $C = (5/9)(F - 32)$. To obtain Kelvin (K) readings, use $K = (5/9)(F - 32) + 273.15$.

WAVE ANALYSIS OF MAT FOUNDATIONS TO RESIST DIFFERENTIAL SOIL MOVEMENTS

PART I. INTRODUCTION

Background

1. Soil differential movement patterns cause considerable damage to all types of structures and pavements such as military facilities, commercial buildings, housing, streets, highways, parking lots, and airfields. These damages occur primarily from differential movements caused by nonuniform soil volume changes and can occur almost immediately following construction, particularly after unusual wetting and drying seasons. Damages can also accumulate gradually over long periods of time and may not become readily discernable for some years following construction. Annual damages to structures excluding pavements have been estimated in 1988 to exceed six billion dollars (Gnaedinger 1988), but under todays' conditions may well exceed ten billion. Although differential movements often occur slowly with little loss of life and may not be observed immediately, economic loss to structures has consistently been greater than that caused by other natural hazards including earthquakes and floods (Jones and Holtz 1973). Types of soils in which damages from foundation movements can be significant to structures consist of a wide range of natural earth materials and include expansive and collapsible soils, clayey shales and siltstones, marls, and saprolites. Soil differential movements are becoming an increasing problem as more new construction is required to be placed in less suitable soil.

2. Existing methodology for analyzing soil deformations provides little information on differential movements responsible for damage to structures. These older methods evaluate differential soil-foundation movements primarily from differences in loading patterns and use consolidation theory, empirical equations, and soil-structure interaction computer programs. These differential movements are caused by only a small fraction of the possible mechanisms. Very little is known about soil deformation patterns that occur from soil volume changes caused by a variety of mechanisms that involve wetting, drying, nonuniform soil profiles and many others. Limited progress has therefore been made in reducing damages to structures constructed in

unstable soil areas such as expansive or collapsible soils using existing methods. New techniques are needed to understand the mechanisms that cause soil-foundation distortions. This understanding may lead to improved methodology for reducing destructive soil distortions, methodology for estimating potential soil-foundation deformation patterns and more effective techniques for design and construction of foundations in unstable soils.

3. A methodology that may provide a new approach for analysis of soil-foundation distortion is the wave pattern concept illustrated in Figure 1.

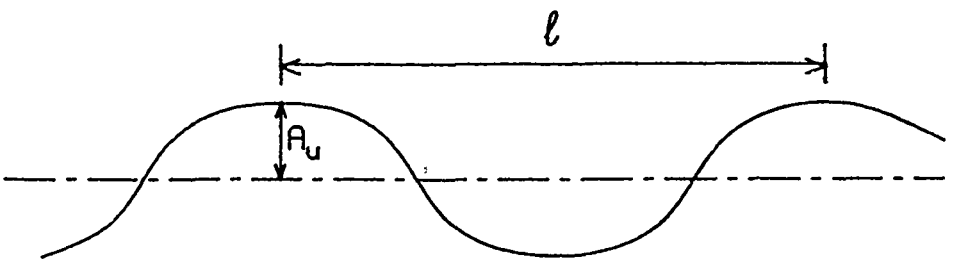

Figure 1. Wave pattern of differential surface soil movement

The surface of a soil profile not restricted by the stiffness of a foundation is hypothesized to move in a periodic pattern with wavelength ℓ and an unrestrained amplitude A_u. A mat foundation placed on the soil surface will restrict soil deformation and reduce the amplitude. Wave patterns have been applied by Professor Robert Lytton, Texas A&M University, and his associates in several studies related with pavement and slab analysis (McKeen 1981, McKeen and Lytton 1984, Gay and Lytton 1988, McKeen and Eliassi 1988). The wave pattern concept may be an appropriate approach because different types of soil distortions appear to have a periodic and modulating pattern such as gilgai (O'Neill and Poormoayed 1980) and moisture extraction by heavy vegetation such as trees (Cheney 1988). Gilgai are bumps of soil on otherwise "smooth" or "flat" undisturbed ground surfaces about 6 inches high by several feet in diameter spaced 5 to 15 feet (ft) apart. These bumps may occur from migration of moisture down fissures into deep desiccated expansive soil layers with extrusion of the expansive material up the fissures. "Smooth" or "flat" in this study refers to a plane surface that is not necessarily horizontal or level. Figure 1 represents a soil surface that is not smooth or flat. "Level" refers to a horizontal surface that is not necessarily plane, but may

have numerous bumps or ridges in which a straight line evaluated by least square regression analysis of all the elevation or level points of a profile has a zero slope. The wave pattern of Figure 1 is level. An elevation profile is a series of closely spaced points usually in a straight line that measures at each point the vertical distance above a datum elevation or level. The datum elevation in this study is zero and all initial elevation readings of the profile are taken at this zero datum.

4. The wave pattern concept was applied in pavement studies by measuring the elevation profile of a fixed length of pavement such as 128 ft using close spacings between measurement points such as 0.5 ft. These data provide 256 measurement points that were analyzed using the fast Fourier transform (FFT) (Gay and Lytton 1988). The FFT decomposes the data into discrete amplitudes and wavelengths that can be used to provide a measure of the surface roughness of the pavement. Surface roughness indices using FFT analysis for a given pavement length indicate reasonably well the effects of soil stabilization treatments such as lime or lime-flyash slurry injection or moisture barriers.

Purpose and Scope

5. The purpose of this study is to apply the wave pattern approach of soil distortion analysis to determine new methodology for evaluating displacement behavior in unstable soils caused by various mechanisms, to verify that soil-foundation differential movement patterns can be modeled by a wave pattern of motion, to develop a suitable performance rating system and to evaluate the potential of a wave model for foundation design. The concept of angular distortion defined in Figure 2 is also used with this wave pattern methodology because angular distortions have correlated well with damages in structures (Burland and Wroth 1974, Wahls 1981, Boscardin and Cording 1989, Day 1990). Knowledge of the characteristics of surface soil movement patterns will assist in determining sources of soil distortions, how these distortion patterns influence performance of structures such as maintenance and repair requirements, and how foundations may be better designed and constructed to improve long-term performance.

6. PART II describes mechanisms of soil volume changes and includes development of a wave pattern hypothesis for modeling soil-foundation

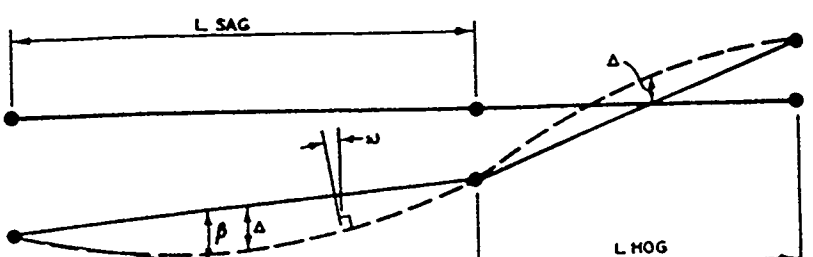

a. COMBINATION L_{SAG} AND L_{HOG}

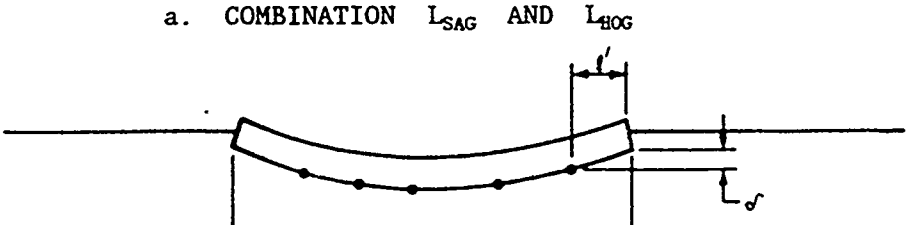

b. REGULAR SETTLEMENT

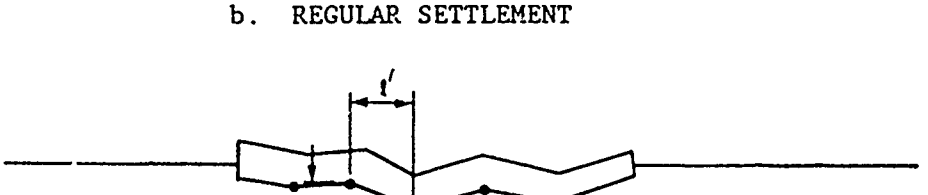

c. IRREGULAR SETTLEMENT

Figure 2. Schematic illustration of angular distortion $\beta = \delta/\ell'$ and deflection ratio Δ/L for settling (sagging) and heaving (hogging) profiles. ω is the tilt of a profile. From Figure 2-1, EM 1110-1-1904, Headquarters, US Army Corps of Engineers (HQACE 1990)

distortions. A mat foundation or slab is assumed in this study to lie on top of the surface soil movement pattern, to have an ability to squeeze down or reduce the unrestrained amplitude and to always remain in contact with the soil such that there will not be edge lift-off. PART II also derives a simplified wave model for calculating the thickness or a mat foundation required to limit soil-foundation distortions to within acceptable levels that will not contribute to significant damage. A new term, relative thickness D_{rel}, is found independent of soil and foundation characteristics that can be used to rate performance. A performance rating system is necessary to provide a basis of comparison between the foundation behavior of different types and sizes of structures. The maximum relative thickness D_{relmax} required to restrain soil-foundation distortion to a limiting angular distortion and

therefore limit damage is found to be a function of only the limiting permissible angular distortion and potential heave $2A_u$ for foundations with no lift-off. $2A_u$ is the peak-to-peak differential heave in Figure 1. PART II also introduces the maximum relative thickness D_{relm} measured from an elevation profile for use as an indicator of foundation performance. PART III defines and compares various performance rating indices such as F-numbers, wave index, angular distortion indices and a macrorelief index. Useful performance rating systems should indicate the potential for structural damage and operational efficiency. Idealized simple and complex wave patterns are used in PART III to determine the most appropriate indices for analyzing performance of actual structures. PART IV verifies that field elevation profiles may be modeled by wave patterns and applies the selected rating indices to field measurements of elevation profiles in various facilities to determine the most suitable indices for rating foundation performance.

7. The performance rating systems use profilograph or elevation change measurements taken at close spacings of 1 ft on first floor surfaces that should be representative of soil-foundation distortion patterns. Elevation changes have been measured at close spacings $\leq$ 1 foot on floor surfaces, but these have only been applied to evaluation of surface roughness for small wavelengths $\leq$ 5 ft related with concrete finishing techniques. Such elevation change measurements have not yet been applied to analysis of foundation performance. Elevation profile measurements used in PART IV were accomplished with a dipstick profilometer capable of elevation difference measurements of 0.001 inch at a 12-inch spacing. Closed loop profiles were made to allow correction for operator bias. The profile data were automatically recorded and could be accessed by personal computer systems. Computer software was prepared to reduce the data, perform analysis, and prepare graphs of the results. Soil exploration data, site inspections and interviews with users of facilities assisted in evaluation of facility performance. Structures investigated in this study include one or two story administrative buildings, clinics, laboratories and warehouses with many located in Texas because of significant potential for differential movements in the expansive soil found there.

PART II. HYPOTHESES OF SOIL MOVEMENT PATTERNS

8. A hypothesis is developed describing how soil volume changes can lead to a wave pattern of surface soil movements. Mechanisms of how soil volume changes can occur are also illustrated to assist detection of causes of soil-foundation distortion in the field. A concise theory of soil-foundation movement by wave patterns is subsequently derived to evaluate the thickness of foundations required to restrain a given amount of surface soil movement while maintaining acceptable performance of the supported structure. The hypothesis also provides a simple index for rating performance of foundations that can be applied toward development of methodology for reducing soil-foundation movements and improvement of guidelines for design and construction.

Causes of Soil Volume Changes

9. Soil is a nonhomogeneous porous material consisting of three phases: solids, fluid (normally water), and air. These three phases interact with external influences such as surface loading that lead to volume changes from causes described in Table 1. Nonuniform volume changes lead to differential soil movement patterns at the ground surface. The amount of volume changes and surface deformation depend on the type of soil; i.e., whether the soil is a cohesionless sand or gravel, cohesive clay or cohesive mixture of silt-sand-clay materials. Surface deformation patterns from soil volume changes caused by changes in the stress balance, water content, particle bonding, and thermal effects (excluding freeze/thaw) are discussed below. Other causes of volume change such as particle reorientation from dynamic loading, temperature change causing freeze/thaw of silty sands, and mass change from erosion may cause similar surface deformation patterns. Refer to Engineer Manual 1110-1-1904, "Settlement Analysis" (HQACE 1990) for information on soil characteristics and standard methodology for estimating soil volume changes and differential movements.

Stress Balance

10. Foundation and superstructures placed in soil introduces stress in the soil causing the soil to deform leading to total and differential settlement of the structure. This deformation may be calculated through constitutive relationships or models of continuum mechanics that relate stress

Table 1. Causes of Soil volume Changes

Cause	Description
Stress Balance	Compression/rebound of soil particles from changes in applied loads
Water Content	Primary consolidation in saturated soil or heave/ shrinkage in partly saturated soil from gradients in soil pore water pressure
Particle Bonding	Collapse of large void ratio silty/clayey sands or sands following wetting and subsequent solution of soluble chemical bonds, bonding agents between particles or loss of cohesion from negative pore water pressure
Thermal	Consolidation or swell from thermal gradients in pore water; expansion/contraction from density changes in pore water; expansion/contraction of water in ice following freezing/melting of surface soil; water vapor movement from warmer to cooler areas (hydrogenesis)
Particle reorientation	Density increase following sliding and reorientation of particles in cohesionless soil from dynamic/earthquake loads
Mass	Loss of support from erosion

and strain state at a macroscopic level. Parameters relating stress to strain are measures of soil stiffness or elastic modulus required for design of foundations.

11. Concept of Effective Stress. Constitutive relationships can calculate change in soil volume such as settlement or heave in response to a change in effective stress

$$\frac{\Delta V}{V} = f(\Delta \sigma') \tag{1}$$

where

V = volume of the soil, ft^3

ΔV = change in volume, ft^3

σ' = effective stress, ksf

$\Delta \sigma'$ = change in effective stress, ksf

$f(\Delta \sigma')$ = function of a change in effective stress

The above relationship is such that the volume of soil decreases if the

effective stress increases. The change in effective stress from applied forces occurs through particle-to-particle contacts in cohesionless friction soil and bonding between particles in cohesive soil that causes particles to roll, slide, compress or rebound leading to a volume change.

12. A fundamental equation of effective stress in saturated soil at constant temperature is (Terzaghi and Peck 1967)

$$\sigma' = \sigma - u_w \tag{2}$$

where

σ = total pressure applied to the soil, ksf

u_w = pore water pressure, ksf

are the stress state variables. A decrease in pore water pressure leads to an increase in effective stress and strength and a decrease in soil volume. A satisfactory stress state equation relating effective to total stress and negative pore water pressure (suction) in partly saturated soil has not yet been developed because of conceptual problems with the three phases air, water, and solids and deviation of the soil mass from a continuum due to fissures, shrinkage cracks, discontinuous air voids and other macroscopic features.

13. Constitutive Relationships. Constitutive equations for soils are typically nonlinear, particularly for foundation soils supporting heavy structures with loads applied only once. These equations include material dependent parameters such as the stiffness or Young's elastic modulus of the soil and foundation, compression and swell indices of the soil, maximum past pressure of the soil, Poisson's ratio of the materials, and geometry of the foundation. A satisfactory general equation for all soils is difficult to develop because the response of different soils under the same or different forces may or may not be related. The time-dependent deformation response of a cohesive clay, for example, is different than that of a cohesionless sand.

14. Experience has shown th . solutions based on linear elasticity are simple and will provide deformations in soil that are at least qualitatively correct. Numerous other constitutive relationships have been proposed for soil, but most of these are primarily research tools and have not been commonly applied to practical computations of settlement. The hyperbolic (Duncan and Chang 1970) and Cam Clay (Chang and Duncan 1977) models have been successfully applied to the solution of engineering problems.

15. Stress Distribution in Soil. Successful application of constitutive relationships to solution of volume change in soil and other engineering problems requires evaluation of a realistic distribution of stresses in the soil. The Boussinesq (1885) distribution is commonly used to calculate stresses at depth in a soil from foundation and soil overburden pressures. This distribution is applicable to linear elastic isotropic soils. The Westergaard (1938) distribution is applicable to soils that are stratified with strong layers of rigid, thin sheets interspersed between weak layers. These solutions assume validity of the superposition of stresses and St. Venant's principle.* A third method based on the normal statistical distribution of particulate media (Harr 1977) calculates similar vertical stresses as the Boussinesq method, but lateral stresses attenuate more rapidly. These stress distributions largely replace the early approximate 2:1 stress distribution widely used before the introduction of the computer. The 2:1 distribution provides an increase in vertical stress (HQACE 1990)

$$\Delta\sigma_z = \frac{Q}{(B+z)\cdot(L+z)} \tag{3}$$

where B and L are the foundation width and length, respectively, and z is the depth below the foundation. This distribution is most useful in quick hand calculations of settlement.

16. Solutions of stress distribution in soil based on linear elasticity for simple applied surface loads may be combined to form stress distributions of more complicated load patterns. The stresses at each point in a soil mass caused by each simple surface load may be summed to determine the total stress at each point for the geometry of a given foundation. Each of the applied surface loads may be either a positive (downward) or negative (upward) applied load. EM 1110-1-1904 (HQACE 1990) provides examples of stress distributions beneath different loads.

---

*St.-Venant's principle, which states that if the forces acting on a small portion of the surface of an elastic body are replaced by other statistically equivalent forces, this change has negligible effect on the state of stress in the body at distances which are large with respect to the linear dimension of the surface where the change took place. This principle allows approximate solutions of stress distribution at large distances from applied foundation loads where solutions may not exist, such as stresses due to strip loads, by replacing the strip load with a statically equivalent line load.

17. Deformation Patterns. The deformation pattern of the foundation and supporting soil depends on the (1) loading pattern, (2) geometry, size, and stiffness of the foundation and (3) type of soil. Figure 3 illustrates some soil contact pressure and deformation patterns of uniformly loaded rigid and flexible footings and mat foundations on uniform cohesionless and cohesive soils. The difference in the distributions strongly depends on the effect of confining pressure on the soil stiffness. The elastic modulus of cohesionless soil may increase with increasing confining pressure, while the elastic modulus of cohesive soil may be independent of confining pressure. Most actual soils are some combination of cohesive and cohesionless materials where the degree of cohesiveness often relates closely with the type and amount of clay minerals present.

18. Tests of small rigid footings of about 1 ft dimension on sands indicated a parabolic pressure distribution, Figure 3a (Kögler and Scheidig 1927). Cohesionless soil tends to be pushed aside near the edges because of the reduced confining pressure. Tests of larger footings on sands with loads much less than the ultimate bearing capacity of the soil indicated a saddle-shaped pressure distribution, Figure 3b (Kögler and Scheidig 1927, Murzenko 1965). Cohesionless soil appears to be subject to significant confining pressure at the perimeter. The influence of adjacent soil particles on the

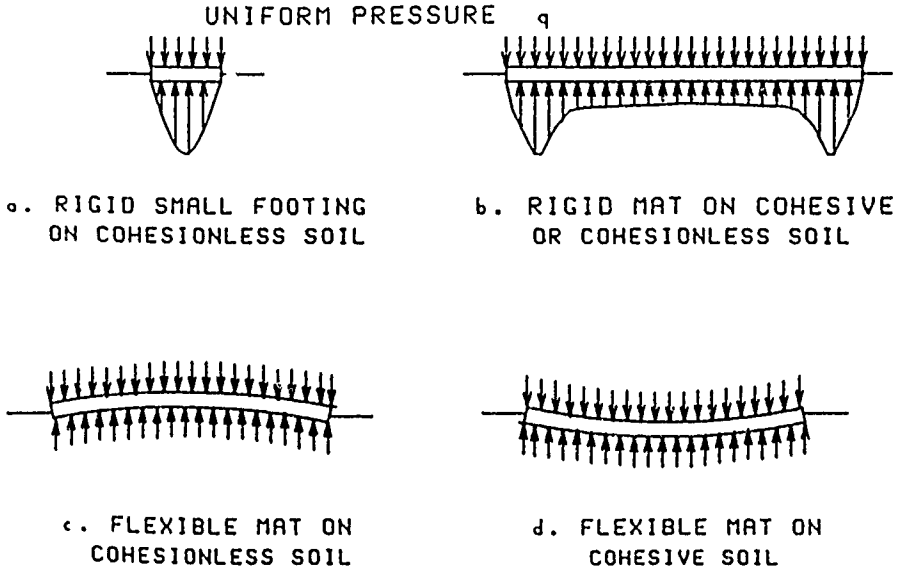

Figure 3. Some contact pressure and deformation patterns

stress distribution and pressure required for edge shear displacements causes greater soil contact pressure near the perimeter (Burmister 1963). The distortion of a uniformly loaded flexible mat on cohesionless soil will be concave downward, Figure 3c, because the soil near the center is stressed under higher confining pressure such that the modulus is higher near the center. A uniform pressure applied to a flexible foundation on laterally homogeneous cohesive soil, Figure 3d, causes greater settlement near the center than near the edge because the elastic modulus of the soil is constant laterally and cumulative stresses are greater near the center as a result of the pressure bulb stress distribution. Deformation analysis of uniformly loaded square flexible plates on elastic or cohesive soil indicates settlement at corners about 1/4 and at edges about 1/2 of that at the center (Lysmer and Duncan 1969). A uniform pressure applied to a large mat foundation on cohesive soil will also cause the saddle-shaped soil contact pressure distribution (Johnson 1989a, 1989b). This occurs because pressure is required to shear or cut the soil at the perimeter leading to relative displacement between the foundation and soil. Concentrated loads on footings or stiffening beams of flexible ribbed mats may cause a cyclic pattern of soil deformation with a spacing between cycles or waves equal to the spacing between concentrated loads.

Water Content

19. Soil volume change and deformation from water content changes occur from flow of moisture into and out of soil voids. Soils most susceptible to volume change from changes in water content are plastic CH clays* such as expansive clays, organic soil, and cohesive silty sands with high void ratios. The cause of moisture flow is a gradient in the pore pressure where moisture flows from regions of higher potential energy to lower potential energy or pressure. Table 2 illustates some factors that can change the pore pressure. The total potential head of a soil-water system differs from that of free water and may be given by Dempsey (1976)

$$\Omega = z_e + h_p + h_o + h_g \tag{4}$$

where

*Soil descriptions follow the Unified Soil Classification System (HQDA 1960)

Table 2. Factors Leading to Changes in Pore Pressures

Factor	Description
Mechanical pressure	Mechanical pressure applied to or removed from a soil mass changes the state of stress in the solids and pores, normally filled with air and water
Climate	Arid climates promote desiccation, while humid climates promote wet soil profiles
Groundwater	Fluctuating and shallow water tables (less than 20 ft from the ground surface) provide a source of moisture change for heave or settlement
Shrinkage cracks	Vertical and horizontal shrinkage cracks may be a major conduit for fluid and vapor moisture flow
Temperature gradients	Fluid and vapor moisture flow is influenced by temperature gradients tending to move from warmer to cooler regions
Drainage	Poor surface drainage leads to moisture accumulations or ponding
Vegetative cover	Trees, shrubs, and grasses are conducive to moisture depletion by transpiration; moisture tends to accumulate beneath areas denuded of vegetation
Utility lines	Leaking underground water and sewer conduits and pipes provide a source of subsurface moisture
Construction	Foundations supporting facilities cover the soil preventing evaporation of water from the ground surface and transpiration of moisture from any previously existing vegetation

Ω = total potential, ft

z_e = gravitational potential or elevation relative to a datum, ft

h_p = pressure potential, ft

h_o = osmotic potential, ft

h_g = gas potential, ft

The pressure potential in saturated soil is u_w/γ_w where γ_w is the unit weight of water, 0.063 kip/ft^3. The pressure potential in unsaturated soil is the matric (matrix) potential or suction of the pore water. The osmotic potential occurs from the concentration of soluble salts in pore water. This

may be a factor if a desiccated foundation soil with a high salt content is exposed to wetting from relatively pure surface water. The gas potential occurs from variation in gas pressure which is not expected to be a major factor in practical cases. Equation 4 for unsaturated soils simplifies to the total head $\Omega = z_e + h_t$ where h_t is the sum of matrix and osmotic suctions.

20. Moisture Flow From Applied Pressure. Moisture flow in saturated soil may occur by primary consolidation if a mechanical pressure such as from foundation or footing surcharge loads is applied to change the total potential head, Table 2. The hydrostatic excess pressure caused by an applied load and its gradient decrease with time as water drains from the soil causing the load to be gradually carried by the soil skeleton. This load transfer is accompanied by a decrease in volume of the soil mass equal to the volume of water drained from the soil. Primary consolidation is complete when all excess pressure has dissipated. The reverse of primary consolidation (rebound of cohesive soils such as clays, clay shales, and claystones) can occur beneath cut areas over lengthy time periods as moisture flows into these soils to restore pore pressures back to near original values prior to the cuts. Substantial differential soil heave between the perimeter and center of cut areas can occur over several years.

21. Secondary compression and creep may also occur following placement of mechanical pressure, but these appear to occur at essentially constant effective stress with negligible change in pore water pressure. Secondary compression and creep may be a dispersion process in the soil structure causing particle movement and may be associated with electrochemical reactions and flocculation. Although creep is caused by the same mechanism as secondary compression, they differ in the geometry of confinement. Creep is associated with deformation without volume and pore water pressure changes in soil subject to shear, while secondary compression is associated with volume reduction without significant pore water pressure changes. Secondary compression or creep may be a significant contribution to settlement where soft soil exists, particularly soil containing organic matter, or where a deep compressible stratum is subject to small pressure increments relative to the magnitude of the effective consolidation pressure. Refer to EM 1110-1-1904 (HQUSACE 1990) for further details.

22. Moisture Flow From Wetting/Drying. Volume changes may occur from any of the factors described in Table 2 that can wet or dry foundation soil. Moisture flow will occur from higher pressure potential to a lower potential. Shrinkage cracks in soil provide paths for liquid and vapor water to move long distances. Temperature differences in soil beneath a building or in soil beneath shaded and sunny areas can be significant and influence moisture over long periods of time. Models for calculating equilibrium moisture, rate of flow, and volume change or vertical heave are available in the literature (Knight and Greenberg 1970, Lytton and Woodburn 1973, McKeen 1981, Johnson and Snethen 1978, Fredlund and Dakshanamurthy 1982).

23. Construction of foundation systems on grade eliminates evaporation of moisture from the ground surface and transpiration of moisture in the soil by heavy vegetation such as trees. The subsurface soil beneath the foundation often becomes wetter over time. Long-term wetting can vary from a few months to many years and includes seasonal climate changes, irrigation and rainfall patterns, droughts, subsurface drains and leaking sewer or water utilities. Wetting can be sufficient to cause a shallow perched water table or elevation increase in the groundwater of soil supporting the structure. Changes in groundwater levels lead to heave or settlement (Blight 1987, Brandl 1987, Papadopoulos and Anagnostopoulos 1987).

24. Deformation Patterns. Some factors that contribute to changes in soil moisture and cause deformation patterns are described in Table 3 with illustrations in Figure 4. All of these patterns can exist simultaneously and may be superimposed to cause a complex pattern of differential foundation movement characteristic of all types of military facilities, housing, commercial structures and pavements. These surface distortions coupled with deformations from changes in soil stress are hypothesized in this study as being representative of wave motion with relatively long wavelengths exceeding 4 ft (measured wavelengths are discussed in paragraph 39.

Particle Bonding

25. Soil volume change and deformation may occur from solution of calcareous cementation or other soluble salts or clays bonding larger particles such as silts or sands together. These "collapsible" soils may be mudflows or windblown silt deposits of loess. A collapsible soil at natural water content may support a given foundation load with negligible

Table 3. Factors That Cause Nonuniform Surface Deformations

Item	Factor	Description
1	Heavy vegetation	Heavy vegetation desiccates the soil; locations of previously existing trees should show greatest heaves from wetting of desiccated soil following construction (Figure 4a)
2	Fissures	Large cracks provide high permeable paths for moisture flow down to desiccated expansive soil leading to gilgai (Figure 4b)
3	Old drainage areas	Drainage and ponding areas wet the foundation soils with possible settlement from consolidation and creep following construction (Figure 4c)
4	Underground utilities	Leaking water and sewer lines can cause local heave in expansive soil or settlement in collapsible and eroding soil (Figure 4d)
5	Perimeter wetting	Perimeter soil may heave from seasonal wetting and irrigation of plants and shrubs leading to edge heave (Figure 4e)
6	Elimination of natural evaporation and transpiration	Foundations on the ground surface eliminate natural evaporation of moisture from the ground surface and transpiration of moisture from vegetation leading to a long-term center heave pattern
7	Variations in type and amount of clay minerals	Lateral and vertical point-to-point variations in clay minerals characteristic of alluvially deposited clays and vertical clay stratifications; soils may be complicated by permeable inclusions of silts, sands, and gravels
8	Variations in dry density	Spatial dry density variations affect differential soil movement where changes in field moisture vary only with time and not with location
9	Hot areas	Migration of moisture from hot areas in soil such as beneath furnaces or boilers causing shrinkage and heave in cooler regions leading to differential movement (similar to Figures 4c or 4e)
10	Changes in water table elevations	Perched water may induce localized heave in a soil above or below the water; receding or rising water tables may proceed at different vertical rates at different locations due to variations in soil permeability and clay mineral content

Table 3 (Concluded)

Item	Factor	Description
11	Long-term changes in moisture	Soil moisture at equilibrium under natural precipitation can be drastically altered following construction of structures and irrigation
12	Barriers to water movement	Manmade barriers such as horizontal or vertical membranes and natural geologic structures induce nonuniform soil deformations
13	Pipelines for water movement	Natural highly permeable layers, granular bedding or backfills such as in utility trenches induce nonuniform soil deformations (similar to Figure 4d)
14	Bedrock	Bedrock and its depth influence soil shrink/swell; drying proceeds more rapidly where bedrock is more shallow and proceeds more rapidly than a site having a permanent water table
15	Organic soil	Organic soil may consolidate unevenly because of fossil tree stumps, buried boulders, and other inclusions

Note: Data from Lytton and Woodburn 1973, Technial Manual 5-818-7 (HQDA 1983), Blight 1987, Cheney 1988, and D. Earl Jones by personal communication

settlement, but when water is added to this soil bonding agents may dissolve and the volume can decrease significantly through particle rolling and sliding and cause substantial settlement of overlying foundations even under relatively low applied stress or at the overburden pressure. Lowering of water tables in some Karst areas may induce increased soil/rock stresses from loss of bouyancy and accelerate collapse of below-grade cavities. An associated problem can be lateral sliding of soil and supported structures as sinks form.

26. Soils subject to collapse may have a honeycombed structure of bulky shaped particles or grains held in place by a bonding material such as clay or soluble salts of cementitious material. Typical collapsible soils are lightly colored, low in plasticity with liquid limits below 45, plasticity indices below 25, and relatively low dry densities between 65 and 105 lbs/cubic foot (60 to 40 percent porosity). Local shallow or deep wetting, slow uniform rise in the groundwater, or a slow increase in the soil water content can trigger

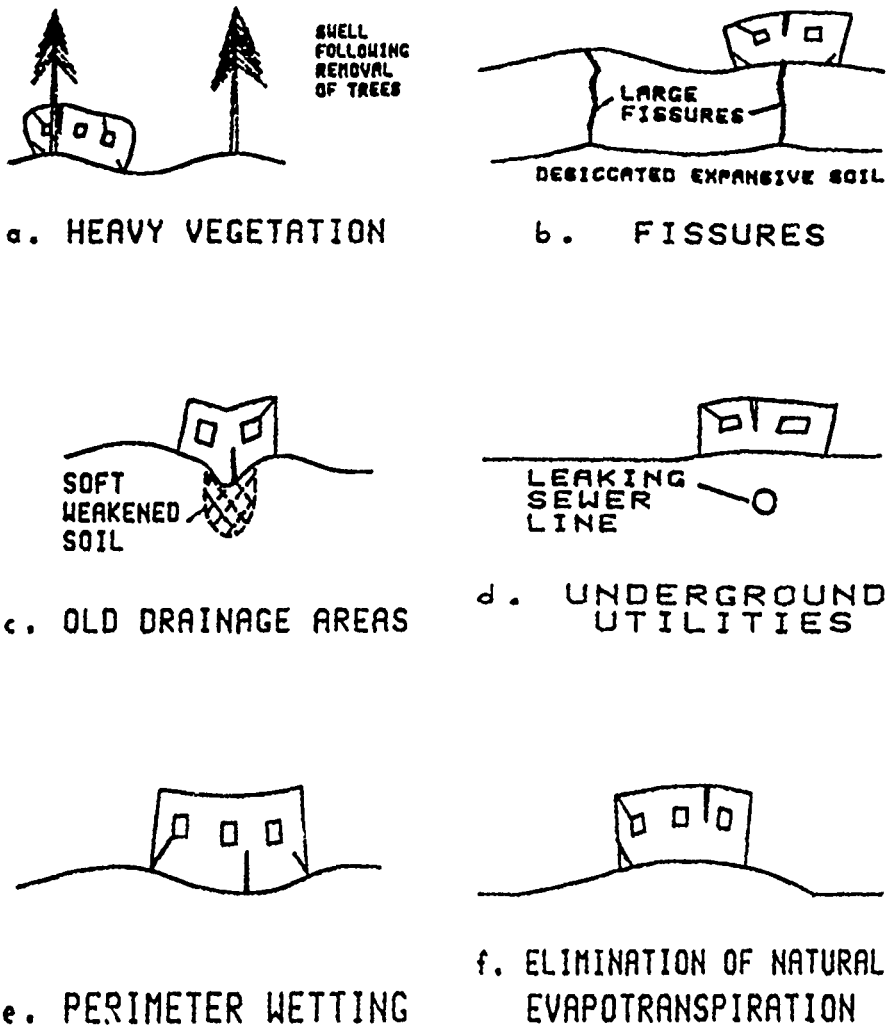

Figure 4. Deformation patterns from water content changes

collapse settlement. Collapsible soils exposed to perimeter watering of vegetation around structures or leaking underground water or sewer lines are most likely to settle. Collapse may be initiated beneath the ground surface and propagate toward the surface leading to sudden settlement of overlying facilities.

27. Collapse or erosion of subsurface particles such as into leaking sewer lines will cause local subsurface voids and eventually settlement above the wetted or eroded soil areas. The wave pattern may appear similar to Figure 4c or Figure 4e.

Thermal Effects

28. Soil volume change and deformation may occur from thermal consolidation of thick and soft soil layers such as silt and clay. Thermal expansion/contraction of the pore fluid may occur because of changes in the fluid density that alter the buoyancy force of the fluid supporting the solid matrix. A rise in the surface temperature above the soil can sufficiently reduce the buoyancy force and effective stress in the soil overcoming thermal expansion of the fluid and causing the soil to compress rather than swell (Mei and Tyvand 1988). Laboratory experiments and analysis have shown that partial saturation of the soil is necessary for a flow of moisture under a temperature gradient. Moisture flow is probably from the transfer of vapor caused by the temperature gradients (Jennings et al, 1952). Hydrogenesis in Table 1 is a significant factor under some conditions, especially deterioration of asphalt pavements on clay subgrades. Actual measurements to determine thermal effects on soil distortion are limited. Wave patterns could resemble Figure 4e or 4f.

Differential Movement of Soil Surfaces

29. The hypothesis that soil movement may be modeled by wave patterns provides a new way of interpreting differential movement by causes illustrated in Table 1. Deformation patterns caused by soil volume changes shown in Figure 4 illustrating factors in Table 3 relate commonly used terms such as edge and center heave with soil wave patterns, Figure 5. Maximum differential movement commonly denoted as "y_m" in the literature is used in several ribbed mat design procedures (Post-Tensioning Institute 1980, Hartman and James 1988). y_m is the maximum differential vertical heave that will occur beneath a fully flexible weightless mat or a flexible impervious membrane placed on the ground surface. y_m is associated with edge heave such as cyclic perimeter wetting and drying of item 5 and even items 1 to 4 of Table 3 depending on the location of the mat relative to the various factors. y_m is also associated with center heave such as elimination of natural evaporation and transpiration of moisture of item 6 and also items 1 to 4 depending on the location of the mat.

Edge Heave

30. Differential movement from edge heave may vary from 1/2 to the total maximum unrestrained heave $2A_u$ (Figure 1) beneath a weightless covered

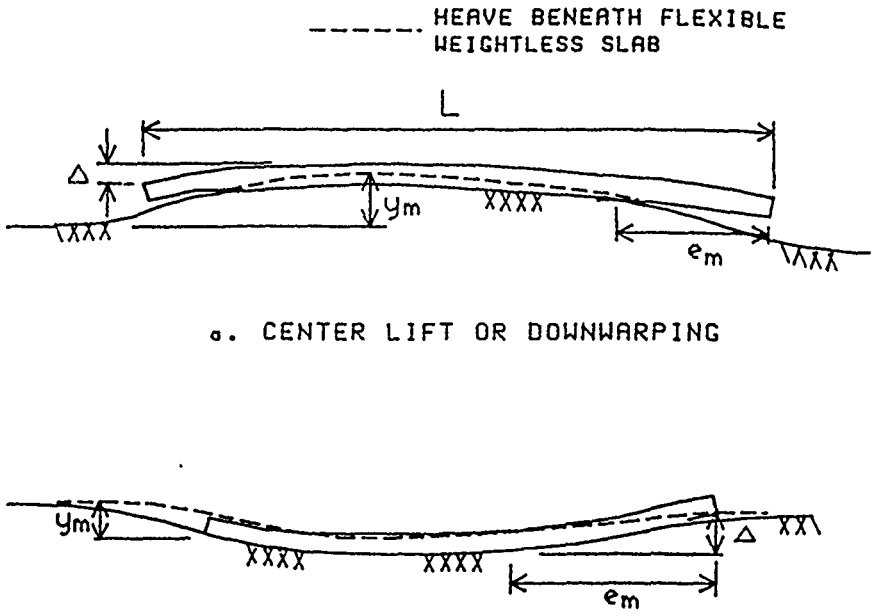

Figure 5. Differential movement beneath mats

area depending on when the mat is constructed relative to seasonal moisture changes or when local sources of water or leaks occur; e.g., y_m is A_u if the mat is placed midway between the wet and dry periods or y_m is $2A_u$ if the mat is placed when the soil is fully wetted or fully dried by the climate or leaks occur in utility lines beneath the mat. A_u is the amplitude of a periodic unrestrained soil wave pattern given by, Figure 1

$$\phi(x) = A_u \cdot \sin\left(2\pi \frac{x}{\ell}\right) \tag{5}$$

where

$\phi(x)$ = elevation of the wave at lateral distance x, in.

A_u = unrestrained amplitude, in.

x = lateral distance, ft

ℓ = wavelength, ft

$2A_u$ is the peak-to-trough amplitude of the wave and the maximum unrestrained soil heave.

31. Maximum Unrestrained Heave. The maximum unrestrained heave $2A_u$ may be estimated from results of swell tests

$$2A_u = f \cdot \Delta h \sum_{i=1}^{N_{za}} \frac{e_{f(i)} - e_{o(i)}}{1 + e_{o(i)}} \qquad (6a)$$

where

f = soil fabric factor

Δh = increment of depth, ft

$e_{f(i)}$ = final void ratio of depth increment i

$e_{o(i)}$ = initial void ratio of depth increment i

N_{za} = number of depth increments to reach Z_a

Z_a = depth of the active zone for heave $N_{za} \cdot \Delta h$, ft

Changes in void ratio commonly occur from moisture changes, but other causes in Table 1 may contribute. The fabric factor f converts volumetric heave to vertical heave and may vary from 1/3 for loose soil to 1.0 for dense soil. Much of the swell of expansive clay minerals from increasing moisture in loose soil is used to reduce the volume taken by fissures, while clay mineral swell in dense soil is mostly transmitted through the soil structure and contributes to surface heave. The factor f = 1.0 if results of one-dimensional swell tests are used because vertical dimensional changes are measured directly. The final void ratio e_f is determined from a model such as soil suction (Johnson and Snethen 1978, McKeen 1981) or consolidation swell (ASTM D 4546). The initial void ratio e_o may be determined as part of the tests performed on undisturbed soil prior to construction.

32. McKeen and Lytton (1984) found from pavement studies

$$2A_u = 0.37 \cdot f \cdot C_t \cdot Z_a \cdot CV_{ct} \cdot \Delta pF \qquad (6b)$$

where

C_t = suction compression index $(\Delta V/V)/\Delta pF$, $(pF)^{-1}$*

$\Delta V/V$ = change in volume V

CV_{ct} = coefficient of variation of C_t

ΔpF = change in average suction, $(pF)^{-1}$

C_t is the fraction change in volume per change in pF. Equations 6 show that the amplitude is a function of the fabric factor, expansiveness of the soil and depth of the active zone for heave.

* pF is the logarithm to the base 10 of the negative pressure head in centimeters of water.

33. Depth of Active Zone. The depth of the active zone for heave Z_a or depth within which vertical dimensional changes are significant is an elusive parameter that has been observed to vary from several to 20 or more feet (HQDA 1983). This depth for seasonal climatic changes has been determined to be (McKeen and Johnson 1990, Johnson 1989b)

$$Z_{ae} = \frac{\ln\left[\frac{\Delta U_{max}}{2U_o}\right]}{-\left[\frac{n\pi}{\alpha}\right]^{0.5}} \tag{7}$$

where

Z_{ae} = depth of active zone for edge heave, ft

$2U_o$ = suction change at the ground surface (Figure 6), pF

ΔU_{max} = maximum suction change below which movement is insignificant, pF

n = frequency of the suction change, cycle/yr

α = diffusion coefficient, ft^2/yr

The magnitude of soil moisture at depth Z_a or below is at equilibrium suction U_e and will not change provided external sources of moisture are not present, Figure 6. Within Z_a soil suction changes are bounded by an envelope. The maximum width of the envelope $2U_o$ is at the ground surface and may vary from about 5 pF for extremely damaging climatic changes to about 1 pF for mild climates. $\Delta U_{max} = (\Delta V/V)_z/C_t$ where $(\Delta V/V)_z$ is the fraction

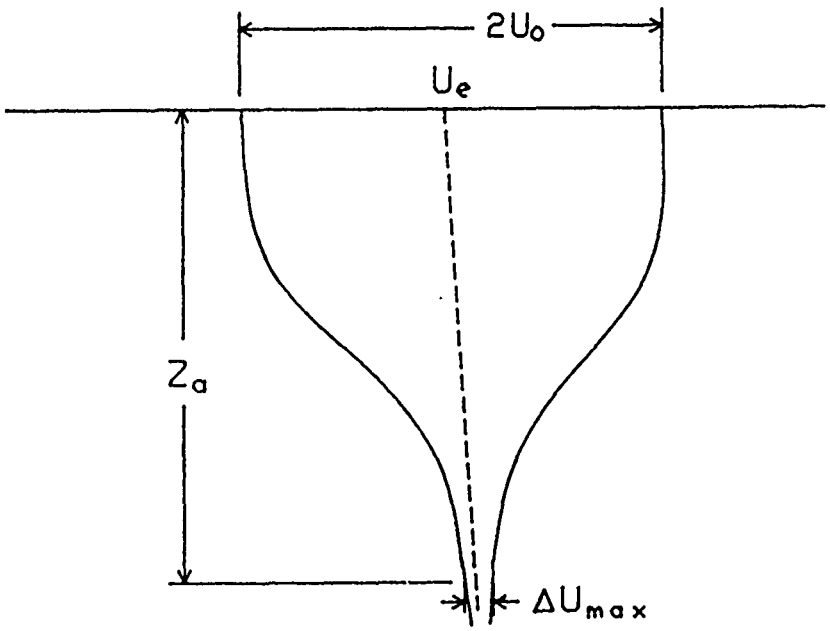

Figure 6. Envelope of soil suction changes

volume change that is significant at depth Z_{ae}. C_t typically varies from 0.01 for low expansive to 0.07 or more for high expansive soils (denoted as γ_h in McKeen 1981, McKeen and Johnson 1990). ΔU_{max} from 0.1 to 0.4 pF provide Z_{ae} that is consistent with observations, depths that vary from 5 to 20 ft or so (HQDA 1983). The frequency n appears to vary from 0.5 to 1.4 for sites in Texas and Mississippi. The diffusivity α of field soils is about 9 ft^2/yr for Yazoo clay near Jackson, Mississippi, to 120 ft^2/yr for some soils in Texas (McKeen and Johnson 1990). Diffusivities of these unsaturated soils are quantitatively similar to the coefficient of consolidation observed in similar plasticity saturated clays (Lambe and Whitman 1969).

34. Little information is available on the maximum suction change at the depth of the active zone ΔU_{max}. A computer analysis using program SWELZA.FOR given in Appendix A indicates that ΔU_{max} may be approximated by

$$\Delta U_{max} = \frac{0.007}{C_t} \tag{8}$$

where the coefficient of correlation $r^2 = 0.716$. Equation 6 may therefore be rewritten in terms of the suction compression index

$$Z_{ae} = \frac{\ln\left[\frac{0.0035}{U_o \cdot C_t}\right]}{-\left[\frac{n\pi}{\alpha}\right]^{0.5}} \tag{9}$$

C_t may be estimated from charts using soil cation exchange capacity data or measured from results of soil suction-volume change laboratory tests on soil specimens (McKeen and Johnson 1990).

35. Edge Moisture Variation Distance. The edge moisture variation distance for edge heave required for some design methodologies (Post-Tensioning Institute 1980, Hartman and James 1988) is (McKeen and Johnson 1990)

$$e_{me} = Z_{ae} - D \tag{10}$$

where

e_{me} = edge moisture variation distance for edge heave, ft

Z_{ae} = active zone depth for edge heave, ft

D = depth of the exterior stiffening beam, ft

Equation 10 is confirmed in Appendix A. e_{me} could approach half of the wavelength of the soil surface wave pattern $\ell/2$ beneath and adjacent to a

structure as the soil wets and drys with the season, but would not exceed L/2 where L is the length of the mat or foundation. Therefore, $Z_{ae} < \ell/2$ if D = 0. McKeen and Lytton (1984) found for some pavements

$$Z_a = 0.027 \cdot \ell^{1.727} \tag{11}$$

for $\ell \leq 35$ ft. The wavelength of the soil surface movement pattern appears to be a primary function of the active zone depth. Equation 11 calculates $Z_a < \ell/2$ if $\ell \leq 35$ ft and $Z_a = 13$ ft if $\ell = 35$ ft.

Center Heave

36. Differential movement from center heave (or shrinkage) y_{mc} will occur if (1) the soil suction within the active depth of heaving soil for center heave Z_{ac} is less or more than the equilibrium suction U_e, Figure 6, or (2) the level of equilibrium moisture changes at and below depth Z_{ac}.

37. Depth of Active Zone. If the equilibrium suction U_e does not change below depth Z_a, then $Z_{ac} = Z_{ae}$ because the edge active zone depth Z_{ae} controls when moisture changes occur from climate changes outside the perimeter of the facility. The depth of the active zone for center heave Z_{ac} may be found approximately from Equations 10 or 11. y_{mc} may be as much as half of the heave or A_u, amplitude of the wave pattern, as the soil wets up within depth Z_a from the maximum surface suction to U_e or drys out from the minimum suction to U_e.

38. Edge Moisture Variation Distance. The edge moisture variation distance for center heave $e_{mc} = e_{me}$ if $Z_{ac} = Z_{ae}$. If the soil wets from surface watering or leaking underground utility lines such as shown in item 4 of Table 3 or Figure 4d, edge moisture variation distance for center heave e_{mc} may exceed e_{me} caused only by seasonal climatic changes, especially in dry climates. e_{mc} will be limited to L/2. The Post-Tensioning Institute (1980) indicates e_{mc} of about 5 to 6 ft compared to e_{me} of 2 to 3 ft for dry climates. The wavelength for center heave is therefore expected to be greater than for edge heave if the soil is initially dry as in a dry climate. Center heave of soil in a wet climate can be limited so that e_{mc} may be less than e_{me} as indicated by the Post-Tensioning Institute (1980).

Field Elevation Measurements

39. Field elevation profile measurements on pavement surfaces taken at relatively small spacings from 0.5 to 1.0 ft indicate wavelength distributions

caused by soil movement patterns usually exceed 4 ft and are more likely to be in the range of 10 to 35 ft for pavements (McKeen and Lytton 1984, Gay and Lytton 1988). Active zone depths for these wavelengths may therefore be 5 to 17 ft or less assuming $Z_a \leq \ell/2$. These observations are consistent with past experience that indicates Z_a from 5 ft to 20 ft or more (HQDA 1983). Actual wavelengths may be much more than 35 ft if Equation 10 is valid because some active zone depths exceed 20 ft such as in areas where fissured deep desiccated soil exist such as in Texas. Wavelengths less than about 4 ft indicate surface disturbances and finishing characteristics of floors and pavements, which are beyond the scope of this study. Wavelengths larger than 4 ft indicate soil volume changes attributed to soil deformation mechanisms (McKeen and Eliassi 1988). Edge moisture variation distances are often 5 to 17 ft or less (Post-Tensioning Institute 1980, HQDA 1983), which are consistent with wavelengths of soil surface movement greater than 10 ft.

Differential Foundation Movements

40. Damage to facilities may occur from excessive differential movement of the foundation. One or two story lightly loaded structures often experience more deformation or damage than taller structures because the smaller loads of one or two story and light structures are less able to restrict differential movement of the foundation soil. Tools for rating foundation performance and for design are developed below using guidelines for tolerable differential movements and the influence of foundation stiffness on limiting potential differential movements.

Definition of Differential Movement

41. Differential movement may be defined in terms of diagonal (shear) or tensile bending modes, Figure 7. Diagonal shear and bending fractures occur when the critical tensile strains of the building materials are exceeded. The orientation of Figure 7 illustrates fractures to a concrete structure from elastic center settlement or edge heave. Rotating Figure 7 by 180 degrees illustrates edge settlement or center heave. The diagonal tension cracking or shear mode of failure is favored in structures with small length to height ratios or where deformation occurs over small lengths compared to the height of the structure (Boscardin and Cording 1989). Diagonal tension cracking will usually occur first in facilities constructed on soils subject

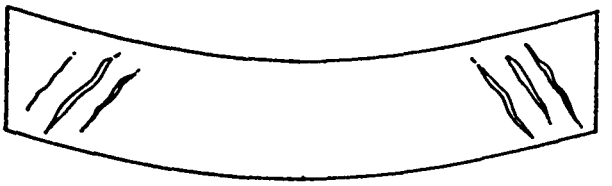

a. DIAGONAL SHEAR STRAIN

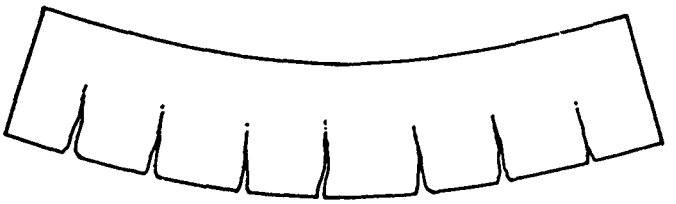

b. TENSILE BENDING STRAIN

Figure 7. Cracking due to types of deformation in structures

to volume change because deformation often begins over short lengths. In practice, cracking that is observed may be a combination of both shearing and bending modes. Differential movement that leads to damage may be defined in terms of angular distortion for shear mode deformation and deflection/span length ratio for bending mode deformation.

42. Angular Distortion. Angular distortion β is the rotation of a straight line joining two reference points on the structure minus any rigid body tilt that the structure may have incurred, Figure 2 in PART I. Figure 8a illustrates the definition of angular distortion in radians from a sinusoidal wavelength motion

$$\beta = \frac{2A}{\ell/2} = \frac{4A}{\ell}, \quad A \ll \ell \tag{12}$$

where ℓ is the wavelength and $2A$ is the peak-to-peak (or peak-to-trough) amplitude of the actual waveform beneath the foundation. β is the average angular distortion of all values between the peak and trough of the wave. The amplitude A is less than A_u and A may be defined in terms of a sinusoidal vertical movement restrained by the foundation. β exceeding 1/500 may lead to cracking and structual damage in structures (HQDA 1983, HQACE 1990). The angular distortion is often correlated with the deflection to span

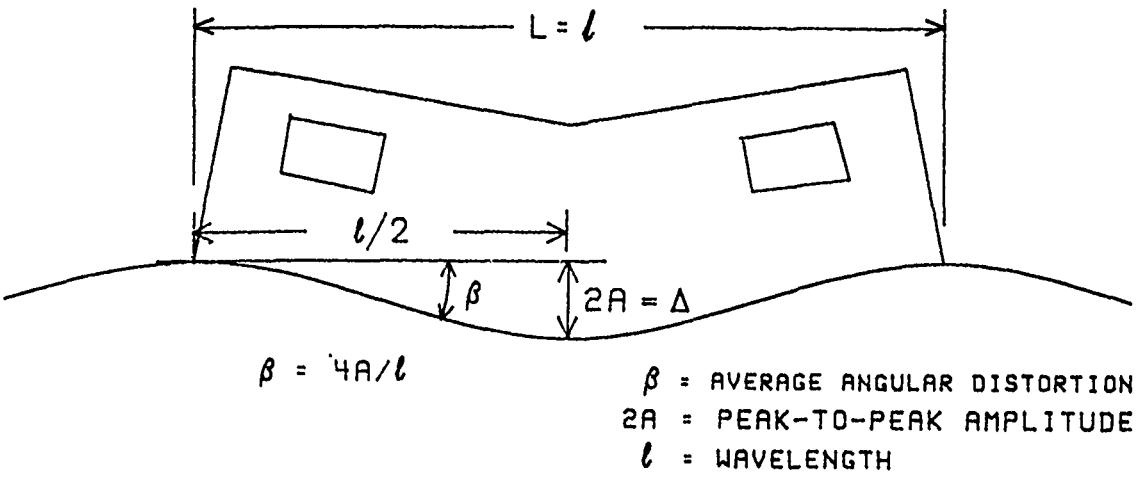

a. ANGULAR DISTORTION β

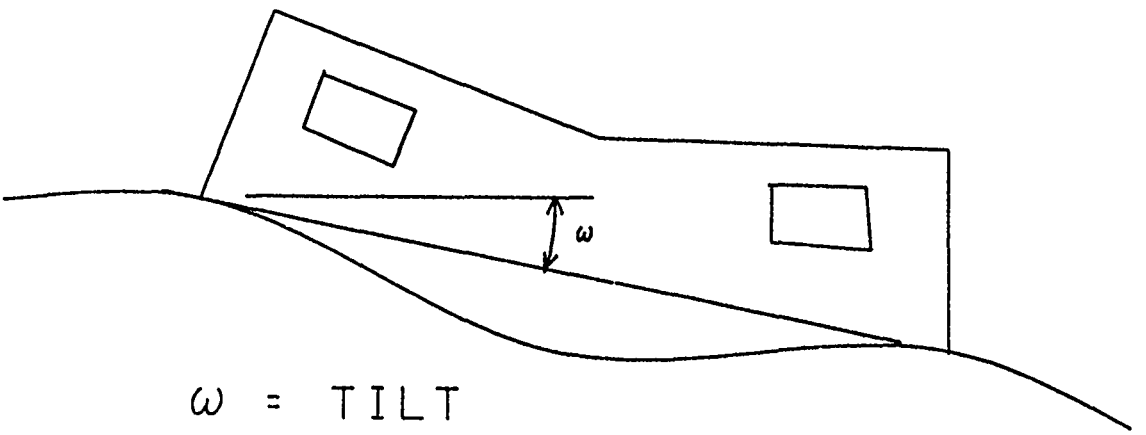

b. TILT ω

Figure 8. Angular distortion related with wave motion

length ratio and may be in the range of 2 to 3 times this ratio. Tilt ω is the rotation of the peaks of the wave from the horizontal as shown in Figure 8b. Tilt exceeding 1/250 or 0.4 percent can be noticeable (HQACE 1990).

43. Deflection/Span Length Ratio. The deflection Δ divided by the span length L between two reference points is defined as the deflection/span length ratio. The two reference points can be taken as adjacent crests of a wave with crest-to-crest distance ℓ. Δ/L may be defined in terms of wavelength motion by

$$\frac{\Delta}{L} = \frac{2A}{\ell} \tag{13}$$

where L is the distance ℓ between peaks of the wave form in Figure 8a. The Δ/L of Figure 8a is 1/2 of the angular distortion β.

44. Degree of Damage. The degree of damage observed in structures is a function of differential movement which is defined herein as the crest-to-trough amplitude 2A divided by the crest-to-trough length $\ell/2$. Many studies have been completed that characterize the degree of damage such as extent of cracking, particularly in masonry walls, with angular distortion (Polshin and Tokar 1957, Burland and Wroth 1974, Wahls 1981). Table 4 characterizes the degree of damage in masonry walls for various angular distortions. The angular distortions selected accommodate some horizontal strain from self-weight of the structure.

Foundation Stiffness to Resist Damage

45. Stiffness of the foundation may be adjusted to accommodate or reduce the unrestrained soil vertical movement A_u or the foundation could be designed to isolate vertical soil movement as in a deep foundation, whether heave or settlement. A mat foundation constructed on grade is required to reduce the soil wave surface motion to tolerable levels of angular distortions. Settlement analyses are also necessary to check that applied loads will not cause excessive differential movement. Structural analyses should check for adequate shear and bending resistance in the foundation.

46. The wavelength of the vertical soil movement pattern is critical to the performance of a particular mat foundation. Two models are described for analysis of mats using soil surface wave patterns. Model I proposes that the critical wavelength is when $\ell = 2R$ where R is the radius of a circular mat. A mat radius R simulates circular foundations (Kay and Cavagnaro 1983) and therefore considers two-dimensional slabs using only one length parameter,

$$R = \sqrt{\frac{LB}{\pi}} \tag{14}$$

where

R = equivalent radius, ft

L = length of the mat, ft

B = width of the mat, ft

Kay and Cavagnaro recommended that the L/B ratio should not exceed two. Model II proposes that the critical wavelength is when $\ell = 4R$. These models assume

Table 4. Characterization of Degree of Damage

Degree of Damage in Masonry	Critical Tensile Strain ϵ_c	Angular Distortion β	Description of Damage	Approximate Width of Cracks, mm
Negligible	< 0.0005	< 0.0010	Hairline cracks	< 0.1
Very Slight	0.0005	0.0010	Easily treated fine cracks; possible slight fracture; cracks visible in outside brick on close inspection	< 1.0
Slight	0.0007	0.0015	Easily filled cracks; several slight fractures inside structure; exterior cracks visible and repointing may be required for weathertightness; doors and windows may stick slightly	< 5.0
Moderate	0.0013	0.0031	Cracks may require cutting out and patching; tuckpointing and possible replacement of some brickwork; doors and windows stick; utility service may be interrupted; weathertightness impaired	5 to 15 several > 3
Severe	0.0027	0.0062	Extensive repair requires removal/replacement of walls, especially over doors and windows; windows and door frames distorted; floor slopes noticeably; walls lean or bulge noticeably; some loss of bearing in beams; utility service disrupted	15 to 25
Very Severe	> 0.0027	> 0.0062	Major repair or complete reconstruction required; beams lose bearing; walls lean badly and require shoring; windows broken; danger of instability	usually > 25

Note: Data from Boscardin and Cording, 1989

that the (1) mat will not lift off the soil at any point, thus conforming to the shape of the soil surface and (2) foundation stiffness does not influence wavelength ℓ. These models assume uniform loads and do not consider

concentrated loads. These models are proposed to be used with existing design methodologies such as the PTI (Post-tensioning Institute 1980) and SWD (Hartman and James 1988) procedures and may be most useful in designing the interior portions of mat foundations.

47. Model I: $\ell = 2R$. Figure 9 illustrates the dimension of a rigid, weightless mat in relation to the wavelength ℓ of the unrestrained vertical movement A_{eu}. If the length of the mat exceeds ℓ, then the mat will be supported by two or more bumps, Figure 9a, and A_{eu} is the total potential heave $2A_u$. A real mat foundation has weight and it will conform some with the surface soil wave pattern, but the amplitude will be reduced from $2A_u$ to 2A, Figure 8a. This model is representative of edge heave as in Figure 8a and center heave by the dotted line in Figure 9a.

48. Kay and Cavagnaro (1983) after the work of Brown (1969) indicated that the stiffness of the mat can be made to reduce the unrestrained differential movement through a stiffness reduction factor. This factor is

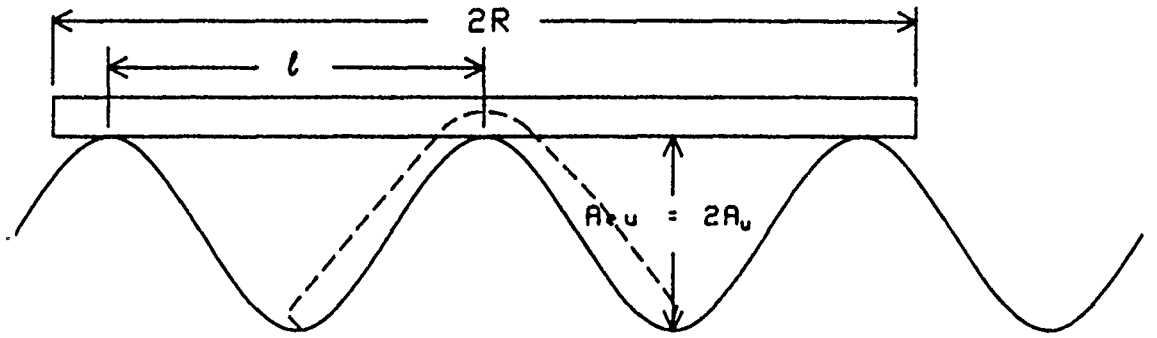

Aeu = UNRESTRAINED HEAVE BENEATH FOUNDATION

2Au = PEAK-TO-PEAK UNRESTRAINED HEAVE

a. MAT LENGTH GREATER THAN WAVELENGTH

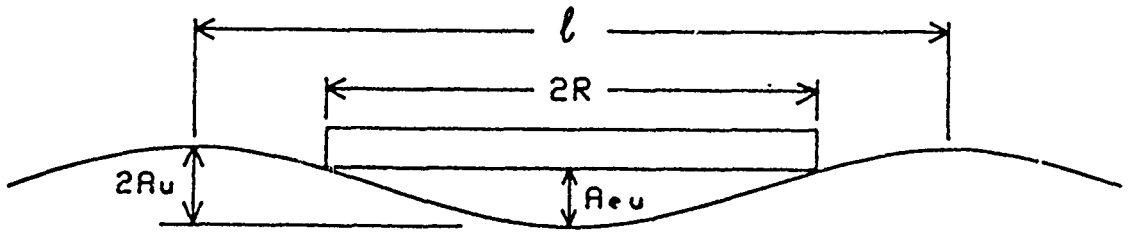

b. MAT LENGTH LESS THAN WAVELENGTH

Figure 9 Relationship of mat length with the wavelength of soil movement

the differential settlement beneath the mat restrained by the slab stiffness divided by the unrestrained differential settlement of a fully flexible mat. A reduction factor R_f may similarly be defined that relates the restrained differential heave or crest-to-crest amplitude $2A$ beneath a mat with stiffness as in Figure 8a with the unrestrained differential heave A_{eu} of the surface soil wave pattern beneath a fully flexible mat foundation

$$R_f = \frac{2A}{A_{eu}} = \frac{A}{A_u} \tag{15a}$$

where A is related to angular distortion of the foundation β and wavelength ℓ by Equation 12. The unrestrained heave beneath a fully flexible mat A_{eu} is $2A_u$, the crest-to-crest unrestrained amplitude of the wave motion where $2R \geq \ell$. $2A_u$ approaches maximum differential heave "y_m" or that calculated using Equations 6 for lighter, more flexible mat foundations. R_f may be redefined in terms of angular distortion assuming wavelengths are not changed by compression from the foundation

$$R_f = \frac{\beta}{\beta_u} \tag{15b}$$

where β_u is the angular distortion from unrestrained soil heave. Kay and Cavagnaro (1983) and Brown (1969) give R_f as a function of the relative stiffness of the mat K_s as in Figure 10. This relationship is used in program ADATG, Table B4, and placed in a DATA statement of SUBROUTINE STIFF. The relative stiffness is (after Brown 1969)

$$K_s = \frac{E_c}{E_s} \cdot \frac{D_e^3}{\left[r \cdot \frac{\ell}{2}\right]^3} \cdot [1 - \upsilon_s^2] \tag{16}$$

where

E_c = modulus of concrete elasticity, ksf

D_e = equivalent mat thickness, ft

ν_s = soil Poisson's ratio

E_s = modulus of soil elasticity, ksf

r = ratio of effective mat diameter to the wavelength, $2R/\ell$

ℓ = wavelength of soil movement, ft

For a given relative stiffness and E_c/E_s ratio, D_e required to accommodate a given angular distortion is a maximum when $r \cdot \ell/2 = R_c$ and $r = 1$. R_c is the effective mat radius, $\ell/2$. R_c equals R only when $2R = \ell$.

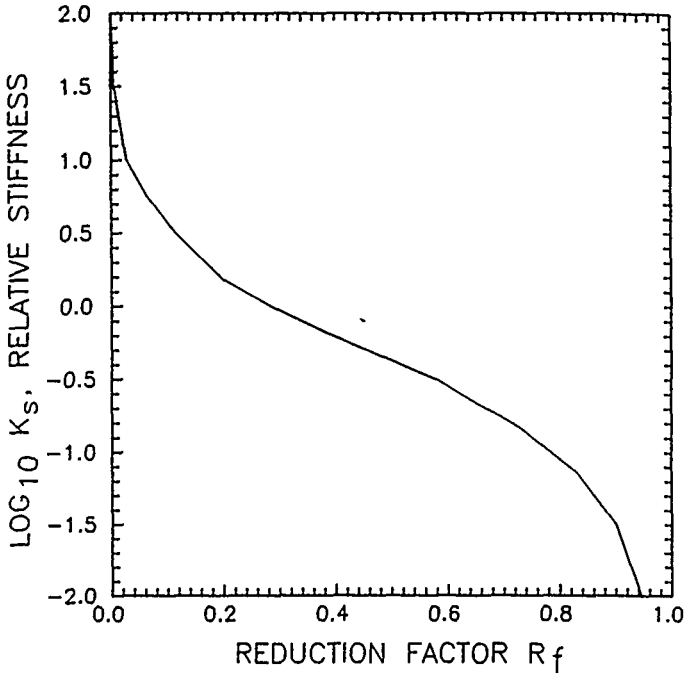

Figure 10. Relationship between relative stiffness (data from Kay and Cavagnaro 1983)

49. The equivalent mat thickness D_e may be the thickness of a flat mat or it may be found from ribbed mat dimensions, Figure 11

$$D_e = \left[\frac{12 \cdot I_{rm}}{B}\right]^{1/3} \tag{17a}$$

$$I_{rm} = \frac{wt^3 + BD^3}{12} + wt\left(h_c - \frac{t}{2}\right)^2 + BD\left(h_c - t - \frac{D}{2}\right)^2 \tag{17b}$$

$$h_c = \frac{wt^2 + BD^2 + 2BDt}{2(wt + BD)} \tag{17c}$$

where

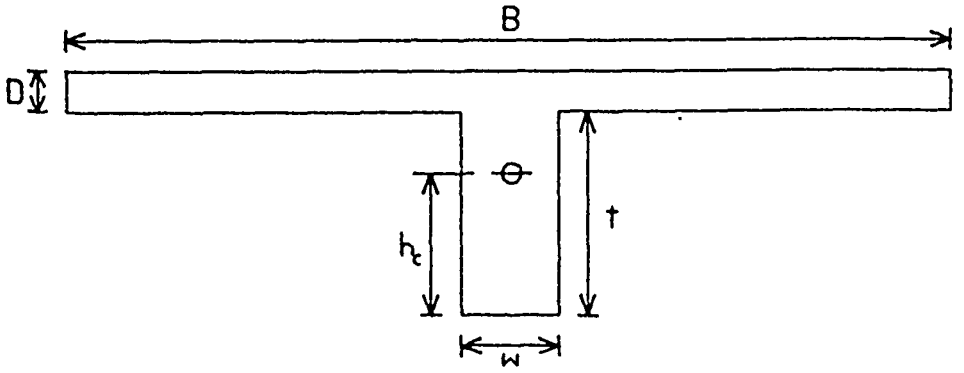

Figure 11. Cross-section of stiffened ribbed mat

I_{rm} = ribbed mat moment of inertia, ft^4

w = stiffening beam width, ft

t = stiffening beam depth below flat portion of mat, ft

B = width of stiffening beam T-section, ft

D = thickness of flat portion of mat, ft

The Post-Tensioning Institute (1980) provides design aids for determining section dimensions. Stiffened ribbed mats that have been economically constructed for supporting lightly loaded 1 or 2 story structures usually have dimensions less than or equal: w = 1.5 ft, t = 3 ft and D = 0.42 ft. B may be $\geq$ 12 ft. Solution of Equations 17 using these dimensions lead to D_e = 2.2 ft. D_e should not be much thicker than 2 to 3 ft for mats supporting one or two story structures. Thick mats supporting heavy multistory structures may be 3 to as much as 8 ft thick.

50. The effective mat diameter $2R_c = \ell$ when 2R exceeds the wavelength ℓ because the mat is supported at the peaks, Figure 9a, and $r \cdot \ell/2 = R_c$. When $2R < \ell$, Figure 9b, the mat may tilt into the depression of the wave and the unrestrained heave beneath the mat is

$$A_{eu} = A_u[1 + \cos\pi(1-r)] \tag{18a}$$

The critical case for Figure 9b is also when D_e is maximum and $2R = 2R_c = \ell$ such that $r = 1$ and the mat just spans the wavelength similar to edge heave or elastic settlement. This situation is also true for center heave. Differential heave A_{eu} is a fraction of total heave $2A_u$

$$\frac{A_{eu}}{2A_u} = \frac{1 + \cos\left[\pi\left(1 - \frac{2R}{\ell}\right)\right]}{2} \tag{18b}$$

D_e required to accommodate the distortion for mats when $2R < \ell$ in Figure 14b is less than if the mat spans the peaks.

51. Figure 12a was developed using Equation 12 and the relationship between R_f and K_s given in Figure 10 for a limiting angular distortion β = 0.0015. β = 0.0015 (1/667), which may cause a slight degree of damage from Table 4, is used as a reference tolerable distortion in this study. The parameters $r = 1$ and $2R = 2R_c = \ell$. Figure 12a shows the logarithm of the relative stiffness K_s required to reduce the unrestrained peak-to-peak amplitude $2A_u$ to a restrained amplitude 2A (leading to a β = 0.0015) for an

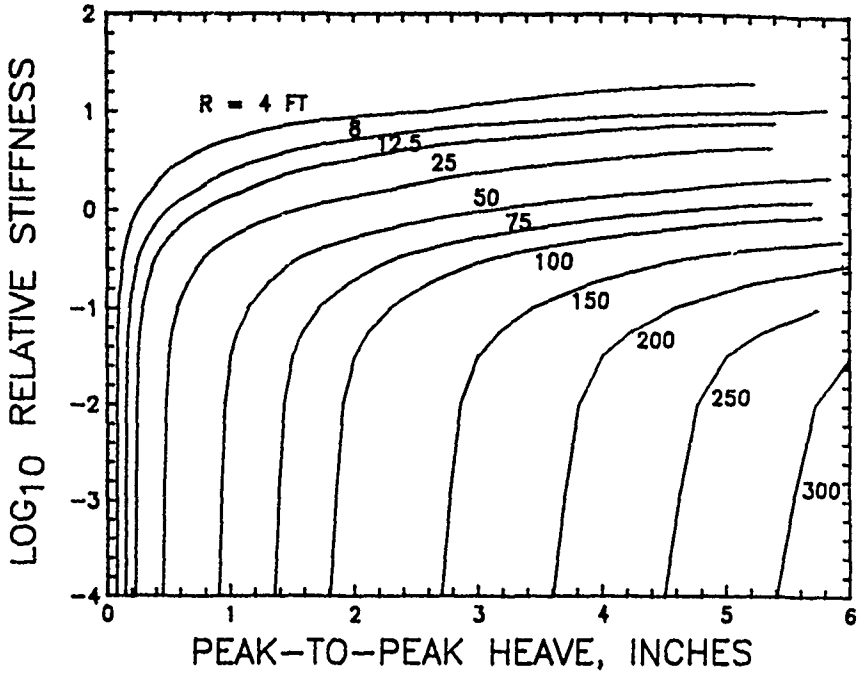

a. RELATIVE STIFFNESS K_s AND HEAVE $2A_u$

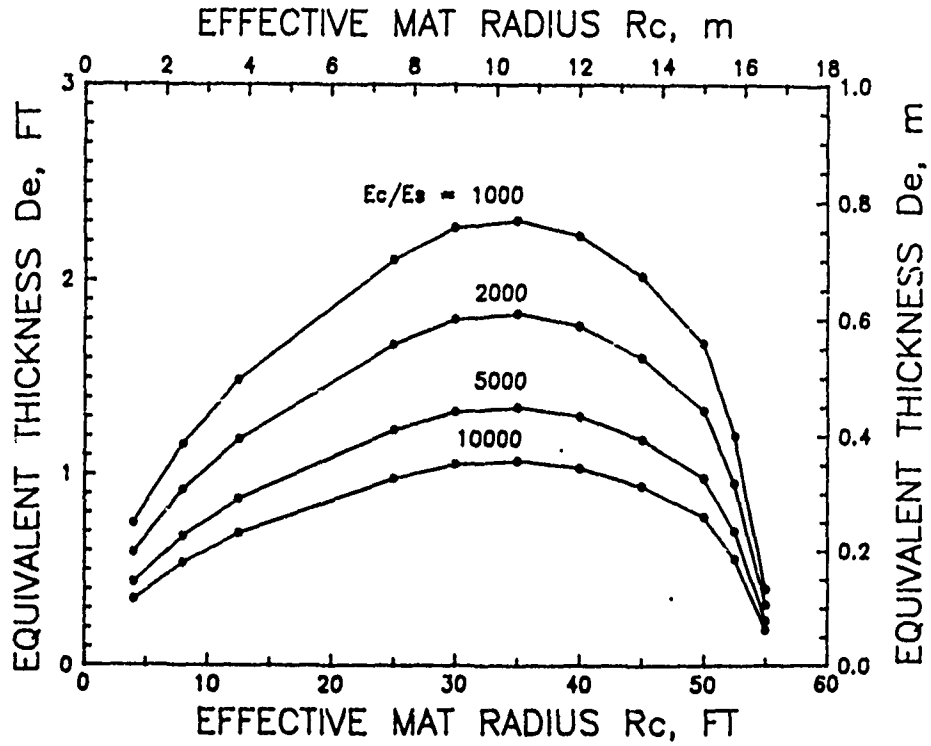

b. THICKNESS FOR $2A_u$ = 1 INCH UNRESTRAINED HEAVE

Figure 12. Relationship of mat stiffness for angular distortion β = 0.0015 and 2R = 2Rc = ℓ

effective diameter $2R_c = 2R = \ell$, the diameter that spans one wavelength. Note that the requirement for relative stiffness decreases rapidly below a certain crest-to-crest heave. This is because the wave amplitude becomes insufficient to cause $\beta \geq 0.0015$ in a completely flexible mat.

52. The equivalent thickness D_e of the mat may be calculated from relative stiffness using Equation 16 for given $R = R_c = \ell/2$ and E_c/E_s ratios. Poisson's ratio of the soil ν_s was assumed 0.4 simulating a saturated clay (HQACE 1990, Bowles 1988). The equivalent thickness from the relative stiffness of Figure 12a for given R_c was plotted in Figure 12b for a peak-to-peak heave $A_{eu} = 2A_u = 1$ inch (limiting $\beta = 0.0015$). Amplitude A required in Equation 15a is found from Equation 12. K_s is subsequently evaluated from R_f and Figure 10. Figure 12b shows that D_e is larger for stiffer soils. The maximum thickness occurs at an equivalent radius R_c of about 35 ft and is on the order of the maximum practical value of 2 to 3 ft for $E_c/E_s = 1000$. If $E_c/E_s = 1000$ and $E_c = 432{,}000$ ksf (3,000,000 psi) for a concrete mat, then $E_s = 432$ ksf which is a medium stiff foundation soil commonly encountered for surface soils. E_c of 432,000 ksf is relatively low corresponding to a concrete strength of about 2800 psi (Winter and Nilson 1979). Calculated values of D_e are on the order of those thicknesses currently constructed for ribbed mats. Deformations in stiffer foundation soils are harder to reduce and require stiffer mats. Therefore, the top several feet of soil supporting mat foundations should have limited stiffness, while still minimizing settlement, to promote the ability of the mat to squeeze out deformation and should not be expansive or collapsible.

53. Mat radii greater than 35 ft reduce the stiffness needed to resist a given unrestrained heave for larger wavelengths because the angular distortion is reduced. Without additional information on soil movement wavelengths, mat foundations with radius > 35 ft should be designed for the worst case situation, which corresponds to a mat thickness given by the peak D_e in Figure 12b if the appropriate limiting $\beta = 0.0015$ for the onset of cracking or any structural damage and the peak-to-peak heave is 1.0 inch.

54. Mat thickness required for limiting angular distortion to $\beta = 0.0015$ when peak-to-peak amplitude of unrestrained heave is only 1 inch can be substantial, especially for $\ell/2$ between 10 and 50 ft. Figure 12 supports the observation by Hartman that heaves greater than 1 inch may be uneconomical

for design and construction of mat foundations (Johnson 1988). Design practice sometimes creates more flexibility in the superstructure than masonry structures to maintain damage within tolerable levels. Therefore, a larger angular distortion than 0.0015 may be appropriate in some cases. Field measurements are required to determine an appropriate limiting β so that Figures 12 may be "fine tuned" to current construction practice. Field measurements will also indicate soil movement patterns and wavelengths that may be most appropriate for design.

55. A new term may be introduced that is independent of soil and mat characteristics using Equation 16. This term is called the relative thickness D_{rel} and it is dependent only on the mat radius and relative stiffness

$$D_{rel} = D_e \left[\frac{E_c}{E_s} \cdot (1 - \upsilon_s^2) \right]^{1/3} = R(K_s)^{1/3} \qquad (19)$$

where R is defined in Equation 14. R and D_{rel} are in units of ft. D_{rel} may be calculated for a given mat radius R or span length ℓ as follows:

1. Determine heave or unrestrained amplitude $2A_u$ in inches for a span length ℓ in feet
2. Calculate $\beta_u = 4A_u/(12 \cdot \ell)$ after Equation 12
3. Select a tolerable angular distortion β that will prevent unacceptable damage to the structure
4. Calculate $R_f = \beta/\beta_u$, Equation 15b
5. Evaluate $\log_{10}K_s$ from R_f using Figure 10, then calculate K_s
6. Calculate D_{rel} from Equation 19 using R or $R = \ell/2$

Many D_{rel} may be calculated for real soil-foundation elevation profiles such as the profile of survey line ATC1 taken over the 8-inch thick slab-on-grade of the Automated Technology Center, Waterways Experiment Station, Figure 13. Survey line ATC1 includes both forward and backward profiles to make a loop. As an example calculation, ATC1 shows a dip between 200 and 246 ft with a peak-to-peak (relatively) unrestrained amplitude $2A_u = 1$ inch and span length $\ell = 46$ ft. $\beta_u = 2 \cdot 2A_u/\ell = 2 \cdot 1/(12 \cdot 46) = .00362$. If tolerable $\beta = 0.0015$, then $R_f = \beta/\beta_u = 0.0015/0.00362 = 0.41$. $\text{Log}_{10}K_s = -0.22$ from Figure 10 and $K_s = 0.6$. $D_{rel} = R(K_s)^{1/3} = (46/2) \cdot (0.6)^{1/3} = 19.3$ ft, which is probably the maximum value D_{relm} for this elevation profile. Program ADATG calculates D_{relm} at this same location, but slightly less at 18.7 ft as shown in PART IV.

56. The maximum relative thickness calculated from Equation 19 for a given elevation profile is denoted as D_{relm} and it is the critical thickness

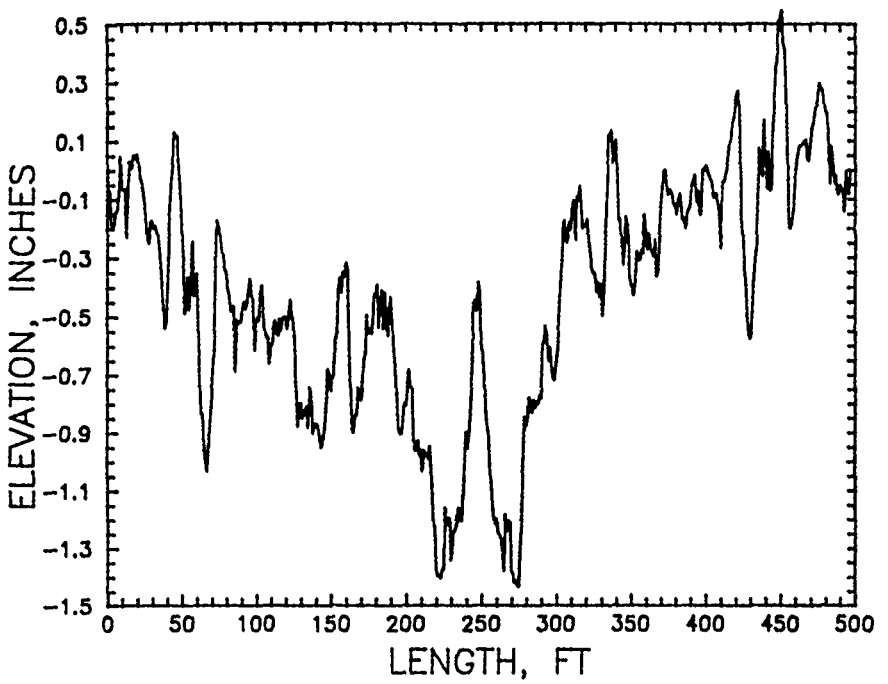

Figure 13. Elevation profile of survey line ATC1, Automated Technology Center

required to prevent a certain amount of damage based on the tolerable angular distortion β. D_{relm} is expected to have the most potential for damage and it can be determined for a specific location. D_{relm} may therefore be useful for rating performance of foundations while also indicating the location of the most damaging distortion in an elevation profile. Program ADATG, Table B4, calculates D_{rel} for span lengths between 4 and 120 ft and determines the span length and location of D_{relm} in an elevation profile. The span length in program ADATG is calculated as nonobstructed distances between adjacent and non-adjacent peaks of the elevation profile. The possibility of support by crests between dominating non-adjacent peaks is considered in evaluating the unrestrained angular distortion β_u used to calculate R_f from Equations 15. Program ADATG uses 0.0015 for the limiting restrained angular distortion β.

57. The relative thickness, calculated from Equation 19 using Equation 15a, may be plotted versus $1/2R_c$ (or $1/\ell$) for different angular distortions to determine how critical frequencies of soil movement change depending on acceptable angular distortions. The critical frequency $f_c = 1/\ell_c$ is where the relative thickness is maximum D_{relmax}, Figure 14. D_{relmax} is the maximum D_{rel} calculated from Equation 19 for a given β and A_{eu}, while D_{relm} is the maximum D_{rel} measured from a given elevation profile. Figure 14 illustrates

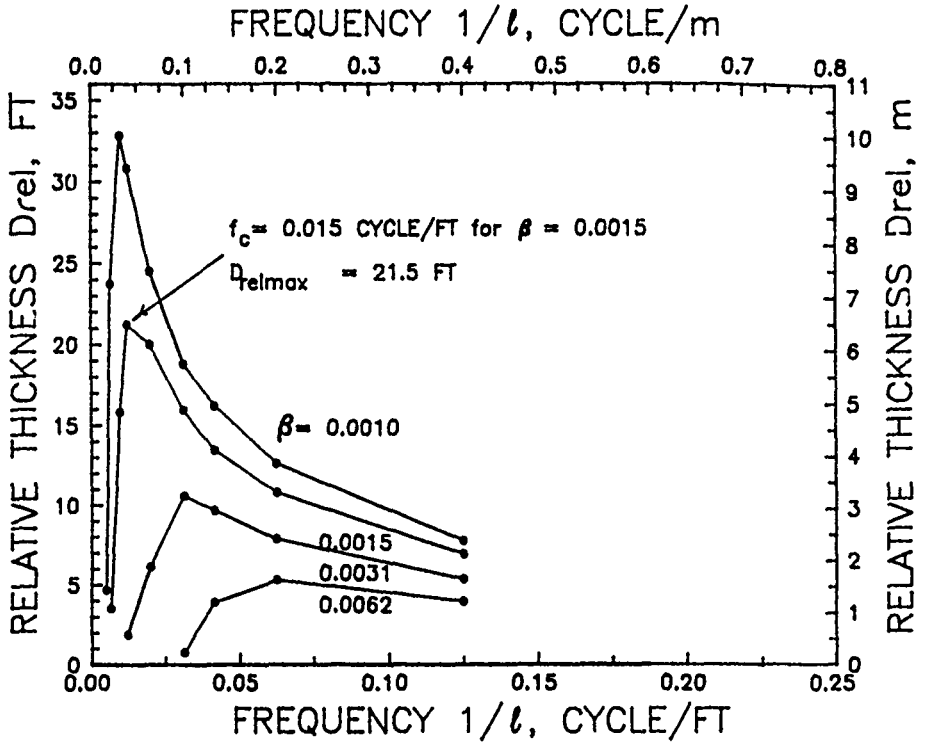

Figure 14. Relative thickness as a function of the reciprical of the span length for A_{eu} = 1 inch

that larger acceptable β can substantially decrease D_{rel} and D_{relmax} and increase the critical frequency. If the acceptable β = 0.0015, then the critical frequency is 0.015 cycle/ft or the critical span (or soil wavelength ℓ_c) is 67 ft for a peak-to-peak amplitude of 1 inch. Mats with diameter 2R greater than 67 ft should be designed with the maximum D_{relmax} of 21.5 ft to consider the possibility that 67 ft wavelengths with amplitude of 1 inch may occur. Mats with 2R less than 67 ft should be designed with D_{rel} found from Figure 14 using frequency 1/2R. If peak-to-peak amplitudes are 2 inches or twice that in Figure 14, then the same curves may be used except that the limiting β values are doubled; e.g., the curve for β = 0.0031 in Figure 14 is that for β = 0.0062 if peak-to-peak amplitudes are 2 inches so that D_{rel} values are approximately doubled. If the acceptable β = 0.0031, then D_{rel} is 1/2 of that for β = 0.0015 and the critical frequency is 0.029 cycle/ft (ℓ_c is 34 ft). These relationships may be expressed by simple equations. Substitution of R = ℓ/2, $\ell = A_{eu}/6\beta_u$ after Equation 12 where $A_{eu} = 2A_u$ and $R_f = \beta/\beta_u$ into Equation 19 gives

$$D_{rel} = R(K_s)^{1/3} = \frac{A_{eu}R_f}{12\beta}K_s^{1/3} \qquad (20a)$$

where

R = equivalent mat radius, Equation 14

K_s = relative stiffness, Equation 16

A_{eu} = soil heave unrestrained by mat stiffness, $2A_u$, Figure 9a

R_f = reduction factor, Equation 15a

β = tolerable angular distortion, Table 4

A plot of R_f versus $R_f \cdot K_s^{1/3}$ in Figure 15 shows that $R_f \cdot K_s^{1/3}$ reaches a peak when $R_f = 0.625$ and $R_f \cdot K_s^{1/3} = 0.398$. Therefore

$$D_{relmax} = \frac{A_{eu}}{12\beta} \cdot 0.398 = \frac{0.033 \cdot A_{eu}}{\beta} \quad (20b)$$

$$f_c = \frac{9.6\beta}{A_{eu}} \quad (20c)$$

where D_{relmax} is in feet, A_{eu} is in inches and f_c is in cycle/ft.

58. Equations 20 show how to calculate the maximum thickness of a mat that can accommodate crest-to-crest unrestrained differential heave $A_{eu} = 2A_u$ and still maintain the limiting angular distortion β. If mat dimension $2R < 1/f_c$, then mat thickness may be less. D_e and D_{rel} may be used as a design tool for estimating the thickness (and stiffness) of a mat foundation, Table 5, from estimates of the appropriate limiting angular distortion β and

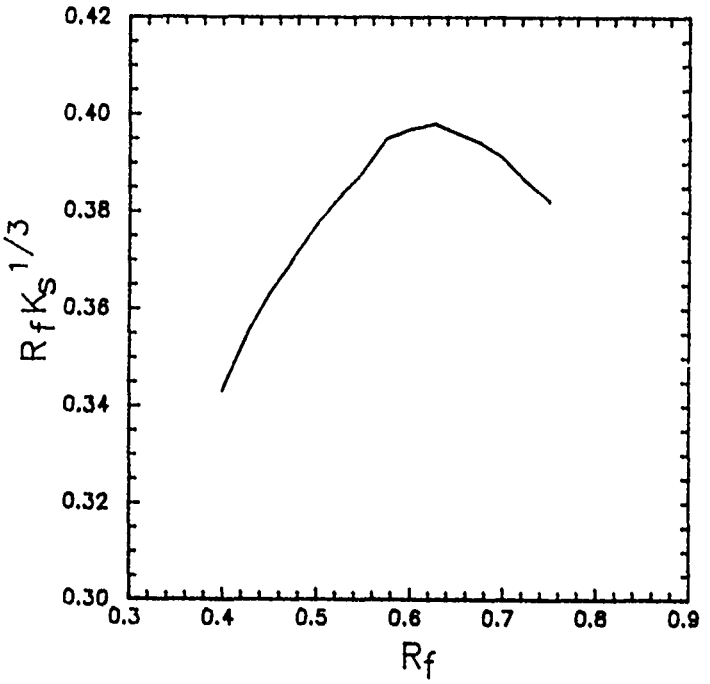

Figure 15. R_f versus $R_f \cdot K_s^{1/3}$

Table 5. Estimation of Mat Thickness

Step	Procedure	Illustration
1	Determine input data: mat length L and width B, potential heave A_{eu} in inches and elastic soil modulus E_s in ksf using procedures in EM 1110-1-1904, assume υ_s, maximum angular distortion β tolerated by structure and foundation modulus E_c. Assume ribbed mat T-section dimensions, Figure 11; reinforcement steel, concrete cover COV	L=70 ft, B = 50 ft, A_{eu} = 3 inches E_s = 200 ksf, υ_s = 0.4 and $1-\upsilon_s^2$ = 0.84, tolerable β = 1/360, E_c = 432,000 ksf. E_c/E_s = 2160; ribbed mat T-section dimensions: w = 1.5 ft, t = 3.25 ft, B = 12 ft, D = 0.5 ft. 2 bars steel top and bottom, NB = NT = 2, steel yield strength f'_s = 60 ksi = 8640 ksf, COV = 0.25 ft
2	Determine foundation diameter in feet, $2R = 2(LB/\pi)^{1/2}$	$2R = 2(70\cdot50/\pi)^{1/2}$ = 66.75 ft, R = 33.38 ft
3	Calculate critical frequency $f_c = 9.6\beta/A_{eu}$ from Equation 20c. If $2R \geq 1/f_c$, then go to step 7 and use $D_{rel} = D_{relmax} = 0.033\cdot A_{eu}/\beta$; if $2R < 1/f_c$, then go to step 4	$f_c = 9.6\cdot(1/360)/3 = 0.00889$ cycle/ft or $1/f_c$ = 113 ft; 2R = 66.75 ft < 113 ft, therefore, go to step 4
4	Calculate reduction factor $R_f = 12\beta R/A_{eu}$ (assumes ℓ = 2R or worst case wavelength)	$R_f = 12\cdot(1/360)\cdot33.38/3 = 0.37$
5	Determine $\log_{10}K_s$ from Figure 10	$\log_{10}K_s$ = -0.18 and K_s = 0.66
6	Calculate $D_{rel} = R(K_s)^{1/3}$ from Equation 19	$D_{rel} = 33.38\cdot(0.66)^{1/3}$ = 29.07 ft
7	Calculate: $D_e = D_{rel}/[(E_c/E_s)(1 - \upsilon_s^2)]^{1/3}$, from Equation 19; then, use assumed T-section dimensions to calculate D_e; if calculated D_e is $\geq D_e$ from Equation 19, then ok	$D_e = 29.07/[2160\cdot0.84]^{1/3}$ = 2.38 ft from T-section dimensions, step 1 Equation 17c: h_c = 2.66 ft Equation 17b: I_{rm} = 13.87 ft^4 Equation 17a: D_e = $(12\cdot13.87/12)^{1/3}$ = 2.40 ft: ok
8	Estimate bending moment $M \approx 4E_cI\beta/\ell$, Equation 22. Use $I = I_{bcr}$ for a bottom cracked T-section, Equation 23e. A_s = Area steel = $M/[f'_s\cdot j\cdot(D+t-COV)]$ from Eshbach (1954, p 5-66)	Calculate I_{bcr}: Equation 23a: h_{cb} = 3.42 ftt Equation 23b: I_{stb} = 0.125 ft^4 Equation 23c: I_{stt} = 0.000 ft^4 Equation 23d: I_{rmbc} = 0.380 ft^4 Equation 23e: I_{bcr} = 1.63 ft^4 $M = (4\cdot432,000\cdot1.63\cdot1/360)/66.75$ = 117.21 kips-ft $A_s \approx 117/[8640\cdot.86\cdot(.5+3.25-0.25)]$ ≈ 0.0046 ft^2 = 0.7 in^2 Use 2 Number 9 bars bottom

potential soil heave A_{eu}. β may be determined from structural limitations as in Table 4, while $A_{eu} = 2A_u$ may be estimated from Equations 6 using the active zone depth Z_a. Edge moisture variation distance e_m is not required. D_e calculated using Table 5 appears reasonably consistent with some design examples (Post-Tensioning Institute 1980, Hartman and James 1988), but may be more conservative than the Post-tensioning Institute method. An example calculation is provided in Table 5 to illustrate the simplicity of this method. Note from Figure 12b, Figure 13 and Table 5 that D_{rel} is approximately 10 to 20 times D_e for a concrete foundation depending on the ratio of the concrete and soil moduli and soil Poisson's ratio. Equations 20 may also be applicable to pavements except that R and R_c are not used. Limiting angular distortions appear applicable to airport pavements as confirmed in design charts developed by McKeen (1981). These charts indicate that nearly linear amplitude versus wavelength relationships separate acceptable from unacceptable performance. The slope of the linear relationship is a function of angular distortion, Equation 12.

59. The bending moment of a cross-section in the mat foundation may be estimated from flexure theory (Popov 1956)

$$M = \frac{E_c I}{\rho} \tag{21a}$$

where

M = bending moment, kips-ft

ρ = radius of curvature, ft

E_c = Modulus of elasticity of foundation, ksf

I = cross-section moment of inertia, ft^4

If the mat is assumed to deflect as a circular arc, Figure 16a, then

$$\rho = \frac{\ell(1+\beta^2)}{4\beta} \tag{21b}$$

$\ell = \ell_c$ if $2R \geq \ell_c$ or $\ell = 2R$ if $2R < \ell_c$. Substituting Equation 21b into 21a

$$M = \frac{4E_c I\beta}{\ell(1+\beta^2)} \approx \frac{4E_c I\beta}{\ell} \tag{22}$$

This bending moment may not be realistic because assumption of a circular arc deflection is inconsistent with the soil wave pattern of Figure 8 or 9; the foundation must shape the soil-foundation interface into a circular arc.

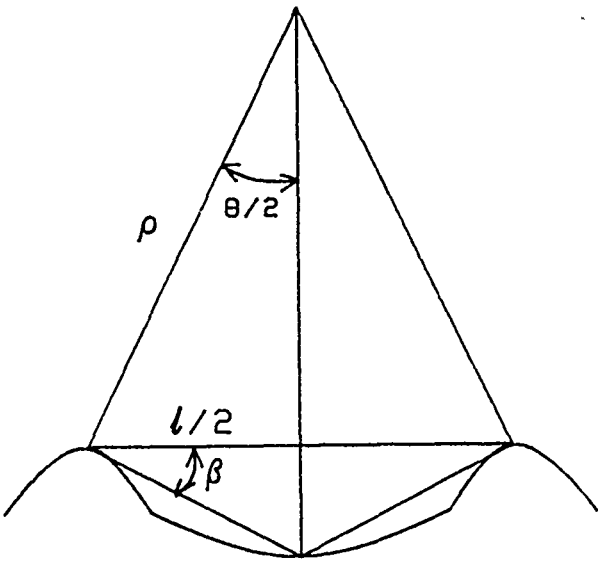

a. Model I

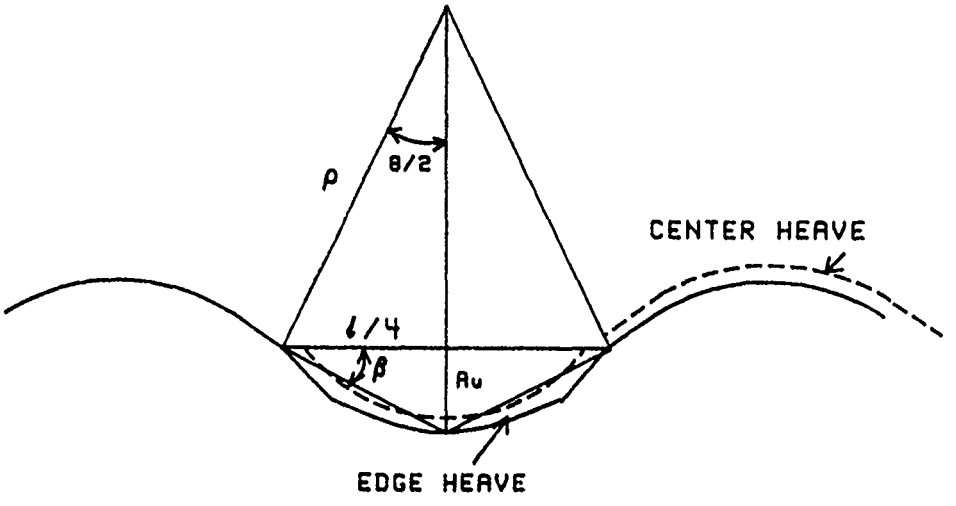

b. Model II

Figure 16. Radius of curvature ρ and angular distortion β

Steel requirements are excessive using a moment of inertia I_{rm} calculated for an uncracked T-section, Equation 17b. Assuming a T-section cracked below the center of gravity h_c, Figure 11, yields reasonable steel requirements (Johnson 1989b)

$$h_{cb} = \frac{w\cdot(t+D-h_c)\,(D+t+h_c)/2. + D\cdot(B-w)\,(t+D/2.) + NB\cdot\pi r_s^2\cdot COV}{w\cdot(t+D-h_c) + D\cdot(B-w) + NB\cdot\pi r_s^2} \qquad (23a)$$

$$I_{stb} = NB\left[\frac{\pi r_s^4}{4} + \pi r_s^2\,(h_{cb}-COV)^2\right] \qquad (23b)$$

$$I_{stt} = NT\left[\frac{\pi r_s^4}{4} + \pi r_s^2 (t+D-h_{cb}-COV)^2\right] \tag{23c}$$

$$I_{rmbc} = \frac{BD^3+w(t-h_c)^3}{12} + BD\left(\frac{D}{2}+t-h_{cb}\right)^2 + w(t-h_c)\left(h_{cb}-\frac{h_c+t}{2}\right)^2 \tag{23d}$$

$$I_{bcr} = I_{rmbc} - I_{stt} + \frac{E_{st}}{E_c}(I_{stb}+I_{stt}) \tag{23e}$$

where

h_{cb} = bottom cracked center of gravity

COV = concrete thickness over steel

NB = number of bottom bars

NT = number of top bars

I_{stb} = moment of inertia of bottom steel, in.^{4}

I_{stt} = moment of inertia of top steel, in.^{4}

r_s = radius of steel, in.

I_{rmbc} = bottom cracked moment of inertia excluding steel, in.^{4}

I_{bcr} = effective bottom cracked moment of inertia including steel, in.^{4}

E_{st} = modulus of elasticity of steel, $29 \cdot 10^6$ psi

E_c = modulus of elasticity of concrete, $3 \cdot 10^6$ psi

Table 5 provides an example calculation of bending moment and required steel reinforcement to illustrate the potential of this methodology.

60. Model II: $\ell = 4R$. This model simulates edge and center heave using the distortion pattern in Figure 16b, which may be more realistic than that of Model I. Calculations are the same, except that amplitude $A_{eu} = A_u$ or half the amplitude of Model I. The critical frequency $f_c = 4.8\beta/A_{eu}$. Calculation of mat thickness and bending moment are the same as Model I for the same amplitude beneath the mat.

PART III. SELECTION OF PERFORMANCE RATING SYSTEMS

Introduction

61. Performance rating systems can quantify damage to structures and assist in rating operational efficiency. This information is required to check and compare the value of existing and new design and construction technology. These systems are also able to evaluate performance techniques for stabilizing expansive, collapsible, soft and other unstable soils. A satisfactory rating system may also have potential as a design tool for foundations. Several systems have been proposed for analysis of foundation performance as described below, but these systems have not been systematically compared to evaluate their relative value in rating performance.

62. The purpose of PART III is to select rating systems that show sufficient potential of being able to adequately rate foundation performance. These systems use elevation change measurements taken at close spacings ≤ 1 ft. Useful rating systems should be independent of length because foundations vary over a wide range of sizes. Useful systems should also have some independence from each other so that each potentially useful system is capable of measuring distortion characteristics in a unique way. This will enhance the potential for selection of optimum rating systems. Simple and complex periodic wave motions are used to check for potential application and for independence between rating systems. A technique referred to as "fractals" is used to confirm that soil-foundation deformation is either a wave pattern motion or another pattern such as a space-filling curve similar to edges of fine particles or coastlines (Whalley and Orford 1989).

Applications With Simple Wave Patterns

63. Potential for application of a rating system is evaluated by determining if ratings provided by a proposed system are independent of the length of the foundation slab. The degree of independence between rating systems is evaluated by regression analysis that attempt to relate the rating systems with each other. Rating systems available for analysis are Fourier transform parameters, F-numbers, wave index, angular distortion parameters and relative thickness parameters. Computer programs prepared to assist analysis of surface soil and foundation movement patterns are described in Appendix B.

Fourier Transform of Surface Movement

64. The Fourier transform is an ideal method of decomposing a wave pattern into sine or cosine waves to evaluate dominant soil wavelengths and amplitudes. These transforms have previously been applied in some pavement studies to rate performance and to assist in design (McKeen 1981, McKeen and Lytton 1984, Gay and Lytton 1988).

65. Definition of Fourier transform. Wave patterns of surface soil movements may be transformed into a family of sinusoidal functions at discrete frequencies and amplitudes using Fourier transform analysis (Brigham 1974). The transform function $\Phi(f)$ is given by

$$\Phi(f) = \int_{-\infty}^{\infty} \phi(x) \cdot e^{-j2\pi fx} \cdot dx \tag{24}$$

where

$\phi(x)$ = arbitrary waveform to be decomposed into sinusoids $\Phi(f)$, in.

x = horizontal distance, ft

dx = differential increment of distance, ft

f = frequency, cycle/ft

j = $\sqrt{-1}$

The arbitrary waveforms of interest are the elevation profiles of the first floor supported by the foundation and soil surfaces.

66. Equation 24 may be solved for each frequency f_k for any complex function by numerical integration

$$\Phi(f_k) = \frac{1}{\Delta x \cdot NRE} \cdot \sum_{i=1}^{NRE} \phi(x_i) \cdot e^{-j \cdot 2\pi f_k x_i} \Delta x \qquad k=1,2\ldots,NRE \tag{25a}$$

or

$$\Phi(f_k) = \frac{1}{\Delta x \cdot NRE} \cdot \sum_{i=1}^{NRE} [\cos(2\pi f_k x_i) - j \cdot \sin(2\pi f_k x_i)] \cdot \Delta x \tag{25b}$$

$$\Phi(f_k) = R(f_k) + j \cdot I(f_k) \tag{25c}$$

where

f_k = frequency for integer k, cycle/ft

NRE = number of readings used in the Fourier transform calculation

x_i = distance for value i, ft

Δx = increment of distance, ft

$R(f_k)$ = real part of the Fourier Transform for frequency f_k, in.

$I(f_k)$ = imaginary part of the Fourier Transform for frequency f_k, in.

The term $\frac{1}{\Delta x \cdot NRE}$ in Equations 25 is used to normalize the amplitude of the transformed functions. The number of readings NRE used in the Fourier transform calculation may be less than the actual number of readings NREAD in a profile elevation survey. NRE may be approximately NREAD/2 if a closed loop is made where the last reading is at the point of origin. Closed loops are desirable because much of the operator bias may be removed from the readings.

67. The amplitude of each discrete sinusoid is given by

$$A_t(f_k) = \left[[R(f_k)]^2 + [I(f_k)]^2\right]^{0.5} \tag{26}$$

where $A_t(f_k)$ is the amplitude of the transform in units of the sinusoid functions, which is inches for measured elevation changes. The phase angle is given by

$$\Theta(f_k) = \tan^{-1}\left[\frac{I(f_k)}{R(f_k)}\right] \tag{27}$$

and defines the shift in radians (or degrees if multiplied by $180/\pi$) from the amplitude. The phase angle ranges from -90 to +90 degrees.

68. Simple Wave Patterns. The computer program FTRC (Fourier TRansform Complex) listed in Table B1 was prepared to evaluate the Fourier transform of arbitrary waveforms from elevation or elevation change data. This program calculates the amplitude of each wave of the elevation profile from Equation 26 as a function of frequency between 0.0 and 0.25 cycle/ft. The minimum wavelength that can be discerned is $1/f_m = 1/0.25 = 4$ ft and it will be computed at the maximum frequency f_m or 0.25 cycle/ft used in this study. The increment of length Δx should not be greater than 1.0 ft to determine a minimum wavelength of 4 ft. Wavelengths less than 4 ft are not considered because these are attributed to construction characteristics such as concrete finishing. The maximum wavelength that may be discerned depends on the number of readings and the increment change in frequency $\Delta f = 1/(NRE \cdot \Delta x)$. If $\Delta x = 1$ ft and NRE = 100, for example, then a maximum wavelength (minimum frequency f_o) that may be discerned is limited by $1/\Delta f = NRE \cdot \Delta x = 100$ ft ($f_o = 1/100 = 0.01$ cycle/ft). Larger NRE for a fixed Δx will allow larger wavelengths to be discerned. A Δx of 1.0 ft appears to be a reasonably optimum increment for the wavelengths of interest in this study. A plot of the

amplitude of discrete waves versus frequency is defined as an amplitude frequency spectrum. This spectrum is illustrated in the following for a straight line, sine wave and cosine wave.

69. Straight Line. A straight line of constant elevation may indicate uniform heave or settlement, which does not contribute to a damaging distortion, but may adversely influence drainage from the structure and connections to exterior utilities. The Fourier transform of a straight line 200 ft long at an elevation of 0.5 inch shows a peak amplitude of 0.5 inch at a frequency of 0.0, Figure 17. Program FTRC calculates the amplitude of the transform of a straight line at a given elevation equal to the elevation of the line. The width of the peak at zero frequency is controlled by the number of readings taken along the 200 foot length. More frequent readings at closer spacings reduce the width of the spike (amplitude) toward zero.

70. Sine Wave. A sine wave based on elevation profile measurements initiated from the perimeter of a structure may indicate center heave or edge settlement. The elevation of the initial point of wave patterns used in this study is always zero. Figure 18a illustrates the function

$$\phi(x) = \sin\left(\frac{2\pi x}{\ell}\right) \tag{28}$$

where the wavelength ℓ = 32 ft and the amplitude A = 1.0 inch. The peak amplitude of the Fourier transform of this function is at a frequency of

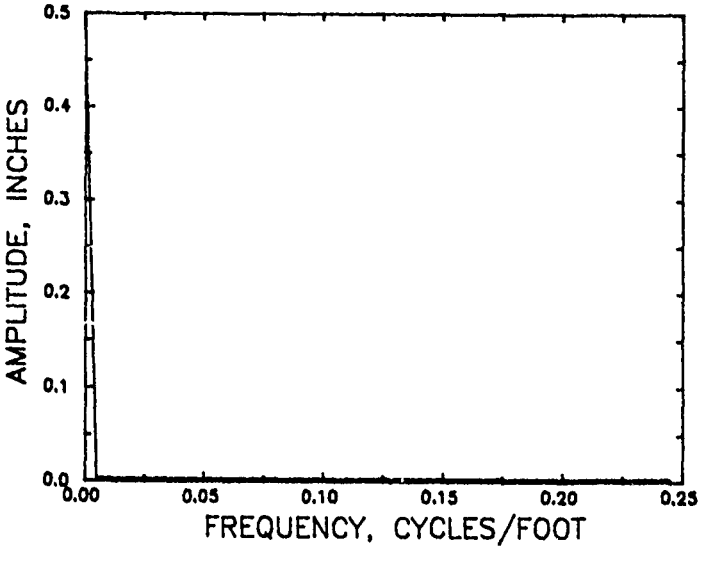

Figure 17. Amplitude frequency spectrum of a straight line

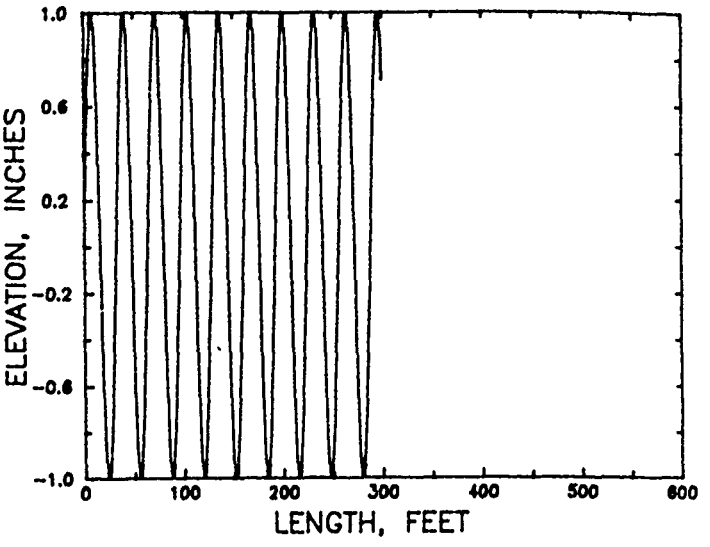

a. SINE WAVE

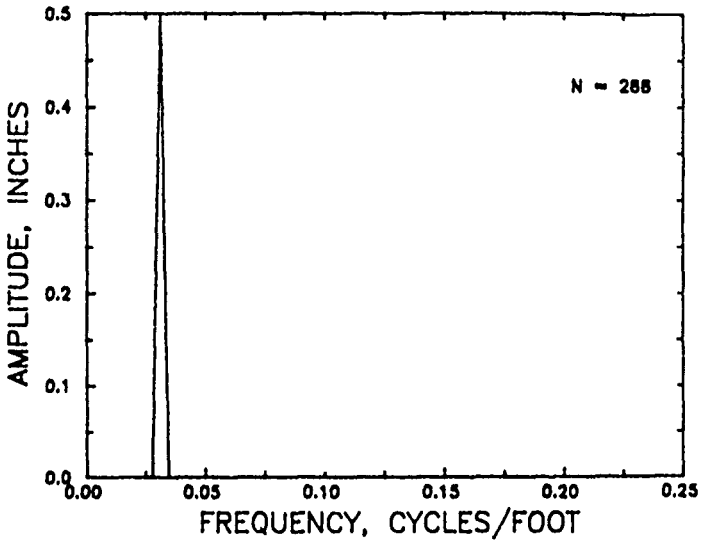

b. AMPLITUDE FREQUENCY SPECTRUM OF SINE WAVE

Figure 18. Fourier transform of the wave $\sin(2\pi x/32)$, N = 288

0.03125 cycle/ft where 1/0.03125 is the wavelength of 32 ft/cycle, Figure 18b. The peak amplitude of the transform A_t from Equation 26 is 0.5 inch for NRE = 288 readings whereas the amplitude of the sine function A in Equation 28 is 1.0 inch. Program FTRC calculates the amplitude of the transform A_t of a sinusoidal function as 1/2 of the amplitude A of the actual waveform, $A = 2A_t$, or 1/4 of the peak-to-peak vertical distance. Input data to program FTRC for a sine wave are illustrated in Table B7a. Output data, Table B7b,

indicate 0.5 inch amplitude at a frequency 0.03125 with a phase angle of 90 degrees. The peak amplitude occurs at a distance of 1/4 wavelength from the point of origin.

71. The shape of the transform depends on the number of readings. Figure 19a illustrates that the amplitude A_t of the waveform is reduced and the shape is distorted if the number of readings is reduced to 270. If NRE = 32, then the amplitude remains at 0.5 because $NRE \cdot \Delta x = 32 \cdot 1.0 = 32$ ft or an

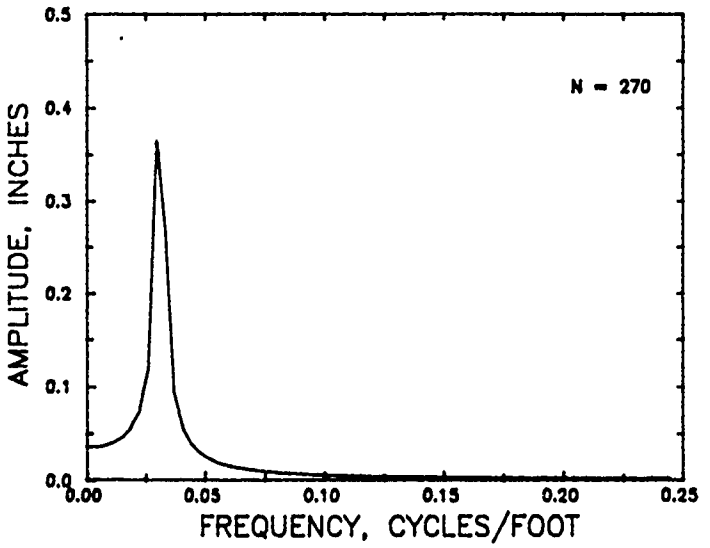

a. N = 270

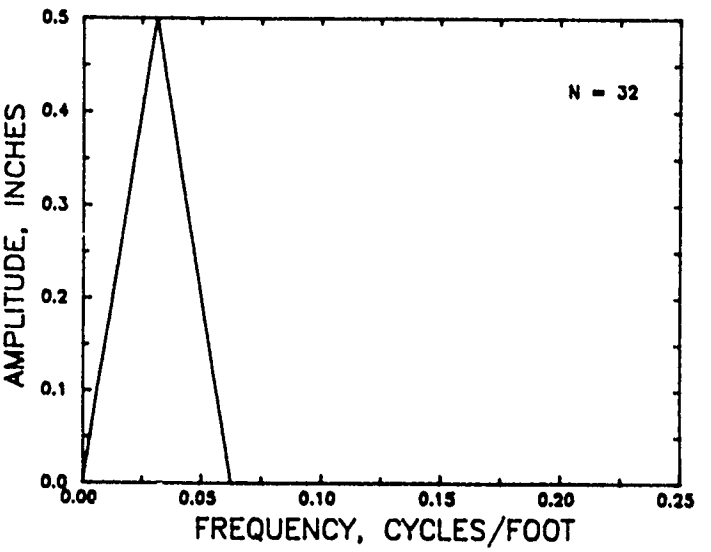

b. N = 32

Figure 19. Influence of number of readings on the amplitude frequency spectrum of wave $\sin(2\pi x/32)$

integral multiple of the wavelength. The width of the transform of this function at NRE = 32 is much greater than if NRE = 270, Figure 19a, or 288, Figure 18b. The number of readings that is an integral multiple of the wavelength will not reduce the amplitude. Reducing the number of readings increases the frequency increment Δf, therefore increasing the width of the transform sinusoidal function and reducing the maximum wavelength that can be discerned from the transform.

72. Optimum frequencies and amplitudes. Fourier transforms of wave patterns can indicate frequencies and amplitudes that are not exactly those of the original wave form. Correction of these errors in the transformed discrete waves may improve results of analysis such as those used to determine Equations 6 and 11 in PART II.

73. Figure 20 illustrates how the frequency and amplitude of the Fourier transform of the sine wave of Figure 18a calculated by program FTRC varies with phase angle θ. The frequency is a linear function of θ and the amplitude is nearly a linear function of the absolute value of sin θ. The frequency of the maximum or peak amplitude of the transform A_{tp} is referred to as the resonant frequency f_r and it occurs at a phase angle of 90 degrees. The resonant frequency may be estimated using equations of linear regression analysis, which for sine waves based on the linear relationships of Figure 20 are

$$f_{rsin} = f_{rosin} + 90 \cdot m_{fsin} \tag{29a}$$

$$f_{rosin} = \frac{\Sigma f_i}{N} - m_{fsin} \cdot \frac{\Sigma \theta_i}{N} \tag{29b}$$

$$m_{fsin} = \frac{\Sigma \theta_i f_i - \frac{\Sigma \theta_i \Sigma f_i}{N}}{\Sigma \theta_i^2 - \frac{(\Sigma \theta_i)^2}{N}} \tag{29c}$$

$$r^2_{fsin} = m_{fsin} \cdot \frac{\Sigma \theta_i f_i - \frac{\Sigma \theta_i \Sigma f_i}{N}}{\Sigma f_i^2 - \frac{(\Sigma f_i)^2}{N}} \tag{29d}$$

where

f_{rsin} = resonant frequency or frequency at the peak amplitude of a sine wave, cycle/ft

f_i = frequency of amplitude of transform wave at phase angle θ_i, cycle/ft

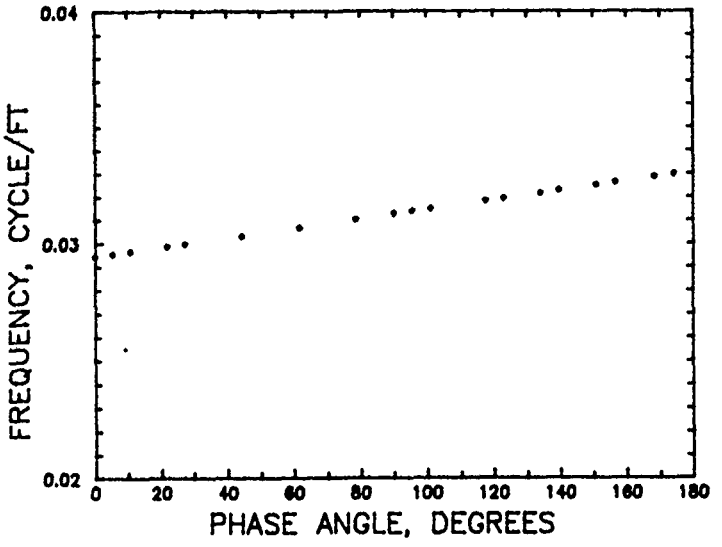

a. FREQUENCY f

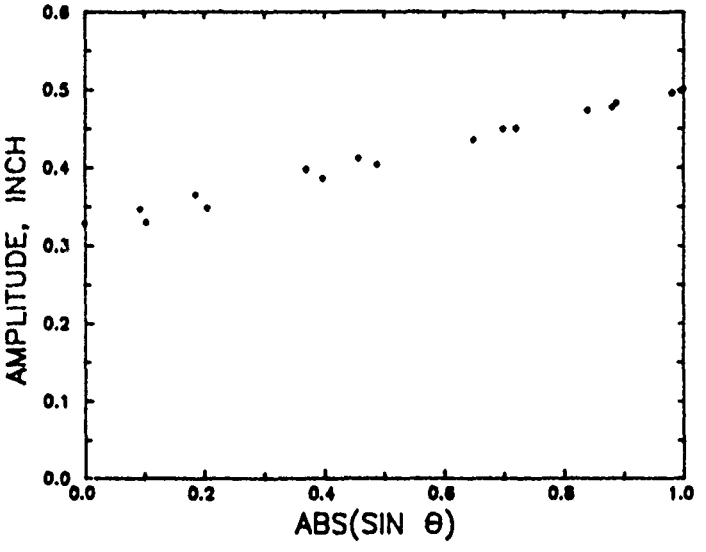

b. AMPLITUDE A_t

Figure 20. Variation of frequency and amplitude of the sine wave Fourier transform with phase angle θ

θ_i - phase angle, degrees; 180 added to negative phase angles

N - number of terms summed; number of points on regression curve, Figure 20

r^2_{fsin} - frequency coefficient of determination of sine wave

Peak amplitudes of the sine wave occur when ABS(SIN θ) = 1.0 or θ = 90 degrees, Figure 20. The resonant frequency of the sine wave f_{rsin} of Figure

20 is 0.03125 at $\theta = 90$ degrees. Some amplitudes may not be large enough to detect from the Fourier transform because the amplitude can decrease substantially if $NRE \cdot \Delta x$ is not a multiple integer of the wavelength. Values of r^2_{fsin} close to 1.00 indicate a better fit of data than values close to zero.

74. The amplitude of the waveform varies linearly with the absolute value of the sine of the phase angle, Figure 20b. The peak amplitude at a phase angle of 90 degrees for the sine wave Fourier transform may be estimated from linear regression analysis by

$$A_{tpsin} = A_{tposin} + m_{asin} \tag{30a}$$

$$A_{tposin} = \frac{\Sigma A_i}{N} - m_{asin} \cdot \frac{\Sigma |\sin\theta_i|}{N} \tag{30b}$$

$$m_{asin} = \frac{\Sigma |\sin\theta_i| A_i - \frac{\Sigma |\sin\theta_i| \Sigma A_i}{N}}{\Sigma |\sin\theta_i|^2 - \frac{(\Sigma |\sin\theta_i|)^2}{N}} \tag{30c}$$

$$r^2_{asin} = m_{asin} \cdot \frac{\Sigma |\sin\theta_i| A_i - \frac{\Sigma |\sin\theta_i| \Sigma A_i}{N}}{\Sigma A_i^2 - \frac{(\Sigma A_i)^2}{N}} \tag{30d}$$

where

$|\sin \theta_i|$ = the absolute value of the sine of the phase angle

r^2_{asin} = amplitude coefficient of determination of sine wave

The peak amplitude A_{tpsin} of the transform wave is 1/2 of the actual amplitude A of the waveform.

75. A cosine wave based on elevation measurements initiated from the perimeter of a structure may indicate edge heave or deformation similar to that of a plate on elastic foundation. The behavior of a cosine wave is similar to that of a sine wave except that the peak amplitude of the transform occurs at a phase angle of zero degrees and the amplitude increases linearly with the cosine of the phase angle from -90 to +90 degrees. The resonant frequency of a cosine wave may be estimated using equations of linear regression analysis by

$$f_{rcos} = \frac{\Sigma f_i}{N} - m_{fcos} \cdot \Sigma \frac{\theta_i}{N} \tag{31a}$$

$$m_{fcos} = \frac{\Sigma\theta_i f_i - \frac{\Sigma\theta_i \Sigma f_i}{N}}{\Sigma\theta_i^2 - \frac{(\Sigma\theta_i)^2}{N}} \tag{31b}$$

$$r^2_{fcos} = m_{fcos} \cdot \frac{\Sigma\theta_i f_i - \frac{\Sigma\theta_i \Sigma f_i}{N}}{\Sigma f_i^2 - \frac{(\Sigma f_i)^2}{N}} \tag{31c}$$

where

f_{rcos} = resonant frequency of cosine wave, cycle/ft

r^2_{fcos} = frequency coefficient of determination of cosine wave

76. The peak amplitude of the transform cosine wave may be estimated by

$$A_{tpcos} = A_{tpocos} + m_{acos} \tag{32a}$$

$$A_{tpocos} = \frac{\Sigma A_i}{N} - m_{acos} \cdot \frac{\Sigma\cos\theta_i}{N} \tag{32b}$$

$$m_{acos} = \frac{\Sigma\cos\theta_i A_i - \frac{\Sigma\cos\theta_i \Sigma A_i}{N}}{\Sigma\cos\theta_i^2 - \frac{(\Sigma\cos\theta_i)^2}{N}} \tag{32c}$$

$$r^2_{acos} = m_{acos} \cdot \frac{\Sigma\cos\theta_i A_i - \frac{\Sigma\cos\theta_i \Sigma A_i}{N}}{\Sigma A_i^2 - \frac{(\Sigma A_i)^2}{N}} \tag{32d}$$

where

A_{tpcos} = the peak amplitude of the cosine wave, cycle/ft.

r^2_{acos} = amplitude coefficient of determination of cosine wave

77. Computer program FTROPT, Table B2, was developed to calculate the peak amplitudes and resonant frequencies of discrete sine and cosine waveforms of complex soil movement patterns calculated from multiple Fourier transform computations of elevation profiles. The initial number of elevation profile readings NRE selected to calculate the Fourier transform is input with the minimum amplitude PEAKA of the wave to be detected from the transformed data. The number NRE is decreased by 2 decrements after each Fourier transform calculation is complete until the number of decrements is NO. Varying the number of readings selected; i.e., NO terms, to calculate the Fourier transforms alters the phase angle θ yielding the type of relationship illustrated in Figure 20. Sometimes altering θ will cause the

amplitude of a particular wave transformed from a measured elevation profile to become undetectable so that $N \leq NO$. The number of transforms to be computed NO is also input in addition to the other data required for computer program FTRC. Program FTROPT will determine and differentiate between cosine and sine wave patterns. The DIMENSION statement is set to detect up to 10 peaks in a transform and up to NO = 30 transform computations. This program was checked with the sine wave of Figures 7 and 8 with NRE = 300 and PEAKA = 0.02 inch. PEAKA = 0.02 is taken as the minimum amplitude of a significant wave. The results of calculations using the sine wave of Equation 28 and different numbers of calculated Fourier transforms NO from 3 to 14 are:

NO	f_{rsin}	r^2_{fsin}	A_{tpsin}	r^2_{asin}
3	0.03124	0.99901	0.49725	0.99978
5	0.03123	0.99994	0.49664	0.99989
7	0.03124	0.99975	0.49819	0.99913
9	0.03126	0.99957	0.49932	0.99809
10	0.03126	0.99963	0.49931	0.99810
14	0.03128	0.99911	0.50128	0.98998

For this case the number of terms summed in the regression analysis N = NO. The coefficients of determinations are approximately 0.999 and essentially independent of the number of terms N; therefore, $3 \leq N \leq 10$ terms are recommended for analysis of the peak amplitudes and resonant frequencies of the waveforms.

78. Angular Distortion. The amplitude and frequency relation for constant angular distortion β associated with various degrees of damage (cracking in masonry walls) may be generated from Equation 12 and the data in Table 4 as illustrated in Figure 21. The amplitude required to cause damage for each β of Table 4 increases with decreasing frequency (or increasing wavelength) as shown because smaller frequencies require larger amplitudes to develop the same angular distortion. The damages characterized in Table 4 are expected to occur in masonry structures if the measured amplitude frequency spectrum indicates any amplitude shown in Figure 21 exceeding the degree of damage ratings for frequencies from 0 to 0.25 cycle/ft. If multiple amplitudes measured in a structure exceed certain damage ratings, then the

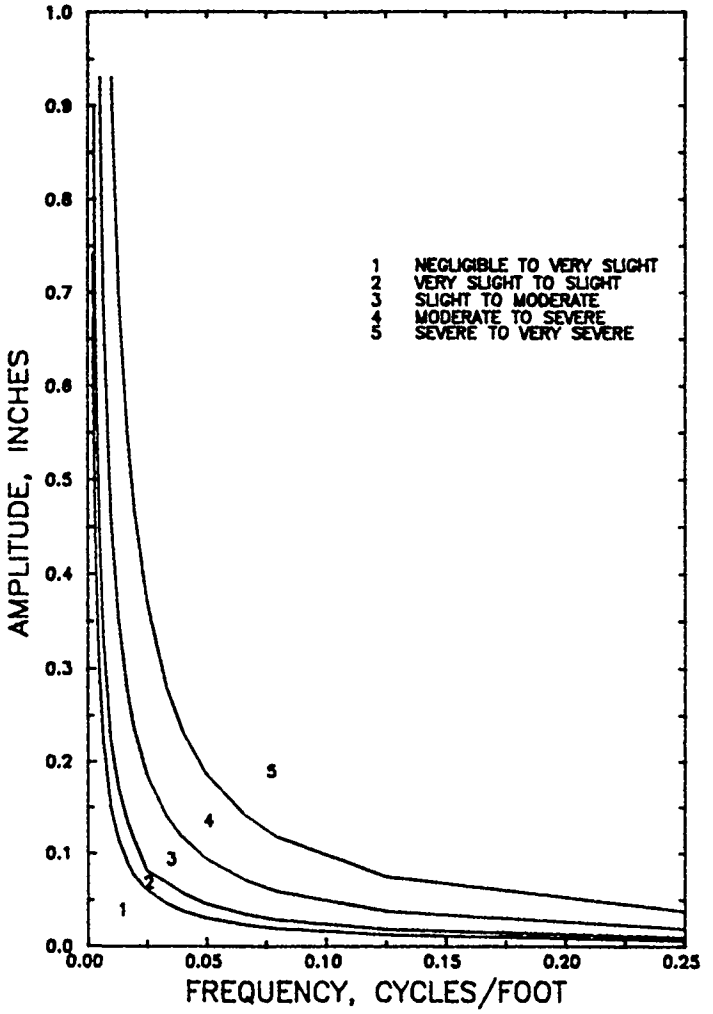

Figure 21. Damage amplitude frequency spectrum from past exprience for masonry structures based on Table 4 and Equation 12

observed damage may be greater. Figure 21 indicates, for example, that a masonry facility with any amplitude of the measured amplitude frequency spectrum in zone 3 should show evidence of slight to moderate damage. Comparison of the sine wave transform of Figure 18b with Figure 21 indicates possible severe to very severe damage of a masonry structure founded on this waveform.

79. Figure 21 may be replotted as a beta frequency spectrum in terms of the angular distortion versus frequency, Figure 22

$$BETA = 100 \cdot \beta \tag{33a}$$

$$\beta = 8 \cdot A_t \cdot \frac{f}{12} \tag{33b}$$

where

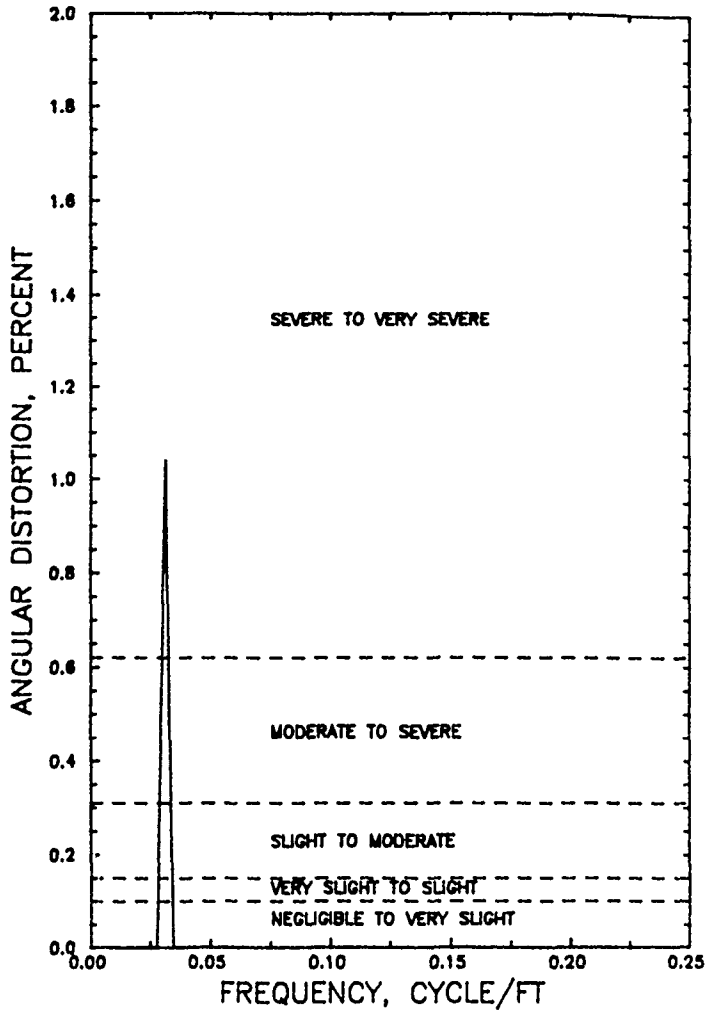

Figure 22. Damage beta frequency spectrum from past experience for masonry structures ($\sin(2\pi x/32)$ is superimposed on this figure)

BETA = angular distortion, percent

β = angular distortion of soil-foundation from Equation 12

A_t = transform amplitude from Equation 26, inches

f = frequency, cycle/ft

A_t is 1/2 of amplitude A of Equation 12 where $f = 1/\ell$. The number 12 in Equation 33b converts feet to inches. Any peak of BETA that exceeds the levels of angular distortion in Table 4 may indicate the corresponding level of damage in the structure. The angular distortion BETA of the sine wave transform of Figure 18b calculated using Equations 33 is shown on Figure 22. BETA exceeds 1 percent, which indicates severe to very severe damage from Table 4. Figures 21 and 22 may require some adjustment for structures built with flexibility such as steel framing with frequent construction joints in

exterior walls. The distortion and reduction in amplitude of the transformed waves, when the number of readings used in the Fourier transform NRE times the spacing between points Δx is not a multiple of the wavelength, may also influence the measured frequency spectrum of structures.

80. Pavement Roughness. Gay and Lytton (1988) calculated a measure of the roughness R_t of pavements as the area underneath the curve of the amplitude versus frequency plots of the amplitude frequency spectrum

$$R_t = \frac{2}{f_m} \cdot \int_{f_o}^{f_m} A_t(f) \cdot df = \frac{2}{f_m} \cdot \sum_{i=1}^{M} \frac{A_t(i) + A_t(i-1)}{2} \cdot \Delta f \qquad (34)$$

where

R_t = transform roughness, in.

$A_t(i)$ = amplitude of the transform wave as a function of frequency f, inches

f_m = maximum frequency, 0.25 cycle/ft

f_o = minimum frequency, cycle/ft

Δf = $1/(NRE \cdot \Delta x)$, cycle/ft

M = number of points in the amplitude-frequency system, $f_m/\Delta f$.

NRE = number of readings used in Fourier transform calculation

If $i=1$, then $A_t(0)$ is the amplitude at a minimum frequency f_o. A minimum frequency (maximum wavelength) is required because increasing wavelengths contribute decreasing damage for a given amplitude such that the effectiveness of larger wavelengths is less. The maximum frequency f_m is 0.25 cycle/ft; therefore, $M = 0.25 \cdot NRE \cdot \Delta x$. The transform roughness R_t is converted to units of "in." by the factor "$2/f_m$" or 8 ft/cycle. The factor "2" in "$2/f_m$" upgrades the roughness to the actual roughness for sine and cosine waves because the amplitude of the transform is 1/2 of the actual amplitude of the wave.

81. Figure 23 illustrates the transform roughness R_t of the amplitude frequency spectrum of the sine wave function $\sin(2\pi x/32)$ as a function of length $L = NRE \cdot \Delta x$. The minimum frequency f_o is determined by the sine wave frequency. The transform roughness shown in Figure 23 was calculated from Equation 34 for a given number of readings using a spacing $\Delta x = 1.0$ ft. The roughness indicates low readings at increments of 32 ft consistent with the wavelength of the sine function or frequency 0.03125 cycle/ft. The roughness is larger for fewer readings or smaller lengths L consistent with the

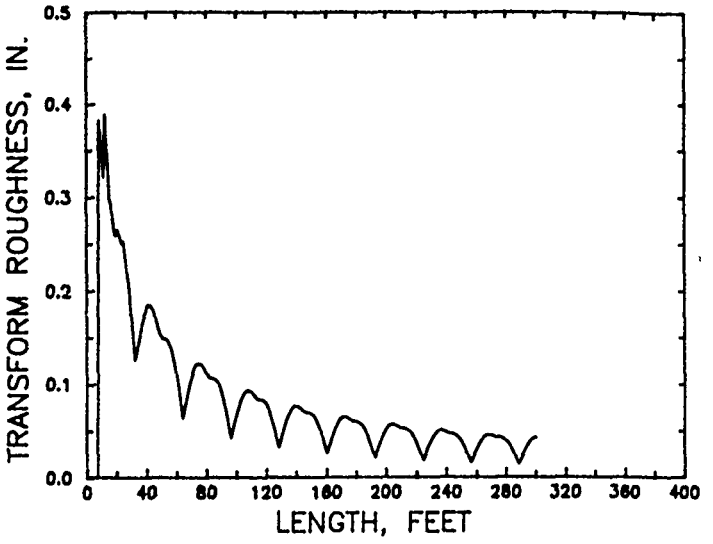

Figure 23. Roughness spectrum of wave $\sin 2\pi x/32$

widening of the transform of this function illustrated in Figures 18 and 19. The roughness levels off to a relatively small value less than 0.05 in. for large numbers of readings. The bump height (Gay and Lytton 1988) given by the sum of the amplitudes of all frequencies will cause a waveform similar to Figure 23 for different lengths L or readings NRE. The bump height for a particular set of readings is the area beneath the amplitude-frequency curve, Figure 17. This transform roughness and bump height are not used further in this study because they vary with the number of readings NRE and length L. The transform roughness and bump height also do not differentiate between the effectiveness of different wavelengths in contributing to damage because different wavelengths calculate the same roughness provided amplitude and number of readings are the same.

F-Numbers

82. Face (1984) developed a quantitative system to describe the flatness and levelness of industrial floors. Elevation differences DEL are measured at equal intervals of length Δx such as 1.0 ft over the length of the floor, Figure 24. The curvatures ΔDEL, the difference between adjacent DEL measurements, are also determined. These measurements from numerous floors were used to develop a series of F-number equations which describe the flatness FF and the levelness FL of floors. A perfectly flat (plane) floor occurs when the difference between adjacent DEL is zero, while a perfectly level (zero slope) floor occurs when the difference between adjacent

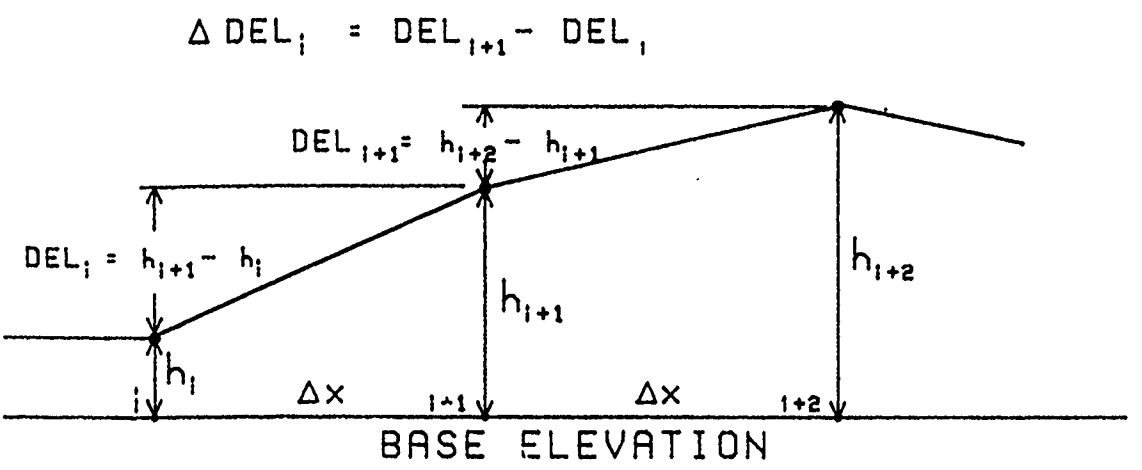

Figure 24. Assumed linear elevation profile between points Δx

ΔDEL is zero. A level floor is horizontal, while a flat floor is planar and may be at any angle to the horizontal. F-numbers may be calculated by (Edward W. Face Company 1983)

$$FF = \frac{6.585}{DCMAX} \cdot |\cos(0.105 \cdot \Delta x) - 1| \qquad \Delta x \leq 15 \text{ in.} \tag{35a}$$

$$FL = \frac{4.175}{DDMAX} \cdot \sinh^{-1}(0.083 \cdot \Delta x) \qquad \text{any } \Delta x \tag{35b}$$

where

FF = F-number for floor flatness

FL = F-number for floor levelness

DCMAX = the maximum curvature ΔDEL over the length interval Δx, STDC·3 + ABS(MEANΔ), in.

DDMAX = the maximum elevation difference DEL over the length interval Δx, STDD·3 + ABS(MEANDEL), in.

STDC = mean standard deviation of curvatures for NRE readings, in.

STDD = mean standard deviation of the elevation differences for NRE readings, in.

MEANΔ = mean curvature, in.

MEANDEL = mean elevation difference, in.

Specifications may allow a certain maximum curvature and elevation difference required to obtain a sufficiently flat and level floor. DCMAX and DDMAX as defined above provide confidence that 99 percent of the floor will conform to F-numbers greater than those given by Equations 35 provided the measured maximum curvature ΔDEL and elevation difference DEL are within the allowed specifications. The units of Δx in Equations 35 are in inches. Refer to

ASTM D 1155-87 for a standard test method to determine floor flatness and levelness from F-numbers.

83. F-numbers FF and FL should be identical for a particular floor if there is no bias toward flatness or levelness. F-numbers typically range from 25 to 35 for average floors and at least 50 for superflat floors. Superflat floors require placement widths less than 20 ft and straightedge-machine float-restraightedge-machine finish.

84. Substandard floors typically have some bias which may be estimated by (Face 1984)

$$P_b = 200 \cdot \frac{FL - FF}{FL + FF} \tag{35c}$$

A negative bias indicates that the floor is more planar than it is level and that the floor may not have been struck off as it was finished.

85. Computer program FNUMR, Table B3, was developed to calculate F-numbers of floors from elevation or elevation change data. Figure 25 illustrates the F-number calculation of the sine wave distortion of Figure 18a as a function of length. This "wavy" floor is considerably more flat than it is level. The floor levelness is essentially independent of length, while the flatness increases with length, especially at small lengths. Introducing a

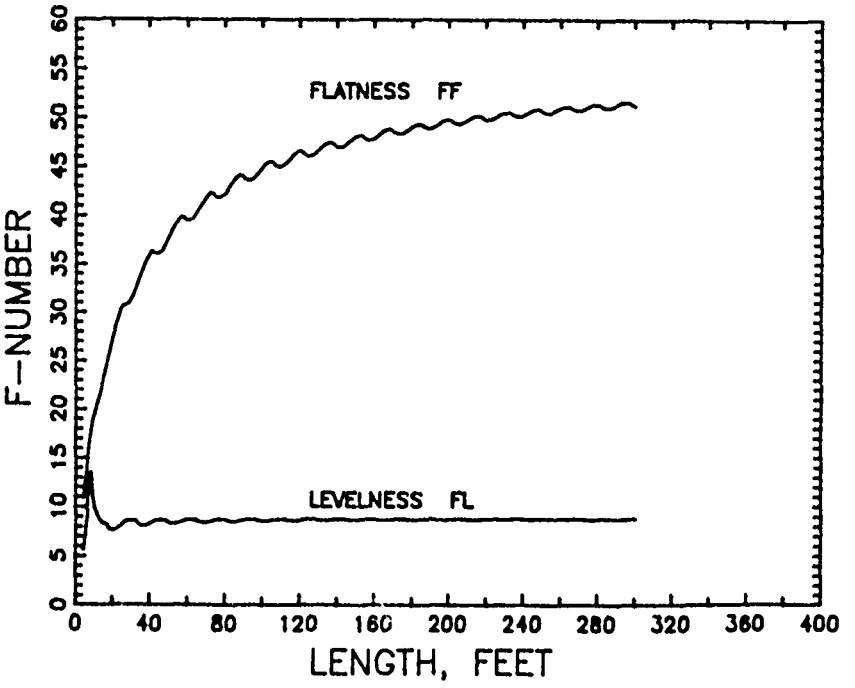

Figure 25. F-number distribution of a sine wave

constant slope such as 0.01 in./ft into the sine wave did not influence the plot in Figure 25. F-numbers therefore appear not to be sensitive to slope. Equation 35a and 35b appear to be reversed for the sine wave to be consistent with the definition of levelness and flatness. The sine wave is horizontal and should be level, but not flat.

Wave Index

86. This system was developed to determine the level of effort and cost necessary to enforce construction specifications (Kalman Laboratories Note 1, 1989). The wave index of an elevation profile is

$$WI = \left[\frac{\sum_{i=1}^{NS} A_{rms}^2}{NS} \right]^{0.5} \tag{36a}$$

where A_{rms} is the root mean square amplitude of the waves in inches for a spacing Δx and NS is the number of different spacings. The spacing of points is varied from a minimum to a maximum distance.

87. The root mean square amplitude may be determined from

$$A_{rms} = \left[\frac{\sum_{i=1}^{NRE} a_i^2}{2 \cdot NRE} \right]^{0.5} \tag{36b}$$

where

a_i = 1/2 peak-to-peak amplitude, inches

NRE = number of survey points or readings

a_i, Figure 24, is the amplitude of a wave that spans $2 \cdot \Delta x$, which is the vertical offset distance at point "i+1" relative to a straight line between h_i and h_{i+2}. This amplitude is (Kalman Laboratories Note 3, 1989)

$$a_i = h_{i+1} - \frac{h_i + h_{i+2}}{2} \tag{36c}$$

where

h_i = elevation of left end point i of the elevation profile, inches

h_{i+1} = elevation of center point of wave section at distance Δx from left end point, inches

h_{i+2} = elevation of right point of wave section at distance $2 \cdot \Delta x$ from left end point, inches

The maximum spacing between measurement points Δx is limited to $\leq$ NRE/2. $2 \cdot$NRE in Equation 36b causes A_{rms} to be independent of the number of

readings. The root-mean-square amplitude A_{rms} can be plotted versus the spacing between measurement points Δx to form a wave spectrum.

88. Program WAVEI, Table B5, calculates the wave spectrum and wave index from elevation profile readings using a minimum to maximum spacing from 1 to 50 ft where spacings increase in increments of 1 ft such that NS = 50. Refer to standard CSA-A23.1-M90 (CSA 1990) for further details. The wave spectrum of the sine wave function $\sin(2\pi x/\ell)$ when amplitude A = 1.0 inch and ℓ = 32 ft, Figure 26a, is a reproduction of the sine wave of Figure 18a,

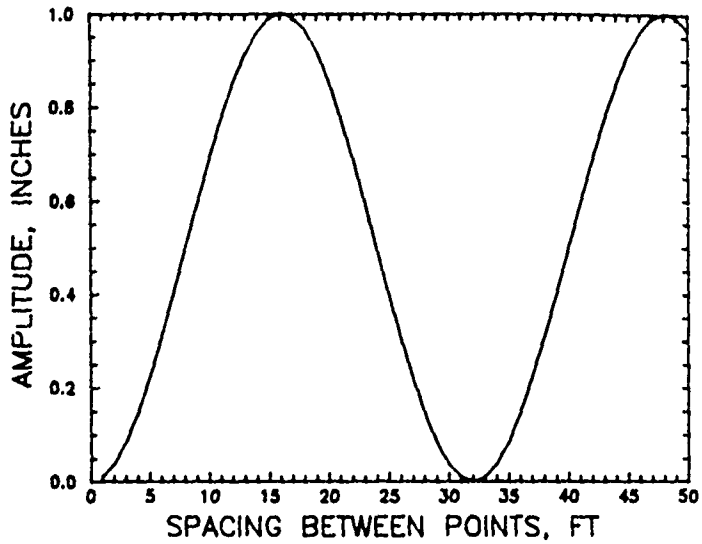

a. WAVE SPECTRUM

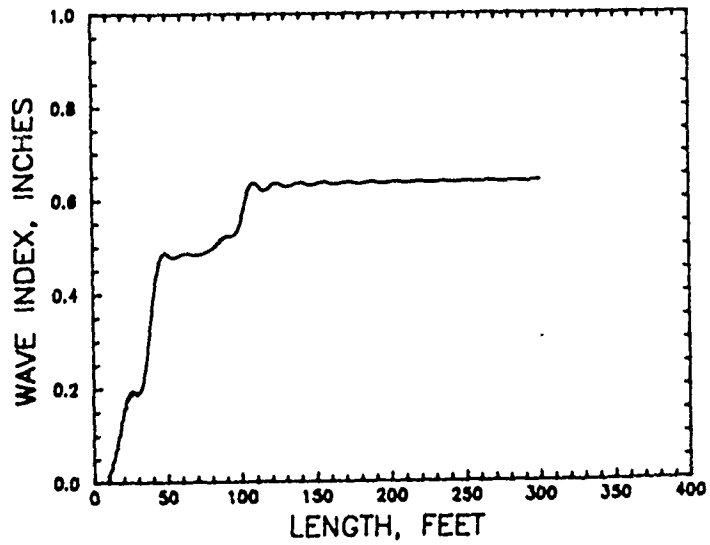

b. WAVE INDEX WI

Figure 26. Wave Index system of roughness for $\sin(2\pi x/32)$

except that the peak-to-peak amplitude is amplitude A. Slope is not considered because Equation 36c eliminates slope. The wave index of the sine wave, Figure 26b, is independent of the spacing between points for $L = NRE \cdot \Delta x$ greater than about 3 times the wavelength ℓ and is about 0.63 inch for the sine wave of Figure 18a. This wave index is an amplitude function.

Macrorelief Index

89. A dimensionless macrorelief index MRI is analogous to a parameter (Römken and Wang 1986), which is the product of an area bounded by an elevation profile within a length L and number of peaks in the profile

$$MRI = \frac{MI}{L} \cdot \frac{NL}{L} \tag{37}$$

where

MI = area within a given L bounded by the elevation profile and a regression line through the measured elevations, ft^2

NL = number of peak elevations within L

L = profile length, ft

The regression line is the least-squares line through all elevation points within the profile length L. Lehrsch et al (1988) found that such a parameter was the best of eight descriptors of surface roughness of soils because of its sensitivity to simulated rainfall and independence of the parameter with length L.

90. Program ADATG (Angular Distortion and Tilt), Table B4, calculates the MRI parameter. Figure 27 illustrates the MRI with length L for $\sin(2\pi x/32)$. This MRI is essentially independent of length L. The spikes in Figure 27 are caused by a sudden reduction in the number of elevation peaks calculated by program ADATG. The regression line parameters and the MRI for NRE = 300 with and without a slope of 0.01 in./ft are:

Regression Line Parameters

Slope, in./ft	Intercept, in.	Slope, in./ft	r^2	MRI, Percent
0.00	0.04516	-0.00012	0.00020	0.17737
0.01	0.04516	0.00988	0.59076	0.17737

The above table shows that introducing a slope of 0.01 in./ft into the sine wave does not influence the MRI of 0.17737 percent, but the regression line indicates the proper slope.

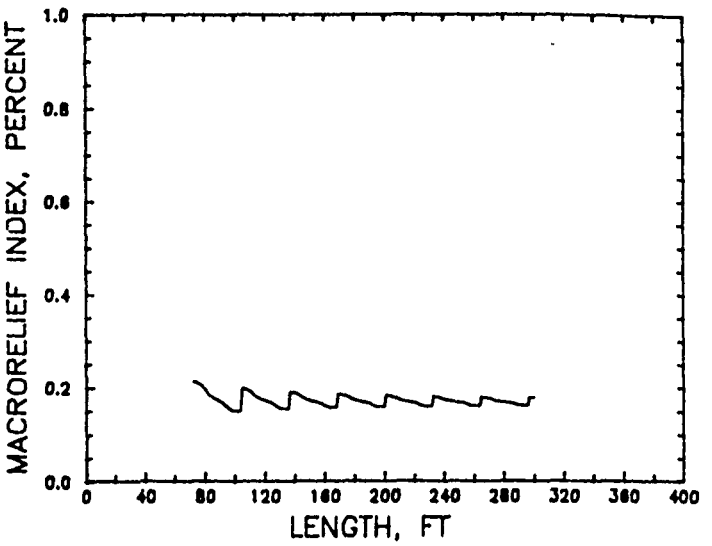

Figure 27. Macrorelief index of wave $\sin(2\pi x/32)$

Angular Distortion

91. Program ADATG calculates the mean and standard deviation of the angular distortion, maximum angular distortion, mean ratio and standard deviation of the mean ratio of the angular distortion and span length, maximum ratio of the angular distortion and span length, and the mean and standard deviation of the tilt of elevation profiles for span lengths less than 120 ft and greater or equal to 4 ft. The angular distortion of wave $\sin(2\pi x/32)$ is 1.043 percent and the tilt is 0.0. Introducing a slope of 0.01 in./ft does not alter the angular distortion, but tilt is 0.083 percent. Tilts may have some value in detecting slope.

92. Beta Roughness. Program ADATG also calculates a measure of the overall roughness of the angular distortion

$$R\beta = \frac{1}{L} \cdot \sum_{i=1}^{n} \beta_i \tag{38}$$

where

$R\beta$ = beta angular distortion roughness; normalized roughness of the angular distortion, percent/ft

L = length of the elevation profile, ft

β_i = angular distortion between peaks i and $i+1$ of the elevation profile, percent

n = number of angular distortions calculated within the elevation profile

Two beta angular distortion roughness parameters are determined: $R\beta_1$, roughness summing all β_i of adjacent elevation peaks over length L divided by L and $R\beta_T$, roughness summing $R\beta_1$ plus sum of all β_i of nonadjacent elevation peaks over length L divided by L. Figure 28a illustrates the roughness distribution spectrum $R\beta_1$ of wave $\sin(2\pi x/32)$, which is also $R\beta_T$

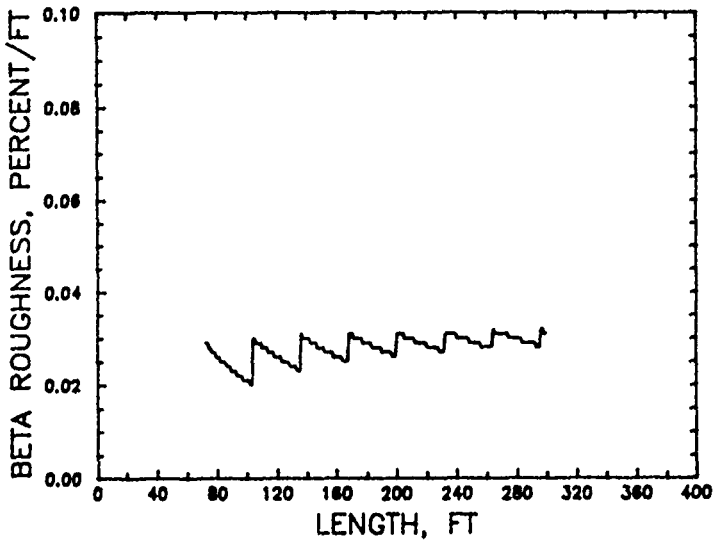

a. BETA $R\beta_1$

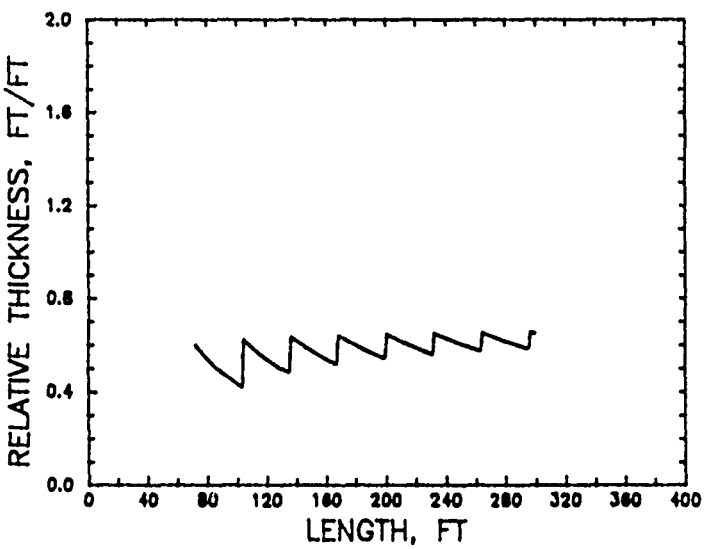

b. RELATIVE THICKNESS RD_{rel1}

Figure 28. Roughness related with angular distortion of wave $\sin(2\pi x/32)$

because all amplitudes are equal. This roughness is reasonably independent of length similar to the macrorelief index.

93. Relative Thickness. The relative thickness is a measure of the foundation thickness required to reduce deformation to limit angular distortion to 0.15 percent. Program ADATG calculates

$$RD_{rel} = \frac{1}{L} \cdot \sum_{i=1}^{n} D_{reli} \tag{39}$$

where

RD_{rel} = normalized roughness of the relative thickness, ft/ft

L = length of the elevation profile, ft

D_{reli} = relative thickness for a given span length and length between peaks i and $i+1$ of the elevation profile, ft

n = number of relative thickness calculated within the elevation profile

Paragraph 55, PART II, illustrates hand calculation of D_{rel} for a span in survey line ATC1. Program ADATG calculates two normalized relative thickness roughness parameters from span lengths between 4 and 120 ft: RD_{rel1}, roughness summing all D_{reli} of adjacent elevation peaks over length L divided by L, and RD_{relT}, roughness summing RD_{rel1} plus sum of all D_{reli} of nonadjacent peaks over length L divided by L. Figure 28b is the roughness distribution of RD_{rel1} of wave $\sin(2\pi x/32)$. The behavior of RD_{rel1} is similar to $R\beta_1$ for this sine wave.

Comparison of Surface Roughness Systems

94. Regression analyses were performed on a series of simple waves of 300 ft length with amplitudes 0.05, 0.10, 0.20, 0.50, 1.0, and 2.0 inch and wavelengths of 4, 7, 10, 15, 20, 30, and 50 ft to determine log-log, linear-log, or linear relationships between angular distortion β, intensity of angular distortion $I_m = \beta/\ell$ (ratio of angular distortion to wave length), floor levelness FL, floor flatness FF, wave index WI, macrorelief index MRI, beta roughness $R\beta$, relative thickness roughness RD_{rel} and maximum relative thickness D_{relm}. Parameters that show least correlation with each other may indicate independent indices applicable to rating performance of foundations subject to soil movement patterns. Parameters that correlate best with each other may indicate duplication of ratings. The results of this analysis for 36 amplitude and wavelength combinations are shown in Table 6 for regression

Table 6. Comparison of Surface Roughness of Simple Sine Waves

Type of Distortion		Equation	Regression Coefficient, r^2
Mean Angular Distortion β_m	(40a)	FL = $9.1903\ \beta_m^{-0.9934}$	0.9987
	(40b)	MRI = $0.1528\ \beta_m^{0.9825}$	0.9956
	(40c)	RD_{rel} = $0.6309+0.6002\log_{10}\beta_m$	0.9847
	(40d)	FF = $23.9106\ \beta_m^{-1.2177}$	0.8472
	(40e)	I_m = $0.0745\ \beta_m^{1.2601}$	0.8207
	(40f)	$R\beta$ = $0.07018\ \beta_m^{1.2779}$	0.8061
Intensity of Mean Angular Distortion Angular $I_m = (\beta/\ell)_m$	(41a)	$R\beta$ = $-0.00235+0.98940\ I_m$	0.9999
	(41b)	FF = $2.0366\ I_m^{-0.95000}$	0.9976
	(41c)	RD_{rel} = $1.0798+0.4055\log_{10}I_m$	0.8699
	(41d)	FL = $1.7978\ I_m^{-0.64358}$	0.8111
	(41e)	MRI = $0.7484\ I_m^{0.62776}$	0.7863
Relative Thickness RD_{rel}	(42a)	$\log_{10}$FL = $1.9924-1.6287\ RD_{rel}$	0.9820
	(42b)	$\log_{10}$MRI = $-1.8315+1.6073\ RD_{rel}$	0.9746
	(42c)	$\log_{10}$FF = $2.6804-2.0670\ RD_{rel}$	0.8929
	(42d)	$\log_{10}R\beta$ = $-2.5258+2.1794\ RD_{rel}$	0.8577
	(42e)	D_{relm} = $12.0481\ RD_{rel}^{0.8072}$	0.8309
Beta Roughness $R\beta$	(43a)	FF = $2.0483\ R\beta^{-0.9276}$	0.9959
	(43b)	FL = $0.5460\ R\beta^{-0.6234}$	0.7967
	(43c)	MRI = $0.7344\ R\beta^{0.6078}$	0.7718
Floor Levelness FL	(44a)	MRI = $1.3738\ FL^{-0.9899}$	0.9986
	(44b)	FF = $-40.4254 + 6.3816$ FF	0.8599
Floor Flatness FF	(45)	MRI = $1.2471\ MRI^{-0.6726}$	0.8166

coefficients $r^2 > 0.7$. Table 6 shows that FL and MRI correlate best with the mean angular distortion β_m and FF and $R\beta$ correlate best with the mean intensity of the angular distortion I_m with regression coefficients r^2 exceeding 0.99. The angular distortion roughness $R\beta$ is similar to I_m for simple sine waves. WI and D_{relm} indicate little correlation with any of these variables for these simple sine waves. Maximum angular distortion and maximum intensity of angular distortion are the same as mean values because standard deviations are negligible. Parameters that may be useful for rating performance may include FF, FL, MRI, WI and D_{relm}.

Application of Idealized Complex Wave Pattern

95. Simple waves superimposed on each other in foundation soil may cause a composite wave pattern with different and even larger amplitudes than the discrete waves. Soil surface deformation made of superimposed simple waves from a variety of causes could increase damage contributing to reduced performance of structures supported by these soils. This situation was investigated by a parametric analysis of an idealized composite waveform

$$y = A_1 \cdot \sin\left(\frac{2\pi x}{\ell_1}\right) + A_2 \cdot \sin\left(\frac{2\pi x}{\ell_2}\right) + \ldots\ldots + A_n \cdot \sin\left(\frac{2\pi x}{\ell_n}\right) \qquad (46)$$

where

A_n = amplitude of the waveform n, inches

ℓ_n = wavelength of the waveform n, ft

Three complex waves were considered to be composed of four terms, Table 7. The elevation profiles of these waveforms are shown in Figure 29. These elevation profiles were analyzed in terms of Fourier transforms, differential movement, and surface roughness indices to determine their potential application in evaluating the influence of complex waveforms in causing damage to structures. Elevations of the initial points are always zero.

Fourier Transforms

96. The Fourier transforms of each of these waves will indicate peak transform amplitudes A_t approximating those shown in Table 7 at the frequencies 0.125, 0.067, 0.042, and 0.031 cycle/ft. An example beta frequency spectrum of case 1, constant amplitude, Figure 30, illustrates decreasing angular distortion with decreasing frequency as expected because smaller frequencies (larger wavelengths) require more amplitude to cause

Table 7. Illustration of Complex Waveforms

Case	Amplitude	Amplitude, inch				Wavelength, ft			
		A_1	A_2	A_3	A_4	ℓ_1	ℓ_2	ℓ_3	ℓ_4
1	Constant	0.25	0.25	0.25	0.25	8	16	24	32
2	Decreasing	0.40	0.30	0.20	0.10	8	16	24	32
3	Increasing	0.10	0.20	0.30	0.40	8	16	24	32

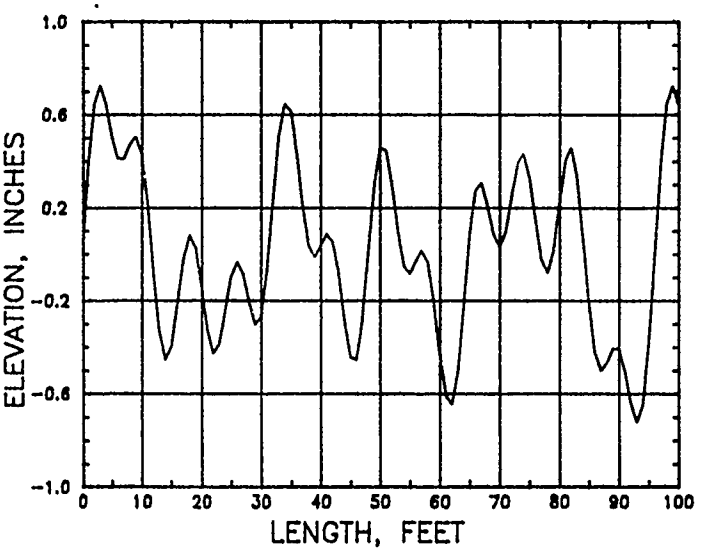

a. CASE 1 - CONSTANT AMPLITUDE

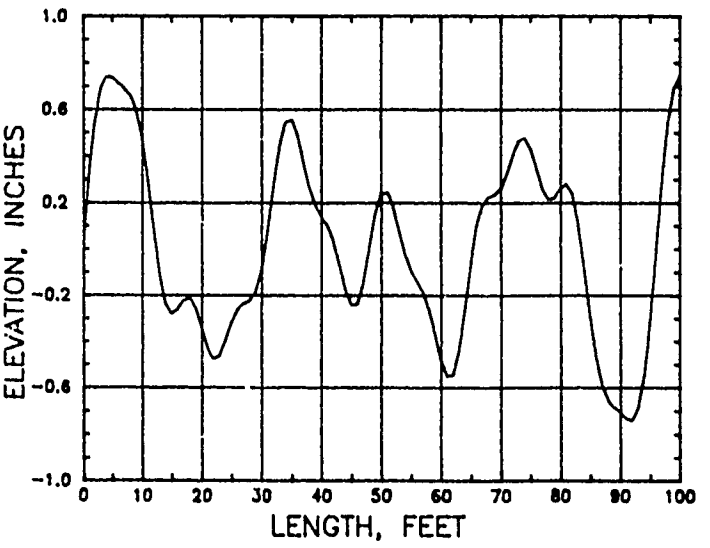

b. CASE 2 - DECREASING AMPLITUDE

Figure 29. Elevation profiles of composite waves

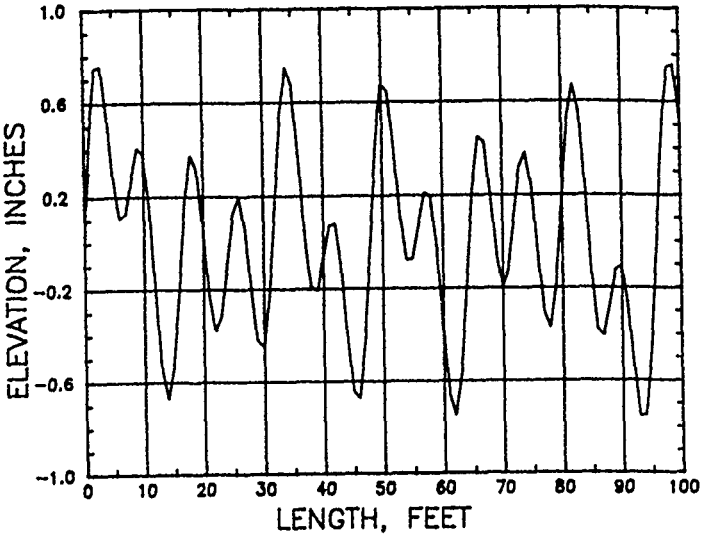

c. CASE 3 - INCREASING AMPLITUDE

Figure 29. (Concluded)

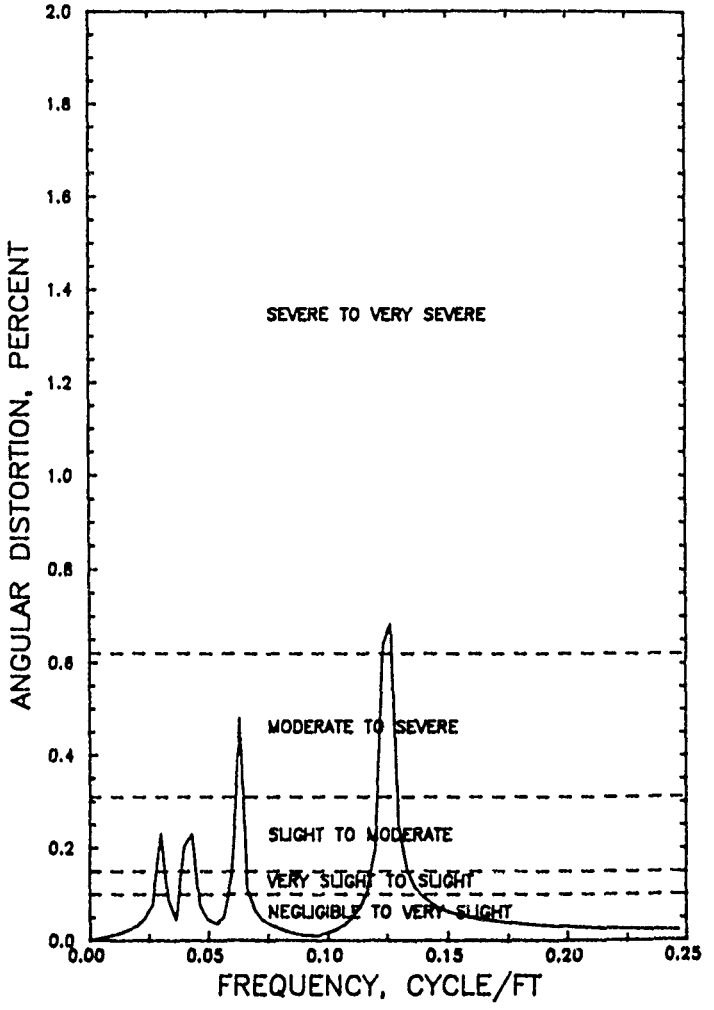

Figure 30. Beta frequency spectrum of Case 1 - Constant Amplitude

damage. The frequency spectrums of discrete waves of a complex wave form calculated by the Fourier transform can show amplitudes A_t and angular distortions β of discrete waves for identification of wave patterns that may be potentially destructive, but these spectra provide limited information on angular distortion and tilt of the composite wave pattern that can lead to potential damage of structures or interference with operations.

Angular Distortion

97. Figure 31 illustrates the angular distortion of the composite waveforms of Figure 29 calculated by program ADATG, Table B4. Each of these cases is for a mat spanning between different sets of elevation peaks where the maximum settlement is in the center of the span. The frequency in Figure 31 is the reciprocal of the span between peaks. Comparison of Figures 30 and 31a for Case 1 illustrate that superimposed waves may give composite waves with amplitudes much greater than those of discrete waves. The amplitudes of case 1 are 0.25 inch, while the amplitudes of the superimposed waves approach 0.35 inch, Figure 29a. Case 2, decreasing amplitudes with increasing span (decreasing frequency), appears to cause more severe angular distortion than cases 1 and 3. The maximum acceptable tilt, $\delta = 1/250$ (0.4 percent), was exceeded for cases 1 and 2, constant and decreasing amplitude. Negative tilts represent decreasing slope with increasing length, while positive tilts represent increasing slope with increasing length.

98. Each of the composite waves in Figure 29 requires a certain minimum stiffness in a mat foundation to accommodate this soil deformation. The required relative thickness versus the reciprocal of the span length (frequency) for limiting $\beta = 0.0015$ is shown in Figure 32 for case 1, constant unrestrained amplitude $A_u = 0.25$ inch. The greatest relative thickness of 13.2 ft is required for a frequency of 0.032 cycle/ft (span length 31 ft) with a peak-to-peak amplitude of 0.70 inch to reduce or accommodate the unrestrained wave motion. Cases 2 and 3 will provide similar plots.

Comparison of Surface Roughness Systems

99. Analyses of the surface roughness systems described earlier and applied to cases 1, 2 and 3 indicate that all of the systems are independent of length, except for the Fourier transform roughness. These systems generally indicate that case 2 is more severe than cases 1 and 3 consistent with observations of angular distortion in Figure 31. F-numbers for case 1,

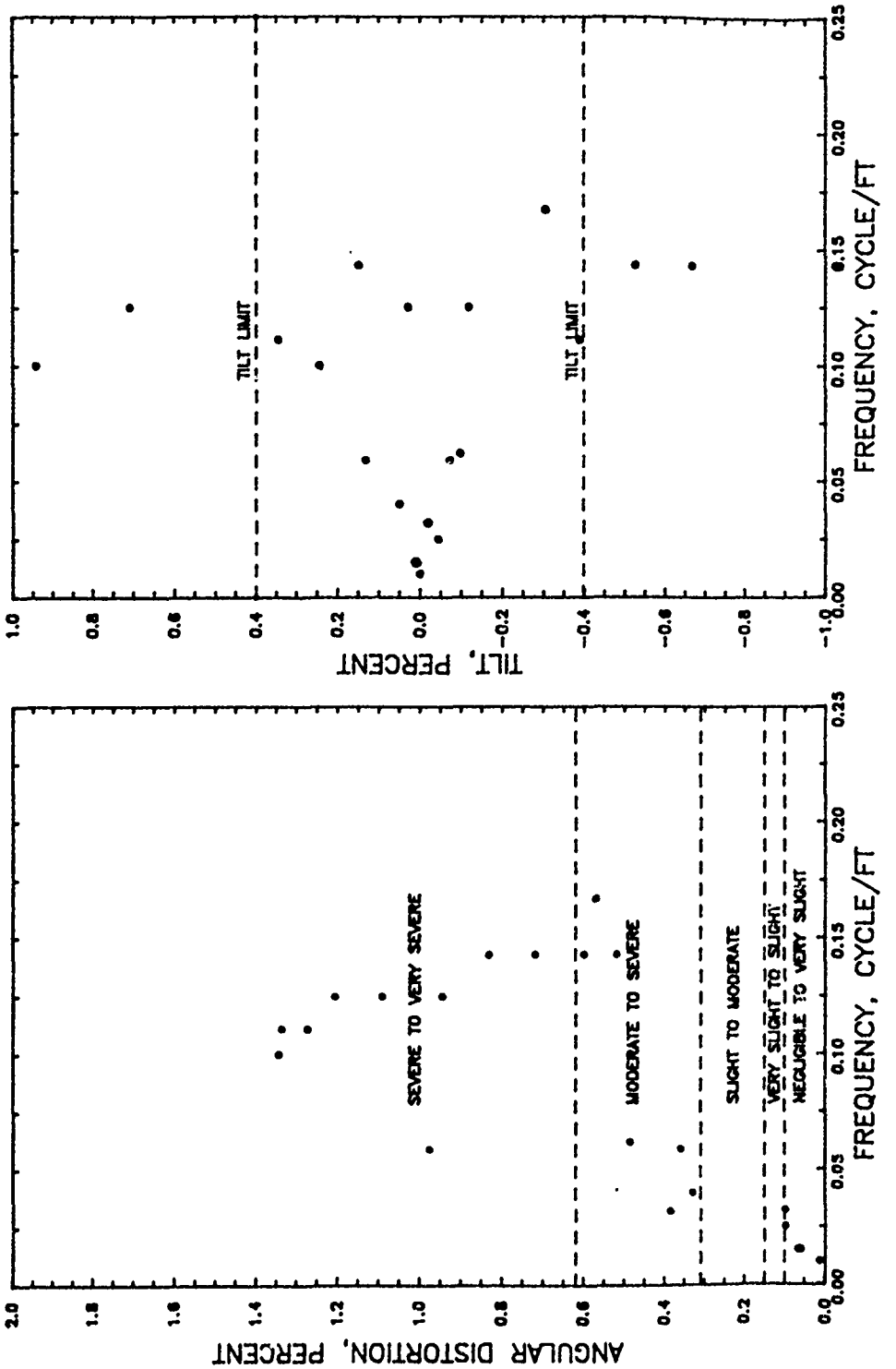

a. CASE 1- CONSTANT AMPLITUDE

Figure 31. Angular distortion and tilt relationships of the three cases

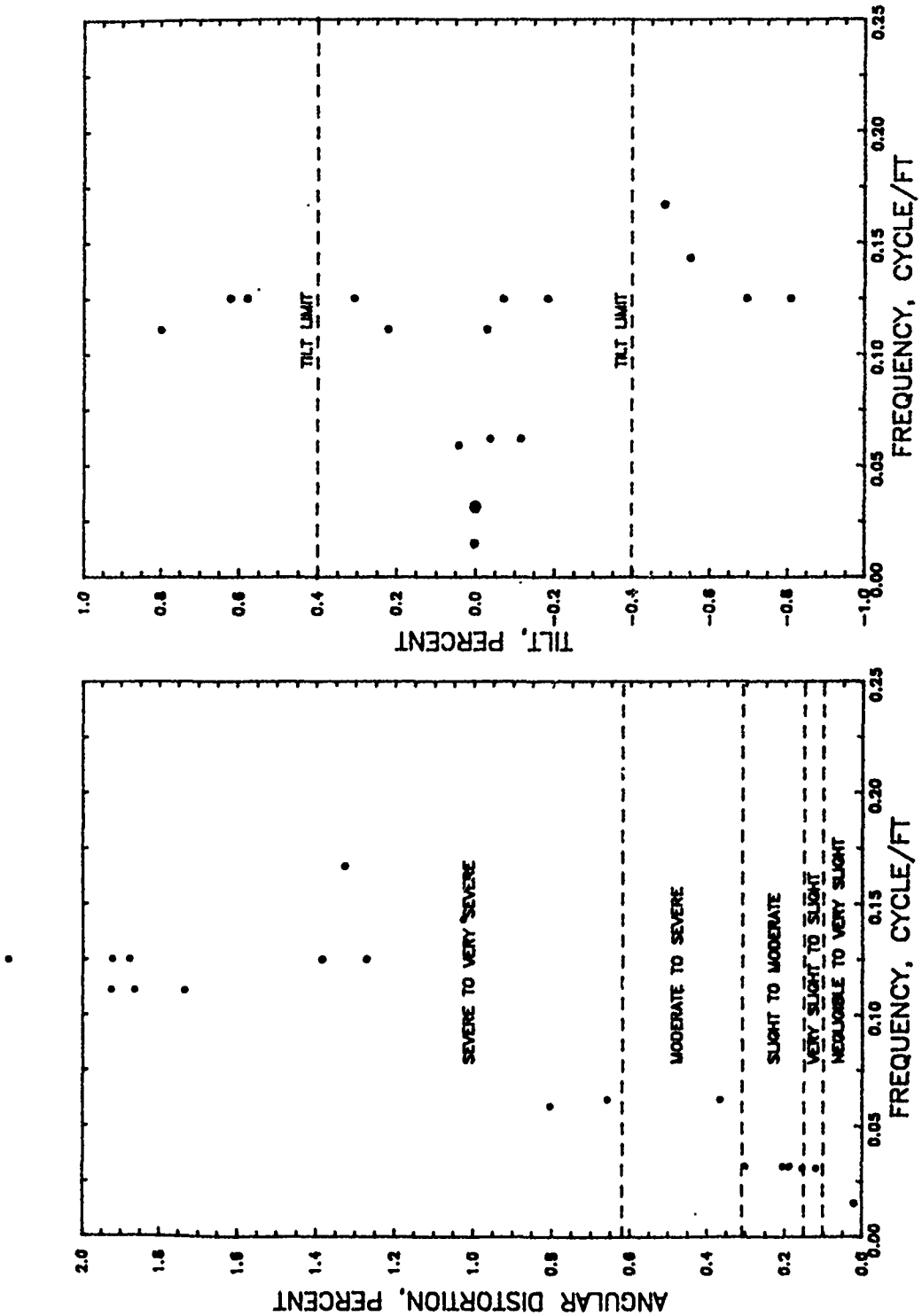

b. CASE 2 - DECREASING AMPLITUDE

Figure 31. (Continued)

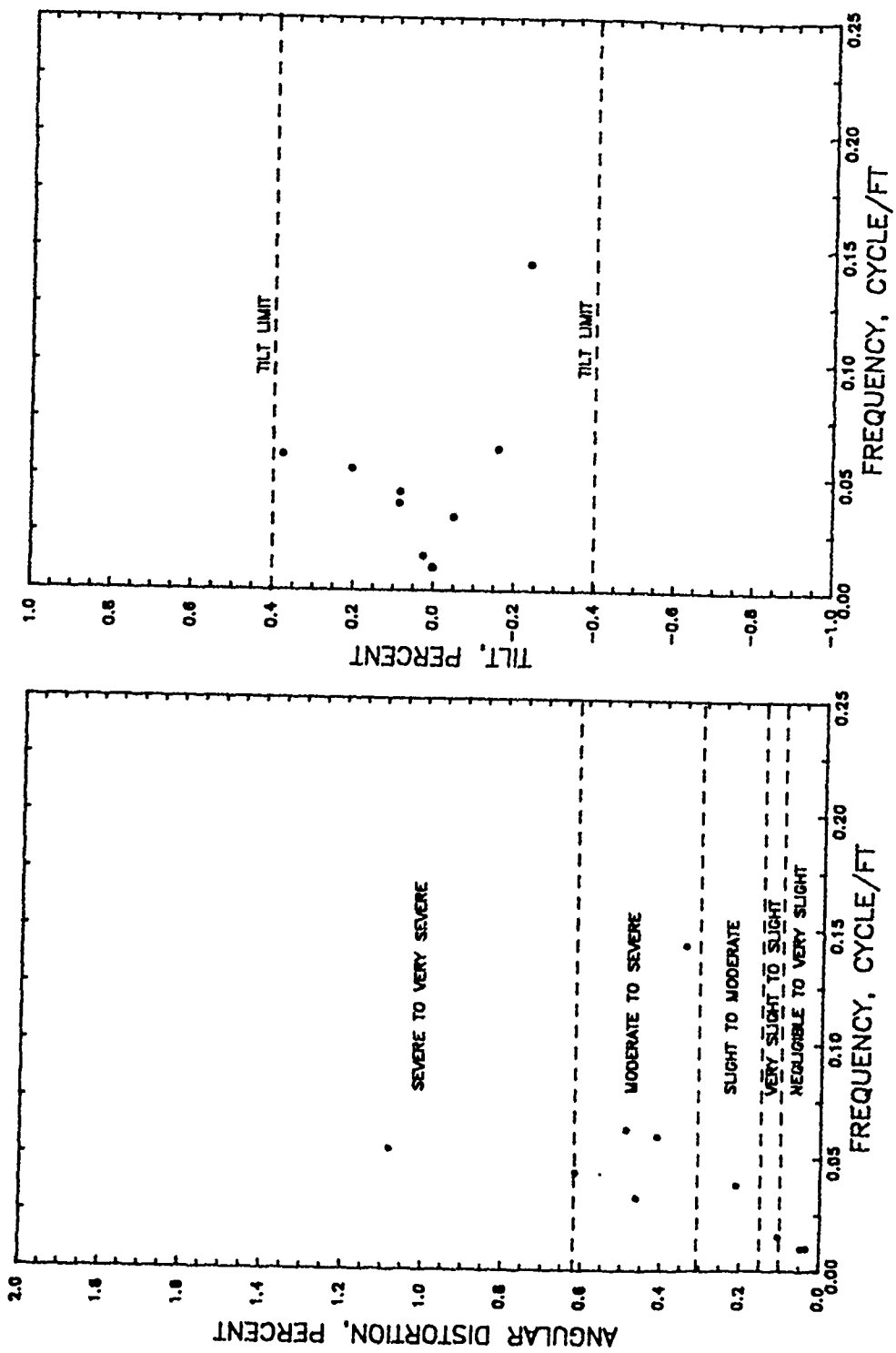

c. CASE 3 - INCREASING AMPLITUDE

Figure 31. (Concluded)

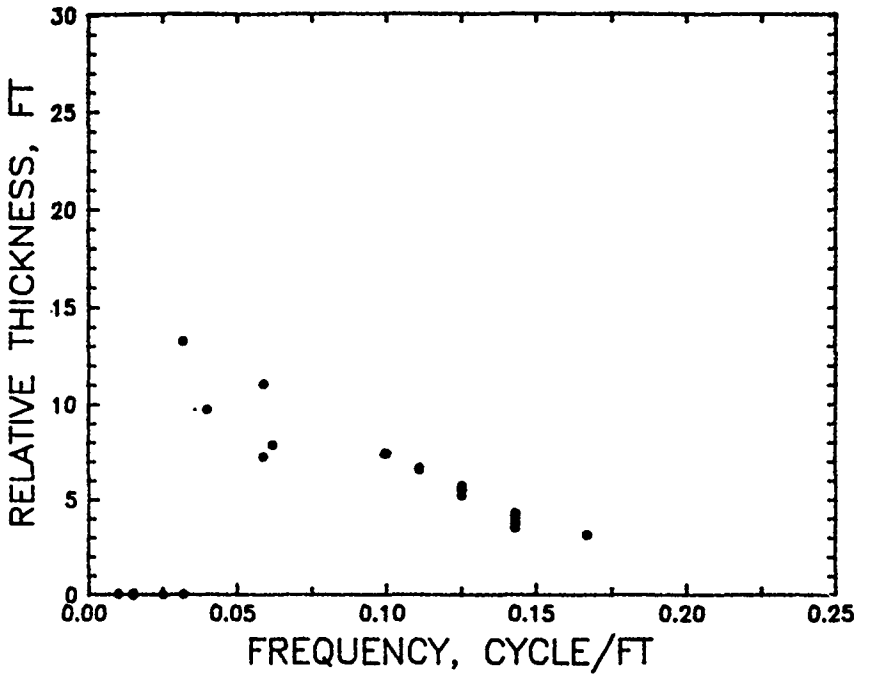

Figure 32. Relative thickness for Case 1, constant amplitude

however, were least at about FF = FL = 4 indicating that case 1 should have been the roughest floor.

97. Regression analyses were performed on 40 combinations of complex wave patterns consisting of 7 sine waves with wavelengths of 4, 7, 10, 15, 20, 30, and 50 ft and amplitudes of 0.005, 0.01, 0.02, 0.03, 0.04, 0.05, 0.1, 0.2, and 0.3 inch over a total length of 300 ft. These analyses were performed to determine any relationship between angular distortion β, intensity of angular distortion I, beta roughness $R\beta$, relative stiffness roughness RD_{rel}, floor levelness FL, floor flatness FF, microrelief index MRI, wave index WI and tilt angle ω. The results, Table 8, show

(a) floor levelness FL is a strong function of the angular distortion parameters and the floor flatness FF is a strong function of the intensity of the angular distortion parameters with r^2 usually > 0.98; this is consistent with the derivation of the F-number system (Face 1984)

(b) standard deviations of the parameters appear to be a strong function of the parameters; mean + 3 times the standard deviation represents a 99 percent probability that the observed value will be less than this magnitude.

(c) FF, FL and MRI are related with relative stiffness RD_{rel}, beta distortion $R\beta$ and the angle of tilt ω.

Table 8. Comparison of Surface roughness, Complex Waves, $r^2 > 0.7$

a. Angular Distortion

Type of Distortion		Equation	Regression Coefficient, r^2
Mean Angular Distortion β_m	(47a)	$I_m = 4.2320\beta_m^{0.9761}$	0.9857
	(47b)	$\beta + 3\sigma_\beta = 2.5383\beta_m^{0.9212}$	0.7663
	(47c)	$\sigma_\beta = 0.5906\ \beta_m^{0.9212}$	0.7634
	(47d)	$FL = 6.2866\ \beta_m^{-0.8830}$	0.7634
	(47e)	$\beta_{mm} = 0.1836 + 1.9484\ \beta_m$	0.7026
Standard Deviation of Mean Angular Distortion σ_β	(48a)	$\beta_m + 3\sigma_\beta = 0.0248 + 4.2412\ \sigma_\beta$	0.9996
	(48b)	$\beta_{mm} = 3.4323\ \sigma_\beta^{0.9716}$	0.9805
	(48c)	$FL = 3.8041\ \sigma_\beta^{-0.9571}$	0.9797
	(48d)	$R\beta_T = -0.0372 + 0.5759\ \sigma_\beta$	0.9578
	(48e)	$I_m = -0.0163 + 0.2854\ \sigma_\beta$	0.9566
	(48f)	$I_m + 3\sigma_I = -0.0829 + 1.4654\ \sigma_\beta$	0.9559
	(48g)	$\sigma_I = -0.0220 + 0.3931\ \sigma_\beta$	0.9594
	(48i)	$R\beta_1 = -0.0366 + 0.5032\ \sigma_\beta$	0.9490
	(48j)	$I_{mm} = -0.0299 + 0.7726\ \sigma_\beta$	0.9353
	(48k)	$FF = 3.6735\ \sigma_\beta^{-1.2649}$	0.9006
	(48l)	$MRI = 0.5986\ \sigma_\beta^{1.0045}$	0.8914
	(48m)	$\omega = 0.4009\ \sigma_\beta^{0.8963}$	0.8575
	(48n)	$\sigma_\omega = 0.4470\ \sigma_\beta^{0.9074}$	0.8707
Mean + 3 Times Standard Deviation of Mean Angular Distortion $\beta_m + 3\sigma_\beta$	(49a)	$FL = 15.6470(\beta_m + 3\sigma_\beta)^{-0.9815}$	0.9826
	(49b)	$\beta_{mm} = 0.8167(\beta_m + 3\sigma_\beta)^{0.9959}$	0.9826
	(49c)	$R\beta_T = -0.0401 + 0.1355(\beta_m + 3\sigma_\beta)$	0.9532
	(49d)	$I_m = -0.0177 + 0.0671(\beta_m + 3\sigma_\beta)$	0.9521
	(49e)	$I_m + 3\sigma_I = -0.0904 + 0.3447(\beta_m + 3\sigma_\beta)$	0.9514

Table 8. (Continued)

Type of Distortion		Equation	Regression Coefficient, r^2
	(49f)	$\sigma_I = -0.0240 + 0.0925(\beta_m+3\sigma_\beta)$	0.9510
	(49g)	$R\beta_1 = -0.0390 + 0.1183(\beta_m+3\sigma_\beta)$	0.9435
	(49h)	$I_{mm} = -0.0340 + 0.1819(\beta_m+3\sigma_\beta)$	0.9327
	(49i)	$FF = 23.8013(\beta_m+3\sigma_\beta)^{-1.2988}$	0.9056
	(49j)	$MRI = 0.1357(\beta_m+3\sigma_\beta)^{1.0312}$	0.8960
	(49k)	$\sigma_\omega = 0.1170(\beta_m+3\sigma_\beta)^{0.9313}$	0.8747
	(49l)	$\omega = 0.1067(\beta_m+3\sigma_\beta)^{0.9213}$	0.8642
Maximum Angular Distortion β_{mm}	(50a)	$FL = 12.8307\ \beta_{mm}^{-0.9832}$	0.9953
	(50b)	$MRI = 0.1690\ \beta_{mm}^{1.0554}$	0.9474
	(50c)	$\sigma_\omega = 0.1431\ \beta_{mm}^{0.9600}$	0.9382
	(50d)	$\omega = 0.1304\ \beta_{mm}^{0.9531}$	0.9335
	(50e)	$FF = 18.2898\ \beta_{mm}^{-1.3028}$	0.9197
	(50f)	$I_{mm} = -0.0504 + 0.2441\ \beta_{mm}$	0.9180
	(50g)	$\sigma_I = -0.292 + 0.1210\ \beta_{mm}$	0.8901
	(50h)	$I_m+3\sigma_I = -0.1095 + 0.4509\ \beta_{mm}$	0.8896
	(50i)	$R\beta_T = -0.0474 + 0.1770\ \beta_{mm}$	0.8891
	(50j)	$I_m = -0.0212 + 0.0876\ \beta_{mm}$	0.8859
	(50k)	$R\beta_1 = 0.0769\ \beta_{mm}^{1.4141}$	0.8760
Mean Intensity of Angular Distortion $I_m = (\beta/\ell)_m$	(51a)	$I_m+3\sigma_I = 0.0006 + 5.1356\ I_m$	0.9995
	(51b)	$\sigma_I = 0.0004 + 1.3779\ I_m$	0.9993
	(51c)	$R\beta_T = -0.0042 + 2.0150\ I_m$	0.9982
	(51d)	$R\beta_1 = -0.0081 + 1.7665\ I_m$	0.9958
	(51e)	$FF = 1.0675\ I_m^{-0.9623}$	0.9806
	(51f)	$I_{mm} = 3.4940\ I_m^{-1.0542}$	0.9800

Table 8. (Continued)

b. Intensity of Angular Distortion

Type of Distortion		Equation	Regression Coefficient, r^2
	(51g)	FL = $1.9927\ I_m^{-0.6479}$	0.8448
	(51h)	MRI = $1.2452\ I_m^{0.6950}$	0.8028
	(51i)	σ_ω = $0.8763\ I_m^{0.6310}$	0.7921
	(51j)	ω = $0.7844\ I_m^{0.6250}$	0.7846
Standard Deviation of Mean Intensity of Angular Distortion σ_I	(52a)	$I_m + 3\sigma_I$ = $-0.0009 + 3.7266\ \sigma_I$	0.9999
	(52b)	$R\beta_T$ = $-0.0047 + 1.4613\ \sigma_I$	0.9937
	(52c)	$R\beta_1$ = $-0.0084 + 1.2796\ \sigma_I$	0.9926
	(52d)	I_m = $2.4000\ \sigma_I^{1.0396}$	0.9865
	(52e)	FF = $1.5106\ \sigma_I^{-0.9476}$	0.9843
	(52f)	FL = $2.5181\ \sigma_I^{-0.6380}$	0.8478
	(52g)	MRI = $0.9789\ \sigma_I^{0.6875}$	0.8131
	(52h)	σ_ω = $0.7037\ \sigma_I^{0.6239}$	0.8016
	(52i)	ω = $0.6300\ \sigma_I^{0.6174}$	0.7924
Mean + 3 Times Standard Deviation of Mean Intensity of Angular Distortion $I_m + 3\sigma_I$	(53a)	$R\beta_T$ = $-0.0043 + 0.3922(I_m+3\sigma_I)$	0.9976
	(53b)	$R\beta_1$ = $-0.0081 + 0.3435(I_m+3\sigma_I)$	0.9933
	(53c)	I_m = $0.5995(I_m+3\sigma_I)^{1.0190}$	0.9820
	(53d)	FF = $5.3572(I_m+3\sigma_I)^{-0.9280}$	0.9781
	(53e)	β_{mm} = $0.0144 + 0.5257(I_m+3\sigma_I)$	0.9729
	(53f)	FL = $5.9350(I_m+3\sigma_I)^{-0.6223}$	0.8356
	(53g)	MRI = $0.3899(I_m+3\sigma_I)^{0.6722}$	0.8055
	(53h)	σ_ω = $0.3068(I_m+3\sigma_I)^{0.6128}$	0.8012
	(53i)	ω = $0.2776(I_m+3\sigma_I)^{0.6072}$	0.7943

Table 8. (Continued)

Type of Distortion		Equation	Regression Coefficient, r^2
Maximum Intensity of Angular Distortion I_{mm}	(54a)	$FF = 3.4054\ I_{mm}^{-0.9056}$	0.9850
	(54b)	$R\beta_T = 0.6210\ I_{mm}^{1.0062}$	0.9788
	(54c)	$R\beta_1 = 4.4936\ I_{mm}^{0.9968}$	0.9647
	(54d)	$FL = 4.3900\ I_{mm}^{-0.6064}$	0.8390
	(54e)	$RI = 0.5569\ I_{mm}^{0.6671}$	0.8389
	(54f)	$\sigma_\omega = 0.4253\ I_{mm}^{0.6087}$	0.8359
	(54g)	$\omega = 0.3831\ I_{mm}^{0.6027}$	0.8273

c. Relative Thickness System

Type of Distortion		Equation	Regression Coefficient, r^2
Relative Thickness RD_{rel1}	(55a)	$RD_{relT} = 0.6990\ RD_{rel1}^{0.9565}$	0.9657
	(55b)	$\log_{10}FL = 1.8701 - 1.5944\ RD_{rel1}$	0.9239
	(55c)	$\log_{10}R\beta_1 = -2.2529 + 2.4156\ RD_{rel1}$	0.9023
	(55d)	$\log_{10}R\beta_T = -2.1607 + 2.4077\ RD_{rel1}$	0.8926
	(55e)	$\log_{10}FF = 2.2827 - 2.1571\ RD_{rel1}$	0.8900
	(55f)	$\log_{10}\sigma_I = 2.2145 + 2.2472\ RD_{rel1}$	0.8811
	(55g)	$\log_{10}(I_m+3\sigma_I) = -1.6606+2.2715 RD_{rel1}$	0.8690
	(55h)	$\log_{10}I_{mm} = -1.9024 + 2.2802\ RD_{rel1}$	0.8281
	(55i)	$D_{relm} = 18.67802\ RD_{rel1}^{0.7333}$	0.8239
	(55j)	$\log_{10}MRI = -1.5699 + 1.6543\ RD_{rel1}$	0.8216
	(55k)	$\log_{10}\sigma_\omega = -1.5639 + 1.4868\ RD_{rel1}$	0.7943
	(55l)	$\log_{10}\omega = -1.5988 + 1.4758\ RD_{rel1}$	0.7901
	(55m)	$\beta_{mm} = 1.3750\ RD_{rel1}^{0.4078}$	0.7156

Table 8. (Continued)

Type of Distortion		Equation	Regression Coefficient, r^2
Total Relative Thickness RD_{relT}	(56a)	$MRI = 0.0072 + 0.2694\ RD_{relT}$	0.9682
	(56b)	$\omega = 0.0104 + 0.1939\ RD_{relT}$	0.9350
	(56c)	$\sigma_\omega = 0.0101 + 0.2163\ RD_{relT}$	0.9184
	(56d)	$FF = 8.3007 - 40.1109 \log_{10} RD_{relT}$	0.9099
	(56e)	$\beta_{mm} = -0.0156 + 1.6750\ RD_{relT}$	0.8937
	(56f)	$\log_{10} FL = 1.7652 - 0.7383\ RD_{relT}$	0.8673
	(56g)	$\log_{10}(\beta_m+3\sigma_\beta) = -0.5756 + 0.7425\ RD_{relT}$	0.8599
	(56h)	$\log_{10}\sigma_\beta = -1.2280 + 0.7550\ RD_{relT}$	0.8478
	(56i)	$D_{relm} = 13.4822\ RD_{relT}^{0.7325}$	0.7789
	(56j)	$\log_{10} I_m = -2.1619 + 0.9759\ RD_{relT}$	0.7530
	(56k)	$\log_{10} R\beta_T = -1.9665 + 1.0564\ RD_{relT}$	0.7522
	(56l)	$\log_{10}\sigma_I = -2.0370 + 0.9922\ RD_{relT}$	0.7519
	(56m)	$\log_{10}(I_m+3\sigma_I) = -1.4817 + 1.0038\ RD_{relT}$	0.7428
	(56n)	$\log_{10} R\beta_1 = -2.0370 + 0.9922\ RD_{relT}$	0.7519
	(56o)	$\log_{10}\beta_m = -0.9816 + 0.6514\ RD_{relT}$	0.7016
Maximum Relative Thickness D_{relm}	(57)	$FL = 63.1933 - 44.0230 \log D_{relm}$	0.7550

d. Beta System

Type of Distortion		Equation	Regression Coefficient, r^2
Beta Distortion $R\beta_1$	(58a)	$R\beta_T = 0.0054 + 1.1376\ R\beta_1$	0.9970
	(58b)	$FF = 1.9212\ R\beta_1^{-0.8872}$	0.9736
	(58c)	$FL = 2.8953\ R\beta_1^{-0.6042}$	0.8580
	(58d)	$MRI = 0.8248\ R\beta_1^{0.6446}$	0.8067

Table 8. (Continued)

Type of Distortion		Equation	Regression Coefficient, r^2
Total Beta Distortion $R\beta_T$	(59a)	FF = $2.2816\ R\beta_T^{-0.8907}$	0.9856
	(59b)	FL = $3.2537\ R\beta_T^{-0.6068}$	0.8691
	(59c)	MRI = $0.7437\ R\beta_T^{0.6542}$	0.8345

e. Tilt

Type of Distortion		Equation	Regression Coefficient, r^2
Angle of Tilt ω	(60a)	σ_ω = $1.0922\ \omega^{0.9996}$	0.9897
	(60b)	MRI = $1.4973\ \omega^{1.0776}$	0.9610
	(60c)	FL = $1.8666\ \omega^{-0.9619}$	0.9270
	(60d)	FF = $1.3838\ \omega^{-1.2855}$	0.8713
	(60e)	$R\beta_T$ = $1.5101\ \omega^{1.3833}$	0.8122
	(60f)	$R\beta_1$ = $1.1412\ \omega^{1.3535}$	0.7809
Standard Deviation of Tilt σ_ω	(61a)	MRI = $1.3382\ \sigma_\omega^{1.0708}$	0.9581
	(61b)	FL = $2.0457\ \sigma_\omega^{-0.9595}$	0.9311
	(61c)	FF = $1.5584\ \sigma_\omega^{-1.2838}$	0.8773
	(61d)	$R\beta_T$ = $1.5108\ \sigma_\omega^{1.3833}$	0.8122
	(61e)	$R\beta_1$ = $1.1412\ \sigma_\omega^{1.3535}$	0.7809

f. Floor Levelness/Flatness

Type of Distortion		Equation	Regression Coefficient, r^2
Floor Levelness FL	(62a)	MRI = $2.6184\ FL^{-1.0738}$	0.9525
	(62b)	FF = $0.6456\ FL^{1.3127}$	0.9069
	(62c)	$\log_{10}$WI = $0.5797 - 0.3104\ FL$	0.8078
Floor Flatness FF	(63)	MRI = $1.4507\ FF^{-0.7522}$	0.8880

Simple convenient parameters that appear most independent of each other and may be useful for rating performance of facilities include F-numbers FF and FL, WI, MRI, D_{relm} and mean angular distortion β_m. These systems for rating performance are the same as those indicated from analysis of the simple sine wave, except β_m is added. These parameters are selected for rating performance of facilities in PART IV.

Fractal System

100. The concept of fractals as self-similarity "space-filling" curves is a quantitative measure of the form of a perimeter or edge of given lengths enclosing a space. A fractal may be an effective way of expressing nondifferentiable curves and a nonintegral dimensionality (Whalley and Orford 1989). The fractal applies the idea that the length of a given irregular segment L_s increases when the length is measured by summing up smaller equal increments ΔL_s stepped off by a pair of dividers. The logarithm of L_s plotted versus the logarithm of the increment ΔL_s provide a "Richardson Plot". A linear regression analysis may be performed to find the best linear line segment through the data points. The slope of the line is negative $-b = 1 - D$ where D falls between 1 and 2 and is the Hausdorff-Besicovitch dimension (Whalley and Orford 1989). A $D = 1$ indicates a Euclidean shape while D approaching 2 indicates a line that becomes increasingly plane filling. The Richardson plot may sometimes be better fitted to two parts, the first part is a horizontal line and relates to textural details D_T. The second part becomes increasing plane filling and relates to structural details D_S (Kaye 1978).

101. Figure 33 is a Richardson plot of the wave $\sin(2\pi x/32)$ for different number of readings NRE. Differences in the number of readings make little difference in the form of the plot. Furthermore, the Richardson plots of the complex wave forms of Figure 29 are also similar to Figure 33. The slope of the first part of the curve is zero indicating $D_T = 1$ consistent with a Euclidean or wave pattern of motion. The second part becomes increasingly plane filling.

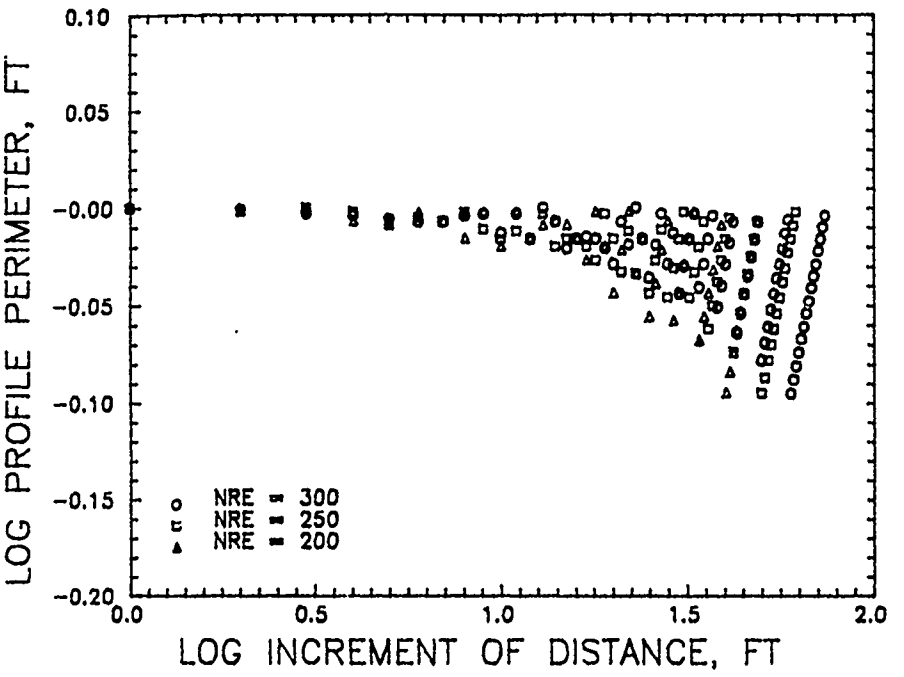

Figure 33. Richardson Plot of wave $\sin(2\pi x/32)$

PART IV: ANALYSIS OF FOUNDATION MOVEMENT PATTERNS

Introduction

102. Actual foundation and soil movement patterns may differ from sine or cosine combinations of wave patterns considered in PART III. The superposition of soil movement patterns caused by the various factors described in Table 3 may also complicate simple methods of determining soil parameters needed for foundation design such as the depth of the active zone for heave and edge moisture variation distance. Field measurements of elevation profiles were therefore made on the first floors of various structures to obtain data for analysis of foundation performance using indices F-numbers FL and FF, Wave Index WI, relative thickness D_{relm}, macrorelief index MRI and mean angular distortion β_m. These indices were calculated using the computer programs in Appendix B. The reproducibility of these indices was checked by evaluating their mean, standard deviation and coefficient of variation for multiple profile measurements of a typical slab-on-grade. Elevations of the first measured point of each profile are taken zero.

103. Elevation profiles taken on first floors of new construction may indicate floor finishing characteristics and elastic or immediate deformations of foundation soils from structural loads, while elevation profiles taken on first floors of older construction also include deformations from long-term soil movements. First floors of one or two story structures were selected to minimize the influence of superstructure stiffness on floor deformation. Lightly loaded slabs-on-grade were expected to provide the best data for analysis.

Measurement of Elevation Profiles

104. Elevation profiles were measured using the Auto-Read Imperial Floor Profiler Dipstick, Figure 34, manufactured by Edward W. Face Company, Inc. The two small circular feet of the dipstick shown in Figure 34 are spaced exactly 1.0 ft apart. The dipstick is rotated 180° as shown in Figure 35 to obtain each reading. The switch and computer should be facing forward for the initial reading; otherwise the elevation profile will be inverted. Each reading is a measure of the difference in elevation between the two feet and it is displayed on two LCD panels on the top surface of the dipstick. The

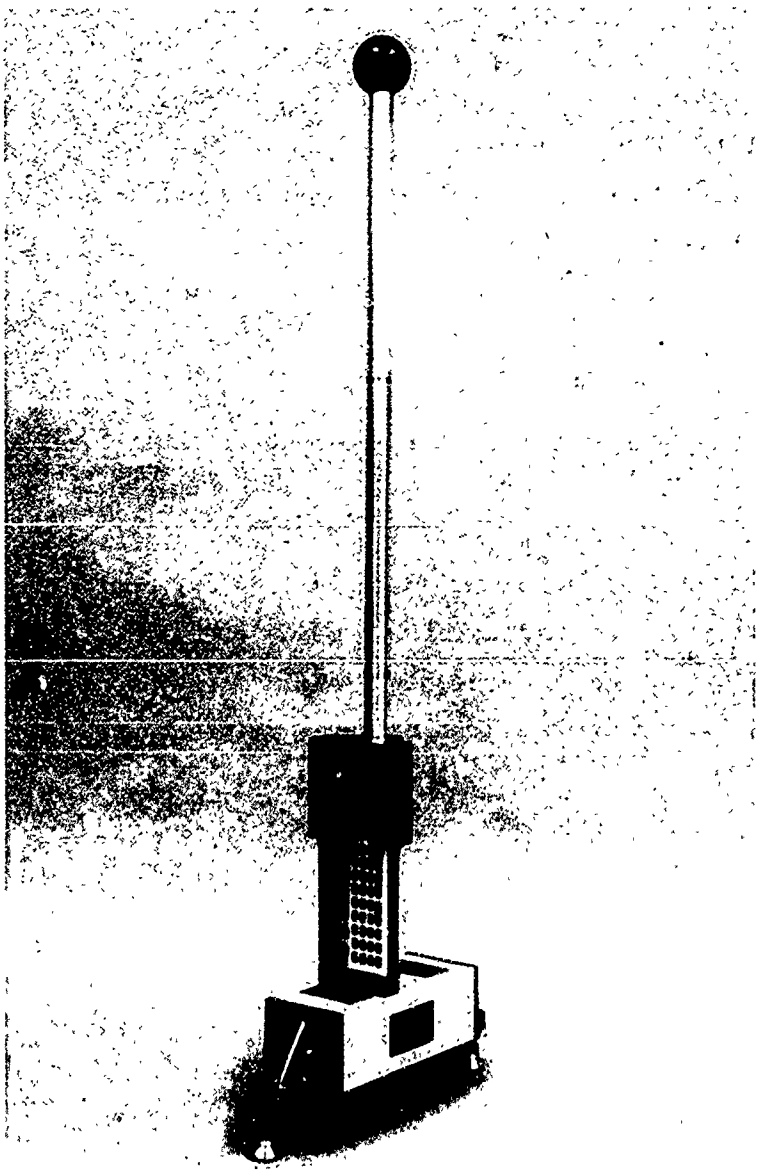

Figure 34. The Auto-read Profiler Dipstick

reading is also recorded in the memory of a pocket computer mounted on the dipstick handle. The dipstick is calibrated for a reproducibility of ± 0.001 inch.

105. The computer was programmed to collect up to 600 elevation difference readings per survey line in each of 10 data files. A set of readings entered into each data file consists of forward and reverse readings such that the final reading is on the original starting point to complete a

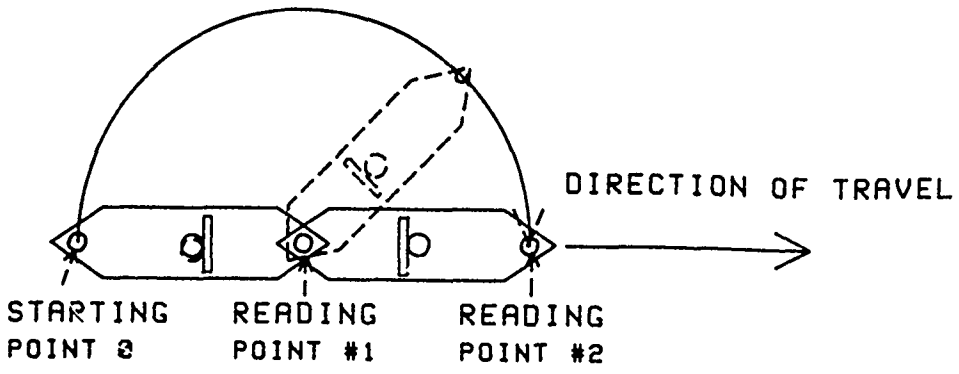

Figure 35. Schematic plan view of rotating the dipstick

loop. When the data files are filled or surveys completed the contents saved in the files of the computer could be read as necessary to a tape for storage permitting the computer memory to be purged and prepared for accepting new data. After all readings for a field survey project have been obtained the files can be read back into the pocket computer from tape, then read from the pocket computer into a personal computer for analysis.

106. Data obtained from the pocket computer were initially converted to a format capable of analysis by the computer programs in Appendix B. Prior to analysis, the elevation profile of each loop was calculated by adding the elevation differences of each reading beginning from the initial point, which was taken as zero elevation. The elevation of this same point determined by adding the elevation difference readings of all of the data points of a survey line was denoted as the total operator bias (TOB). The TOB of a perfect set of readings is zero. The actual TOB of each survey line is given by the last elevation reading in the tables of Appendix C, except Table C1 indicates elevation change readings only. The data in Table C1 had been collected during an earlier project by McKeen and Eliassi (1988). The TOB was divided by the total length of the loop to determine the operator bias/ft, which was then subtracted from each reading of the elevation profile to determine the corrected elevation profile. All subsequent analysis was then performed using the corrected elevation profile. The operator bias is a measurement error which depends on characteristics of the operator, nature of the floor and accuracy/reproducibility of readings measured by the dipstick profiler.

Reproducibility of Selected Performance Ratings

107. Ten profilometer readings wer taken of the full loop of a 78-ft length of the first floor slab-on-grade joining the two buildings of the Geotechnical Laboratory, Waterways Experiment Station. The statistics of these indices listed with increasing coefficient of variation are shown in Table 9. The statistics are based on the full loop, except for MRI; MRI was determined for the half loop so that the influence of slope was retained.

108. All of the coefficients of variation (COV) are less than 10 percent indicating sufficient reproducibility for this study. WI has the least COV, while D_{relm} has the largest. D_{relm} is a maximum value. The COV of D_{relm} may be reduced by using a profilometer with a smaller spacing Δx permitting greater accuracy in measuring the elevation profile. The F-numbers and WI are independent of the orientation (i.e., inversion) of the elevation profile.

Table 9. Statistics of Selected Rating Indices

Index	Mean	Coefficient of Variation, Percent
Wave Index WI	0.22	0.71
Floor Levelness FL	23.31	2.20
Mean Angular Distortion β_m	0.15	2.54
Floor Flatness FF	24.75	3.87
Macrorelief Index MRI	0.30	5.81
Maximum Relative Thickness D_{relm}	12.33	7.96

Analysis of Elevation Profiles

109. Elevation (level) profilometer surveys were obtained from three new facilities and seven older facilities located in Mississippi and Texas. Mississippi provides a wet, humid climate in contrast to the semi-arid climate of Texas. Elevation profiles of the new facilities provide initial data that can be applied in later years to analyze the increase in differential movement caused by soil distortions. Elevation profiles of older facilities provide accumulated foundation distress that may be useful in developing performance rating systems and to determine the potential value of performance rating systems as a design tool for foundations in unstable soil.

New Construction

110. Red River Army Depot. Elevation changes were measured on floors of buildings 333 and 312 of the Red River Army Depot (RRAD) in May 1987 using a dipstick similar to the device described in paragraph 104, but without the advantage of a computer to automatically record the data (McKeen and Eliassi 1988), Table C1. Construction of the mat foundations and floors of these facilities was initiated in 1984, while operations were initiated in 1987.

111. The foundation soil consists of 5 to 8 ft of engineered cohesive fill with plasticity index less than 20 and liquid limits less than 35 compacted to greater than 92 percent optimum density after ASTM D 1557. Underlying the fill is potentially expansive high plasticity clay and clay shale identified as the Midway group of Tertiary age. A perched water table exists immediately beneath the fill extending hydrostatically to at least 40 ft, then decreasing with increasing depth. Elevation measurements using survey levels have indicated mostly dish-shaped elastic settlement of floor slabs through 1988, except for a dip near the south end of building 333 (Johnson 1989a, 1989b).

112. Building 333. Building 333, an automated maintenance repair facility for military vehicles, is supported on a stiffened ribbed mat 678 ft long from North to South and 304 ft wide from East to West, Figure 36a. The mat is stiffened to accommodate a maximum differential heave of 1.5 inches. The ribbed mat consists of 3 independent adjacent monoliths each 304 ft long from East to West by 226 ft from South to North. These monoliths are separated by expansion joints parallel with the East-West direction.

113. The layout of survey line 3 with 649 readings, Figure 36b, taken May 1987 (McKeen and Eliassi 1988) is parallel and near an automated vehicle track oriented in the North-South direction. Near survey point 185 is a joint between monoliths 1/3 from the South end of the mat, Figure 36b. The elevation profile, Figure 37a, calculated by program FTRC from the elevation change readings after correction for operator bias illustrates a substantial dip approaching 1.6 in. near 185 ft coincident with the joint between monoliths, Figure 37a. This is attributed to softened foundation soil in this area caused by a previously existing drainage ditch in this location which ran parallel with the joint. The Fourier transform for readings NRE-311 over 1/2 of the loop, Figure 37b, shows a large peak approaching 0.6 in. or 1.2 in.

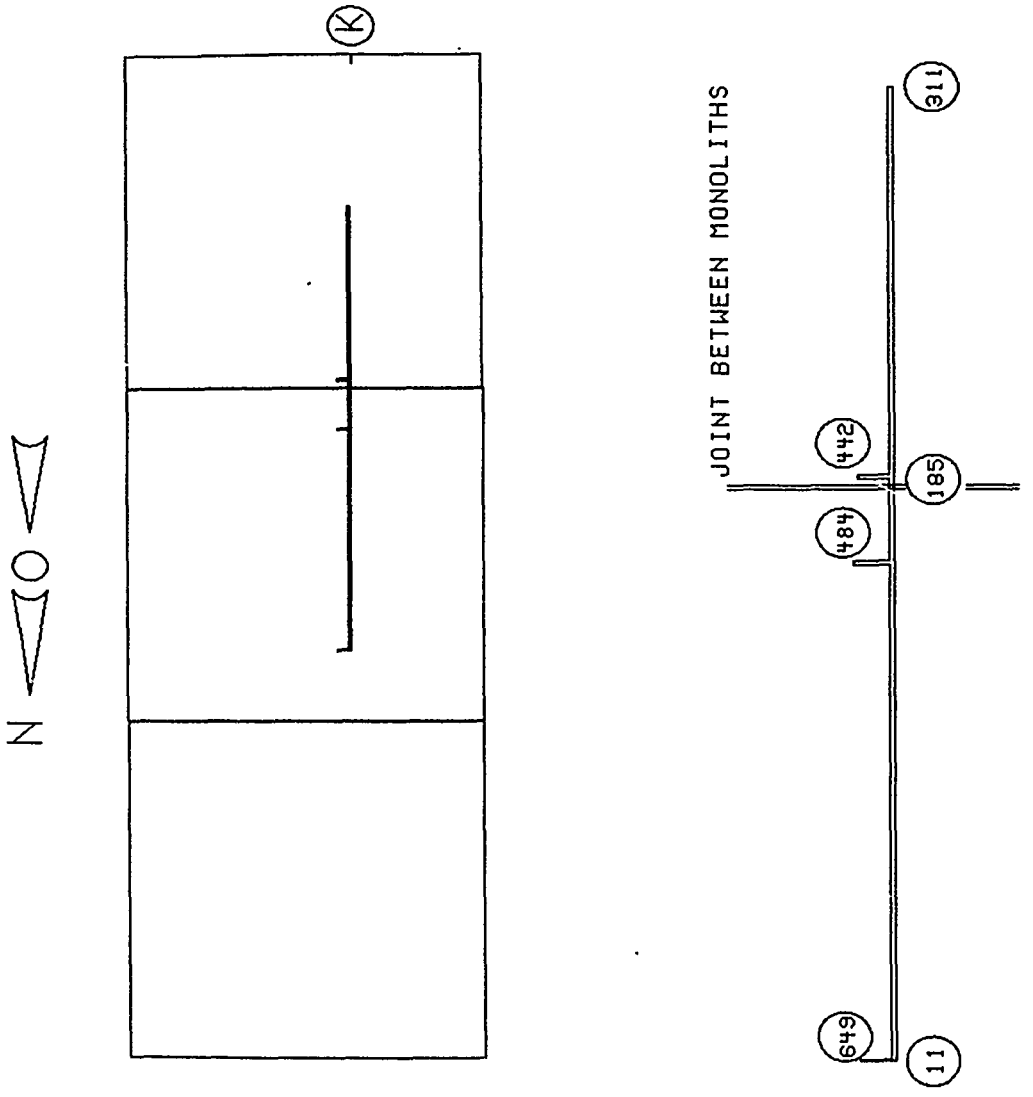

a. PLAN b. SURVEY LINE 3

Figure 36. Survey line 3 of Building 333

actual amplitude near a frequency of zero. Other peaks in amplitude occur near 0.03, 0.08, and 0.13 cycle/ft. The large peak near 0.0 cycle/ft may be related with the 1.6 in. dip in the floor.

114. Peak amplitudes exceeding 0.02 in. and resonant frequencies of these peak amplitudes from program FTROPT for survey line 3 with regression coefficients > 0.5 are as follows:

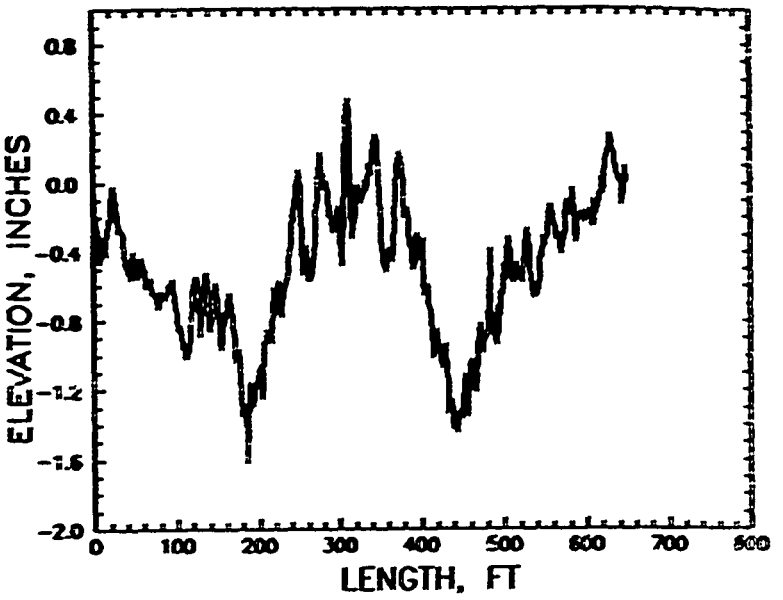

a. ELEVATION PROFILE

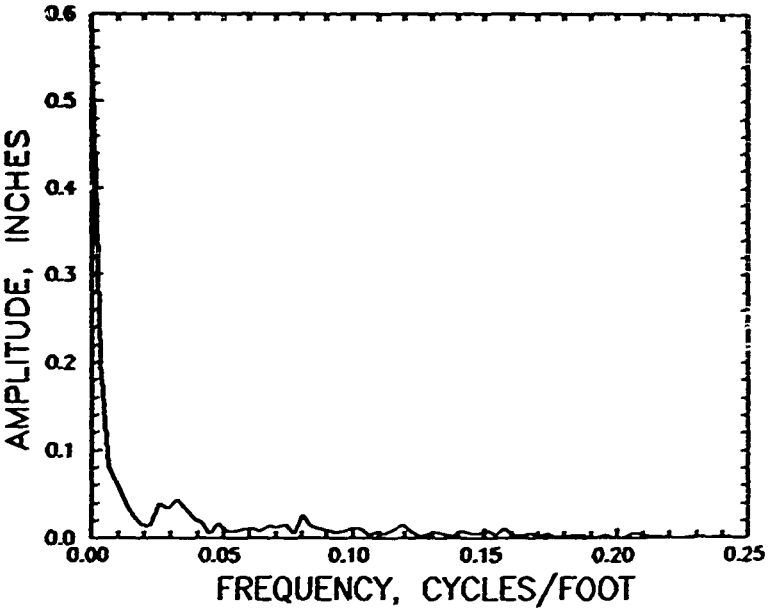

b. FOURIER TRANSFORM OF ELEVATION PROFILE

Figure 37. Elevation profile and Fourier transform of line 3, Building 333

Number Readings NRE	Number of Terms N	Resonant Frequency f_r, cycle/ft	Regression Coefficient r_f^2	Peak Amplitude A_{tp}, in.	Regression Coefficient r_a^2	Wave
311	4	0.0265	0.9940	0.0528	0.9940	Cosin
	5	0.0265	0.9923	0.0527	0.9955	Cosin
	7	0.0266	0.9916	0.0539	0.9555	Cosin
305	4	0.0266	0.9967	0.0546	0.6037	Cosin
		0.0405	0.9971	0.0335	0.5074	Cosin

Peak amplitudes for these calculated cosine waves from program FTROPT are 1/2 of the actual amplitudes. Calculated amplitudes by FTROPT are about 0.11 inch (twice transform amplitudes or half actual peak-to-peak amplitudes), which are less than the observed amplitudes in Figure 37a, especially the 1 inch peak-to-peak dip near 185 ft on the forward run or 440 ft on the reverse run. Dominant frequencies are 0.0266 and 0.0405 cycle/ft (wavelengths of 38 and 25 ft). These frequencies may be related with the immediate compression of the foundation soil over the length of the floor from structural and equipment loads and the 25-ft spacing of stiffening beams supporting the mat foundation and floor in the area of the measured profile.

115. Building 312. Building 312 is an automated warehouse adjacent to and north of building 333 that provides materials for work performed in building 333. This building is supported by a stiffened ribbed mat similar to that of building 333. The system of transporting materials from building 312 to building 333 is accomplished with automated robot vehicles and lift trucks. There are 21 rows of racks on the West end and 34 rows on the East end, Figure 38. Automated lift trucks travel in the aisles between the rows to retrieve supplies from the bins in the racks and then transfers these supplies to the automated vehicles for transport to building 333. The racks are over 40 ft high, therefore, the floors must be exceptionally level to prevent the lift trucks from ramming the racks and to provide optimum operational performance. Table 10 provides a brief description of survey lines 4 through 17 performed within numbered aisles in building 312 between the racks and bins, Figure 38. The elevation change profiles of these survey lines are listed in Table C1.

116. Figure 39a illustrates the elevation profile of line 12, a typical profile, between racks 39 and 40 in the East end of the building. The Fourier

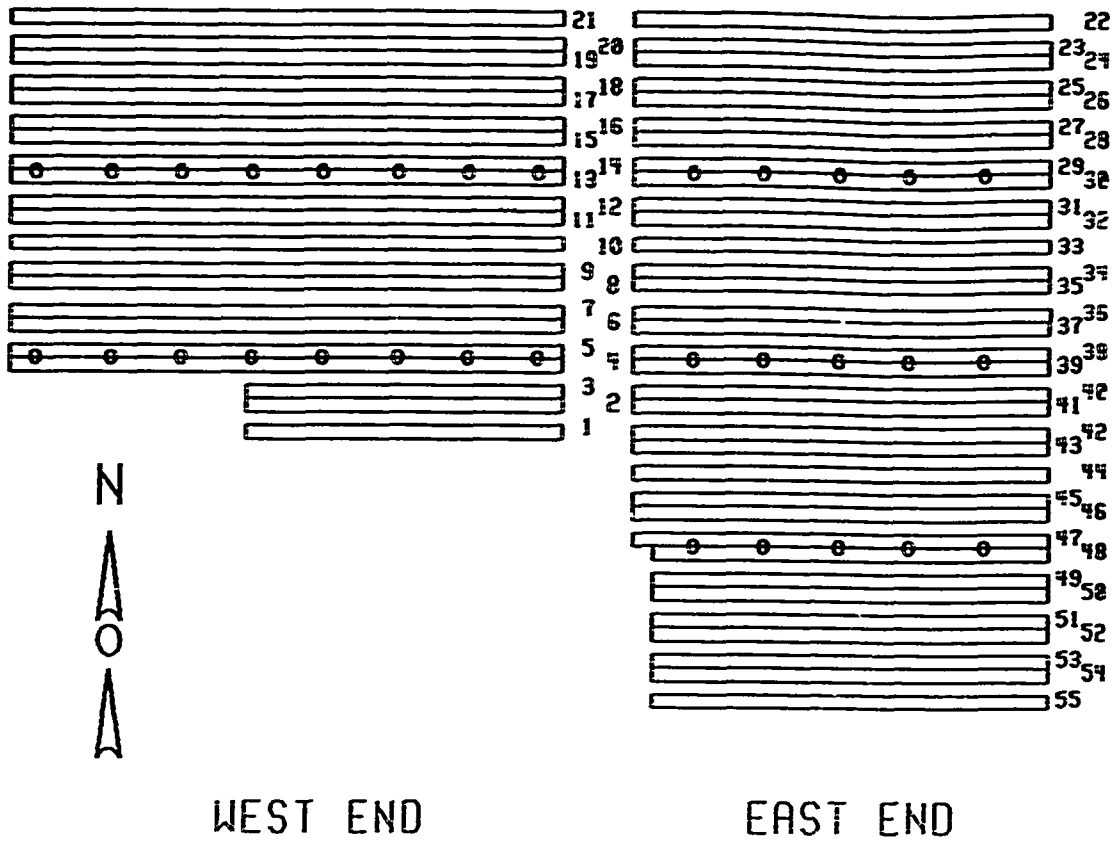

Figure 38. Rack and bin plan of Building 312

Table 10. Description of Survey Lines in Building 312

Line	Readings NREAD	Readings Used NRE	Fourier Runs NO	Description
4	353	176	5	E to W loop between racks 48 & 49
5	372	186	9	E to W loop between racks 24 & 25
6	372	186	4	E to W loop between racks 37 & 38
7	516	258	5	E to W loop between racks 20 & 21
10	515	251	8	E to W loop between racks 12 & 13
11	517	258	7	E to W loop between racks 3 & 4
12	371	183	5	E to W loop between racks 39 & 40
13	372	Not Used		E to W loop between racks 37 & 38
14	372	186	6	E to W loop between racks 28 & 29
15	353	171	6	E to W loop between racks 54 & 55
16	354	177	6	E to W loop between racks 48 & 49
17	372	186	6	E to W loop between racks 45 & 47

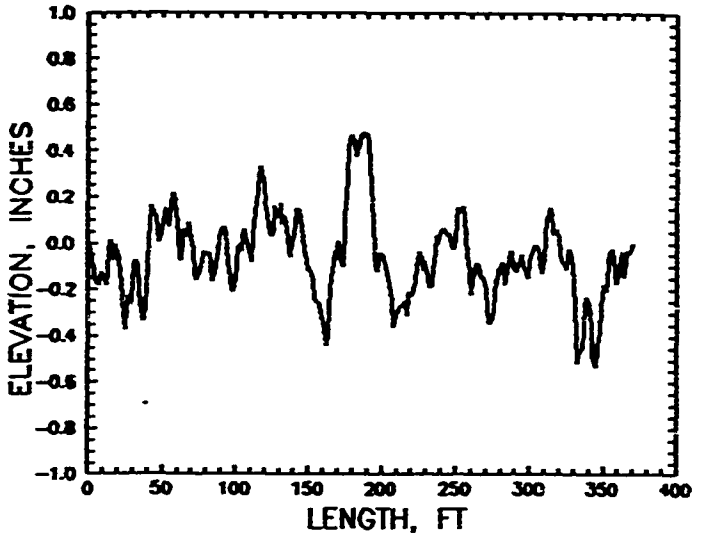

a. ELEVATION PROFILE

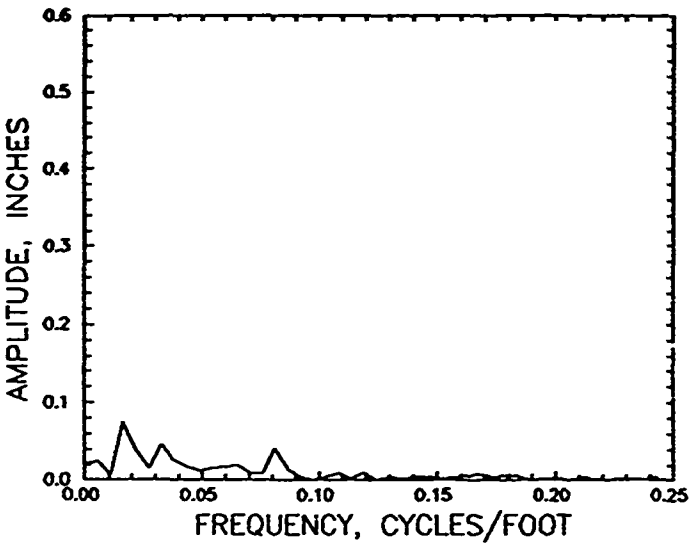

b. FOURIER TRANSFORM OF ELEVATION PROFILE

Figure 39. Elevation profile and Fourier transform of line 12, Building 312

transform of the elevation profile of half of the loop calculated with program FTRC and shown in Figure 39b indicates dominant frequencies with peak amplitudes of about 0.015, 0.03, and 0.08 cycle/ft (wavelengths of about 60, 30, and 13 ft). These wavelengths are similar to the 60-ft North-South and 30-ft East-West spacing of the column loads, Figure 38, indicated by the circle symbols in rows 4-5, 13-14, 29-30, 38-39 and 47-48. The 30 and 13 ft wavelengths are similar to the spacings between stiffening beams.

117. Resonant frequencies and dominant amplitudes calculated with Program FTROPT of half of the survey loops along lines 4 through 7 and 10 through 17 described in Table 10 are shown in Table 11. Transforms of line 13 were not used because regression coefficients were < 0.5. Dominant frequencies are in the range of 0.015, 0.03, and 0.08 cycle/ft or wavelengths of about 60, 30, and 13 ft attributed to elastic settlement from column loads and spacings of stiffening beams. The maximum calculated peak-to-peak

Table 11. Dominant Waves of Building 312 Survey Lines

Line	Number of Terms N	Resonant Frequency f_r, cycle/ft	Regression Coefficient r_f^2	Peak Amplitude A_{tp}, in.	Regression Coefficient r_a^2	Wave Type
4	5	0.0021	0.9352	0.1446	0.8741	Sine
	4	0.0155	0.9997	0.0439	0.9899	Sine
	5	0.0267	0.9959	0.0318	0.8851	Cosine
	5	0.0809	0.9972	0.0254	0.6358	Cosine
5	6	0.0214	0.9394	0.0385	0.9706	Cosine
6	4	0.0166	0.9195	0.0689	0.6292	Cosine
	2	0.0374	0.9963	0.0252	1.0000	Sine
7	5	0.0144	0.9994	0.0818	0.9970	Sine
	5	0.0241	0.9849	0.0233	0.9904	Sine
	3	0.0432	0.9999	0.0282	0.7580	Sine
10	8	0.0136	0.6377	0.0563	0.6904	Sine
	7	0.0281	0.9916	0.0295	0.8871	Cosine
11	7	0.0098	0.9992	0.0869	0.9847	Sine
	7	0.0295	0.9939	0.0435	0.9928	Cosine
12	5	0.0063	0.7640	0.0639	0.8256	Cosine
	5	0.0165	1.0003	0.0636	0.7844	Cosine
	2	0.0675	1.0627	0.0213	1.0052	Cosine
	3	0.0830	0.6145	0.0462	0.9463	Cosine
14	6	0.0165	0.9996	0.0614	0.9395	Cosine
15	6	0.0165	0.9976	0.0570	0.9714	Cosine
16	6	0.0235	0.9998	0.0294	0.9815	Cosine
17	3	0.0157	0.9989	0.0681	0.9995	Cosine
	6	0.0344	0.9960	0.0240	0.7203	Cosine

amplitudes of line 12 are about 0.26 inch, which are much less than the maximum observed peak-to-peak amplitudes observed for line 12 in Figure 39a.

118. Automated Technology Center. The Automated Technology Center (ATC) with plan view illustrated in Figure 40 consists of a main complex, Area

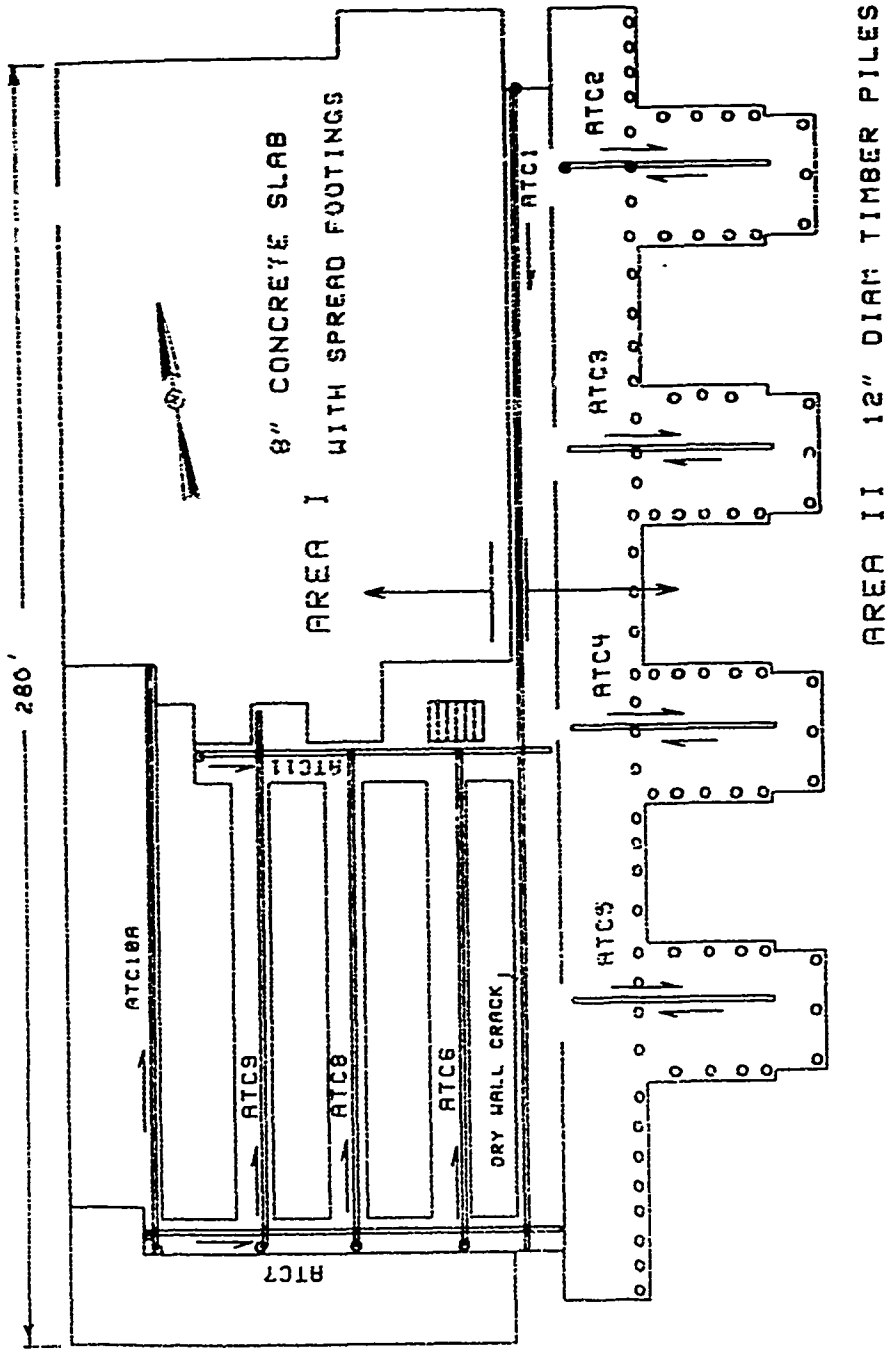

Figure 40. Floor plan of the Automated Technology Center

I, supported by spread footings, while the office complex, Area II, is supported by reinforced concrete grade beams on timber piles. The 10-ft by 10-ft spread footings in Area I support pressures up to 2.5 ksf from column and 2.0 ksf from wall loads. The floor in Area I consists of two 4-inch thick concrete slabs placed directly on top of each other. The building is approximately 280 ft by 180 ft.

119. The south, south-west and west portions of the facility, primarily consisting of Area I, are constructed in a cut area where up to 15 ft of the original overburden soil was removed. Profile lines ATC6, ATC8, ATC9 and ATC10A are included in the cut area. The southern half of profile line ATC1 runs over the cut area, while the northern half runs over fill. Profile lines ATC2 through ATC5 are all over fill and in area II which is supported by piles. Line ATC1 is at the edge of the 8-inch floor slab supported by concrete grade beams running between the concrete slab and the timber piles. Profile ATC1 will be strongly influenced by the deformation of the concrete slab of Area I. The initial floor was level at 180 ft elevation.

120. The in situ soils supporting the ATC are predominantly medium dense clay silts (ML) of low plasticity with plasticity index PI < 15. Fill material is similar material compacted to ≥ 95 percent of optimum density after ASTM standard test methods D 698. The minimum density of any soils beneath any part of the facility is ≥ 95 percent of optimum density after D 698. The groundwater level was about 24 ft below the elevation of the first floor in 1987.

121. Initial elevation profiles listed in Table C2 were made December 12, 1989. Figure 41a illustrates the full loop elevation profile of line ATC1. The floor along survey lines ATC1 and ATC10A slopes slightly down toward the south from 0.8 to 1.5 inch after excluding operator bias. Survey line ATC7 indicated a slight rise of about 0.5 inch to the east. The survey lines, except for ATC10A, were taken over floor carpet which significantly increased operator bias. The Fourier transform of the half loop of ATC1 indicates several dominant amplitudes, Figure 41b, which increase with decreasing frequencies.

122. The most distress observed in this structure to date was the appearance of a jagged crack in the dry wall adjacent to line ATC1 of the main hallway. This diagonal wall fracture appeared near December 28, 1989 about

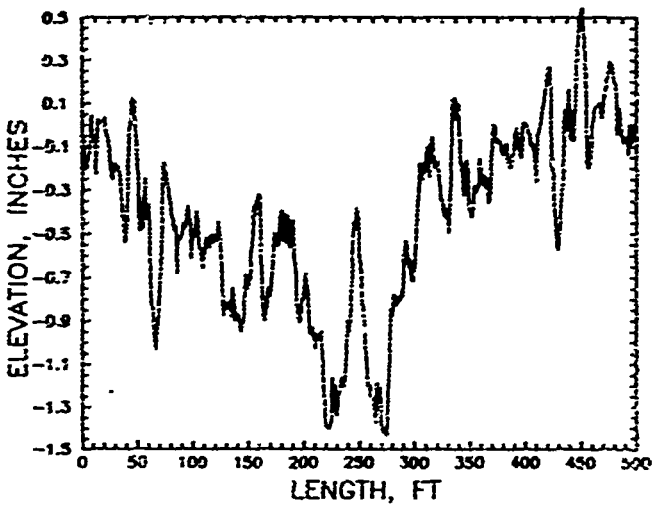

a. FULL LOOP ELEVATION PROFILE

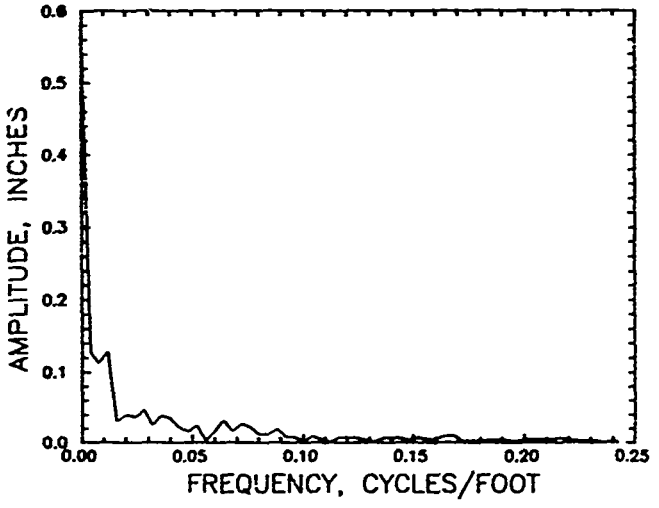

b. FOURIER TRANSFORM OF ELEVATION PROFILE

Figure 41. Survey line ATC1 in the Automated Technology Center

the time of a record cold when outside temperatures dropped to 0° F. This crack was up to 0.25 inch wide extending up about 8 ft to the top of the dry wall. The location of this fracture is about 60 ft from the south end of survey line ATC1, Figure 40, within the large dip in the elevation profile near 220 ft, Figure 41a. Line ATC1 was resurveyed February 21, 1990 to check for significant changes; significant changes were not observed.

123. Dominant frequencies and peak amplitudes of discrete deformation waves in the slab-on-grade floor of the ATC are given in Table 12. These frequencies vary from 0.012 to 0.08 cycle/ft with peak amplitudes decreasing

Table 12. Dominant Waves of Automated Technology Center Survey Lines

Line	Number of Terms N	Resonant Frequency f_r, cycle/ft	Regression Coefficient r_f^2	Peak Amplitude A_{tp}, in.	Regression Coefficient r_a^2	Wave Type
1	8	0.0124	0.9865	0.1313	0.9205	Sine
	3	0.0294	0.9349	0.0612	0.9009	Sine
	5	0.0273	0.6018	0.0680	0.8782	Cosine
7	5	0.0402	1.0000	0.0979	0.9769	Sine
8	3	0.1032	0.6463	0.0292	0.4285	Cosine
9	5	0.0851	0.9983	0.0479	0.4862	Sine
10A	5	0.0144	0.9927	0.0750	0.9886	Sine
	4	0.0428	0.9974	0.0254	0.9133	Cosine
	5	0.0601	0.9994	0.0336	0.9737	Sine
1*	5	0.0123	0.9986	0.1315	0.6916	Sine
	5	0.0214	0.9969	0.0627	0.8570	Sine
	4	0.0313	0.9962	0.0586	0.9928	Cosine
	5	0.0363	1.0003	0.0412	0.8408	Sine
	5	0.0697	0.7837	0.0397	0.8691	Sine
	2	0.0764	0.9930	0.0281	1.0000	Cosine

*Survey line ATC1 repeated 02/21/90

from 0.13 to 0.03 in. as the frequency increases. Line ATC1 appears to have more significant peaks when recorded 02/21/90 than the earlier line recorded 12/12/89.

Existing Construction

124. Coastal Engineering Research Center Building 3296. Building 3296 located in the US Army Engineer Waterways Experiment Station contains many of the offices of the Coastal Engineering Research Center (CERC), Figure 42. This building consists of four sections. CERC-1 (completed June 1965), CERC-2 (completed June 1973), and CERC-3 (completed August 1986) are single story brick masonry structures supported by continuous and shallow spread footings placed 2 ft below the ground surface at an elevation of about 186 ft. Loading pressures on footings are designed not to exceed 1 ksf. Spacings between footings are about 9 or 10 ft. Conventional 4-inch thick concrete slabs were placed on grade. Several minor fractures < 0.06 inch wide are visible below the exterior brick in the continuous footings above the ground surface in

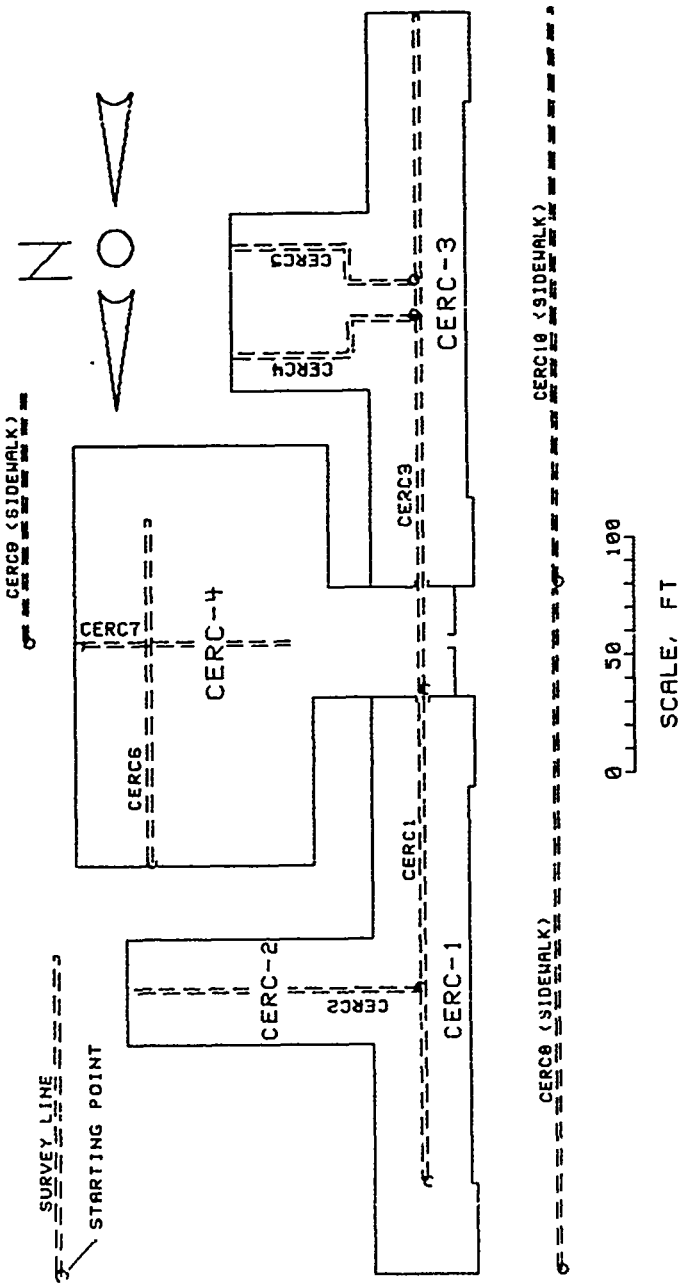

Figure 42. Plan view of building 3296

CERC-1. Opposite exterior walls in CERC-3 about 15 ft from the East end contain severe fractures 1/4 to 3/8 inch wide near the top. These fractures decrease in width with decreasing height to hairline cracks below the windows and in visible parts of the continuous footings above the ground surface. No other distress is apparent.

125. CERC-4 (completed August 1989) is a two-story addition with the first floor at an elevation of about 176 ft supported by grade beams on auger-cast piles. The auger-cast piles are 16 inches in diameter by 65 ft long and spaced from 15 ft to 30 ft apart. The maximum anticipated column load is 19 kips. The greatest loads are placed on columns located at the West end where CERC-4 joins a hall leading to CERC-1 and CERC-3. A structural floor slab in this hall is supported at the west end of CERC-4 by columns and at CERC-1/CERC-3 by granular fill of PI < 20 and LL < 35 compacted to 95 Percent of optimum density after D 698.

126. Foundation soil consists of a crust of strong soil (STP blowcount 11 to 18) underlain by 10 to 20 ft of soft (STP 3 to 8) silty clay and clay silt, sandy silts, and silty sands. Total settlement of CERC-3 was estimated at about 1 inch with differential settlement of 0.75 inch (GEO Construction Testing 1985).

127. Detailed elevation profiles were measured in August 1989, Appendix C3, in the halls of building 3296, lines CERC1 through CERC7, and on sidewalk surfaces, lines CERC8, CERC9, and CERC10 in Figure 42. Survey lines 6 and 7 in CERC-4 were measured on the ground floor supported directly by piles. The elevation profile of CERC1, Figure 43a, indicates a rise, then depression from building unit CERC-1 toward CERC-3 with a differential movement of about 0.6 inch, perhaps from long-term consolidation. Similar wavelengths were not

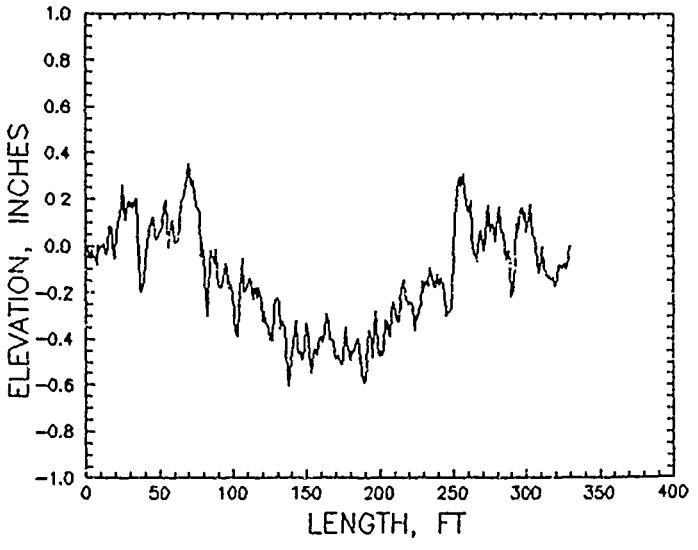

a. CERC1

Figure 43. Elevation profiles of survey lines CERC1, CERC4 and CERC5

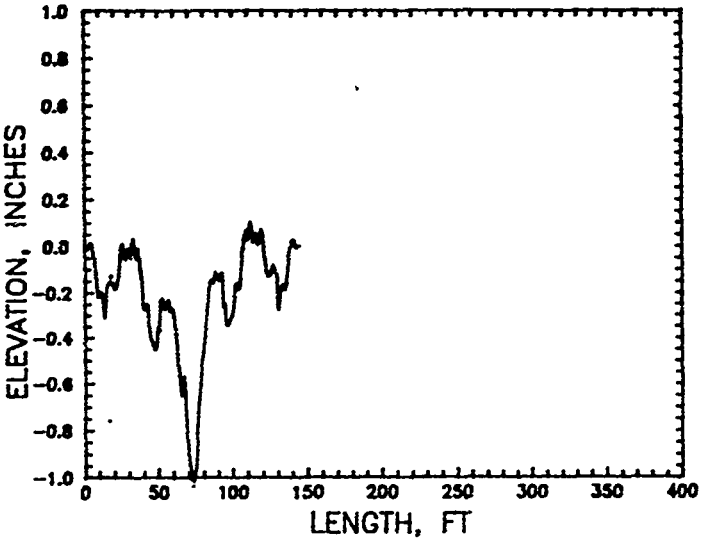

b. CERC4

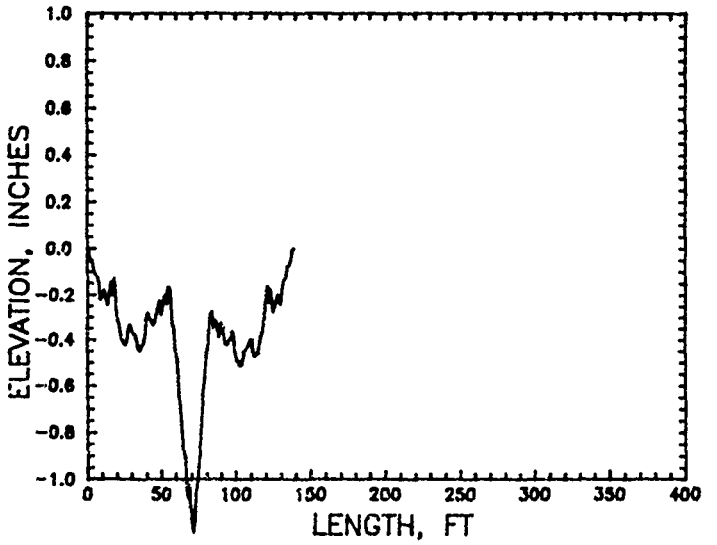

c. CERC5

Figure 43. Concluded

observed in the newer buildings. The elevation profiles of CERC4, Figure 43b, and CERC5, Figure 43c, show settlement exceeding 1 inch at the east end of unit CERC-3, which is probably related to the fractures in the exterior walls observed in building unit CERC-3.

128. Table 13 illustrates dominant frequencies and amplitudes calculated from program FTROPT. The oldest building CERC-1 indicates a highly probable sine wave of about 0.005 cycle/ft or 200 ft wavelength. Line CERC5 in building CERC-3 indicates a highly probable frequency of about 0.02

Table 13. Dominant Waves of Building 3296 Survey Lines

Line	Number of Terms N	Resonant Frequency f_r, cycle/ft	Regression Coefficient r_f^2	Peak Amplitude A_{tp}, in.	Regression Coefficient r_a^2	Wave Type
CERC1	5	0.0048	0.9895	0.1435	0.9651	Sine
	5	0.0185	0.4854	0.0618	0.9391	Cosine
	5	0.0460	0.9973	0.0338	0.4605	Sine
CERC2	5	0.0350	0.0624	0.0694	0.4544	Cosine
CERC3	5	0.0184	0.9801	0.0395	0.8654	Sine
	5	0.0426	0.9550	0.0534	0.8109	Sine
	2	0.0507	1.0003	0.0261	0.9679	Sine
CERC4	3	0.1230	0.9801	0.0257	0.7547	Sine
CERC5	3	0.0223	0.9949	0.1635	0.9988	Sine
	2	0.1102	0.9994	0.0360	1.0000	Cosine
CERC7	2	0.0189	1.0000	0.1544	1.0000	Sine
	2	0.1543	0.9998	0.0232	1.0000	Sine
CERC8	5	0.0465	0.9999	0.1540	0.9949	Sine
	3	0.0446	0.9876	0.1343	0.9990	Cosine
	5	0.1076	0.9558	0.0603	0.0496	Sine
	5	0.1369	0.9261	0.0502	0.5839	Sine
	5	0.1737	0.8230	0.0308	0.7596	Sine
	4	0.2413	0.9979	0.0299	0.4249	Sine
CERC10	5	0.0116	0.9946	0.1540	0.4313	Cosine
	4	0.0233	0.9387	0.0738	0.7500	Cosine
	5	0.0394	0.9928	0.0867	0.8104	Sine
	5	0.0498	0.8463	0.0875	0.7525	Sine
	5	0.0743	0.7435	0.0717	0.5891	Cosine
	3	0.0770	0.9967	0.0365	0.9899	Sine

cycle/ft or wavelength of about 45 ft with a strong 0.16 inch amplitude, which is probably associated with the distortion causing the severe fracture in exterior walls of CERC-3. The maximum observed peak-to-peak amplitude in Figure 43b and 43c is about 1 inch, which is much larger than the 0.3 inch peak-to-peak amplitude of CERC5, Table 13. CERC7 indicates a strong transform amplitude of about 0.15 inch at 0.019 cycle/ft (wavelength of 52 ft), which may be associated with a depression at the west end of CERC-4 where the heavily loaded piles are located. Frequencies characteristic of all these buildings are 0.02, 0.04, and 0.15 cycle/ft (wavelengths of about 50, 25, and

6 ft). Half of these wavelengths appear consistent with spacings between footings and piles. The sidewalk distortion patterns indicate a range of frequencies from 0.02 to 0.15 cycle/ft.

129. Fort Sam Houston. Elevation profilometer surveys recorded in Table C4 were performed in Fort Sam Houston, TX, during February 1, 1990 on the Pest Management Facility, Troop Medical and Dental Clinics, and Maintenance Building. These structures have suffered slight to moderate damage from differential soil movements. The Pest Management Facility and Maintenance Building have floor slopes to promote drainage; therefore, only limited analyses were performed on these initial profilometer surveys because of possible confusion of the slopes with differential movement.

130. Pest Management Facility. This single story rectangular structure located in Fort Sam Houston, TX, was constructed during 1978 and 1979 with load bearing concrete masonry units and a metal roof deck. The structure is supported by a ribbed mat foundation with beam spacings varying from 7 to 23 ft, Figure 44. Beam depth is 30 inches from the mat top, beam width is 12 inches, and mat thickness between stiffening beams is 5 inches. Steel reinforcement in the stiffening beams consists of two number 9 bars placed both top and bottom. The floor surface of the Pest Management Facility (PMF) has built-in slopes to drain rain water away from the open hall along line PMF1. This facility also has a built-in floor rise in line PMF2 connecting with the open hall.

131. The top 18 inches of natural soil is replaced with compacted low plasticity fill. The natural soil consists of about 9 ft of expansive CH clay overburden overlying a thin layer of clayey gravel. Beneath the clayey gravel is the primary formation of Taylor marl of upper Cretaceous age. Strength parameters are assumed similar to the troop medical and troop dental clinics described below.

132. Troop Medical and Dental Clinics. These structures were constructed 1980 and 1981 in Fort Sam Houston. The Troop Medical (TMC) and Dental (TDC) clinics are single story, rectangular brick and concrete masonry structures supported on ribbed mats, Figure 45. Vertical construction joints were closely spaced in the superstructure at approximately 4-ft intervals to increase flexibility. The site slopes down from northwest to southeast at a slope of about 3 percent leading to a grade differential close to 8 ft across

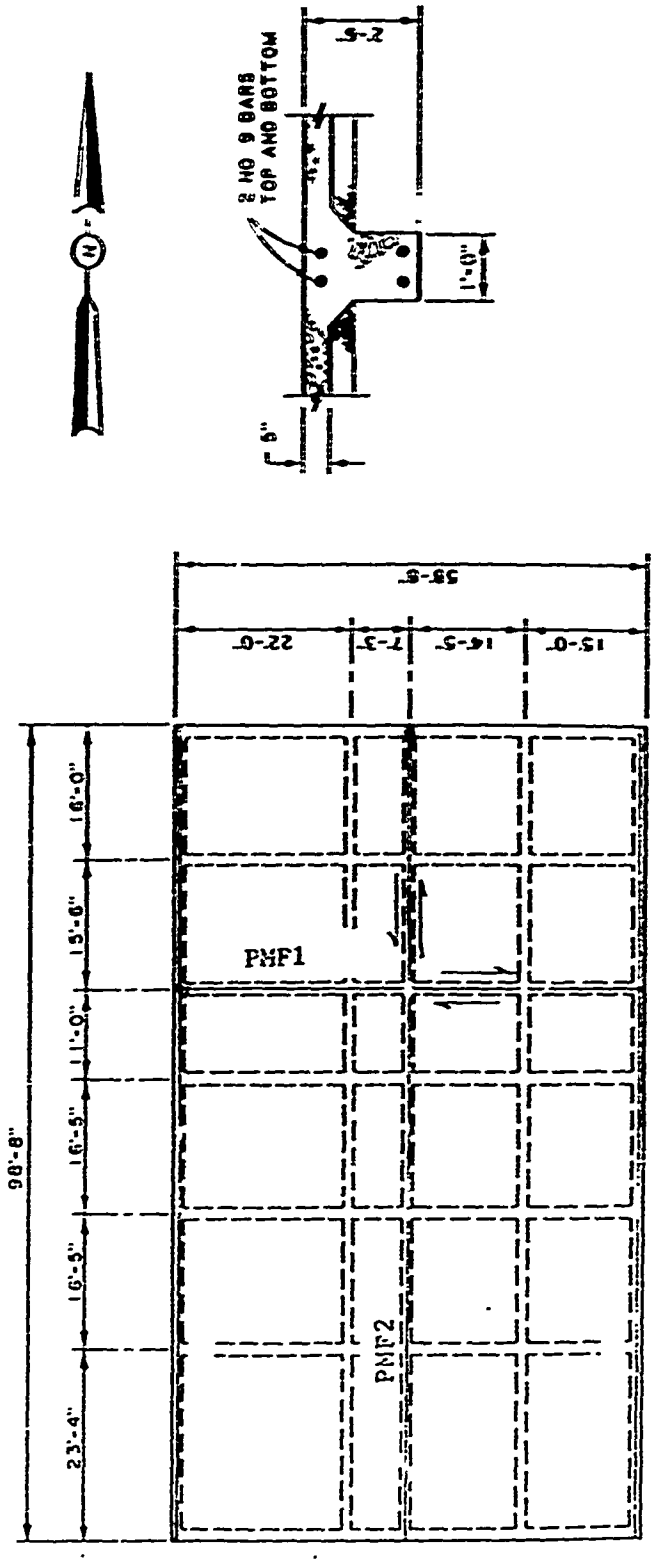

Figure 44. Foundation plan Pest Management Facility

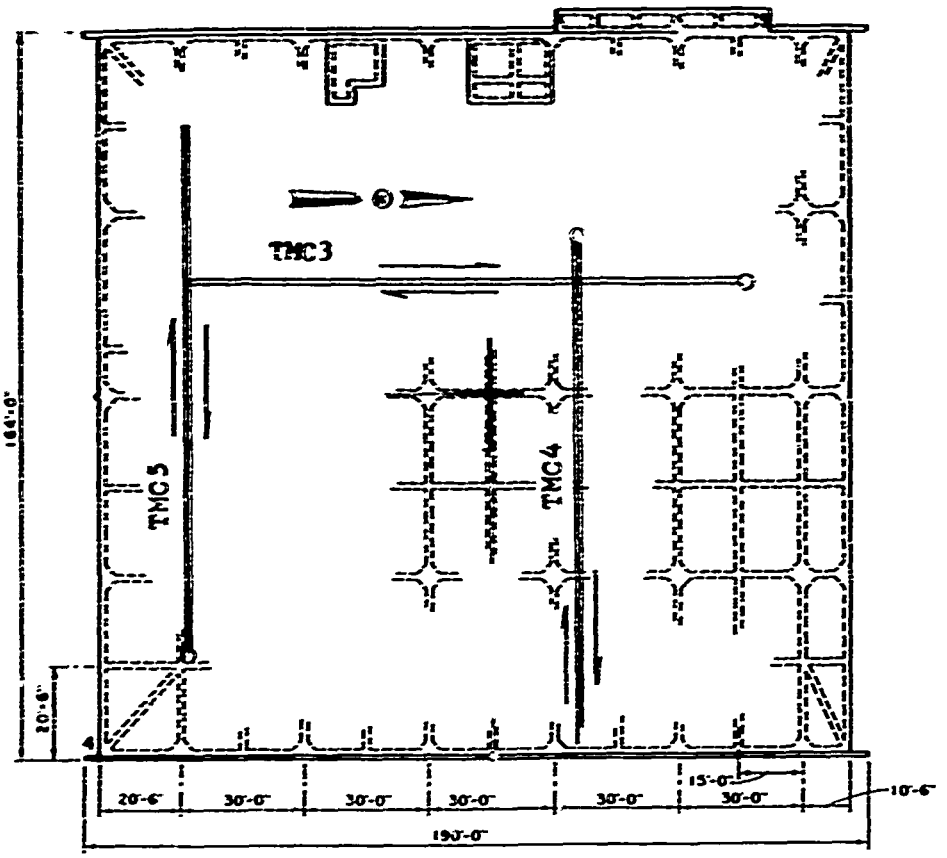

a. TROOP MEDICAL CLINIC

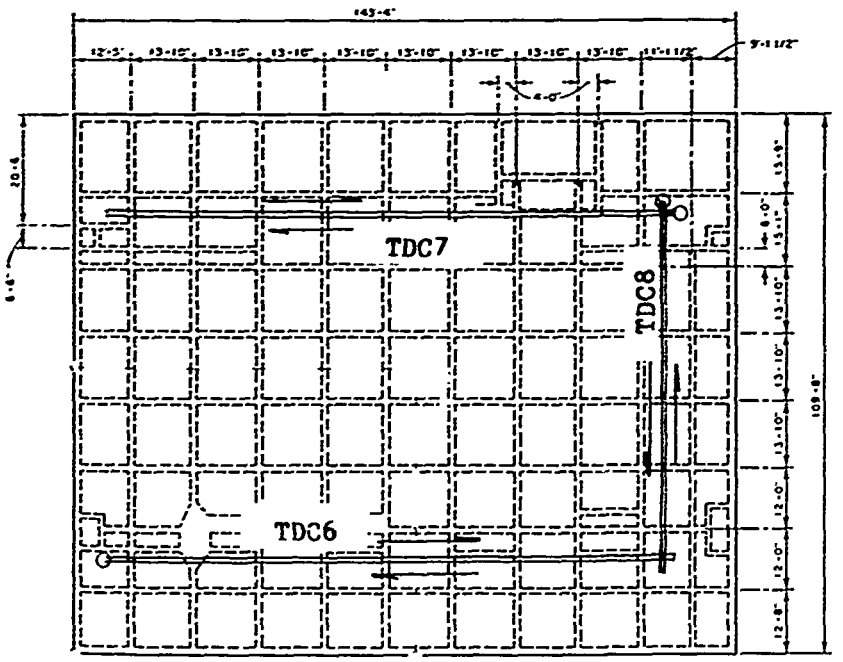

b. TROOP DENTAL CLINIC

Figure 45. Floor plan of Medical and Dental Clinics

the diagonal of both structures. Beam spacings vary from 10 to 15 ft in the TDC and 11 to 30 ft in the TMC. Beam depth of the dental clinic mat is 2 ft 8 inches from the mat top with beam width of 1 ft 4 inches. Beam depth of the medical clinic is 3 ft from the mat top with beam width of 1 ft 6 inches. Thickness of the flat part of the mat is 6 inches. Reinforcement steel consists of three number 9 bars placed both top and bottom in the stiffening beams.

133. Overburden material varies from 6 to 16 ft thick and consists of dark brown to black, gravelly, medium CL to high CH plasticity clay and clayey gravel GC. The clayey gravel contains a perched water table with water level 7 to 12 ft below ground surface. The primary material below the overburden is the Taylor formation of upper Cretaceous age. This material is yellow-brown, calcareous, slightly silty, soft to moderately hard clay shale containing occasional hard marl up to 3 ft thick. The shale is expansive CH jointed and weathered clay up to 50 or 60 ft below ground surface. The soil elastic modulus varies from 200 to 400 ksf within the top 15 ft of soil and 600 to 1000 ksf below 15 ft from the ground surface.

134. The TMC contains a plaster wall with significant cracking parallel with and adjacent to profile line TMC5. The TDC contains a wall with minor cracking and floor distortion adjacent to profile line TDC7.

135. Maintenance Building. The Maintenance Building (MB) is also located in Fort Sam Houston, TX, and consists of a steel frame rectangular building with metal siding and concrete masonry unit walls, Figure 46. Beam depth is 3 ft including the 5 inch thickness of the flat portion of mat between stiffening beams. Beam width is 12 inches. Steel reinforcement consists of two number 11 bars top and bottom in the long direction and two number 7 bars top and bottom in the short direction.

136. Overburden materials consist of about 2 ft of medium plasticity (CL) black clay, 3 to 4 ft of high plasticity (CH) brown clay, approximately 7 ft of white, calcareous medium plastic (CL) clay, and about 3 ft of clayey gravel. The gravel contains a perched water table with water level beginning about 14 ft below ground surface. The primary material underlying the overburden is a tan to gray, weathered and jointed clay shale of the Anacacho formation of Cretaceous age. The soil elastic modulus is about 400 ksf down to 30 ft and 800 ksf or more below this depth.

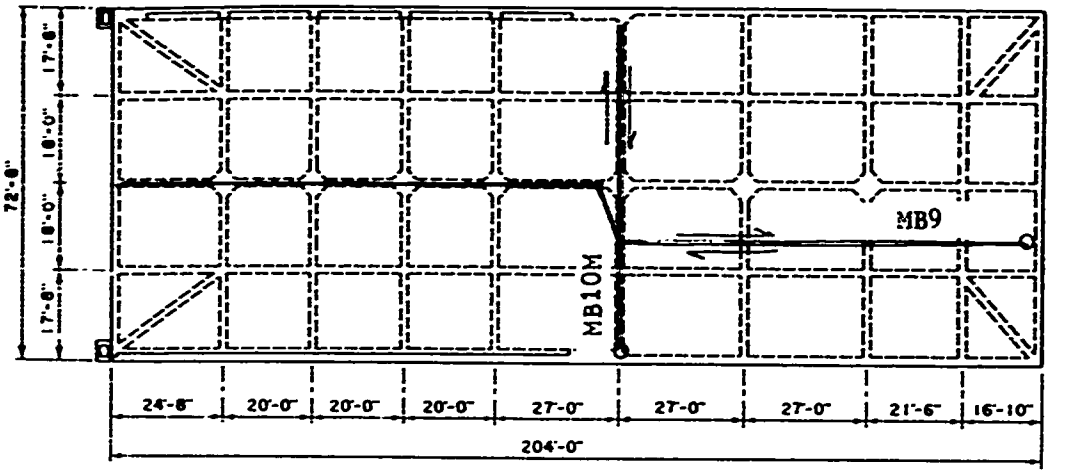

Figure 46. Plan of the Maintenance Building

137. Table 14 provides dominant frequencies and transform amplitudes of the survey lines made in the troop medical clinic and troop dental clinic. The pest management facility and maintenance building had built-in slopes that assist drainage and that may influence the results; therefore, these waves were not included in the table.

138. Red River Army Depot. Line profilometer surveys, Table C5, were made on several old facilities constructed 40 to 50 years ago at the Red River Army Depot that had suffered severe and obvious deformations from the foundation soils to assist the analysis of performance rating systems. These

Table 14. Dominant Waves of Old Facilities, Red Rivery Army Depot

Line	Number of Terms N	Resonant Frequency f_r, cycle/ft	Regression Coefficient r_f^2	Peak Amplitude A_{tp}, in.	Regression Coefficient r_a^2	Wave Type
TMC3	4	0.0278	0.9417	0.0504	0.7918	Cosine
TMC4	5	0.0285	0.9999	0.0573	0.8321	Sine
TMC5	3	0.0583	0.9989	0.0216	0.9709	Sine
	2	0.0769	0.9973	0.0234	1.0000	Sine
TDC6	5	0.0036	0.9973	0.2366	0.9795	Sine
	5	0.0326	0.9992	0.1090	0.9817	Sine

facilities are the headquarters building (HDQ), Dynamometer building (DYNA) and Warehouse A (WHS). Soil and design information for these facilities were not available.

139. The headquarters building consists of a brick central unit and wings, Figure 47a. Two line surveys, HDQ1 and HDQ3, were conducted in the north-south direction on the slab-on-grade of the ground floor. The wing walls are supported on piles. The north wing had been thrust up as indicated by the elevation profile, Figure 47b, causing a 1/150 slope that interferes with the office functions of the building.

140. The dynamometer facility is a long narrow metal frame structure consisting of a basement and main floor, Figure 48. The basement contains the DC converters and power supply for the equipment used to test engines on the main floor. Line surveys were made on both floors to check how distortions can be attenuated on an upper level. DYNA4 and DYNA5 were made on the main floor and DYNA6 and DYNA7 were made on the basement slab-on-grade. The basement slab-on-grade had been thrust up nearly 5 inches as indicated by the elevation profile of DYNA7 made in the short direction on the basement floor, Figure 45a, causing severe longitudinal fractures in this slab. The elevation profile of DYNA5 in the short direction on the main floor, Figure 49a, indicates a slump in the short direction.

141. Warehouse A is a large single story masonry rectangular structure, Figure 50. This warehouse exhibits severe repaired fractures up to 1 inch wide in the walls of the north end. Numerous other less severe fractures occur in the other walls. Five profilometer survey lines were obtained in the warehouse as illustrated in Figure 50. Figure 51 shows the elevation profiles of survey lines WHS1, WHS2 and WSH5, which are parallel with the short direction. WHS1 (dashed) and WHS2 (solid) are near the north end. WHS1 was measured on the narrow slab supported by drilled shafts and which supports the north end wall. WHS2 is on the slab-on-grade isolated from the north end narrow slab, but adjacent to WHS1. Line WHS1 and WHS2 settle in the middle, but heave nearly 4 inches toward the west end of the survey line leading to a differential heave of about 6 inches. Line WHS5, taken several hundred feet south of the north end, but parallel with WHS1 and WHS2 is similar to lines WHS1 and WHS2, but has much less distortion.

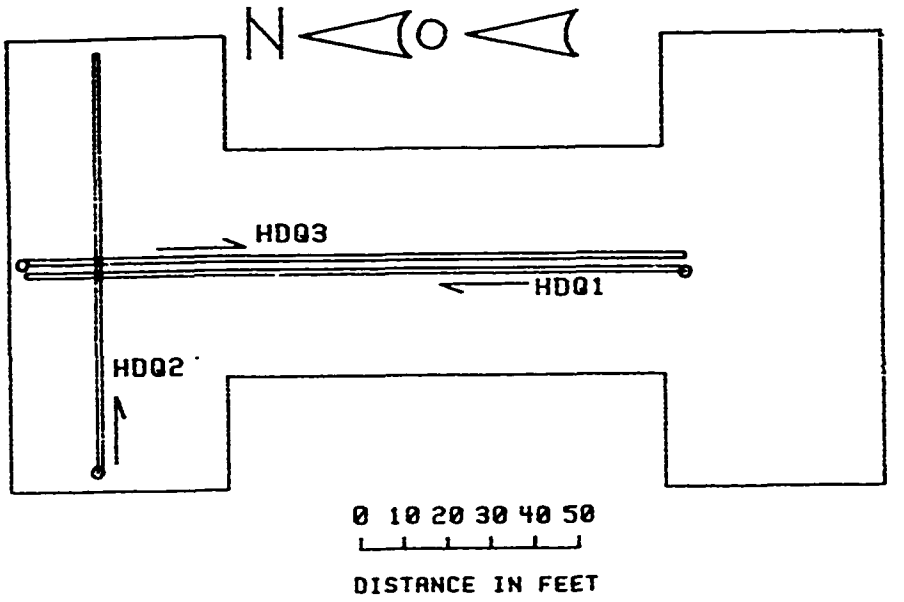

a. HEADQUARTERS BUILDING

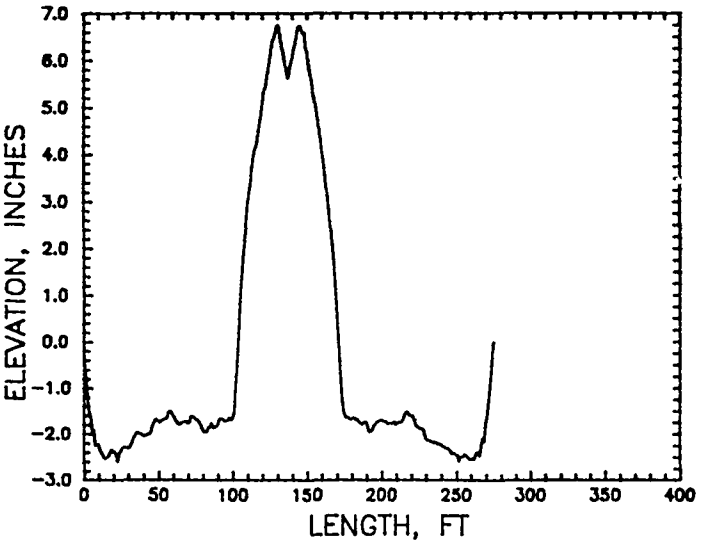

b. ELEVATION PROFILE OF SURVEY LINE HDQ1

Figure 47. Layout and elevation profile of the headquarters building, RRAD

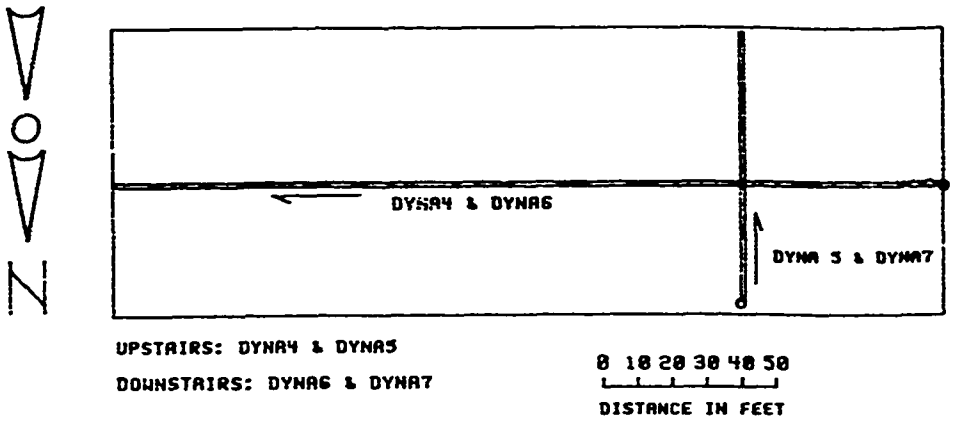

Figure 48. Dynamometer facility, RRAD

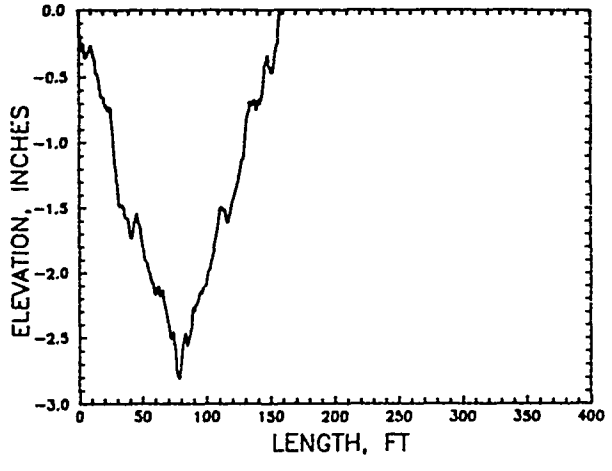

a. MAIN FLOOR, DYNA5

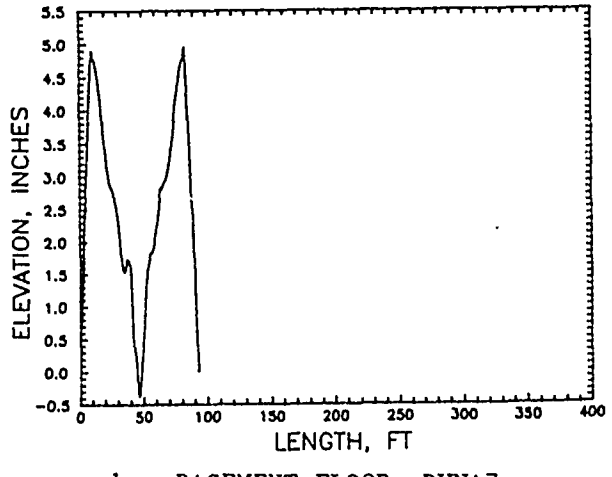

b. BASEMENT FLOOR, DYNA7

Figure 49. Short direction elevation profiles of the dynamometer facility

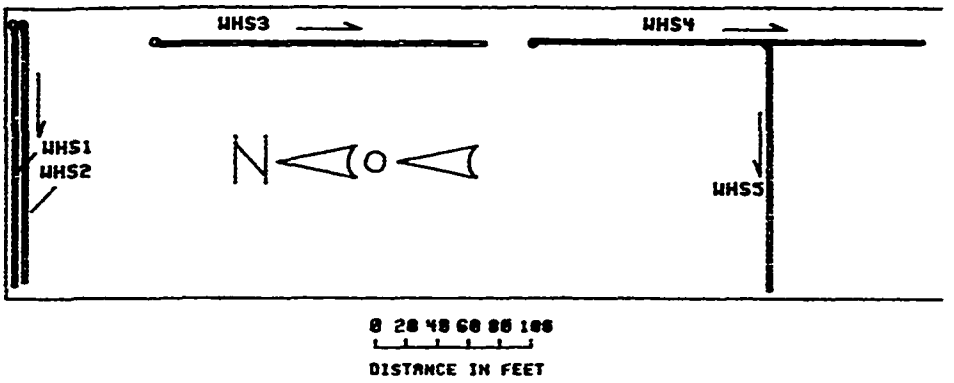

Figure 50. Layout of Warehouse A

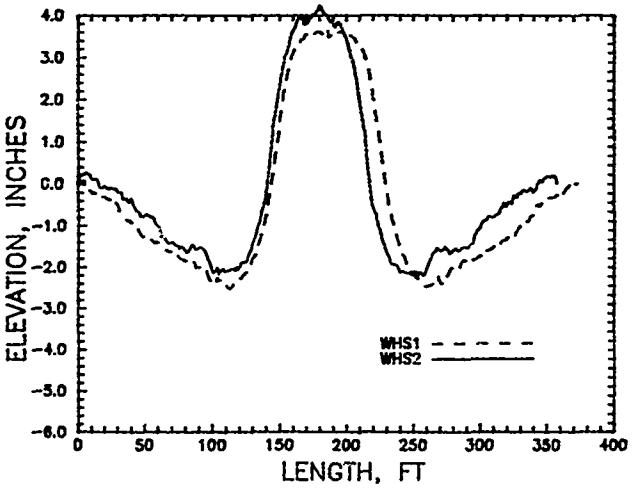

a. SURVEY LINES WHS1 AND WHS2

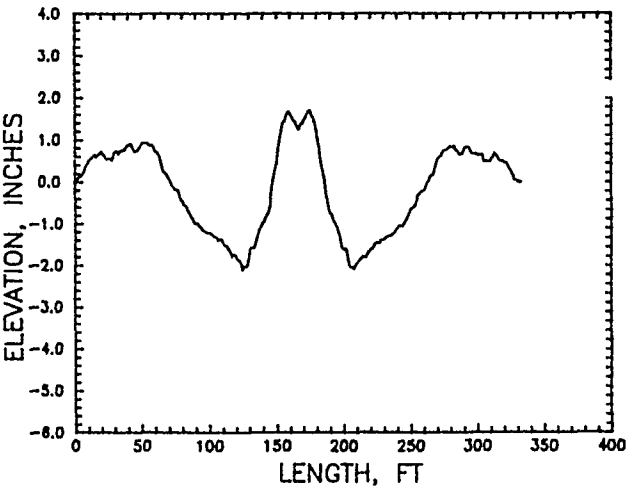

b. SURVEY LINE WHS5

Figure 51. Elevation profiles of survey lines WHS1, WHS2, and WHS5 from Warehouse A, RRAD

142. Table 15 illustrates the dominant frequencies of the discrete wavelengths calculated from program FTROPT for these old facilities of the RRAD. Lines HDQ1 and WHS1 have frequencies 0.0038 and 0.0035 (wavelengths 263 and 286 ft) with large half transform amplitudes of 2.8 and 1.7 inches. Peak-to-peak amplitudes are on the order of 10 and 7 inches, which are reasonably consistent with the observed elevation profiles for these facilities in

Table 15. Dominant frequencies and amplitudes for old facilities, RRAD

Line	Number of Terms N	Resonant Frequency f_r, cycle/ft	Regression Coefficient r_f^2	Peak Amplitude A_{tp}, in.	Regression Coefficient r_a^2	Wave Type
HDQ1	5	0.0038	0.9905	2.7753	0.9862	Sine
	5	0.0465	0.2340	0.2475	0.9332	Sine
	5	0.2493	0.8094	0.0577	0.5686	Sine
HDQ2	5	0.0866	0.9866	0.0742	0.4820	Sine
	3	0.1007	0.9997	0.0499	0.9841	Sine
HDQ3	5	0.0698	0.9206	0.0815	0.8856	Sine
DYNA4	5	0.0222	0.9762	0.1246	0.9396	Sine
	5	0.0263	0.9105	0.0999	0.9112	Sine
	2	0.1109	1.0030	0.0242	0.9989	Cosine
DYNA5	2	0.0498	0.9990	0.1263	1.0132	Sine
DYNA6	5	0.0224	0.7000	0.2645	0.4692	Cosinc
	5	0.0687	0.7591	0.0449	0.6015	Cosine
	5	0.1363	0.7613	0.0271	0.7401	Sine
	2	0.1620	0.9950	0.0215	0.9999	Cosine
WHS1	5	0.0035	0.9981	1.7000	1.0000	Sine
WHS2	5	0.0058	0.4760	1.7612	0.9582	Sine
WHS3	5	0.0128	0.9945	0.1530	0.9413	Cosine
	5	0.0380	0.9988	0.0622	0.9999	Sine
	3	0.0474	0.9841	0.0326	0.8775	Sine
	5	0.0701	0.9888	0.0316	0.6909	Sine
WHS4	5	0.0106	0.9988	0.1342	0.5513	Cosine
	5	0.0832	0.7891	0.0351	0.4962	Sine
	2	0.1286	1.1121	0.0220	0.9892	Sine
WHS5	5	0.0065	0.9997	0.6535	0.9959	Sine
	5	0.0770	0.9078	0.0208	0.5779	Sine

Figures 47b and 51a. Amplitudes tend to decrease with increasing frequencies as previously observed.

Fractal Pattern

143. The fractal pattern of actual measurements of the elevation profiles is similar to that in Figure 33 indicating that floor distortions may be modeled by wave motion.

Performance Ratings

144. The elevation profiles of the new and existing construction provide useful field data toward development of simple indices for rating performance of facilities. Indices selected for analyzes are F-numbers FL and FF, wave index WI, maximum relative thickness D_{relm}, macrorelief index MRI and mean angular distortion β_m. Reproducibility of these indices are all within 10 percent or less. The influence of length was checked prior to comparison of these indices as performance raters.

Influence of Length on Rating Systems

145. Ratings using the selected systems were calculated as a function of length for survey line 3 of building 333 to determine how the length of the readings may actually influence field measurements of distortion patterns. The F-numbers increase with floor length up to about 25 at 100 ft, Figure 52,

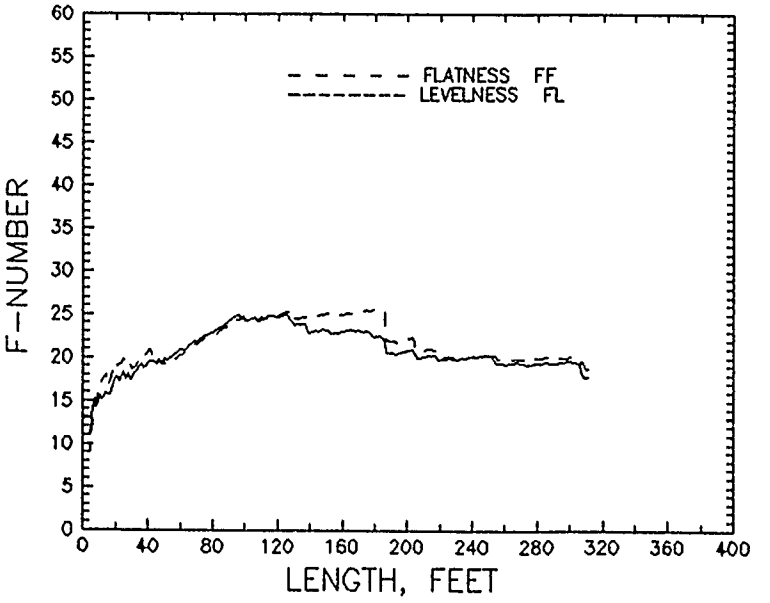

Figure 52. F-number distribution of mat foundation supporting building 333 for NRE-311

indicating overall increasing flatness and levelness up to this 100 ft. These numbers decrease to a minimum of 18 at 311 ft indicating decreasing flatness and levelness, which is attributed to the dip in the floor near 185 ft in Figure 37a. Both FF and FL F-numbers are similar indicating low bias or a standard quality floor. The MRI, Figure 53, and WI, Figure 54, both have similar patterns initially increasing then decreasing and increasing after 185 ft with increasing length. The mean angular distortion and mean tilt, Figure 55, also have similar trends. The variation in MRI with length appears to indicate greater sensitivity than the other indices.

146. The changes in these ratings with length are attributed to an uneven distribution of floor distortion over the length of the mat foundation, especially near the south end of the building and the expansion joint at length 185 ft. These selected rating parameters: F-numbers, WI, MRI and β_m therefore appear sensitive to variations in floor distortion which is a needed characteristic for providing an adequate rating system. The maximum relative thickness D_{relm} calculated from an elevation profile, in contrast, is not dependent on measurement length, but indicates the extent of the worst distortion and its location within a given measurement length. Mean tilt ω_m will not be investigated further because tilt is not a characteristic of distortion damage such as β_m.

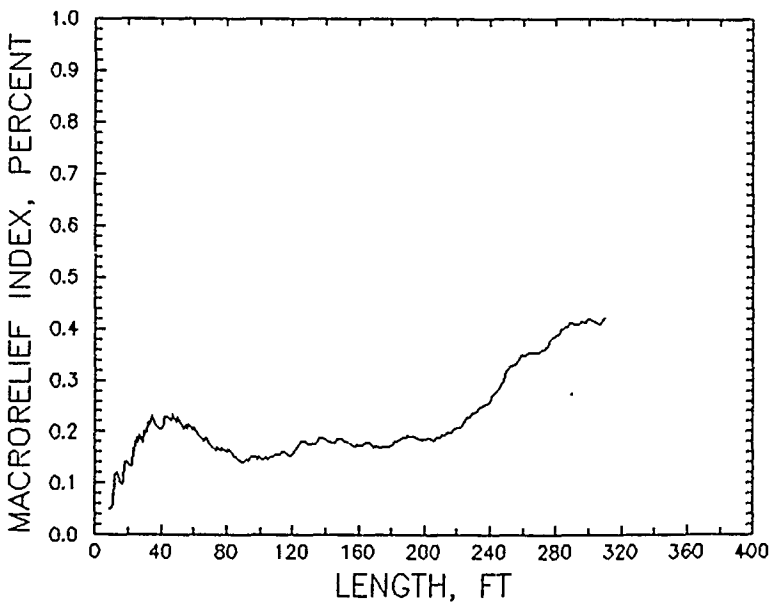

Figure 53. Macrorelief Index MRI distribution of mat foundation supporting building 333 for NRE=311

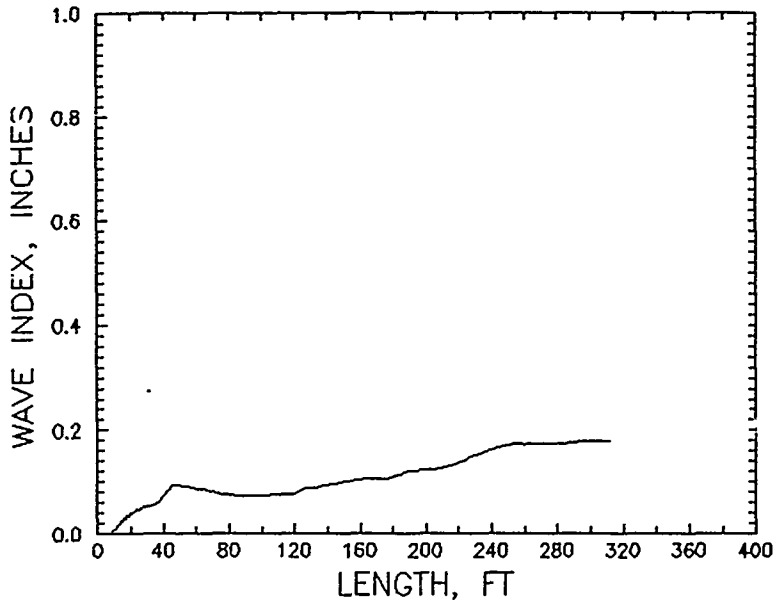

Figure 54. Wave Index WI distribution of mat foundation supporting building 333 for NRE=311

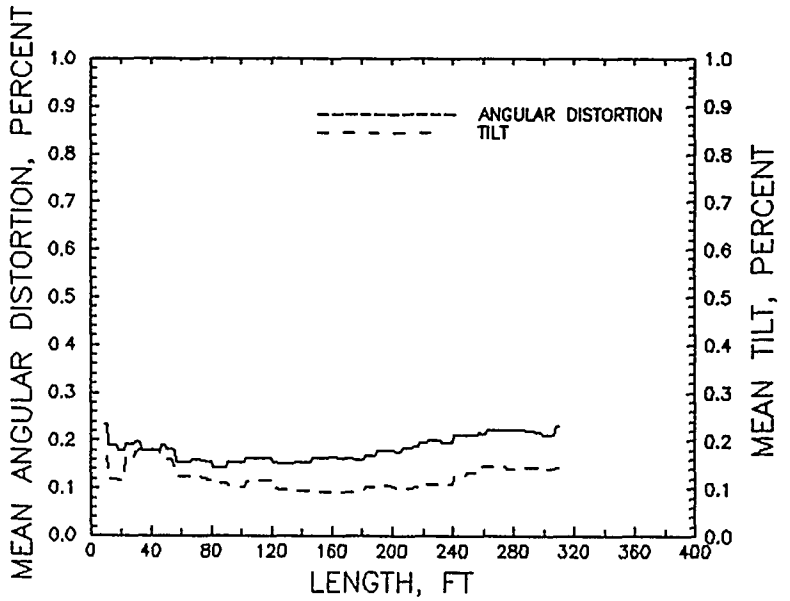

Figure 55. Distribution of mean angular distortion β_m and mean tilt ω_m with length of Building 333

Comparison of Performance Rating Systems

147. Table 16 provides values of the selected rating indices - FL, FF, WI, MRI, β_m, and D_{relm} - of all elevation profiles of the surveyed facilities. The ratings for floors that are supported by piles or had slopes for drainage will be useful for comparison of results from later surveys. An initial

Table 16. Performance Ratings of Surveyed Facilities

a. New Construction

Facility	Date of Survey	Visual Observations	Type of Loop	Survey Line	Selected Rating Systems								
					F-Numbers		Wave Index WI	Macro-relief Index, MRI	Mean Angular Distortion β_m, Percent	Maximum Relative Thickness			
					FL	FF				D_{relm}, ft	Location, ft	Span, ft
Building 333	05/11/87	Floor cracks near length 200 ft	First Half	3	17.80	18.70	0.1788	0.4222	0.2305	11.9893	263	27
			Full	3	17.62	17.83	0.1798	0.4844	0.2244	13.1557	357	31
Building 312		Automated lift trucks ram racks	First Half	4	28.42	28.59	0.0746	0.1606	0.1278	5.3440	142	11
				5	34.45	32.60	0.0807	0.1388	0.1077	2.9691	46	11
				6	27.10	33.43	0.1596	0.1916	0.1345	6.4261	99	38
				7	24.99	24.60	0.0965	0.1677	0.1497	5.0815	231	16
				10	27.92	27.43	0.0903	0.1509	0.1340	4.1074	63	12
				11	28.01	28.25	0.0980	0.1751	0.1227	4.9810	223	25
				12	22.19	26.75	0.1330	0.1542	0.1873	8.0476	168	37
				13	25.67	31.83	0.1602	0.1874	0.1421	7.0986	103	41
				14	28.20	28.94	0.1019	0.1542	0.1305	4.3085	117	10
				15	23.07	26.35	0.1158	0.1681	0.1850	7.3520	43	16
				16	28.62	28.49	0.0784	0.1575	0.1244	4.3359	141	9
				17	21.59	25.59	0.1738	0.2165	0.1821	5.7091	92	35
			Full	4	26.12	24.95	0.0909	0.1761	0.1347	5.3440	142	11
				5	32.62	30.97	0.0831	0.1630	0.1090	3.3783	343	12
				6	25.20	27.62	0.1514	0.2264	0.1402	6.4261	99	38
				7	26.30	26.20	0.1034	0.3044	0.1497	8.3854	296	28
				10	26.74	25.21	0.1049	0.2370	0.1385	5.3583	294	18
				11	27.98	27.95	0.1177	0.2630	0.1255	6.0122	301	24
				12	23.39	27.72	0.1600	0.1620	0.1708	8.0476	168	37
				13	24.89	28.07	0.1579	0.2027	0.1494	7.0986	103	41
				14	28.24	29.54	0.1290	0.1955	0.1276	6.2275	219	43
				15	22.53	24.57	0.1120	0.1751	0.1757	7.3520	43	16
				16	26.28	25.05	0.0886	0.1688	0.1446	4.9243	223	11
				17	22.06	24.11	0.1935	0.1989	0.1769	7.0139	276	39

Table 16. (Continued)

Facility	Date of Survey	Visual Observations	Type of Loop	Survey Line	Selected Rating Systems							
					F-Numbers		Wave Index WI	Macro-relief Index, MRI	Mean Angular Distortion β_m, Percent	Maximum Relative Thickness		
					FL	FF				D_{reim}, Ft	Location, Ft	Span, Ft
Automated Technology Center	12/12/89	Large diagonal, jagged crack in dry wall appeared about 12/28/89 following unusual cold weather to 0° F; crack is adjacent to ACT1 about 60 ft from south end < 0.3 inch wide from floor up to 8 ft high	First Half	ATC1	14.38	13.91	0.1829	0.3158	0.2239	16.3441	229	56
				ATC2	15.60	12.10	0.0455	0.1690	0.1993	2.8157	38	6
				ATC3	21.14	23.85	0.0540	0.1336	0.1777	2.2181	31	7
				ATC4	14.18	11.64	0.0665	0.1748	0.2240	4.7187	15	11
				ATC5	15.12	16.13	0.0847	0.1699	0.2953	6.0474	38	12
				ATC6	16.63	15.65	0.0868	0.1511	0.2617	4.4020	30	20
				ATC7	14.83	14.17	0.2086	0.4457	0.2454	5.8649	31	14
				ATC8	16.27	18.69	0.1541	0.2249	0.2278	8.6827	10	26
				ATC9	15.95	17.96	0.1480	0.2333	0.2564	9.3981	15	32
				ATC10A	17.82	17.76	0.1185	0.1825	0.2005	3.8556	55	7
				ATC11	13.96	14.43	0.1105	0.2014	0.3027	5.6894	69	8
	02/21/90			ATC1	15.11	14.55	0.1840	0.3331	0.2318	16.1310	233	53
	12/12/89		Full	ATC1	14.75	14.25	0.2029	0.5627	0.2325	18.7418	260	58
				ATC2	16.62	12.73	0.1289	0.2413	0.2010	2.8157	38	6
				ATC3	20.92	22.78	0.0895	0.1488	0.1821	7.6883	101	15
				ATC4	14.91	12.37	0.0896	0.2112	0.1931	6.0567	86	14
				ATC5	16.19	16.73	0.2019	0.2689	0.2827	6.0581	87	12
				ATC6	16.63	15.25	0.0814	0.1471	0.2599	6.6845	99	20
				ATC7	15.22	14.34	0.2638	0.4147	0.2278	8.4740	158	22
				ATC8	16.66	18.46	0.1257	0.2144	0.2246	8.6827	10	26
				ATC9	16.30	17.94	0.1353	0.2305	0.2532	11.4439	198	31
				ATC10A	19.51	19.05	0.1454	0.2071	0.1923	5.5272	160	19
				ATC11	13.76	13.70	0.1499	0.2319	0.2713	9.5875	84	25
	02/21/90			ATC1	15.88	15.53	0.2067	0.5283	0.2457	17.3940	272	41

Table 16. (Continued)

b. Existing Construction

Facility	Date of Survey	Visual Observations	Type of Loop	Survey Line	Selected Rating Systems: F-Numbers FL	F-Numbers FF	Wave Index WI	Macro-relief Index, MRI	Mean Angular Distortion β_m, Percent	Maximum Relative Thickness D_{relm}, Ft	Maximum Relative Thickness Location, Ft	Maximum Relative Thickness Span, Ft
Coastal Engineering Research Center	07/20/89	Minor cracking less 0.063 inch below exterior brick of building unit CERC-1 Severe cracks unit CERC-3, CERC4 and CERC5, of 0.25 inch toward top middle of wall	First Half	CERC1	19.76	20.04	0.1094	0.1718	0.1987	5.5162	45	12
				CERC2	17.38	18.12	0.1294	0.1867	0.2134	6.1643	14	14
				CERC3	23.22	23.24	0.0943	0.1621	0.1395	6.8294	17	20
				CERC4	20.86	23.25	0.1201	0.1849	0.1565	2.6593	50	8
				CERC5	21.66	23.98	0.0985	0.1765	0.1071	3.6329	29	11
				CERC6	19.21	17.57	0.1143	0.1731	0.1806	8.1403	56	21
				CERC7	13.63	11.81	0.0628	0.1755	0.2530	2.3833	21	5
				CERC8	8.10	14.63	1.2149	1.1303	0.4745	38.7845	121	97
				CERC9	12.44	12.62	0.2214	0.3145	0.2735	6.7180	63	18
				CERC10	10.02	10.89	0.3908	1.8920	0.4102	10.8663	161	50
			Full	CERC1	20.71	20.73	0.1061	0.3131	0.2245	5.7944	254	12
				CERC2	16.82	17.64	0.1172	0.2276	0.2584	6.4958	152	21
				CERC3	23.79	23.37	0.1020	0.1630	0.1472	6.8294	17	20
				CERC4	22.20	24.20	0.2261	0.2604	0.1463	7.7983	86	19
				CERC5	23.40	25.28	0.2160	0.2103	0.1269	13.7278	69	29
				CERC6	19.51	17.72	0.1242	0.1776	0.1670	8.1403	56	21
				CERC7	14.44	12.26	0.1454	0.1824	0.2267	10.0346	42	19
				CERC8	8.53	16.02	1.1743	1.2910	0.3587	38.7845	121	97
				CERC9	13.12	13.20	0.2655	0.3739	0.3036	7.1244	88	19
				CERC10	10.83	11.67	0.3642	1.7346	0.4397	10.4794	80	37
Pest Management Facility	02/01/89	Multiple diagonal wall fractures up to 0.5 inch; negligible fractures in mat; floors constructed with slope	First Half	PMF1	7.41	22.73	0.8575	0.4218	0.2969	5.5042	51	18
				PMF2	6.51	15.68	0.9680	1.1502	0.3243	8.3504	21	12
			Full	PMF1	7.79	22.07	0.9163	0.4876	0.2637	21.9341	51	54
				PMF2	6.83	15.90	0.8206	1.2623	0.2541	9.4979	159	13
Troop Medical Clinic	02/01/89	Significant cracking in plaster walls adjacent line TMC5 up to 0.2 inch wide	First Half	TMC3	21.59	23.33	0.2008	0.3221	0.1822	8.1598	10	22
				TMC4	26.15	24.89	0.0768	0.1881	0.1628	4.3590	92	10
				TMC5	18.40	21.50	0.1947	0.3503	0.1762	6.5963	112	13
			Full	TMC3	22.43	23.73	0.2027	0.5148	0.1620	12.0680	245	42
				TMC4	27.19	26.11	0.0982	0.1828	0.1317	5.3678	136	10
				TMC5	18.91	21.73	0.2856	0.4685	0.1988	23.6370	158	50

Table 16. (Continued)

Facility	Date of Survey	Visual Observations	Type of Loop	Survey Line	Selected Rating Systems: F-Numbers FL	F-Numbers FF	Wave Index WI	Macro-relief Index, MRI	Mean Angular Distortion β_m, Percent	Maximum Relative Thickness D_{relm}, Ft	Maximum Relative Thickness Location, Ft	Maximum Relative Thickness Span, Ft
Troop Dental Clinic	02/01/89	Satisfactory overall performance; minor cracking and floor distortion adjacent line TDC7	First Half	TDC6	16.77	17.61	0.1363	0.2100	0.2052	8.7688	7	23
				TDC7	15.83	17.34	0.3070	0.2538	0.2466	10.6478	30	31
				TDC8	14.08	20.64	0.1523	0.1858	0.2437	8.6779	62	17
			Full	TDC6	17.43	18.64	0.1353	0.2013	0.2065	8.8534	259	24
				TDC7	16.42	18.07	0.2709	0.3256	0.2674	10.6759	142	35
				TDC8	14.40	20.21	0.2610	0.2069	0.2450	8.6779	62	17
Maintenance Building	02/01/89	Satisfactory overall performance; minor cracking in floor slab; floor sloped for drainage; no wall distress	First Half	MB9	13.83	16.03	0.2400	0.2446	0.2240	12.1019	99	19
				MB10M	10.10	14.83	0.8220	0.5559	0.3488	13.0039	63	27
			Full	MB9	13.65	16.30	0.2375	0.2578	0.2024	12.8876	325	23
				MB10M	9.70	13.61	0.9218	0.6374	0.4405	38.7832	71	69
Headquarters RRAD	04/26/90	Diagonal cracking of wings and corners; wing distortion disrupts area function due to high 1/150 slope; original building okay	First Half	HDQ1	6.38	12.71	1.2868	1.5045	0.5441	49.4323	98	72
				HDQ2	5.88	11.99	1.4450	1.2318	0.4238	5.2327	53	18
				HDQ3	7.00	14.66	1.2849	2.0454	0.4814	48.9375	41	71
			Full	HDQ1	6.82	13.90	1.8013	2.8850	0.5639	55.0484	217	120
				HDQ2	6.29	13.96	1.1994	1.0105	0.3797	20.2457	64	47
				HDQ3	7.10	12.69	0.8438	1.7821	0.4369	48.3563	160	107
Dynamometer Facility RRAD	04/26/90	Visible basement floor distortion due to soil center heave; major longitudinal cracks in basement floor 0.375 to 0.625 inch wide	First Half	DYNA4	18.07	20.88	0.2681	1.2612	0.2234	15.8810	79	35
				DYNA5	17.93	20.84	0.1158	0.1196	0.1831	8.0966	34	21
				DYNA6	8.14	8.96	0.8719	1.1712	0.4317	45.4885	137	114
				DYNA7	4.17	9.66	0.6193	0.4736	0.3263	6.6992	83	19
			Full	DYNA4	18.77	21.02	0.2350	0.3775	0.2152	15.8810	79	35
				DYNA5	19.01	21.91	0.3891	0.8015	0.2021	13.0649	92	102
				DYNA6	9.65	10.72	0.7147	1.3818	0.3698	45.4885	137	114
				DYNA7	4.24	9.90	1.3121	0.5296	0.6573	41.4954	37	73

Table 16. (Concluded)

Facility	Date of Survey	Visual Observations	Type of Loop	Survey Line	Selected Rating Systems: F-Numbers FL	F-Numbers FF	Wave Index WI	Macro-relief Index, MRI	Mean Angular Distortion β_m, Percent	Maximum Relative Thickness: D_{relm}, Ft	Location, Ft	Span, Ft
Warehouse A RRAD	04/27/90	Significant cracks North wall up to 1 inch wide running full height adjacent lines WHS1 and WHS2; cracks to 0.25 inch in wall parallel with WHS4; WHS5 parallel with WHS1 but 500 ft South	First Half	WHS1	13.74	23.98	0.7782	2.2927	0.2717	18.4654	111	63
				WHS2	12.23	20.92	0.8104	1.7825	0.3432	70.2742	124	136
				WHS3	19.62	23.02	0.2506	0.4992	0.1805	7.0535	110	18
				WHS4	15.43	18.00	0.4339	0.9971	0.2222	27.1071	121	71
				WHS5	14.60	22.15	0.6425	0.9154	0.2227	52.2706	127	101
			Full	WHS1	14.57	24.13	0.9211	2.3586	0.2882	23.3760	262	59
				WHS2	12.90	20.33	1.0290	2.0025	0.3624	74.7699	235	149
				WHS3	20.67	23.40	0.2390	0.5657	0.1972	7.0535	110	18
				WHS4	15.96	18.71	0.4557	1.4083	0.2527	27.1071	121	71
				WHS5	15.08	22.53	0.8197	1.1317	0.2319	52.2706	127	101

Note: Program ADATG was modified to increase detection of span length to 150 ft for survey line WHS2

observation of these ratings is that some differences occur between the half loop and full loop surveys. For example, F-numbers FL and FF, wave index WI and mean angular distortion are overall measures of floor distortion independent of slope. Repeating the elevation survey over a given length provides more data on the distortion pattern of the given length and improves accuracy of the rating. The full loop is therefore recommended and used for these indices. The largest maximum relative thickness D_{relm} is nearly always calculated for the full loop because the full loop considers both forward and reverse elevation points providing greater opportunity for reading larger distortions at a particular location. The full loop also permits program ADATG to pick up distortions at the far end of a survey line such as edge heave or edge settlement because the calculation of D_{relm} is based on the span and depression between peak waves. The full loop is also recommended and used for D_{relm}. The macrorelief index MRI is sometimes much larger for the full loop than the half loop because MRI is calculated relative to an average linear regression line through all the elevation points. The full loop may reduce significance of the regression line causing MRI to be greater.

148. A cursory examination of all the rating indices in Table 16a for buildings 312 and 333 show that the floor of building 312 is significantly flatter than the floor of building 333. The floor of building 312, however, is still too distorted for the automated lift trucks to operate efficiently.

149. Survey line ATC1 of the ATC facility, Table 16a, was measured prior to the appearance of a large crack in the dry wall adjacent to ATC1 about December 28, 1989. D_{relm} of ATC1 is 18.7 ft for the full loop, which is the largest value of any of the D_{relm} values and the location of this D_{relm} is where the crack is located. The other indices calculate that some of the other survey lines may have more overall distortion than ATC1. D_{relm} appears capable of indicating potential damage for a particular distortion.

150. The ratings for the basement survey lines of the dynamometer facility, Table 16b, tend to show more distortion than the upper floor consistent with the major floor cracks observed in the basement floor. The F-numbers, WI, β_m , and D_{relm} appear most consistent with the observed damage.

151. Survey lines WHS1 and WHS2 of warehouse A, Table 16b, indicates the potential for most damage according to the values for F-numbers, WI, MRI, and β_m. D_{relm} also indicates the most potential for damage in survey line

WHS2 after program ADATG was modified to extend detected span lengths to 150 ft. Visual observations of the warehouse indicate that the north wall had been heavily damaged by soil distortions. Some cracking also occurs in the wall parallel with survey line WHS4.

152. The surveys shown in Table 17 were performed on facilities with floors with originally level surfaces that exhibited various degrees of damage. The full loops are used for F-numbers FL and FF, wave index WI, mean angular distortion β_m and D_{relm}, while the half loop is used for the macrorelief index MRI. The ratings of each facility in Table 17 are compared in Table 18 with survey lines that are adjacent to the most heavily damaged walls in a particular structure to determine performance rating systems that may be most effective. These ratings consider total deformations including floor distortions from construction. The results in Table 18 indicate that D_{relm} is totally consistent with indicating the observed damage. D_{relm} also correlates reasonably well with observed crack widths in walls of these facilities, excluding the Headquarters building in RRAD, as shown in Table 19. The Headquarters building suffered severe floor distortion exceeding 1/250 reducing operational efficiency, but the exterior brick walls exhibited only minor cracks. WI as defined in this report appears nearly as consistent as D_{relm}. D_{relm} as low as 8 to 10 and WI as low as 0.2 appear to indicate a potential for at least minor damage.

153. The ability of D_{relm} to rate performance with reasonable consistency illustrated in Tables 18 and 19, even using total deformations since construction, shows that the location and magnitude of maximum distortion in a foundation can have a substantial impact on performance. The root mean square summation of amplitudes in an elevation profile as measured by the wave index also has a substantial impact on performance. Average distortions calculated by the mean angular distortion β_m, F-numbers and the MRI are not as significant. Foundations of structures should have thickness or stiffness that can be inferred from the relative thickness (not actual thickness) shown in Table 19 in order to prevent cracking that had occurred. Mat foundations with relative thickness exceeding 40 ft (slab thickness exceeding 2 to 4 ft), which correlates with crack widths > 0.5 inch and differential heave > 5 inches, may not be economical to construct. Alternative foundations that isolate differential movement such as deep

Table 17. Comparison of Performance Ratings for Selected Facilities

Facility	Date of Survey	Visual Observations	Survey Line	Selected Rating Systems: F-Numbers FL	F-Numbers FF	Wave Index WI	Macro-relief Index, MRI	Mean Angular Distortion β_m, Percent	Maximum Relative Thickness D_{relm}, Ft	Maximum Relative Thickness Location, Ft	Maximum Relative Thickness Span, Ft
Automated Technology Center	12/12/89	Large diagonal, jagged crack in dry wall appeared about 12/28/89 following unusual cold weather to 0° F; crack is adjacent to ACT1 about 60 ft from south end < 0.125 inch wide from floor up to 8 ft high	ATC1	14.75	14.25	0.2029	0.3158	0.2325	18.7418	260	58
			ATC6	16.63	15.25	0.0814	0.1551	0.2599	6.6845	99	20
			ATC7	15.22	14.34	0.2638	0.4457	0.2278	8.4740	158	22
			ATC8	16.66	18.46	0.1257	0.2249	0.2246	8.6827	10	26
			ATC9	16.30	17.94	0.1353	0.2333	0.2532	11.4439	198	31
			ATC10A	19.51	19.05	0.1454	0.1825	0.1923	5.5272	160	19
			ATC11	13.76	13.70	0.1499	0.2014	0.2713	9.5875	84	25
	02/21/90		ATC1	15.88	15.53	0.2067	0.3331	0.2457	17.3940	272	41 7 8
Coastal Engineering Research Center	07/20/89	Minor cracking less 0.063 inch below exterior brick of building unit CERC-1 Severe cracks unit CERC-3 of 0.25 to 0.5 inch wide toward top middle of wall	CERC1	20.71	20.73	0.1061	0.1718	0.2245	5.7944	254	12
			CERC2	16.82	17.64	0.1172	0.1867	0.2584	6.4958	152	21
			CERC3	23.79	23.37	0.1020	0.1621	0.1472	6.8294	17	20
			CERC4	22.20	24.20	0.2261	0.1849	0.1463	7.7983	86	19
			CERC5	23.40	25.28	0.2160	0.1765	0.1269	13.7278	69	29
Troop Medical Clinic	02/01/89	Significant cracking in plaster walls adjacent line TMC5 up to 0.2 inch wide	TMC3	22.43	23.73	0.2027	0.3221	0.1620	12.0680	245	42
			TMC4	27.19	26.11	0.0982	0.1881	0.1317	5.3678	136	10
			TMC5	18.91	21.73	0.2856	0.3503	0.1988	23.6370	158	50
Troop Dental Clinic	02/01/89	Satisfactory overall performance; minor cracking and floor distortion adjacent line TDC7	TDC6	17.43	18.64	0.1353	0.2100	0.2065	8.8534	259	24
			TDC7	16.42	18.07	0.2709	0.2538	0.2674	10.6759	142	35
			TDC8	14.40	20.21	0.2610	0.1858	0.2450	8.6779	62	17

Table 17. (Concluded)

Facility	Date of Survey	Visual Observations	Survey Line	Selected Rating Systems: F-Numbers FL	F-Numbers FF	Wave Index WI	Macro-relief Index, MRI	Mean Angular Distortion β_m, Percent	Maximum Relative Thickness D_{relm}, Ft	Maximum Relative Thickness Location, Ft	Maximum Relative Thickness Span, Ft
Head-quarters RRAD	04/26/90	Diagonal cracking of wings and corners; wing distortion disrupts area function due to high 1/150 slope; original building okay	HDQ1	6.82	13.90	1.8013	1.5045	0.5639	55.0484	217	120
			HDQ2	6.29	13.96	1.1994	1.2318	0.3797	20.2457	64	47
			HDQ3	7.10	12.69	0.8438	2.0454	0.4369	48.3563	160	107
Dyna-mometer Facility RRAD	04/26/90	Visible basement floor distortion due to soil center heave; major longitudinal cracks in basement floor 0.375 to 0.625 inch wide	DYNA4	18.77	21.02	0.2350	1.2612	0.2152	15.2810	79	35
			DYNA5	19.01	21.91	0.3891	0.1196	0.2021	13.0649	92	102
			DYNA6	9.65	10.72	0.7147	1.1712	0.3698	45.4885	137	114
			DYNA7	4.24	9.90	1.3121	0.4736	0.6573	41.4954	37	73
Warehouse A RRAD	04/27/90	Significant cracks North wall up to 1 inch wide running full height adjacent lines WHS1 and WHS2; cracks to 0.25 inch in wall parallel with WHS4; WHS5 parallel with WHS1 but 500 ft South	WHS1	14.57	24.13	0.9211	2.2927	0.2882	23.3760	262	59
			WHS2	12.90	20.33	1.0290	1.7825	0.3624	74.7699	235	149
			WHS3	20.67	23.40	0.2390	0.4992	0.1972	7.0535	110	18
			WHS4	15.96	18.71	0.4557	0.9971	0.2527	27.1071	121	71
			WHS5	15.08	22.53	0.8197	0.9154	0.2319	52.2706	127	101

Table 18. Comparison of Survey Lines and Matching Indices

Facility	Survey Line With Most Observed Damage	Index Matching Observed Damage
Automated Technology Center	ATC1	D_{relm}
Coastal Engineering Research Center	CERC4 CERC5	D_{relm}, WI
Troop Medical Clinic	TMC5	D_{relm}, WI, β_m, MRI, FL
Troop Dental Clinic	TDC7	D_{relm}, WI, β_m, MRI, FF
Headquarters RRAD	HDQ1 or HDQ3	D_{relm}, WI, β_m, MRI, FF
Dynamometer RRAD	DYNA 6 or DYNA 7	D_{relm}, WI, MRI, FL
Warehouse A RRAD	WHS2	D_{relm}, WI, β_m, MRI, FL

Table 19. D_{relm} Related with Crack Width

Facility	Crack Width, in.	D_{relm}, ft.
Troop Dental Clinic	< 0.1	10
Troop Medical Clinic	0.2	23
Automated Technology Center	0.25	18
Coastal Engineering Research Center	0.25	13
Dynamometer Facility	0.5	42
Warehouse A	1.0	75

foundations or soil improvement methods that reduce potential heave such as remove and replace with nonexpansive fill or lime stabilization should be used. Note that span lengths of soil-foundation waves measured in the Headquarters, Dynamometer and Warehouse buildings of the RRAD indicate that Z_a, depth of active zone for heave, may be greater than 50 ft if $Z_a \approx \ell/2$ as shown in PART II. e_m, edge moisture variation distance could also be about 50 ft from Equation 10 in PART II for these old structures.

Dominant Wave Patterns

154. Figure 56 illustrates the relationship between amplitude (twice transformed amplitude) and frequency of discrete waves calculated by program FTROPT, excluding large amplitudes of HDQ1, WHS1 and WHS2. Amplitudes tend to be larger with decreasing frequency as observed from pavement studies (Gay and Lytton 1988). This figure shows that wavelengths vary from 4 to more than 120 feet and could be nearly any wavelength.

155. The range of maximum unrestrained or nearly unrestrained angular distortion β_u calculated from Equation 12 using data in Figure 56 is shown in Table 20. These β_u are more than 1/500 indicating that damage could have occurred in some of these facilities as actually observed. Shorter

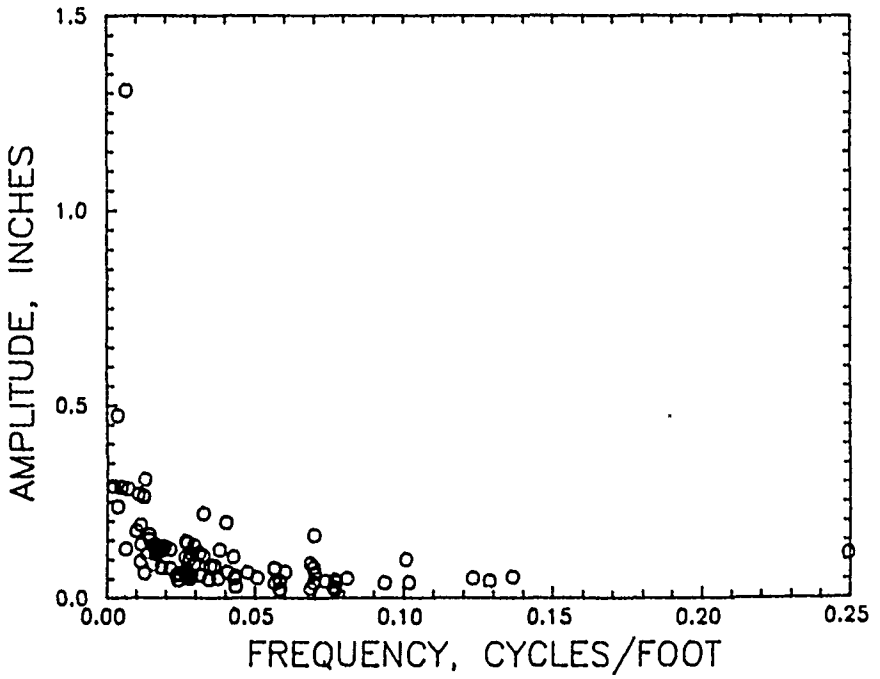

Figure 56. Amplitude and frequency spectrum of discrete waves

Table 20. Unrestrained Angular Distortions and Required Mat Thickness

Frequency f.cycle/ft	wavelength ℓ, ft	Amplitude A, inches	Unrestrained Distortion β_u	Reduction factor R_f	Relative Mat Thicknes D_{rel}, ft
0.007	142.9	1.32	1/325	0.4875	54.5
0.033	30.3	0.23	1/395	0.5925	10.1
0.040	25.0	0.20	1/375	0.5625	8.7
0.070	14.3	0.15	1/286	0.4290	5.9
0.100	10.0	0.10	1/300	0.4500	4.0
0.250	4.0	0.12	1/100	0.1500	1.5

wavelengths tend to have larger β_u. Equation 15b may be used to calculate a reduction factor R_f assuming a tolerable $\beta = 0.0015$ as shown in Table 20. D_{rel} may be calculated from Equation 19 using $R = \ell/2$ and stiffness K_s found from Figure 10 and R_f. Table 20 shows that D_{rel} is thicker for larger wavelengths depending on amplitude. Soil preparation procedures such as removal and replace with engineered fill or soil modification may be necessary to restrict amplitudes of unrestrained soil deformation to reasonably small values. The amplitudes shown in Figure 56 are minimal values whereas actual amplitudes of the elevation profile may be larger because superposition of discrete waves to obtain the actual profile often increases amplitudes.

PART V. CONCLUSIONS AND RECOMMENDATIONS

156. Soil-foundation differential movements can be simulated by wave patterns that occur from many sources such as soil water content changes due to seasonal variations in climate, desiccation from vegetation, leaking subsurface utilities and poor drainage. Soil-foundation wave patterns may also be caused by lateral variations in soils, concentrated loads and many others. Wave patterns may be determined using elevation profiles of the soil surface, surfaces of slab-on-grade or mat foundations, and first floor surfaces. Distances between measurement points should be frequent and about 1 ft or even less. Lengths of measured elevation profiles should exceed 50 ft because measured wavelengths often are greater than 50 ft.

157. Wave patterns of soil-foundation movement provide a direct measure of angular distortion that may be linked with structural distress. The potentially most damaging or critical wavelengths ℓ_c are likely to be greater than 30 ft and may be calculated by $A_{eu}/9.6\beta$ where A_{eu} is the potential heave in inches and β is the tolerable angular distortion. The tolerable angular distortion used in this study is $\beta = 0.0015$, which may lead to slight damage in structures. Many structures are able to tolerate larger angular distortions.

158. Linking wave patterns with angular distortion allows simple methods for estimating the equivalent thickness D_e and steel reinforcement of mat foundations required for reducing potential heave to levels that can be tolerated by structures. The wave pattern model indicates that the top several feet of soil should have limited stiffness to improve the ability of a stiffened mat to reduce differential movement. The mat is assumed to be uniformly loaded and to remain in contact with the soil. Soil-foundation wavelengths are assumed not to be affected by foundation stiffness. The required thickness of mats calculated by technology developed during this study is reasonably consistent with mat dimensions determined by current design methodology. Bending moments calculated using a circular arc may not be representative of actual soil-foundation distortions, especially near the perimeter. This methodology is recommended for use with existing design procedures and may be useful for design of internal areas of foundations. Construction of economical foundations may require soil modification to reduce potential heave to less than 1 inch because this wave model indicates that

heavy, stiffened mats may be required for potential heaves greater than 1 inch.

159. A maximum relative thickness independent of soil and foundation characteristics D_{relmax} can be calculated from potential heave A_{eu} and tolerable angular distortion β as $0.033A_{eu}/\beta$. D_{relmax} may be used to calculate the thickness of mat foundations required to reduce a given potential heave through the ratio of the foundation and soil elastic moduli and soil Poisson's ratio. D_{relmax} should also be useful in pavement design.

160. Several promising indices for rating performance include maximum measured relative thickness D_{relm}, wave index WI, F-numbers floor levelness FL and floor flatness FF, macrorelief index MRI, and mean angular distortion β_m. WI and F-numbers are most reproducibile and indicate an overall measure of floor distortion over the length of measurement. D_{relm}, from which the maximum required D_e can be calculated for the measured elevation profile, was found to be consistently reliable in indicating damage to structures caused by foundation floor distortion. This index is also useful for locating the area of floor that may eventually lead to structural damage. Verification of D_{relm} as a valid performance rating index provides additional evidence that the equivalent thickness D_e is expected to be a potential design aid for calculating the thickness and stiffness of mat foundations and pavements required to resist potential soil deformation. Table 5 demonstrates how the maximum required D_e and D_{rel} may be calculated from the potential heave, tolerable angular distortion and ratio of foundation and soil elastic moduli.

161. The consistency of D_{relm} in indicating damage shows that the location and magnitude of maximum distortion can control performance, even though the measured profiles are based on total deformations. The wave index WI, which is a summation of the root mean square amplitudes in an elevation profile, was found nearly as consistent for indicating potential damage and may also be a useful measure of foundation performance.

162. Soil parameters needed for design include the active zone depth for heave Z_a, which is used to evaluate the potential heave A_{eu}. Z_a was correlated with the suction compression index of the soil simplifying the equation for estimating active zone depth for climate controlled soil moisture changes. Z_a, which also can approach 1/2 of the soil-foundation wavelength, can be large and on the order of 50 ft or more beneath old facilities. The

edge moisture variation distance e_m is not required for the new technology developed in this study for design of mat foundations.

163. The Fourier transform is useful for decomposing elevation profiles into discrete waves of given amplitude and frequency. These discrete waves are commonly plotted in amplitude versus frequency charts, which show that amplitude increases with decreasing frequency. Amplitudes of the decomposed wave pattern are often significantly less than amplitudes of the actual wave forms in the elevation profile. Amplitudes of discrete waves in the transforms depend on the phase angle of the wave. Performance rating indices developed using the area beneath the amplitude-frequency curve were found to be dependent on the length of the measured elevation profile and could not be used for rating performance of foundations because foundations are constructed in nonstandard dimensions.

164. Field studies are needed to determine soil-foundation wave patterns caused by changes in soil moisture such as the change in environment, penetration of moisture beneath a covered surface, vegetation and other effects. The data will be used to confirm the wave model concept developed in this study for characterizing soil-foundation displacement patterns, to confirm the proposed new design technology and to confirm soil-structure interaction models for analyzing performance of mat foundations. These field studies can be accomplished through test sections that can measure migration of moisture beneath a simulated foundation, active zone depth of heave, and distortion of surface soil-foundation movement. Soil-foundation wave patterns should also be correlated with operation and maintenance costs of facilities to assist in determining the extent of damage caused by soil-foundation distortion.

165. Field studies are also required to determine optimum methodology for reducing potential heaves to tolerable levels for economical foundations and to determine ways of avoiding soil movements with the most damaging wavelengths. Soil modification methods that should be tested include lime-flyash slurry pressure injection, water injection, impervious moisture barriers and nonexpansive fill materials.

REFERENCES

American Society for Testing and Materials. 1990a. "Standard Test Method for Determining Floor Flatness and Levelness Using the F-number System", E1155-87, Building Seals and Sealants; Fire Standards; Building Constructions, Vol 04.07, pp 874-879, Philadelphia, PA 19103

American Society for Testing and Materials. 1990b. Standard Test Methods for One-Dimensional Swell or Settlement Potential of Cohesive Soils", D4546-85, Soil and Rock; Dimension Stone; Geosynthetics, Vol 04.08, pp 736-742, Philadelphia, PA 19103

Blight, G. E. 1987. "Lowering of the Groundwater Table by Deep-rooted Vegetation - The Geotechnical Effects of Water Table Recovery", Groundwater Effects in Geotechnical Engineering, Proceedings of the Ninth European Conference on Soil Mechanics and Foundation Engineering, Dublin, pp 285-288

Boscardin, M. D. and Cording, E. J. 1989. "Building Response to Excavation Induced Settlement", Journal of Geotechnical Engineering, Vol 115, No. 1, pp 1-21, American Society of Civil Engineers, New York, NY 10017

Boussinesq, J. 1885. Application of Potential to the Study of the Equilibrium and Movements in Elastic Soils, Gauthier-Villars, Paris, France

Bowles, J. E. 1988. Foundation Analysis and Design, Fourth Edition, Table 2-8, p 100, McGraw-Hill Book Company, New York, NY 10020

Brandl, H. 1987. "Heave and Settlement of Foundations Due to Changes in Groundwater Levels", Groundwater Effects in Geotechnical Engineering, Proceedings of the Ninth European Conference on Soil Mechanics and Foundation Engineering, Dublin, pp 651-656

Brigham, E. O. 1974. The Fast Fourier Transform, Prentice-Hall, Inc., Englewood Cliffs, NJ 07632

Brown, P. T. 1969. "Numerical Analysis of Uniformly Loaded Circular Rafts on Deep Elastic Foundations", Geotechnique, Vol 19, No. 3, pp 399-404

Burland, J. B. and Wroth, C. P. 1974. "Settlement of Buildings and Associated Damage", Proceedings, Conference on Settlement of Structures, Pentech Press, London, England, pp 611-614

Burmister, D. M. 1963. "Prototype Load-Bearing Tests for Foundations of Structures and Pavements", Field Testing of Soils, American Society for Testing and Materials Standard Technical Publication No. 322, pp 98-119, Philadelphia, PA 19103

Canadian Standards Association (CSA). 1990. "Concrete Surfaces: Elevation, Slope and Waviness", Concrete Materials and Methods of Concrete Construction, CSA-A23.1-M90, Appendix E, pp 107-112, Rexdale, Ontario, Canada M9W1R3

Chang, C. S. and Duncan, J. M. 1977. "Analysis of Consolidation of Earth and Rock Fill Dams", Vol I and II, Contract Report S-77-4, U. S. Army Engineer Waterways Experiment Station, P. O. Box 631, Vicksburg, MS 39181

Cheney, J. E. 1988. "25 Years Heave of a Building Constructed on Clay, After Tree Removal", Ground Engineering, Vol 21, pp 13-21

Day, R. W. 1990. "Differential Movement of Slab-on-grade Structures", Journal of Performance of Constructed Facilities, Vol 4, pp 236-241, American Society of Civil Engineers, New York, NY 10017

Dempsey, B. J. 1976. "Climatic effects on Airport Pavement Systems: State-of-the-art", Contract Report S-76-12, US Army Engineer Waterways Experiment Station, Vicksburg, MS 39180

Duncan, J. M. and Chang, C. Y. 1970. "Nonlinear Analysis of Stress and Strain in Soils", Journal of the Soil Mechanics and Foundations Division, Vol 97, pp 1629-1653, American Society of Civil Engineers, New York, NY 10017

Edward W. Face Company, 1983. "Specification of Floor Flatness", Technical Sheet 831, Edward W. Face Company, Inc., Norflk, VA 23508

Eshbach, O. W. 1954. Handbook of Engineering Fundamentals, Second Edition, Fourth Printing, p 5-66, John Wiley & Sons, Inc., New York, NY 10016

Face, A. 1984. "Specification and Control of Concrete Floor Flatness", Concrete International, February, pp 56-63, American Concrete Institute, Detroit, MI 48219

Fredlund, D. G. and Dakshanamurthy, V. 1982. "Prediction of Moisture Flow and Related Swelling or Shrinking in Unsaturated Soils", Journal of the Southeast Asian Geotechnical Society, Vol 13, pp 15-49

Gay, D. A. and Lytton, R. L. 1988. "Moisture Barrier Effects on Pavement Roughness", Measured Performance of Shallow Foundations, Geotechnical Special Publication No. 15, American Society of Civil Engineers, New York, NY 10017

GEO Construction Testing 1985. "Soil Boring Exploration: Waterways Experiment Station Building 3296 - Phase III", Job Number B-3-819, Memphis, TN 38114, submitted to The Pickering Firm, Greenwood, MS 38930

Gnaedinger, J. P. 1988. "It's Time for Some Changes", Journal of Performance of Constructed Facilities, Vol 2, pp 199-207, American Society of Civil Engineers, New York, NY 10017

Harr, M. E. 1977. Mechanics of Particulate Media, pp 215-251, McGraw-Hill Book Company, New York, NY 10020

Hartman, J. P. and James, B. H. 1988. "Development of Design Formulas For Ribbed Mat Foundations On Expansive Soils", Technical Report ITL-88-1, US Army Engineer Waterways Experiment Station, Vicksburg MS 39180

Headquarters, Department of the Army 1960 (HQDA 1060). The Unified Soil Classification System, Technical Memorandum No. 3-357, Washington, D. C. 20314

Headquarters, Department of the Army 1983 (HQDA 1983). Foundations in Expansive Soils, Technical Manual TM 5-818-7, Washington, D. C. 20314

Headquarters, US Army Corps of Engineers 1990 (HQACE 1990). Settlement Analysis, Engineer Manual EM 1110-1-1904, Washington, D. C. 20314

Headquarters, US Army Corps of Engineers 1991 (HQACE 1991). Bearing Capacity of Soils, Engineer Manual EM 1110-1-1914, Washington, D. C. 20314

Jennings, J. E., Heymann, P. R. B., and Wolpert, L. 1952. "Some Laboratory Studies of the Migration of Moisture in Soils Under Temperature Gradients", National Building Research Institute Bulletin No. 9, pp 29-46, Council for Scientific and Industrial Research, Pretoria, South Africa

Johnson, L. D. 1988. "Proceedings of the Workshop on Design, Construction, and Research for Ribbed Mat Foundations", Miscellaneous Paper GL-88-6, US Army Engineer Waterways Experiment Station, Vicksburg, MS 39180

Johnson, L. D. 1989a. "Performance of a Large Ribbed Mat on Cohesive Soil", Foundation Engineering: Current Principles and Practices, Vol 2, F. H. Kulhawy, editor, Northwestern University, American Society of Civil Engineers, New York, NY 10017

Johnson, L. D. 1989b. "Design and Construction of Mat Foundations", Miscellaneous Paper MP GL-89-27, US Army Engineer Waterways Experiment Station, Vicksburg, MS 39180

Johnson, L. D. and Snethen, D. R. 1978. "Prediction of Potential Heave of Swelling Soil", Geotechnical Testing Journal, Vol 1, pp 117-125, American Society for Testing and Materials, Philadelphia, PA 19103

Jones, D. E., Jr. and Holtz, W. G. 1973. "Expansive Soils - The Hidden Disaster", Civil Engineering, Vol 43, pp 49-51, American Society of Civil Engineers, New York, NY 10017

Kalman Laboratories 1989. New Floor Tolerance Specifications, Engineering Notes #1-#4, 1202 Highway 74, Evergreen, CO 80439

Kay, J. N. and Cavagnaro, R. L. 1983. "Settlement of Raft Foundations", Journal of Geotechnical Engineering, Vol 109, No 11, pp 1367-1382, American Society of Civil Engineers, New York, NY 10017

Kaye, B. H. 1978. "Specification of the Ruggedness and/or Texture of a Fine Particle by its Fractal Dimension", Powder Technology, Vol 21, No. 1, pp 1-16

Knight, K. and Greenberg, J. 1970. "The Analysis of Subsoil Moisture Movements During Heave and Possible Methods of Predicting Field Rates of Heave", The Civil Engineer in South Africa, Vol 12, No 2, pp 27-32

Kögler, F. and Scheidig, A. 1927. "Druckverteilung im Baugrunde", Die Bautechnik, Heft 29 and 31

Lambe, T. W. and Whitman, R. V. 1969. Soil Mechanics, John Wiley & Sons, New York, NY 10158, p. 412.

Lehrsch, G. A., Whisler, F. D. and Römkens, M. J. M. 1988. "Selection of a Parameter Describing Surface Roughness", Soil Science Society of America Journal, Vol 52, pp 1439-1445

Lysmer, J. and Duncan, J. M. 1969. Stresses and Deflections in Foundations and Pavements, Fourth Edition, Department of Civil Engineering, Institute of Transportation and Traffic Engineering, University of California, Berkeley, CA

Lytton, R. L. and Woodburn, J. A. 1973. "Design and Performance of Mat Foundations On Expansive Clay", Proceedings 3rd International Conference on Expansive Soils, Haifi, Israel, pp 301-307

McKeen, R. G. 1981. "Design of Airport Pavements for Expansive Soils", Report No. DOT/FAA/RD-81/25, Systems Research and Development Service, US Department of Transportation, Federal Aviation Administration, Washington, D. C. 20590

McKeen, R. G. and Eliassi, M. 1988. "Study of Surface Deformations of Mat Foundations on Expansive Soils", Contract Report DACA39-87-M-0557 prepared for U. S. Army Engineer Waterways Experiment Station, Vicksburg, MS 39180

McKeen, G. R. and Lytton, R. L. 1984. "Expansive Soil Pavement Design Using Case Studies", International Conference on Case Histories in Geotechnical Engineering, editor S. Prakash, Vol III, pp 1421-1427, St. Louis, MO

McKeen, R. G. and Johnson, L. D. 1990. "Climate Controlled Soil Design Parameters for Mat Foundations", Journal of Geotechnical Engineering, Vol 116, pp 1073-1094, American Society of Civil Engineers, New York, NY 10017

Mei, C. C. and Tyvand, P. A. 1988. "Thermal Consolidation of Thick and Soft Soil Layer", Journal of Engineering Mechanics, Vol 114, pp 990-1009, American Society of Civil Engineers, New York, NY 10017

Murzenko, Yu. N. 1965. "Experimental Results on the Distribution of Normal Contact Pressure on the Base of a Rigid Foundation Resting on Sand", Soil Mechanics and Foundation Engineering, Vol 2, pp 69-73, Tokyo, Japan

O'Neill, M. W. and Poormoayed, N. 1980. "Methodology for Foundations on Expansive Clays", Journal of the Geotechnical Engineering Division, Vol 106, pp 1345-1367, American Society of Civil Engineers, New York, NY 10017

Papadopoulos, B. P. and Anagnostopoulos, A. G. 1987. "Groundwater Effects on Settlement Estimation", Groundwater Effects in Geotechnical Engineering, Proceedings of the Ninth European Conference on Soil Mechanics and Foundation Engineering, Dublin, pp 725-729

Polshin, D. E. and Tokar, R. A. 1957. "Maximum Allowable Non-uniform Settlement of Structures", Proceedings, 4th International Conference of Soil Mechanics and Foundation Engineering, Vol 1, London, England, pp 402-405

Popov, E. P. 1956. Mechanics of Materials, pp 269-273, Prentice-Hall Civil Engineering and Engineering Mechanics Series, Prentice-Hall, Inc., Englewood Cliffs, NJ 07632

Post-Tensioning Institute 1980. Design and Construction of Post-Tensioned Slabs-On-Ground, 301 W. Osborn, Suite 3500, Phoenix, AZ 85013

Römkens, M. J. M. and Wang, J. Y. 1986. "Effect of Tillage on Surface Roughness", Transactions of the American Society of Agricultural Engineers, Vol 29, pp 429-433

Terzaghi, K. and Peck, R. B. 1967. Soil Mechanics in Engineering Mechanics, Second Edition, pp 58-59, John Wiley and Sons, New York, NY 10158

Vallabhan, C. V. and Sathiyakumar, N. 1987. "A Computer Program for Analysis of Transient Suction Potential in Clays", Report Submitted to the Waterways Experiment Station, Department of Civil Engineering, Texas Tech University, Lubbock, TX 79409

Wahls, H. E. 1981. "Tolerable Settlement of Buildings", Journal of Geotechnical Engineering, Vol 107, No 11, pp 1489-1504, American Society of Civil Engineers, New York, NY 10017

Westergaard, H. M. 1938. "A Problem of Elasticity Suggested by a Problem in Soil Mechanics: Soft Material Reinforced by Numerous Strong Horizontal Sheets", Contributions to the Mechanics of Solids, Stephen Timoshenko 60th Anniversary Volume, pp 268-277, The MacMillan Company, New York, NY 10022

Whalley, W. B. and Orford, J. D. 1989. "The Use of Fractals and Pseudofractals in the Analysis of Two-Dimensional Outlines: Review and Further Exploration", Computers and Geoscience, Vol 15, No 2, pp 185-197

Winter, G. and Nilson, A. H. 1979. Design of Concrete Structures, Ninth Edition, p 16, McGraw-Hill Book Company, New York, NY 10020

APPENDIX A: CLIMATIC PARAMETERS FROM PROGRAM SWELZA.FOR

1. Moisture diffusion computer program SWEL2D (Vallabhan and Sathiyakamar 1987) was modified to directly calculate the active zone depth Z_a as a function of the lateral distance of a soil profile. The lateral distance extends from the left boundary of uncovered soil to the center of a slab foundation on the right boundary at the ground surface, Figure A1. The slab foundation is fully flexible and includes a stiffening beam of depth D at the perimeter. The active zone depth is determined to be at the depth below ground surface where accumulative moisture changes lead to accumulative vertical dimensional changes less than 0.5 inch. At depths less than Z_a the accumulative moisture changes are greater than 0.5 inch. Accumulative heave is estimated by

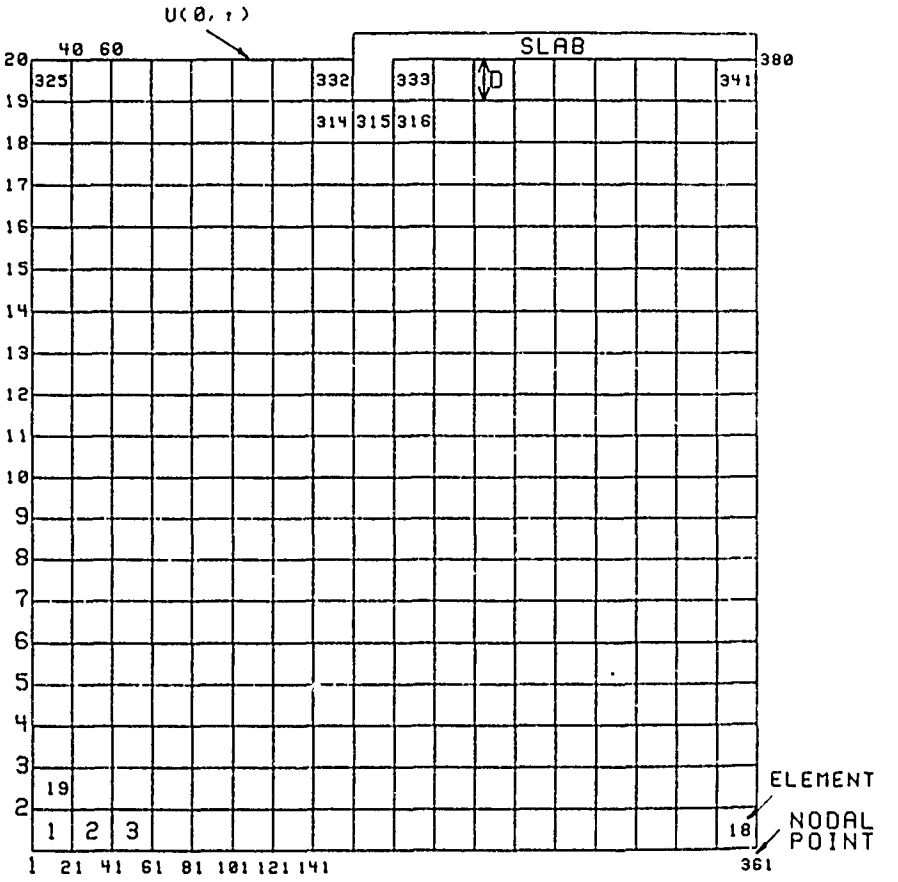

Figure A1. Selected finite element mesh

$$S_{za} = \sum_{i=1}^{N_{Iza}} \Delta h \cdot C_t \cdot \Delta pF_i \qquad \text{(A1a)}$$

$$S = \sum_{i=1}^{N_I} \Delta h \cdot C_t \cdot \Delta pF_i \qquad \text{(A1b)}$$

where

S_{za} = accumulative vertical dimensional change at active depth Z_a, ≤ 0.5 inch

S = accumulative vertical dimensional change at ground surface, in.

N_{Iza} = number of depth increments from bottom of soil to depth Z_a

N_I = number of depth increments from bottom of soil to ground surface

Δh = height of depth increment or element in finite element mesh, in.

C_t = suction compression index of soil

ΔpF_i = change in suction from the initial suction at depth increment i, pF

The suction compression index C_t may be found from charts using cation exchange capacity and soil plasticity data or soil suction-dimensional change laboratory tests on soils (McKeen and Johnson 1990). The change in suction at an increment of depth i, ΔpF_i, occurs from diffusion of moisture through climate changes at the ground surface.

2. Program SWELZA calculates the diffusion of moisture and changes in ΔpF_i from periodic sine changes in climate at the ground surface by

$$U(0,t) = U_o \sin(2n\pi t) + U_e \qquad \text{(A2)}$$

where

$U(0,t)$ = suction at the ground surface at time t, pF

U_o = half of the maximum suction change at the ground surface, pF

U_e = equilibrium suction below active zone depth, pF

n = frequency of climate change, cycle/yr

The program records the maximum change in ΔpF_i at each depth increment i for each time increment up to the maximum allowed time. At the depth Z_a the program sets the maximum suction change $\Delta U_{max} = \Delta pF_i$ where i is the depth increment at the location Z_a.

3. A series of computer runs were performed using program SWELZA.FOR with the finite element mesh, Figure A1. The depth of the mesh should be

sufficient such that any additional heave below the bottom of the mesh will be insignificant. This study assumes this is accomplished if Z_a is less than half of the depth of the mesh. Bottom and right side boundary conditions are such that the suction is constant at the equilibrium suction U_e. These runs were all performed with a uniform equilibrium suction $U_e = 3$ pF. The magnitude of U_e does not influence the active depth Z_a and edge moisture variation e_m values. e_m is the lateral distance from the perimeter beam of depth D to the location beneath the slab where $Z_a \leq 0.5$ inch. The time increment is 0.01 year and the maximum allowed time is 4 years. Results of the computer runs are provided in Table A1.

4. A plot of the maximum change ΔU_{max} in pF units with the suction compression index C_t, Figure A2, provides the approximate correlation

$$\Delta U_{max} = \frac{0.007}{C_t} \tag{A3}$$

where the coefficient of correlation $r^2 = 0.716$. Equation 7 in PART I may threfore be rewritten as

$$Z_{ae} = \frac{\ln \frac{0.007}{2U_o \cdot C_t}}{-\left[\frac{n\pi}{\alpha}\right]^{0.5}} = \frac{\ln \frac{0.0035}{U_o \cdot C_t}}{-\left[\frac{n\pi}{\alpha}\right]^{0.5}} \tag{A4}$$

C_t can be determined while ΔU_{max} is currently an unknown quantity.

5. A plot of Z_a with e_m, Figure A3, indicates that the maximum edge moisture variation distance will be

$$e_m = Z_a - D \tag{A5}$$

Deviations of the data from Equation A5 are largly attributed to the relatively coarse mesh and limited number of elements. Fourier transforms of these elevation profiles such as shown in Figure A4 indicate a peak wavelength at zero frequency. There is no correlation of wavelength of soil heave with the active zone depth from uniform perimeter heave outside of a mat foundation. A program listing of SWELZA is provided in Table A2 with an example listing of the input data given in Table A3.

Table A1

Climatic Parameters

a. Stiffening Beam Depth D = 1 ft

Cycle/yr n	Diffusivity Coefficient α, ft^2/yr	Half Surface Suction Change U_o, pF	Suction Compression Index, C_t	Maximum Suction Change ΔU_{max}, pF	Active Zone Depth Z_a, Ft	Edge Moisture Variation Distance e_m, ft
0.5	120	1.0	0.01	0.802	8	8
		1.5	0.01	0.939	10	10
	60	1.0	0.01	0.768	6	4
			0.02	0.498	9	8
			0.04	0.307	12	10
		1.5	0.01	0.863	8	6
			0.02	0.547	11	10
			0.04	0.382	13	14
		2.0	0.01	0.996	9	8
			0.02	0.613	12	12
		2.5	0.01	1.071	10	10
			0.02	0.767	12	14
1.0	120	1.0	0.01	0.766	6	4
			0.02	0.497	9	8
			0.04	0.311	12	12
		1.5	0.01	0.861	8	6
			0.02	0.550	11	10
			0.04	0.388	13	16
		2.0	0.01	0.993	9	8
			0.02	0.621	12	12
	60	1.0	0.01	0.962	3	2
			0.02	0.522	6	4
			0.04	0.288	9	8
		1.5	0.01	0.958	5	4
			0.02	0.525	8	6
			0.04	0.294	11	10
		2.0	0.01	1.043	6	4
			0.02	0.576	9	8
			0.04	0.322	12	12
		2.5	0.01	1.067	7	6
			0.02	0.593	10	10

b. Stiffening Beam Depth D = 2 ft

Cycle/yr n	Diffusivity Coefficient α, ft^2/yr	Half Surface Suction Change U_o, pF	Suction Compression Index, C_t	Maximum Suction Change ΔU_{max}, pF	Active Zone Depth Z_a, Ft	Edge Moisture Variation Distance e_m, ft
0.5	120	1.0	0.01	0.485	12	8
			0.02	0.306	16	14
			0.04	0.151	22	18
		1.5	0.01	0.581	14	12
			0.02	0.283	20	16
			0.04	0.182	24	18
		2.0	0.01	0.612	16	14
			0.02	0.302	22	18
			0.04	0.193	26	20
		2.5	0.01	0.597	18	14
			0.02	0.303	24	18
			0.04	0.241	26	20
	60	1.0	0.01	0.715	6	2
			0.02	0.391	10	8
			0.04	0.147	16	12

Table A1 (Continued)

Cycle/yr n	Diffusivity Coefficient α, ft^2/yr	Half Surface Suction Change U_o, pF	Suction Compression Index, C_t	Maximum Suction Change ΔU_{max}, pF	Active Zone Depth Z_a, Ft	Edge Moisture Variation Distance e_m, ft
		1.5	0.01	0.586	10	6
			0.02	0.303	14	10
			0.04	0.160	18	14
		2.0	0.01	0.782	10	8
			0.02	0.294	16	12
			0.04	0.154	20	16
		2.5	0.01	0.703	12	8
			0.02	0.367	16	14
			0.04	0.193	20	16
1.0	120	1.0	0.01	0.718	6	4
			0.02	0.297	12	8
			0.04	0.166	16	12
		1.5	0.01	0.598	10	6
			0.02	0.332	14	10
			0.04	0.186	18	16
		2.0	0.01	0.594	12	8
			0.02	0.331	16	12
			0.04	0.186	20	16
		2.5	0.01	0.553	14	10
			0.02	0.310	18	14
			0.04	0.175	22	18
	60	1.0	0.01	0.724	4	0
			0.02	0.484	6	4
			0.04	0.217	10	6
		1.5	0.01	0.725	6	2
			0.02	0.485	8	6
			0.04	0.219	12	8
		2.0	0.01	0.968	6	4
			0.02	0.435	10	6
			0.04	0.196	14	10
		2.5	0.01	0.809	8	4
			0.02	0.365	12	8
			0.04	0.245	14	12

c. Stiffening Beam Depth D = 4 ft

Cycle/yr n	Diffusivity Coefficient α, ft^2/yr	Half Surface Suction Change U_o, pF	Suction Compression Index, C_t	Maximum Suction Change ΔU_{max}, pF	Active Zone Depth Z_a, Ft	Edge Moisture Variation Distance e_m, ft
0.5	120	1.0	0.01	0.478	12	8
			0.02	0.198	20	12
			0.04	0.083	28	20
		1.5	0.01	0.464	16	8
			0.02	0.192	24	16
			0.04	0.080	32	20
		2.0	0.01	0.396	20	12
			0.02	0.165	28	20
			0.04	0.075	36	28
		2.5	0.01	0.494	20	16
			0.02	0.206	28	20
			0.04	0.092	36	32
	›0	1.0	0.01	0.486	8	4
			0.02	0.267	12	8
			0.04	0.144	16	12
		1.5	0.01	0.729	8	4
			0.02	0.216	16	8
			0.04	0.117	20	12

Table A1 (Concluded)

Cycle/yr n	Diffusivity Coefficient α, ft^2/yr	Half Surface Suction Change U_o, pF	Suction Compression Index, C_t	Maximum Suction Change ΔU_{max}, pF	Active Zone Depth Z_a, Ft	Edge Moisture Variation Distance e_m, ft
		2.0	0.01	0.533	12	8
			0.02	0.287	16	12
			0.04	0.090	24	16
		2.5	0.01	0.666	12	8
			0.02	0.195	20	12
			0.04	0.113	24	20
1.0	120	1.0	0.01	0.495	8	4
			0.02	0.283	12	8
			0.04	0.163	16	12
		1.5	0.01	0.425	12	4
			0.02	0.245	16	8
			0.04	0.141	20	16
		2.0	0.01	0.566	12	8
			0.02	0.327	16	12
			0.04	0.108	24	16
		2.5	0.01	0.708	12	8
			0.02	0.236	20	12
			0.04	0.135	24	20
	60	1.0	0.01	0.649	4	0
			0.02	0.303	8	4
			0.04	0.142	12	8
		1.5	0.01	0.973	4	4
			0.02	0.454	8	4
			0.04	0.212	12	8
		2.0	0.01	0.605	8	4
			0.02	0.283	12	8
			0.04	0.132	16	8
		2.5	0.01	0.756	8	4
			0.02	0.354	12	8
			0.04	0.165	16	12

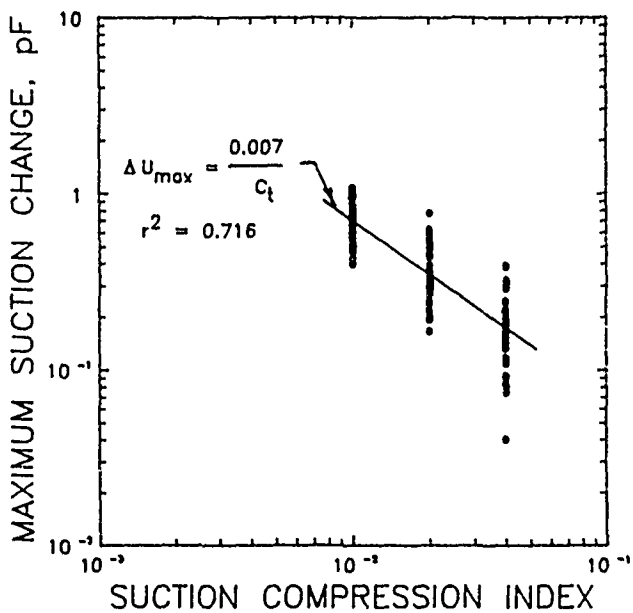

Figure A2. Correlation of Maximum Suction change with the suction compression index

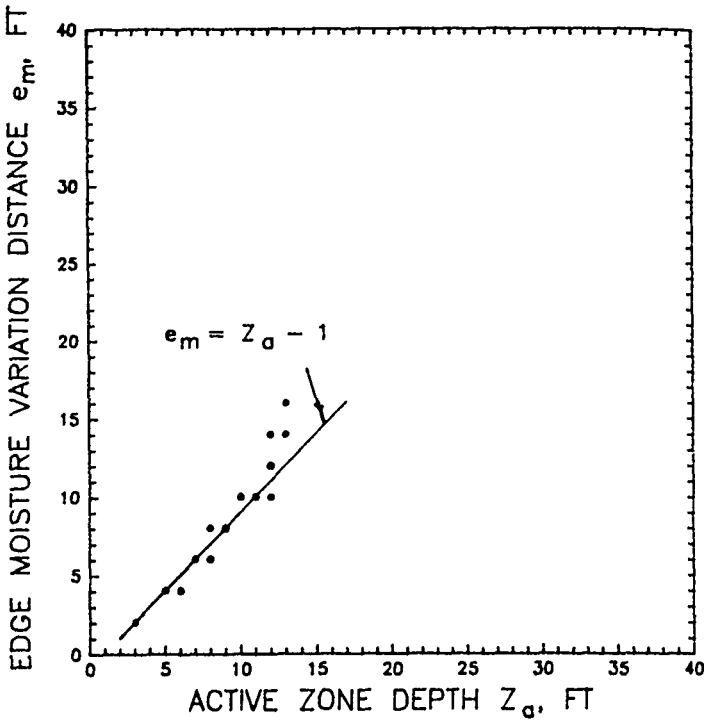

a. STIFFENING BEAM DEPTH = 1 FT

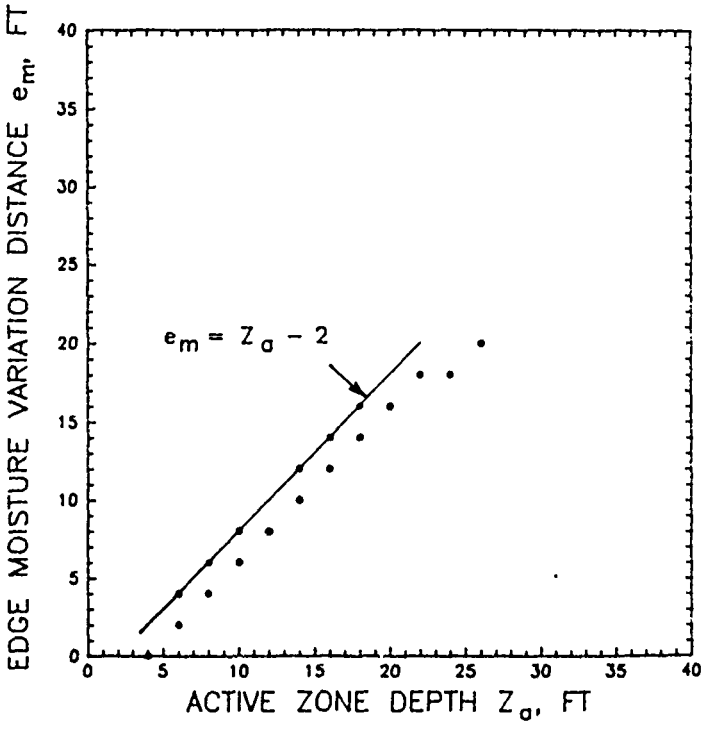

b. STIFFENING BEAM DEPTH = 2 FT

Figure A3. Relationship of the edge moisture variation distance with active zone depth

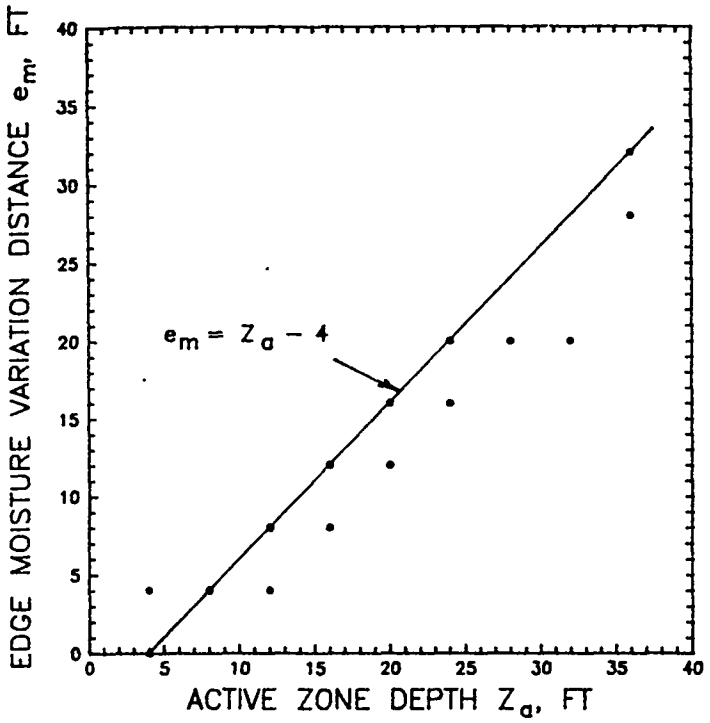

c. STIFFENING BEAM DEPTH = 4 FT

Figure A3. (Concluded)

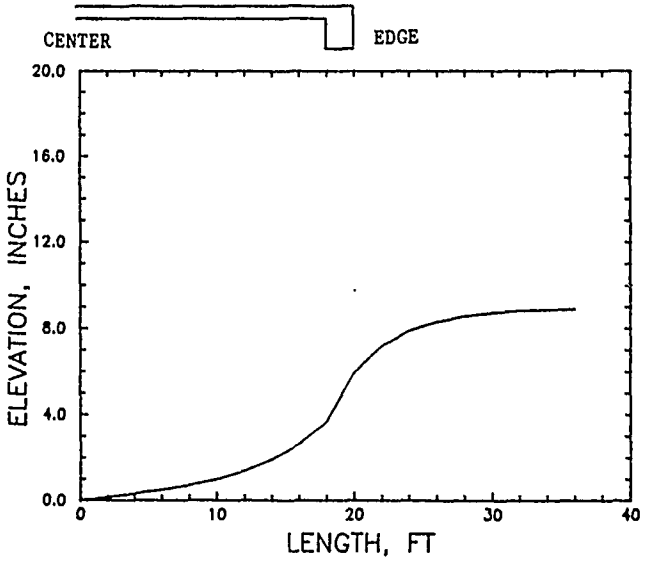

a. ELEVATION PROFILE

Figure A4. Elevation profile and Fourier transform for flexible mat Beam depth D = 1 ft, α = 60 ft^2/day, $2U_o$ = 3 pF, and C_t = 0.04

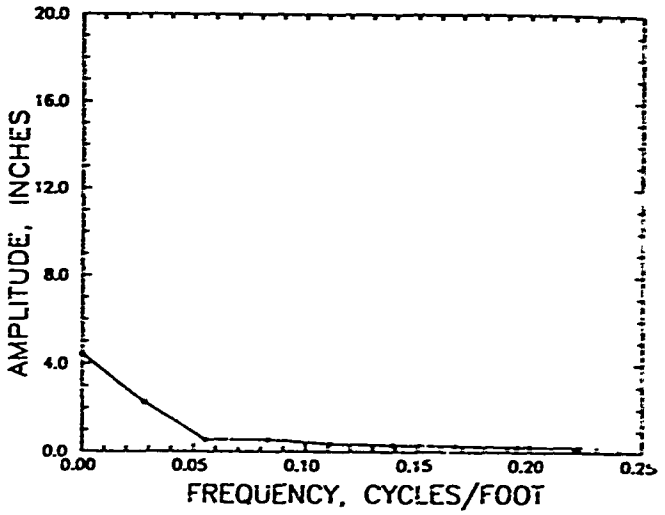

b. FOURIER TRANSFORM

Figure A4. (Concluded)

Table A2.
Listing of Program Swelza.for

```
C        * * * * * * * * * * * * * * * * * * * * * * * * * * * * * *
C        *                                                         *
C        *       SWELZA  A- FINITE ELELMENT PROGRAM FOR            *
C        *                                                         *
C        *        TRANSIENT SUCTION POTENTIAL IN SOILS             *
C        *                                                         *
C        * * * * * * * * * * * * * * * * * * * * * * * * * * * * * *
      IMPLICIT DOUBLE PRECISION (A-H,O-Z)
      PARAMETER (KNO=400)
      DIMENSION NBO(40),BU(40),KK(4),AK(KNO,30),C(KNO,30),PFMIN(40,40),
     &PFMAX(40,40)
      COMMON /COM1/NOD(KNO,4),X(KNO),Y(KNO),SM(4,4),CM(4,4)
      COMMON /COM2/A(KNO,30),P(KNO,30),U(KNO),F(KNO),NF(80)
      OPEN(5,FILE='DIFIN.TXT')
      OPEN(6,FILE='DIFOUT.TXT')
      OPEN(7,FILE='C:\GRAPH\ZA.DAT')
      OPEN(9,FILE='C:ZAOUT.TXT')
  101 FORMAT (6I5,2F10.5)
```

Table A2 (Continued)

```
  102 FORMAT (I5,2F10.2)
  103 FORMAT (7I5,4F8.2)
  104 FORMAT (14I5)
  105 FORMAT (7F10.5)
      READ (5,101) NELM,NODE,NBOUC,NBOUV,NODLS,NOCON,ALPA,CT
      IF (NOCON.EQ.0) READ (5,105) UE
      IF (NOCON.EQ.0) WRITE (9,94) UE
   94 FORMAT (/,6X,'THE INITIAL SUCTION PROFILE IS CONSTANT AT',F10.5
     &, ' pF')
      IF (NBOUV.EQ.0) GOTO 510
      READ (5,105) UOPF,UEPF,CYCLES
      WRITE (9,95) UOPF,UEPF,CYCLES
   95 FORMAT (/,1X,'VARIABLE SURFACE SUCTION',/,6X,'HALF MAXIMUM SUCTION
     & CHANGE =',F10.5, ' pF',/,6X,'EQUILIBRIUM SUCTION=',F10.5,' pF',
     &/,6X,'CYCLES/YEAR=',F10.2)
  510 DELS = 0.0
      TIME = 0.0
      NBOU = NBOUC+NBOUV
C             This program can generate the element numbers using the
C             rectangular or triangular elements with minimal input;
C             however the user has to discretize the domain.  If the
C             user wishes to use both rectangular and triangular elements
C             then the automatic generation provision of this program
C             CANNOT be used. The user must input these parameters.
C             Beam width = element width.
C             The input parameters regardless of nodal generation are:
C             NELM  - Number of elements
C             NODE  - Number of nodes
C             NBOUC - Number of nodes where constant boundary
C                     potentials are prescribed
C             NBOUV - Number of nodes where varying boundary
C                     boundary conditions (with time) are
C                     prescribed
C             NODLS - Left surface node
C             ALPA  - The diffusivity coefficient, ft2/year
C             CT    - Suction Compression Index, pF-1
C             NOCON - Initial suction profile: 0 = constant; 1 = variable
C             UEPF  - Equilibrium suction, pF
C             UOPF  - Half maximum suction change at surface, pF
C             CYCLES- Number of cycles/year of surface suction change  n
C             NDS   - Nodal generation: -1 if yes, -2 if no
C             NTYPE - Type of element: -1 rectangular, -2 triangular
C
C             For nodal generation (NDS = 1):
C             NROW - Number of horizontal rows of elements
C             The following inputs are required for each row
C             NE   - Number of elements in this row
C             NES  - Element number at left (starting)
C             NEL  - Element number at right (ending)
```

Table A2 (Continued)

```
C            N1,N2,N3,N4 - Nodal numbers for this row
C                          in a anti-clockwise manner
C                          N1 is at left lower corner
C                          N2 is ar tight lower corner
C                          N3 is at right upper corner
C                          N4 is at left upper corner
C            X1,Y1,X3,Y3 - X and Y co-ordinates of
C                          N1 and N3 nodes.
C
C            For no nodal generation (NDS = 2):
C            X(I),Y(I), I = 1,NODE
C            I,NODE(I,J) I =1,NELM: J=1,4
C            NOD(I,4) = 0 for triangular elements
C
C            DELT  - Time interval, years
C            TTOT  - Total time, years
C            NFORM - Type of formation: =0, consistent; =1 lumped
C            NALL  - Do you want all element and assembled matrices
C                    = 1, yes; =2, no
C            THETA - Theta should be greater than 0.5
C                    recommended is 0.67
C   ***  HORIZ PERMEABILITY COEFF XKX = 1 AND VERT. COEFF XKY = 1 ******
C   ***  THIS IS FOR FUTURE DEVELOPMENT ONLY **********
      XKX = 1
      XKY = 1
      READ (5,104) NDS,NTYPE
      IF (NDS.EQ.2) GOTO 2450
      IF (NTYPE.EQ.2) GOTO 2110
      READ (5,104) NROW
      DO 2090 NR = 1,NROW
      READ (5,103) NE,NES,NEL,N1,N2,N3,N4,X1,Y1,X3,Y3
      IF (NR.EQ.1) INI = NE + 1
      NINC = (N2-N1)/NE
      XINC = (X3-X1)/NE
      XI = X1
      DO 1920 I = N1,N2,NINC
      X(I) = XI
      Y(I) = Y1
      XI = XI + XINC
 1920 CONTINUE
      XI = X1
      DO 1980 I = N4,N3,NINC
      X(I) = XI
      Y(I) = Y3
      XI = XI + XINC
 1980 CONTINUE
      MINC = (NEL - NES)/(NE-1)
      DO 2070 N = NES,NEL,MINC
      NOD(N,1) = N1
```

Table A2 (Continued)

```
      NOD(N,2) = N1 + NINC
      NOD(N,3) = N4 + NINC
      NOD(N,4) = N4
      N1 = N1 + NINC
      N4 = N4 + NINC
 2070 CONTINUE
 2090 CONTINUE
      GOTO 2510
 2110 READ (5,104) NROW
      DO 2420 NR = 1,NROW
      READ (5,103) NE,NES,NEL,N1,N2,N3,N4,X1,Y1,X3,Y3
      NINC = (N2-N1)/NE
      XINC = (X3-X1)/NE
      XI = X1
      DO 2220 I = N1,N2,NINC
      X(I) = XI
      Y(I) = Y1
      XI = XI + XINC
 2220 CONTINUE
      XI = X1
      DO 2280 I = N4,N3,NINC
      X(I) = XI
      Y(I) = Y3
      XI = XI + XINC
 2280 CONTINUE
      EINC = (NEL - NES)/(NE-1)
      NEINC = IDINT(EINC)
      DO 2400 N = NES,NEL,NEINC
      NOD(N,1) = N1
      NOD(N,2) = N1 + NINC
      NOD(N,3) = N4
      NOD(N+1,1) = NOD(N,2)
      NOD(N+2,2) = NOD(N,2) + 1
      NOD(N+1,3) = N4
      N1 = N1 + NINC
      N4 = N4 + NINC
 2400 CONTINUE
 2420 CONTINUE
      GOTO 2510
 2450 DO 2470 I= 1, NODE
      READ (5,102) J,X(J),Y(J)
 2470 CONTINUE
      DO 2500 I = 1, NELM
      READ (5,104) J,NOD(J,1),NOD(J,2),NOD(J,3),NOD(J,4)
 2500 CONTINUE
 2510 NUM = NODE
      WRITE (9,106) NELM,NODE,NBOUC,NBOUV,NODLS,ALPA,CT
  106 FORMAT (///,
     &'       *           I N P U T   D A T A                *',
```

Table A2 (Continued)

```
     &/,'        * * * * * * * * * * * * * * * * * * * * * * * * * *',/,
     &  '        NO. OF ELEMENTS ..................', I5,/,
     &  '        NO. OF NODES .....................', I5,/,
     &  '        NO. OF NODES BOU POTEN (CONST) ....', I5,/,
     &  '        NO. OF NODES BOU POTEN (VARYING)...', I5,/,
     &  '        NO. OF LEFT SURFACE NODE..........', I5,/,
     &  '        DIFFUSIVITY COEFF, FT2/YEAR.......', F10.5,/,
     &  '        SUCTION COMPRESSION INDEX, pF-1....', F10.5,/)
      WRITE (6,107)
  107 FORMAT ('          COORDINATES OF NODAL NUMBERS ',/,
     &  '      * * * * * * * * * * * * * * * * * * * * *',//,
     &  '          NODE          X-           Y-',/,
     &  '         NUMBER    DIRECTION,FT    DIRECTION,FT',/)
      DO 2890 J = 1,NODE
      WRITE (6,108)J,X(J),Y(J)
 2890 CONTINUE
  108 FORMAT(8X,I5,5X,F10.2,5X,F10.2)
      WRITE (6,109)
  109 FORMAT(//,'                  NODAL NUMBERS OF EACH ELEMENT ',/,
     &  '  * * * * * * * * * * * * * * * * * * * * * * * * * * * * *',/,
     &  '  ELEMENT       FIRST       SECOND        THIRD       FOURTH',/
     &,  '  NUMBER        NODE        NODE          NODE        NODE')
      DO 3020 J = 1,NELM
      WRITE (6,110) J,NOD(J,1),NOD(J,2),NOD(J,3),NOD(J,4)
  110 FORMAT (I5,10X,I5,5X,I5,10X,I5,5X,I5)
 3020 CONTINUE
 3280 NUM=NODE
C       GENERATE INITAL SUCTION POTENTIALS
      IF (NOCON.GT.0) GOTO 3310
      DO 3300 I = 1,NUM
      U(I) = UE
 3300 CONTINUE
      GOTO 3360
 3310 READ(5,105) (BU(I),I=1,NODLS)
      IJO = 0
      DO 3330 I=1,INI
      DO 3320 J=1,NODLS
      IJO=IJO+1
      U(IJO)=BU(J)
 3320 CONTINUE
 3330 CONTINUE
C
 3360 IF (NBOUC.EQ.0) GOTO 3410
      WRITE (6,111)
  111 FORMAT (//,'  CONSTANT BOUNDARY POINTS AND BOUNDARY CONDITIONS',/,
     &  '   * * * * * * * * * * * * * * * * * * * * * * *',/,
     &  '    BOUNDARY NODE      BOUNDARY SUCTION, INCHES',/)
  112 FORMAT (5X,I5,15X,F10.2)
      DO 3400 I = 1,NBOUC
```

Table A2 (Continued)

```
      READ (5,102) NF(I), U(NF(I))
      WRITE (6,112) NF(I), U(NF(I))
 3400 CONTINUE
 3410 WRITE (6,113)
  113 FORMAT (/,'              END OF INPUT DATA',/,
     &'     * * * * * * * * * * * * * * * * * * * * ',///,
     &'              BEGINNING OF OUTPUT',/,
     &'     * * * * * * * * * * * * * * * * * * * * ')
 3600 CONTINUE
      IF(NBOUV.EQ.0) GOTO 3650
      WRITE (9,201)
  201 FORMAT(//,'     VARIABLE BOUNDARY NODES ARE AS FOLLOWS',/)
      NBB = NBOUC + 1
      READ (5,104) (NF(I), I=NBB,NBOU)
      WRITE (9, 104) NBOUV,(NF(I),I=NBB,NBOU)
 3650 READ (5,114) DELT,TTOT
      WRITE (9,199) DELT,TTOT
  199 FORMAT(/,1X,'TIME INCREMENT=',F10.2,'  YEAR    TOTAL TIME=',F10.2,
     &'  YEARS',/)
  114 FORMAT(2F10.2)
      XT=TTOT/DELT
      IT= IDINT(XT) + 1
      WRITE(6,402)IT
  402 FORMAT(/,1X,'IT=',I5)
      READ (5,104) NFORM,NALL
      READ (5,114) THETA
      ANGLE = 1-THETA
C     ************    REM ASSEMBLE STIFFNESS MATRIX    *****************
      DO 3700 L = 1,NUM
      F(L) = 0.0
      DO 3700 M = 1,30
      A(L,M) = 0.0
      AK(L,M) = 0.0
      C(L,M) = 0.0
 3700 CONTINUE
      DO 4450 NN = 1,NELM
      IF (NOD(NN,4).EQ.0) GOTO 4260
      CALL RECT(NN,ALPA,NFORM,NALL,XKX,XKY)
      KK(1) = NOD(NN,1) -1
      KK(2) = NOD(NN,2)-1
      KK(3) = NOD(NN,3)-1
      KK(4)= NOD(NN,4)-1
      DO 4110 I=1, 4
      II = KK(I) + 1
      DO 4100 J=1, 4
      JJ=KK(J)+2-II
      IF (JJ.LE.0) GOTO 4100
      AK(II,JJ) = AK(II,JJ) + SM(I,J)
      C(II,JJ) = C(II,JJ) + CM(I,J)
```

Table A2 (Continued)

```
 4100 CONTINUE
 4110 CONTINUE
      MBS=ABS(KK(1)-KK(2))
      MBS1=ABS((KK(2)-KK(3)))
      MBS2=ABS((KK(3)-KK(4)))
      MBS3=ABS((KK(4)-KK(1)))
      MBS4=ABS((KK(1)-KK(3)))
      MBS5=ABS((KK(4)-KK(2)))
      IF (MBS.LT.MBS1) MBS=MBS1
      IF (MBS.LT.MBS2) MBS=MBS2
      IF (MBS.LT.MBS3) MBS=MBS3
      IF (MBS.LT.MBS4) MBS=MBS4
      IF (MBS.LT.MBS5) MBS=MBS5
      MBS = MBS+1
      IF ((MBS - MBD).GT.0) MBD = MBS
      GOTO 4450
C      ***** CALL SUBROUTINE TRIANGULAR ELEMENTS  *******
 4260 CALL TRIANG(NN,ALPA,NFORM,NALL,XKX,XKY)
      KK(1)=NOD(NN,1)-1
      KK(2)=NOD(NN,2)-1
      KK(3)=NOD(NN,3)-1
      DO 4380 I=1, 3
      II=KK(I)+1
      KL=I
      DO 4370 J = 1, 3
      JJ=KK(J)+2-II
      LL=J
      IF (JJ.GE.0) GOTO 4370
      AK(II,JJ) = AK(II,JJ) + SM(KL,LL)
      C(II,JJ)  = C(II,JJ) + CM(KL,LL)
 4370 CONTINUE
 4380 CONTINUE
      MBS=ABS(KK(1)-KK(2))
      MBS1=ABS(KK(2)-KK(3))
      MBS2=ABS(KK(3)-KK(1))
      IF (MBS.LT.MBS1) MBS=MBS1
      IF (MBS.LT.MBS2) MBS=MBS2
      MBS=MBS+1
      IF((MBS - MBD).GT.0) MBD = MBS
 4450 CONTINUE
      IF (NALL.EQ.2) GOTO 4550
      WRITE (6,120)
  120 FORMAT(//,'                GLOBAL K MATRIX',/,
     &'          ****************************')
      DO 4510 I = 1, NUM
      DO 4510 J = 1, MBD
      WRITE (6,121) I,J,AK(I,J)
 4510 CONTINUE
      WRITE (6,122)
```

Table A2 (Continued)

```
  121 FORMAT (2I5,F20.8)
  122 FORMAT(//,'                    GLOBAL C MATRIX',/,
     &'          ******************************')
      DO 4520 I = 1, NUM
      DO 4520 J = 1, MBD
      WRITE (6,121) I,J,C(I,J)
 4520 CONTINUE
C         *********   FORMULATE A AND P MATRICES   **********
 4550 DO 4610 I=1, NUM
      DO 4600 J=1, MBD
      A(I,J)=(C(I,J)+DELT*THETA*AK(I,J))
      P(I,J)=(C(I,J)-ANGLE*DELT*AK(I,J))
 4600 CONTINUE
 4610 CONTINUE
      IF (NALL.EQ.2) GOTO 4640
      WRITE (6,123)
  123 FORMAT(//,'                    GLOBAL A MATRIX',/,
     &'          ******************************')
      DO 4620 I = 1, NUM
      DO 4620 J = 1, MBD
      WRITE (6,121) I,J,A(I,J)
 4620 CONTINUE
      WRITE (6,124)
  124 FORMAT(//,'                    GLOBAL P MATRIX',/,
     &'          ******************************')
      DO 4630 I = 1, NUM
      DO 4630 J = 1, MBD
      WRITE (6,121) I,J,P(I,J)
 4630 CONTINUE
 4640 CALL BOU(NALL,NUM,MBD,NBOU)
C
C     **********  DECOMPOSE THE A MATRIX  **********
      CALL DECOM(NALL,NUM,MBD)
C
C       SOLVE THE EQUATION AT DIFFERENT TIMES
C
      J=0
      DO 4800 JI=1,INI
      DO 4800 I=1,NODLS
      J=J+1
      PFMIN(JI,I)=U(J)
      PFMAX(JI,I)=U(J)
 4800 CONTINUE
      DO 4900 LL = 1, IT
      IF (LL.EQ.1) GOTO 4820
C
      CALL BOU(NALL,NUM,MBD,NBOU)
C
 4820 CALL PTIMESU(NALL,NUM,MBD)
```

Table A2 (Continued)

```
C
      CALL SOL(TIME,DELT,NUM,MBD)
C
      J=0
      DO 4830 JI=1,INI
      DO 4830 I=1,NODLS
      J=J+1
      IF(U(J).GT.PFMAX(JI,I))PFMAX(JI,I)=U(J)
      IF(U(J).LT.PFMIN(JI,I))PFMIN(JI,I)=U(J)
 4830 CONTINUE
C              READ THE BOUNDARY POTENTIALS FOR THE NEXT TIME
 4890 CALL VARYB(NUM,NBB,NBOU,DELS,DELT,UOPF,UEPF,CYCLES)
 4900 CONTINUE
      WRITE(6,130)
  130 FORMAT(/1X,'  NODE        MIN pF   MAX pF   DIFF')
      WRITE(9,131)
  131 FORMAT(/,1X,'DISTANCE, FT  DELTA UMAX, pF   Za, FT    HEAVE, IN.')
      J=0
      DO 4950 JI=1,INI
      VOLT=0.0
      HEAVE=0.0
      DO 4940 I=1,NODLS
      J=J+1
      DPF=PFMAX(JI,I)-PFMIN(JI,I)
      WRITE(6,137)J,PFMIN(JI,I),PFMAX(JI,I),DPF
      IF(I.EQ.NODLS)GOTO 4940
      DPF1=PFMAX(JI,I+1)-PFMIN(JI,I+1)
      DPF2=PFMAX(JI,I)-PFMIN(JI,I)
      AVEDPF=(DPF1+DPF2)/2.
      DVOL=(Y(I+1)-Y(I))*CT*AVEDPF*12.
      HEAVE=HEAVE+DVOL
      IF(VOLT.GT.0.5)GOTO 4940
      CPF=(DPF1+DPF2)/2.
      VOLT=VOLT+DVOL
      MUM=I
 4940 CONTINUE
      ZA = Y(J)-Y(MUM)-(Y(2)-Y(1))
      WRITE(9,136)X(J),CPF,ZA,HEAVE
      WRITE(7,105)X(J),CPF,ZA,HEAVE
  136 FORMAT(F10.5,5X,F10.5,5X,2F10.5)
  137 FORMAT(I5,3F10.5)
 4950 CONTINUE
      CLOSE (5,STATUS='KEEP')
      CLOSE (6,STATUS='KEEP')
      CLOSE (7,STATUS='KEEP')
      CLOSE (9,STATUS='KEEP')
      STOP
      END
C
```

Table A2 (Continued)

```
C
C      *******    SUBROUTINE RECT  *******
      SUBROUTINE RECT(NN,ALPA,NFORM,NALL,XKX,XKY)
      IMPLICIT DOUBLE PRECISION (A-H,O-Z)
      PARAMETER (KNO=400)
      COMMON /COM1/NOD(KNO,4),X(KNO),Y(KNO),SM(4,4),CM(4,4)
      II=NOD(NN,1)
      JJ=NOD(NN,2)
      KK=NOD(NN,3)
      LL=NOD(NN,4)
      A = (Y(LL) - Y(II))/2
      B = (X(KK) - X(LL))/2
      AREA = 4*A*B
      XKBAR=XKX*A/(6*B)
      YKBAR=XKY*B/(6*A)
      SM(1,1) = XKBAR*2+YKBAR*2
      SM(1,2) = XKBAR*(-2)+YKBAR
      SM(1,3) = XKBAR*(-1)+YKBAR*(-1)
      SM(1,4) = XKBAR+YKBAR*(-2)
      SM(2,2) = XKBAR*2+YKBAR*2
      SM(2,3) = XKBAR+YKBAR*(-2)
      SM(2,4) = XKBAR*(-1)+YKBAR*(-1)
      SM(3,3) = XKBAR*2+YKBAR*2
      SM(3,4) = XKBAR*(-2)+YKBAR
      SM(4,4) = XKBAR*2+YKBAR*2
      IF (NFORM.EQ.2) GOTO 5510
      CM(1,1) = AREA/(9*ALPA)
      CM(1,2) = CM(1,1)/2
      CM(1,3) = CM(1,2)/2
      CM(1,4) = CM(1,2)
      CM(2,2) = CM(1,1)
      CM(2,3) = CM(1,2)
      CM(2,4) = CM(1,3)
      CM(3,3) = CM(1,1)
      CM(3,4) = CM(1,2)
      CM(4,4) = CM(1,1)
      GOTO 5590
 5510 DO 5580 I = 1, 4
      DO 5570 J = 1, 4
      IF (I.NE.J) GOTO 5560
      CM(I,J) = AREA/(4*ALPA)
      GOTO 5570
 5560 CM(I,J)=0
 5570 CONTINUE
 5580 CONTINUE
 5590 DO 5640 J = 1, 4
      DO 5630 K = J, 4
      SM(K,J) = SM(J,K)
      CM(K,J) = CM(J,K)
```

Table A2 (Continued)

```
 5630 CONTINUE
 5640 CONTINUE
      IF (NALL.EQ.2) GOTO 5730
      WRITE (6,114) NN
  114 FORMAT (//,'        ELEMENT NUMBER =',I5,//
     &,'   SM MATRIX   CM MATRIX')
  115 FORMAT (2I5,2F10.4)
      DO 5690 I = 1, 4
      DO 5680 J = 1, 4
      WRITE (6,115) I,J,SM(I,J), CM(I,J)
 5680 CONTINUE
 5690 CONTINUE
 5730 RETURN
      END
C
C
C      ******  SUBROUTINE TRIANGULAR ELEMENTS ********
      SUBROUTINE TRIANG(NN,ALPA,NFORM,NALL,XKX,XKY)
      IMPLICIT DOUBLE PRECISION (A-H,O-Z)
      PARAMETER (KNO=400)
      COMMON /COM1/NOD(KNO,4),X(KNO),Y(KNO),SM(4,4),CM(4,4)
      II=NOD(NN,1)
      JJ=NOD(NN,2)
      KK=NOD(NN,3)
      B1=Y(JJ)-Y(KK)
      B2=Y(KK)-Y(II)
      B3=Y(II)-Y(JJ)
      C1=X(KK)-X(JJ)
      C2=X(II)-X(KK)
      C3=X(JJ)-X(II)
      AR=(C3*B2+C2*B3)/2
      AR=ABS(AR)
      C=4*AR
      XKBAR=XKX/C
      YKBAR=XKY/C
      SM(1,1)=XKBAR*B1*B1+YKBAR*C1*C1
      SM(1,2)=XKBAR*B1*B2+YKBAR*C1*C2
      SM(1,3)=XKBAR*B1*B3+YKBAR*C1*C3
      SM(2,2)=XKBAR*B2*B2+YKBAR*C2*C2
      SM(2,3)=XKBAR*B2*B3+YKBAR*C2*C3
      SM(3,3)=XKBAR*B3*B3+YKBAR*C3*C3
      IF (NFORM.EQ.2) GOTO 6320
C     *******   CONSISTENT FORMULATION    ************
      CON=AR/(12*ALPA)
      CM(1,1)=2*CON
      CM(1,2)=CON
      CM(1,3)=CON
      CM(2,2)=CM(1,1)
      CM(2,3)=CM(1,2)
```

Table A2 (Continued)

```
      CM(3,3)=CM(1,1)
      GOTO 6390
C     *******   LUMPED FORMULATION    ************
 6320 CON=AR/(3*ALPA)
      CM(1,1)=CON
      CM(1,2)=0
      CM(1,3)=0
      CM(2,2)=CON
      CM(2,3)=0
      CM(3,3)=CON
 6390 DO 6440 K=1, 3
      DO 6430 J=K, 3
      SM(J,K)=SM(K,J)
      CM(J,K)=CM(K,J)
 6430 CONTINUE
 6440 CONTINUE
      IF (NALL.EQ.2) GOTO 6530
      WRITE (6,114) NN
  114 FORMAT (//,'         ELEMENT NUMBER =',I5,//
     &,'    SM MATRIX    CM MATRIX')
  115 FORMAT(2I5,2F10.4)
      DO 6520 I = 1, 3
      DO 6510 J = 1, 3
      WRITE (6,115) I,J,SM(I,J), CM(I,J)
 6510 CONTINUE
 6520 CONTINUE
 6530 RETURN
      END
C
C
C     ****** READ THE BOUNDARY (VARYING) SUCTION POTENTIAL IN THE NEXT TIME
      SUBROUTINE VARYB(NUM,NBB,NBOU,DELS,DELT,UOPF,UEPF,CYCLES)
      IMPLICIT DOUBLE PRECISION (A-H,O-Z)
      PARAMETER (KNO=400)
      COMMON /COM2/A(KNO,30),P(KNO,30),U(KNO),F(KNO),NF(80)
      DO 6830 I = 1, NUM
      F(I)=0
 6830 CONTINUE
      DTIME = (DELS+DELT)
      TEM1 = 2*3.14159*CYCLES*DTIME
      TEM1 = UOPF*SIN(TEM1) + UEPF
      IJK = 1
      DELS = DELS+DELT
      DO 6860 I = NBB, NBOU
      U(NF(I)) = TEM1
 6860 CONTINUE
 6870 RETURN
      END
C
```

Table A2 (Continued)

```
C
C        *****  SUBROUTINE PTIMESU  ********************
      SUBROUTINE PTIMESU(NALL,NUM,MBD)
      IMPLICIT DOUBLE PRECISION (A-H,O-Z)
      PARAMETER (KNO=400)
      COMMON /COM2/A(KNO,30), P(KNO,30),U(KNO),F(KNO),NF(80)
      DO 7120 I = 1, NUM
      SUM = 0
      DO 7050 J=1, MBD
      SUM = SUM + P(I,J)*U(I+J-1)
 7050 CONTINUE
      I1 = I
      IF (I1.EQ.1) GOTO 7110
      DO 7100 J = 2, MBD
      I1=I1-1
      SUM = SUM + P(I1,J)*U(I1)
      IF (I1.EQ.1) GOTO 7110
 7100 CONTINUE
 7110 F(I) = F(I) + SUM
 7120 CONTINUE
      IF (NALL.EQ.2) GOTO 7180
      WRITE (6,10)
   10 FORMAT(//,'                F VECTOR (FROM PTIMESU)',/,
     &'        ************************************')
   20 FORMAT (I5,E15.4)
      DO 7170 J = 1, NUM
      WRITE (6,20) J,F(J)
 7170 CONTINUE
 7180 RETURN
      END
C
C
C       *************   SUBVROUTINE BOU ***************
      SUBROUTINE BOU(NALL,NUM,MBD,NBOU)
      IMPLICIT DOUBLE PRECISION (A-H,O-Z)
      PARAMETER (KNO=400)
      COMMON /COM2/A(KNO,30),P(KNO,30),U(KNO),F(KNO),NF(80)
      DO 7550 I = 1, NBOU
      N = NF(I)
      A(N,1)=1.0E+20
      F(N)=F(N) + U(N)*A(N,1)
 7550 CONTINUE
      IF (NALL.EQ.2) GOTO 7650
      WRITE (6,116)
  116 FORMAT (//,'                MATRIX A AFTER THE BOUNDARY CONDITIONS',/,
     &'        ************************************************')
  117 FORMAT (2I5,E15.4)
      DO 7600 I = 1, NUM
      DO 7600 J = 1, MBD
```

Table A2 (Continued)

```
      WRITE (6,117) I,J,A(I,J)
 7600 CONTINUE
      WRITE (6,118)
  118 FORMAT (//,'     F VECTOR (FROM SUB BOU)',/,
     &'         ****************************************')
  119 FORMAT (I5,E15.4)
      DO 7610 J = 1, NUM
      WRITE (6,119) J,F(J)
 7610 CONTINUE
 7650 RETURN
      END
C
C
C       *****  SUBROUTINE DECOM   (BANDED MATRIX)   ********
C  ****  DECOMPOSITION OF UPPER, LOWER, AND DIAGONAL MATRICES  ****
      SUBROUTINE DECOM(NALL,NUM,MBD)
      IMPLICIT DOUBLE PRECISION (A-H,O-Z)
      PARAMETER (KNO=400)
      COMMON /COM2/A(KNO,30),P(KNO,30),U(KNO),F(KNO),NF(80)
      N1=NUM-1
      DO 8140 K=1, N1
      DO 8130 L=2, MBD
      I=K+(L-1)
      IF (NUM.LT.I) GOTO 8130
      C=A(K,L)/A(K,1)
      J=0
      DO 8120 JD=L, MBD
      J=J+1
      A(I,J)=A(I,J)-C*A(K,JD)
 8120 CONTINUE
 8130 CONTINUE
 8140 CONTINUE
      DO 8180 I=1, N1
      DO 8180 J=2, MBD
      A(I,J)=A(I,J)/A(I,1)
 8180 CONTINUE
      IF (NALL.EQ.2) GOTO 8240
      WRITE (6,130)
  130 FORMAT (//,'     MATRIX A AFTER THE DECOMPOSITION',/,
     &'         ************************************************')
  131 FORMAT (2I5,E15.4)
      DO 8230 I = 1,NUM
      DO 8230 J = 1,MBD
      WRITE (6,131) I,J,A(I,J)
 8230 CONTINUE
 8240 RETURN
      END
C
C
```

Table A2 (Concluded)

```
C       *****    SUBROUTINE SOL  **************
      SUBROUTINE SOL(TIME,DELT,NUM,MBD)
      IMPLICIT DOUBLE PRECISION (A-H,O-Z)
      PARAMETER (KNO=400)
      COMMON /COM2/A(KNO,30),P(KNO,30),U(KNO),F(KNO),NF(80)
      IF(TIME.LT.0.0001)NT=0
      NT=NT+1
      TIME =TIME + DELT
      N1=NUM-1
      DO 9090 K=1, N1
      DO 9080 J=2, MBD
      I=K+J-1
      IF (NUM.LT.I) GOTO 9080
      F(I)=F(I)-A(K,J)*F(K)
 9080 CONTINUE
 9090 CONTINUE
C                        READY FOR BACKWARD SUB.
      DO 9130 I=1, NUM
      F(I)=F(I)/A(I,1)
 9130 CONTINUE
C                        FORWARD SUB.
      DO 9220 K= 1, N1
      I=NUM-K
      DO 9210 JD = 2, MBD
      J = I+JD-1
      IF (NUM.LT.J) GOTO 9210
      F(I)=F(I)-A(I,JD)*F(J)
 9210 CONTINUE
 9220 CONTINUE
      IF(NT.EQ.10)WRITE (6,150) TIME
  150 FORMAT(//,' * * * * * * * * * * * * * * * * * * * * * * * * * * * * ',/,
     &'           NODAL SUCTION POTENTIAL AT TIME = ',F10.2,' YEARS',/,
     &'  * * * * * * * * * * * * * * * * * * * * * * * * * * * * * *')
  151 FORMAT(I10,F20.5)
      DO 9490 I = 1, NUM
      U(I)=F(I)
      IF(NT.EQ.10)WRITE (6,151) I,U(I)
 9490 CONTINUE
      IF(NT.EQ.10)NT=0
      RETURN
      END
```

Table A3. Example Input Data

```
e 341   380    38     9    20     0  60.          0.04
   3.
   2.5          3.          1.0
    1     1
   20
   18     1    18     1   361   362     2    0.0      0.0     72.0      4.0
   18    19    36     2   362   363     3    0.0      4.0     72.0      8.0
   18    37    54     3   363   364     4    0.0      8.0     72.0     12.0
   18    55    72     4   364   365     5    0.0     12.0     72.0     16.0
   18    73    90     5   365   366     6    0.0     16.0     72.0     20.0
   18    91   108     6   366   367     7    0.0     20.0     72.0     24.0
   18   109   126     7   367   368     8    0.0     24.0     72.0     28.0
   18   127   144     8   368   369     9    0.0     28.0     72.0     32.0
   18   145   162     9   369   370    10    0.0     32.0     72.0     36.0
   18   163   180    10   370   371    11    0.0     36.0     72.0     40.0
   18   181   198    11   371   372    12    0.0     40.0     72.0     44.0
   18   199   216    12   372   373    13    0.0     44.0     72.0     48.0
   18   217   234    13   373   374    14    0.0     48.0     72.0     52.0
   18   235   252    14   374   375    15    0.0     52.0     72.0     56.0
   18   253   270    15   375   376    16    0.0     56.0     72.0     60.0
   18   271   288    16   376   377    17    0.0     60.0     72.0     64.0
   18   289   306    17   377   378    18    0.0     64.0     72.0     68.0
   18   307   324    18   378   379    19    0.0     68.0     72.0     72.0
    8   325   332    19   179   180    20    0.0     72.0     32.0     76.0
    9   333   341   199   379   380   200   36.0     72.0     72.0     76.0
    1   3.00000
   21   3.
   41   3.
   61   3.
   81   3.
  101   3.
  121   3.
  141   3.
  161   3.
  181   3.
  201   3.
  221   3.
  241   3.
  261   3.
  281   3.
  301   3.
  321   3.
  341   3.
  361   3.
  362   3.
  363   3.
  364   3.
  365   3.
  366   3.
```

Table A3 (Concluded)

```
367   3.
368   3.
369   3.
370   3.
371   3.
372   3.
373   3.
374   3.
375   3.
376   3.
377   3.
378   3.
379   3.
380   3.
 20   40   60   80  100  120  140  160  180
    0.01      4.0
  0    2
    0.67
```

APPENDIX B: COMPUTER PROGRAMS

1. Five computer programs were developed to assist analysis of the detailed elevation profile data obtained from dipstick profilometers:

FTRC.FOR. This program, Table B1, transforms elevation profile data into discrete waveforms of given amplitude frequency by Fourier transforms (Brigham 1974) using data file FTRIN.TXT; output file is FTROUT.TXT

FTROPT.FOR. This program, Table B2, evaluates the optimum amplitude and frequency of dominant discrete waveforms of elevation profiles by Fourier transforms using data file FTRIN.TXT; output file is FTROPT.TXT

FNUMR.FOR. This program, Table B3, evaluates the Face floor levelness FL and floor flatness FF F-numbers of elevation profiles (Edward W. Face Company 1983), Face 1984) using data file DATDIP.TXT; output file is DIPOUT.TXT.

ADATG.FOR. This program, Table B4, evaluates a series of trial surface roughness indices from elevation profiles including relative thickness, angular distortion, intensity of angular distortion, tilt, mean and standard deviations, macrorelief index, and fractal using data file FTRIN.TXT. Output file is FTROUT.TXT

WAVEI.FOR. This program, Table B5, evaluates the wave index WI using a spacing Δx from 1 to 50 ft from elevation data (Kalman Laboratories 1989) using data file DATDIP.TXT; output file is DIPOUT.TXT

Input parameters required for each of these programs are similar, Table B6a, and provided in a data file, FTRIN.TXT or DATDIP.TXT. Output data is given in file FTROUT.TXT or DIPOUT.TXT, Table B6b. Table B7 provides example listing of FTROUT.TXT from a run of program FTRC analyzing the Fourier transform of a simple sine wave of amplitude 1 inch and wavelength 32 ft.

These programs, except FTROPT also generate graphics files to permit plotting of results as follows:

Program	Output File	Plotted Data
FTRC	FTRE.DAT	Elevation profile
	FTR.DAT	Amplitude of discrete waves versus frequency
	FREBETA.DAT	Angular distortion versus frequency

FNUMR	ELEV.DAT	Elevation profile
	FNUM.DAT	F-numbers versus length
ADATG	FTRE.DAT	Elevation profile
	ANGU1.DAT	Angular distortion and tilt versus frequency of adjacent peaks
	ANGU1.DAT	Angular distortion and tilt versus frequency of nonadjacent peaks
	MEAN.DAT	Mean angular distortion, tilt and macrorelief index versus length
	FRACTAL.DAT	Fractal diagram
WAVEI	RWAVE.DAT	Wave index versus length
	WAVE.DAT	Mean square root amplitude versus length increment

Program SINEW.FOR, Table B8, was developed to automatically generate the input files FTRIN.TXT for the simple and complex sine waves studied in PART III.

Table B1. Listing program FTRC.FOR

```
C  PROGRAM FTRC.FOR: TO CALCULATE FOURIER TRANSFORM FROM ELEVATIONS OR
C  ELEVATION CHANGES
C     NOMENCLATURE
C          LOOP      = 1     Closed loop; Operator bias subtracted from
C                            dipstick readings
C                    = 0     Open loop
C          KOPT      = 0     Elevation readings input
C                    = 1     Elevation change readings input
7          NREAD     Number of readings
C          DIFL      Sample length interval of profile data, ft
C          NRE       Number of readings used in Fourier Transform
      DIMENSION HED(20),DEL(1000),ELEV(1000),ALENG(1000),THETA(1000),FRE
     1(1000),H(1000),BETA(1000)
      OPEN(5,FILE='FTRIN.TXT')
      OPEN(6,FILE='FTROUT.TXT')
      OPEN(7,FILE='\GRAPHER\FTR.DAT')
      OPEN(8,FILE='\GRAPHER\FTRE.DAT')
      OPEN(9,FILE='\GRAPHER\FREBETA.DAT')
      STD=0.0
      AMEAN=0.0
      BIAS=0.0
      READ(5,10) (HED(I),I=1,20)
      WRITE(6,12)(HED(I),I=1,20)
   10 FORMAT(20A4)
   12 FORMAT(1X,20A4)
      READ(5,15)LOOP,KOPT,NREAD,DIFL,NRE
   15 FORMAT(3I5,F10.2,I5)
      IF(LOOP.EQ.0) WRITE(6,17)
      IF(LOOP.EQ.1) WR1TE(6,18)
```

Table B1. (Continued)

```
   17 FORMAT(/,10X,'OPEN LINE    UNCORRECTED READINGS')
   18 FORMAT(/,10X,'CLOSED LINE     CORRECTED READINGS')
      WRITE (6,25) NREAD,DIFL,NRE
   25 FORMAT(/,1X,'NUMBER OF READINGS=',11X,I5,/,1X,'ACTUAL SAMPLE',
     1' INTERVAL =',6X,F10.2,'  FEET',/,1X,'READINGS USED =',I5)
      IF(KOPT.EQ.0)WRITE(6,26)
      IF(KOPT.EQ.1)WRITE(6,27)
   26 FORMAT(/,1X,'INPUT DATA ARE ELEVATIONS',/)
   27 FORMAT(/,1X,'INPUT DATA ARE CHANGES IN ELEVATIONS',/)
C     INITIALIZE
      NN = NREAD + 1
      DO 30 I = 1,NN
      DEL(I)=0.0
      ELEV(I) = 0.0
      ALENG(I) = 0.0
   30 CONTINUE
      IF(KOPT.EQ.1)READ(5,40)(DEL(I), I=2,NN)
      IF(KOPT.EQ.0)READ(5,40)(ELEV(I),I=2,NN)
   40 FORMAT(10F7.3)
   41 FORMAT(//,1X,'UNCORRECTED INPUT DATA',//,
     11X,'DEPTH,FT     0      1      2      3     4      5      6',
     2'      7      8      9',/)
      WRITE(6,41)
      JJ = NN/10 + 1
      AK = 0.0
      J1 = 1
      J2 = 10
      DO 45 I = 1,JJ
      IF(I.EQ.JJ)J2 = NN
      IF(KOPT.EQ.1)WRITE(6,47)AK,(DEL(J),J=J1,J2)
      IF(KOPT.EQ.0)WRITE(6,47)AK,(ELEV(J),J=J1,J2)
      AK = AK + 10.*DIFL
      J1 = J1 + 10
      J2 = J2 + 10
   45 CONTINUE
   47 FORMAT(1X,F8.2,10F7.3)
   48 N1 = 2
      N2 = NN
      IF(KOPT.EQ.1)CALL STAND (N1,N2,DEL,STD,AMEAN)
      SUM = AMEAN*FLOAT(NREAD)
      IF(KOPT.EQ.1)WRITE(6,50) SUM, AMEAN, STD
   50 FORMAT(//,4X,'TOTAL  READINGS  =', F7.3,'INCH',/,1X,
     1'MEAN  =',F10.6,'  INCH',/,1X,'STANDARD',
     2' DEVIATION =',F15.5)
      IF(LOOP.EQ.0) GOTO 60
      IF(KOPT.EQ.1)BIAS = AMEAN
      IF(KOPT.EQ.0)BIAS=(ELEV(NN)-ELEV(1))/FLOAT(NREAD)
      WRITE(6,52)BIAS
   52 FORMAT(1X,'BIAS =',F10.5,'  IN./FT',/)
```

Table B1. (Continued)

```
      DO 55 I = 2,NN
      IF(KOPT.EQ.1)DEL(I) = DEL(I) - BIAS
      IF(KOPT.EQ.0)ELEV(I)=ELEV(I) - BIAS*FLOAT(I-1)
   55 CONTINUE
   60 TOTLEN = FLOAT(NREAD)*DIFL
      WRITE(6,61)TOTLEN
   61 FORMAT(/,1X,'TOTAL LENGTH =',F10.2,'  FEET')
      DO 65 I = 2,NN
      ALENG(I) = ALENG(I-1) + DIFL
      IF(KOPT.EQ.1)ELEV(I) =  ELEV(I-1) + DEL(I)
      IF(KOPT.EQ.0)DEL(I)=ELEV(I) - ELEV(I-1)
   65 CONTINUE
   66 FORMAT(//,1X,'CORRECTED READINGS',//,1X,'DEPTH,FT'
     1,'     0      1      2      3      4      5      6      7    8',
     2'      9',/)
      IF(LOOP.GE.1)WRITE(6,66)
      IF(LOOP.EQ.0)GOTO 73
      JJ = NN/10 + 1
      AK = 0.0
      J1=1
      J2 = 10
      DO 70 I = 1,JJ
      IF(I.EQ.JJ)J2 = NN
      IF(KOPT.EQ.1)WRITE(6,72)AK,(DEL(J),J=J1,J2)
      IF(KOPT.EQ.0)WRITE(6,72)AK,(ELEV(J),J=J1,J2)
      AK=AK+10.*DIFL
      J1=J1+10
      J2 = J2 + 10
   70 CONTINUE
   72 FORMAT(1X,F8.2,10F7.3)
   73 AM=DIFL*FLOAT(NRE)/4.
      M=IFIX(AM)
      TOTL=FLOAT(NRE)*DIFL
      WRITE(6,79)NRE
   79 FORMAT(1X,'READINGS USED FOR FOURIER TRANSFORM=',I5,/)
      P=3.14159265*2.
      DO 90 I=1,NN
      WRITE(8,95)ALENG(I),ELEV(I)
   90 CONTINUE
   95 FORMAT(2F10.5)
      WRITE(6,96)
   96 FORMAT(/,1X,'NUMBER  FREQUENCY    REAL   IMAGINARY  AMPLITUDE  PHA
     1SE SHIFT, DEG',/)
      DO 100 I=1,M
      FRE(I)=FLOAT(I-1)/TOTL
      XR = 0.0
      XI = 0.0
      DO 97 J=1,NRE
      ARG=P*FRE(I)*ALENG(J)
```

Table B1. (Continued)

```
      XR=XR+ELEV(J)*COS(ARG)
      XI=XI+ELEV(J)*SIN(ARG)
   97 CONTINUE
      H(I)=ABS(XR)**2.+ABS(XI)**2.
      H(I)=DIFL*(H(I)**0.5)/TOTL
      BA=XI/XR
      THETA(I)=ATAN(BA)*360./P
      WRITE(6,110)I,FRE(I),XR,XI,H(I),THETA(I)
      WRITE(7,120)FRE(I),H(I)
      BETA(I)=100*8.*H(I)*FRE(I)/12.
      WRITE(9,120)FRE(I),BETA(I)
  100 CONTINUE
  110 FORMAT(I5,2F10.5,3F12.5)
  120 FORMAT(2F10.5)
C       ROUGHNESS ESTIMATE
      SUM=0.0
      SUMB=0.0
      DO 250 I=2,M
      TEMP=(H(I)+H(I-1))/2.
      SUM=SUM+TEMP
      TBETA=(BETA(I)+BETA(I-1))/2.
      SUMB=SUMB+TBETA
  250 CONTINUE
      ROUGH=SUM*8./TOTL
      ROUGHB=SUMB/AM
      WRITE(6,300)ROUGH,ROUGHB
  300 FORMAT(/,1X,'AMPLITUDE ROUGHNESS OF TRANSFORM IS',F10.5,'  IN.',/,
     11X,'BETA      ROUGHNESS OF TRANSFORM IS',F10.5)
      SUM=0.0
      DO 350 I=2,NRE
      TEMP=(ABS(ELEV(I))+ABS(ELEV(I-1)))/2.
      SUM=SUM+TEMP
  350 CONTINUE
      ROUGH=SUM/FLOAT(NRE)
      WRITE(6,400)ROUGH
  400 FORMAT(1X,'          ELEVATION ROUGHNESS IS',F10.5, '  IN.')
      CLOSE(5,STATUS='KEEP')
      CLOSE(6,STATUS='KEEP')
      CLOSE(7,STATUS='KEEP')
      CLOSE(8,STATUS='KEEP')
      CLOSE(9,STATUS='KEEP')
      STOP
      END
C
C
      SUBROUTINE STAND (N1,N2,VAR,STD,AMEAN)
      DIMENSION VAR(1000)
      NI=N1
      NJ=N2
```

Table B1. (Concluded)

```
      N=NJ-NI
      NN=N-1
      SUM = 0.0
      SUMSQ = 0.0
      DO 10 I = NI,NJ
      SUM = SUM + VAR(I)
      SUMSQ = SUMSQ + VAR(I)*VAR(I)
   10 CONTINUE
      AMEAN = SUM/FLOAT(N)
      STDSQ = (SUMSQ - SUM*SUM/FLOAT(N))/FLOAT(NN)
      STD = ABS(STDSQ)**0.5
      RETURN
      END
```

Table B2. Listing Program FTROPT.FOR

```
C  PROGRAM FTROPT.FOR: TO OPTIMIZE CALCULATION OF PEAK AMPLITUDES AND
C  RESONANT FREQUENCIES OF FOURIER TRANSFORMS
C     NOMENCLATURE
C          LOOP       = 1     Closed loop; Operator bias subtracted from
C                             dipstick readings
C                     = 0     Open loop
C          KOPT       = 0     Elevation readings input
C                     = 1     Elevation change readings input
C          NREAD      Number of readings
C          DIFL       Sample interval of profile data, ft
C          NRE        Number of readings used in Fourier Transform
C          JOPT       = 0     Minimum output listing
C                     = 1     Maximum output listing
C          NO         Number of Fourier Runs at decrement = 2
C          PEAKA      Limiting peak amplitude used to calculate resonant
C                        frequency, usually 0.02 inch
      DIMENSION HED(20),DEL(1000),IJ(30),IJK(30)
      COMMON/FOUR/FRE(1000),THETA(1000),H(1000),ALENG(1000),ELEV(1000)
      COMMON/AMP/FR(100,30),PHI(100,30),AMP(100,30)
      OPEN(5,FILE='FTRIN.TXT')
      OPEN(6,FILE='FTROPT.TXT')
      OPEN(7,FILE='D:FRE1.DAT')
      OPEN(8,FILE='D:FRE2.DAT')
      OPEN(9,FILE='D:FRE3.DAT')
      OPEN(10,FILE='D:FRE4.DAT')
      OPEN(11,FILE='D:FRE5.DAT')
      OPEN(12,FILE='D:FRE6.DAT')
      OPEN(13,FILE='D:FRE7.DAT')
      OPEN(14,FILE='D:FRE8.DAT')
      OPEN(15,FILE='D:FRE9.DAT')
      OPEN(16,FILE='D:FRE10.DAT')
      STD=0.0
```

Table B2. (Continued)

```
      AMEAN=0.0
      BIAS=0.0
      READ(5,10) (HED(I),I=1,20)
      WRITE(6,12)(HED(I),I=1,20)
   10 FORMAT(20A4)
   12 FORMAT(1X,20A4)
      READ(5,15)LOOP,KOPT,NREAD,DIFL,NRE,JOPT,NO,PEAKA
   15 FORMAT(3I5,F10.2,3I5,F10.5)
      IF(LOOP.EQ.0) WRITE(6,17)
      IF(LOOP.EQ.1) WRITE(6,18)
   17 FORMAT(/,10X,'OPEN LINE    UNCORRECTED READINGS')
   18 FORMAT(/,10X,'CLOSED LINE     CORRECTED READINGS')
      WRITE (6,25) NREAD,DIFL,NRE
   25 FORMAT(/,1X,'NUMBER OF READINGS=',11X,I5,/,1X,'ACTUAL SAMPLE',
     1' INTERVAL =',F5.2,'  FEET'/,1x,'READINGS USED NRE=',I5)
      IF(KOPT.EQ.0)WRITE(6,26)
      IF(KOPT.EQ.1)WRITE(6,27)
   26 FORMAT(/,1X,'INPUT DATA ARE ELEVATIONS',/)
   27 FORMAT(/,1X,'INPUT DATA ARE CHANGES IN ELEVATIONS',/)
C     INITIALIZE
      NN = NREAD + 1
      DO 30 I = 1,NN
      DEL(I)=0.0
      ELEV(I) = 0.0
      ALENG(I) = 0.0
   30 CONTINUE
      WRITE(6,31)NO,PEAKA
   31 FORMAT(1X,'NUMBER OF FOURIER RUNS=',I5,/,1X,'MAXIMUM AMPLITUDE DET
     1ECTED =',F10.5,'  INCH')
      IF(KOPT.EQ.1)READ(5,40)(DEL(I), I=2,NN)
      IF(KOPT.EQ.0)READ(5,40)(ELEV(I),I=2,NN)
   40 FORMAT(10F7.3)
   41 FORMAT(/,1X,'UNCORRECTED INPUT DATA',//,
     11X,'DEPTH,FT     0      1      2      3     4      5      6',
     2'      7      8      9',/)
      IF(JOPT.EQ.1)WRITE(6,41)
      JJ = NN/10 + 1
      AK = 0.0
      J1 = 1
      J2 = 10
      DO 45 I = 1,JJ
      IF(I.EQ.JJ)J2 = NN
      IF(JOPT.EQ.1.AND.KOPT.EQ.1)WRITE(6,47)AK,(DEL(J),J=J1,J2)
      IF(JOPT.EQ.1.AND.KOPT.EQ.0)WRITE(6,47)AK,(ELEV(J),J=J1,J2)
      AK = AK + 10.*DIFL
      J1 = J1 + 10
      J2 = J2 + 10
   45 CONTINUE
   47 FORMAT(1X,F8.2,10F7.3)
```

Table B2. (Continued)

```
48 N1 = 2
   N2 = NN
   IF(KOPT.EQ.0) CALL STAND (N1,N2,ELEV,STD,AMEAN)
   IF(KOPT.EQ.1) CALL STAND (N1,N2,DEL,STD,AMEAN)
   SUM = AMEAN*FLOAT(NREAD)
   WRITE(6,50) SUM, AMEAN, STD
50 FORMAT(//,1X,'TOTAL              =', F7.3,'  INCH',/,1X,'MEAN
  1          =',F10.6,'  INCH',/,1X,'STANDARD DEVIATION =',F9.5)
   IF(LOOP.EQ.0) GOTO 60
   IF(KOPT.EQ.1)BIAS = AMEAN
   IF(KOPT.EQ.0)BIAS=(ELEV(NN)-ELEV(1))/FLOAT(NREAD)
   WRITE(6,52)BIAS
52 FORMAT(/,1X,'BIAS =',F10.5,' IN./FT',/)
   DO 55 I = 2,NN
   IF(KOPT.EQ.1)DEL(I) = DEL(I) - BIAS
   IF(KOPT.EQ.0)ELEV(I)=ELEV(I) - BIAS*FLOAT(I-1)
55 CONTINUE
60 TOTLEN = FLOAT(NREAD)*DIFL
   WRITE(6,61)TOTLEN
61 FORMAT(1X,'TOTAL LENGTH       =',F10.2,'  FEET')
   DO 65 I = 2,NN
   ALENG(I) = ALENG(I-1) + DIFL
   IF(KOPT.EQ.1)ELEV(I) =  ELEV(I-1) + DEL(I)
   IF(KOPT.EQ.0)DEL(I)=ELEV(I) - ELEV(I-1)
65 CONTINUE
66 FORMAT(//,1X,'CORRECTED READINGS',//,1X,'DEPTH,FT'
  1,'     0      1      2      3      4      5      6      7    8',
  2'      9',/)
   IF(LOOP.GE.1)WRITE(6,66)
   IF(LOOP.EQ.0)GOTO 73
   JJ = NN/10 + 1
   AK = 0.0
   J1=1
   J2 = 10
   DO 70 I = 1,JJ
   IF(I.EQ.JJ)J2 = NN
   IF(KOPT.EQ.1)WRITE(6,72)AK,(DEL(J),J=J1,J2)
   IF(KOPT.EQ.0)WRITE(6,72)AK,(ELEV(J),J=J1,J2)
   AK=AK+10.*DIFL
   J1=J1+10
   J2 = J2 + 10
70 CONTINUE
72 FORMAT(1X,F8.2,10F7.3)
73 CONTINUE
   P=3.14159265*2
   NUM=NRE
   DO 75 I=1,NO
   CALL FOURIER(M,I,NUM,DIFL,P,JOPT)
   CALL AMPOPT(M,I,IJ(I),PEAKA)
```

Table B2. (Continued)

```
      NUM=NUM-2
   75 CONTINUE
      WRITE(6,76)IJ(1)
   76 FORMAT(/,1X,'MAXIMUM NUMBER OF PEAKS=',I5)
   77 FORMAT(6F11.5)
      L=6
      DO 80 I=1,IJ(1)
      L=L+1
      IF(I.LT.11.OR.I.GT.11)GOTO 79
      CLOSE(7,STATUS='KEEP')
      CLOSE(8,STATUS='KEEP')
      CLOSE(9,STATUS='KEEP')
      CLOSE(10,STATUS='KEEP')
      CLOSE(11,STATUS='KEEP')
      CLOSE(12,STATUS='KEEP')
      CLOSE(13,STATUS='KEEP')
      CLOSE(14,STATUS='KEEP')
      CLOSE(15,STATUS='KEEP')
      CLOSE(16,STATUS='KEEP')
      OPEN(7,FILE='D:FRE11.DAT')
      OPEN(8,FILE='D:FRE12.DAT')
      OPEN(9,FILE='D:FRE13.DAT')
      OPEN(10,FILE='D:FRE14.DAT')
      OPEN(11,FILE='D:FRE15.DAT')
      OPEN(12,FILE='D:FRE16.DAT')
      OPEN(13,FILE='D:FRE17.DAT')
      OPEN(14,FILE='D:FRE18.DAT')
      OPEN(15,FILE='D:FRE19.DAT')
      OPEN(16,FILE='D:FRE20.DAT')
      L=7
   79 WRITE(L,77)FR(I,1),AMP(I,1),PHI(I,1)
   80 CONTINUE
      IF(IJ(1).LT.11)GOTO 81
      CLOSE(7,STATUS='KEEP')
      CLOSE(8,STATUS='KEEP')
      CLOSE(9,STATUS='KEEP')
      CLOSE(10,STATUS='KEEP')
      CLOSE(11,STATUS='KEEP')
      CLOSE(12,STATUS='KEEP')
      CLOSE(13,STATUS='KEEP')
      CLOSE(14,STATUS='KEEP')
      CLOSE(15,STATUS='KEEP')
      CLOSE(16,STATUS='KEEP')
      OPEN(7,FILE='D:FRE1.DAT',STATUS='OLD')
      OPEN(8,FILE='D:FRE2.DAT',STATUS='OLD')
      OPEN(9,FILE='D:FRE3.DAT',STATUS='OLD')
      OPEN(10,FILE='D:FRE4.DAT',STATUS='OLD')
      OPEN(11,FILE='D:FRE5.DAT',STATUS='OLD')
      OPEN(12,FILE='D:FRE6.DAT',STATUS='OLD')
```

Table B2. (Continued)

```
      OPEN(13,FILE='D:FRE7.DAT',STATUS='OLD')
      OPEN(14,FILE='D:FRE8.DAT',STATUS='OLD')
      OPEN(15,FILE='D:FRE9.DAT',STATUS='OLD')
      OPEN(16,FILE='D:FRE10.DAT',STATUS='OLD')
   81 DF1=1./(FLOAT(NRE)*DIFL)
      L=6
      LL=0
      DO 100 J=1,IJ(1)
      IF(J.LT.11.OR.J.GT.11)GOTO 82
      CLOSE(7,STATUS='KEEP')
      CLOSE(8,STATUS='KEEP')
      CLOSE(9,STATUS='KEEP')
      CLOSE(10,STATUS='KEEP')
      CLOSE(11,STATUS='KEEP')
      CLOSE(12,STATUS='KEEP')
      CLOSE(13,STATUS='KEEP')
      CLOSE(14,STATUS='KEEP')
      CLOSE(15,STATUS='KEEP')
      CLOSE(16,STATUS='KEEP')
      OPEN(7,FILE='D:FRE11.DAT',STATUS='OLD')
      OPEN(8,FILE='D:FRE12.DAT',STATUS='OLD')
      OPEN(9,FILE='D:FRE13.DAT',STATUS='OLD')
      OPEN(10,FILE='D:FRE14.DAT',STATUS='OLD')
      OPEN(11,FILE='D:FRE15.DAT',STATUS='OLD')
      OPEN(12,FILE='D:FRE16.DAT',STATUS='OLD')
      OPEN(13,FILE='D:FRE17.DAT',STATUS='OLD')
      OPEN(14,FILE='D:FRE18.DAT',STATUS='OLD')
      OPEN(15,FILE='D:FRE19.DAT',STATUS='OLD')
      OPEN(16,FILE='D:FRE20.DAT',STATUS='OLD')
      L=6
   82 L=L+1
      LL=LL+1
      REWIND L
      READ(L,77,END=83)FF,AA,TT
   83 NUM=NRE
      IJK(LL)=1
      DO 90 N=2,NO
      NUM=NUM-2
      DF2=1./(FLOAT(NUM)*DIFL)
      DO 85 JI=1,IJ(N)
      D1=FR(J,1)/DF1
      D2=FR(JI,N)/DF2
      DIFT=D2-D1
      IF(ABS(DIFT).LE.1.1)WRITE(L,77)FR(JI,N),AMP(JI,N),PHI(JI,N)
      IF(ABS(DIFT).LE.1.1)IJK(LL)=IJK(LL)+1
      IF(ABS(DIFT).LE.1.1)GOTO 90
   85 CONTINUE
   90 CONTINUE
  100 CONTINUE
```

Table B2. (Continued)

```
      IF(IJ(1).LT.11)GOTO 95
      CLOSE(7,STATUS='KEEP')
      CLOSE(8,STATUS='KEEP')
      CLOSE(9,STATUS='KEEP')
      CLOSE(10,STATUS='KEEP')
      CLOSE(11,STATUS='KEEP')
      CLOSE(12,STATUS='KEEP')
      CLOSE(13,STATUS='KEEP')
      CLOSE(14,STATUS='KEEP')
      CLOSE(15,STATUS='KEEP')
      CLOSE(16,STATUS='KEEP')
      OPEN(7,FILE='D:FRE1.DAT',STATUS='OLD')
      OPEN(8,FILE='D:FRE2.DAT',STATUS='OLD')
      OPEN(9,FILE='D:FRE3.DAT',STATUS='OLD')
      OPEN(10,FILE='D:FRE4.DAT',STATUS='OLD')
      OPEN(11,FILE='D:FRE5.DAT',STATUS='OLD')
      OPEN(12,FILE='D:FRE6.DAT',STATUS='OLD')
      OPEN(13,FILE='D:FRE7.DAT',STATUS='OLD')
      OPEN(14,FILE='D:FRE8.DAT',STATUS='OLD')
      OPEN(15,FILE='D:FRE9.DAT',STATUS='OLD')
      OPEN(16,FILE='D:FRE10.DAT',STATUS='OLD')
   95 WRITE(6,101)
  101 FORMAT(/,2X,'RESONANT  REGRESSION     PEAK     REGRESSION',/,
     11X,'FREQUENCY  COEFFICIENT  AMPLITUDE  COEFFICIENT',/,2X,'CYCLE/FT
     2                INCH')
      L=6
      LL=0
      DO 200 I=1,IJ(1)
      IF(I.LT.11.OR.I.GT.11)GOTO 110
      CLOSE(7,STATUS='KEEP')
      CLOSE(8,STATUS='KEEP')
      CLOSE(9,STATUS='KEEP')
      CLOSE(10,STATUS='KEEP')
      CLOSE(11,STATUS='KEEP')
      CLOSE(12,STATUS='KEEP')
      CLOSE(13,STATUS='KEEP')
      CLOSE(14,STATUS='KEEP')
      CLOSE(15,STATUS='KEEP')
      CLOSE(16,STATUS='KEEP')
      OPEN(7,FILE='D:FRE11.DAT',STATUS='OLD')
      OPEN(8,FILE='D:FRE12.DAT',STATUS='OLD')
      OPEN(9,FILE='D:FRE13.DAT',STATUS='OLD')
      OPEN(10,FILE='D:FRE14.DAT',STATUS='OLD')
      OPEN(11,FILE='D:FRE15.DAT',STATUS='OLD')
      OPEN(12,FILE='D:FRE16.DAT',STATUS='OLD')
      OPEN(13,FILE='D:FRE17.DAT',STATUS='OLD')
      OPEN(14,FILE='D:FRE18.DAT',STATUS='OLD')
      OPEN(15,FILE='D:FRE19.DAT',STATUS='OLD')
      OPEN(16,FILE='D:FRE20.DAT',STATUS='OLD')
```

Table B2. (Continued)

```
      L=6
  110 L=L+1
      LL=LL+1
      REWIND L
      C1=0.0
      C2=0.0
      S1=0.0
      S2=0.0
      T1S=0.0
      A1=0.0
      A2=0.0
      F1=0.0
      F2=0.0
      T1=0.0
      T2=0.0
      SAS=0.0
      SFS=0.0
      CFT=0.0
      CAC=0.0
      T2S=0.0
      DO 190 J=1,IJK(L)
      READ(L,77)F,A,T
      TRAD=T*P/360.
      C=COS(TRAD)
      TS=T
      IF(T.LE.-0.01)TS=T+180.
      SRAD=TS*P/360.
      S=SIN(SRAD)
      C1=C1+C
      C2=C2+C*C
      S1=S1+S
      S2=S2+S*S
      T1=T1+T
      T2=T2+T*T
      T1S=T1S+TS
      T2S=T2S+TS*TS
      F1=F1+F
      F2=F2+F*F
      A1=A1+A
      A2=A2+A*A
      CAC=CAC+C*A
      SAS=SAS+A*S
      CFT=CFT+F*T
      SFS=SFS+F*TS
  190 CONTINUE
      XN=FLOAT(IJK(LL))
      WRITE(6,192)IJK(LL),LL
  192 FORMAT(/,47X,I5,'  TERMS IN FILE',I5)
      C3=CAC-C1*A1/XN
```

Table B2. (Continued)

```
      C4=C2-C1*C1/XN
      SLOAC=C3/C4
      IF(ABS(SLOAC).LT.0.001.AND.ABS(T).LT.45.)GOTO 193
      IF(ABS(SLOAC).LT.0.001.AND.ABS(T).GT.45.)GOTO 195
      IF(SLOAC.LT.0.0)GOTO 195
  193 WRITE(6,194)
  194 FORMAT(50X,'COSINE WAVE')
      AINT=A1/XN - SLOAC*C1/XN
      RSQA=C3*C3/(C4*(A2 - A1*A1/XN))
      AMPLI=AINT + SLOAC
      F3=CFT - T1*F1/XN
      F4=T2 - T1*T1/XN
      SLOFC=F3/F4
      RESF = F1/XN - SLOFC*T1/XN
      RSQF = F3*F3/(F4*(F2 - F1*F1/XN))
      WRITE(6,77)RESF,RSQF,AMPLI,RSQA
      GOTO 200
  195 WRITE(6,197)
  197 FORMAT(50X,'SINE WAVE')
      S3=SAS-S1*A1/XN
      S4=S2-S1*S1/XN
      SLOAS=S3/S4
      AINT=A1/XN-SLOAS*S1/XN
      AMPLI=AINT+SLOAS
      RSQA=S3*S3/(S4*(A2-A1*A1/XN))
      F3=SFS-T1S*F1/XN
      F4=T2S-T1S*T1S/XN
      SLOFS=F3/F4
      FINT=F1/XN-SLOFS*T1S/XN
      RESF=FINT+SLOFS*90.
      RSQF=F3*F3/(F4*(F2-F1*F1/XN))
      WRITE(6,77)RESF,RSQF,AMPLI,RSQA
  200 CONTINUE
      CLOSE(5,STATUS='KEEP')
      CLOSE(6,STATUS='KEEP')
      CLOSE(7,STATUS='KEEP')
      CLOSE(8,STATUS='KEEP')
      CLOSE(9,STATUS='KEEP')
      CLOSE(10,STATUS='KEEP')
      CLOSE(11,STATUS='KEEP')
      CLOSE(12,STATUS='KEEP')
      CLOSE(13,STATUS='KEEP')
      CLOSE(14,STATUS='KEEP')
      CLOSE(15,STATUS='KEEP')
      CLOSE(16,STATUS='KEEP')
      STOP
      END
C
C
```

Table B2. (Continued)

```
      SUBROUTINE STAND (N1,N2,VAR,STD,AMEAN)
      DIMENSION VAR(1000)
      NI=N1
      NJ=N2
      N=NJ-NI
      NN=N-1
      SUM = 0.0
      SUMSQ = 0.0
      DO 10 I = NI,NJ
      SUM = SUM + VAR(I)
      SUMSQ = SUMSQ + VAR(I)*VAR(I)
   10 CONTINUE
      AMEAN = SUM/FLOAT(N)
      STDSQ = (SUMSQ - SUM*SUM/FLOAT(N))/FLOAT(NN)
      STD = ABS(STDSQ)**0.5
      RETURN
      END
C
C
      SUBROUTINE FOURIER(M,N,NRE,DIFL,P,JOPT)
      COMMON/FOUR/FRE(1000),THETA(1000),H(1000),ALENG(1000),ELEV(1000)
      AM=DIFL*FLOAT(NRE)/4.
      M=IFIX(AM)
      TOTL=FLOAT(NRE)*DIFL
      IF(JOPT.EQ.1)WRITE(6,10)NRE
   10 FORMAT(/,1X,'READINGS USED FOR FOURIER TRANSFORM=',I5)
      DO 100 I=1,M
      XR=0.0
      XI=0.0
      FRE(I)=FLOAT(I-1)/TOTL
      DO 20 J=1,NRE
      ARG=P*FRE(I)*ALENG(J)
      XR=XR+ELEV(J)*COS(ARG)
      XI=XI+ELEV(J)*SIN(ARG)
   20 CONTINUE
      H(I)=ABS(XR)**2.+ABS(XI)**2.
      H(I)=DIFL*(H(I)**0.5)/TOTL
      BA=XI/XR
      THETA(I)=ATAN(BA)*360./P
  100 CONTINUE
      IF(JOPT.EQ.1)WRITE(6,150)
  150 FORMAT(/,1X,'NUMBER  FREQUENCY,  AMPLITUDE,  PHASE SHIFT,',/,
     1'          CYCLE/FT      INCH       DEGREES',/)
      DO 200 I=1,M
      IF(JOPT.EQ.1)WRITE(6,210)I,FRE(I),H(I),THETA(I)
  200 CONTINUE
  210 FORMAT(I5,3F12.5)
      RETURN
      END
```

Table B2. (Concluded)

```
C
C
      SUBROUTINE AMPOPT(M,N,J,PEAKA)
      COMMON/FOUR/FRE(1000),THETA(1000),H(1000),ALENG(1000),ELEV(1000)
      COMMON/AMP/FR(100,30),PHI(100,30),AMP(100,30)
      J=0
      WRITE(6,2)N
    2 FORMAT(/,1X,'PEAK FREQUENCY   AMPLITUDE    PHASE ANGLE  FOR RUN',I)
     25)
      DO 10 I=2,M-1
      IF(H(I).GT.H(I-1).AND.H(I).GT.H(I+1))GOTO 5
      GOTO 10
    5 IF(H(I).LT.PEAKA)GOTO 10
      J=J+1
      FR(J,N)=FRE(I)
      PHI(J,N)=THETA(I)
      AMP(J,N)=H(I)
      WRITE(6,15)FR(J,N),AMP(J,N),PHI(J,N)
   10 CONTINUE
   15 FORMAT(3F13.5)
      RETURN
      END
```

Table B3. Listing Program FNUMR.FOR

```
C     PROGRAM FNUMR.FOR:  ANALYSIS OF FLOOR PROFILE USING F-NUMBERS
C     NOMENCLATURE
C          LOOP      = 1     Closed loop; Operator bias subtracted from
C                            dipstick readings
C                    = 0     Open loop
C          KOPT      = 0     Elevation readings input
C                    = 1     Elevation change readings input
C          NREAD     Number of readings
C          DIFL      Sample interval of profile data, ft
C          NRE       Data points used to calculate F-number if IOPT=1
C          JOPT      = 0     Minimum output listing
C                    = 1     Maximum Output listing
C          IOPT      = 0     Calculate F-number for full length
C                    = 1     Calculate F-numbers to  NRE, then NRE+1
C                            to NREAD+1
C                    = 2     Calculate F-numbers at increment of 1
C                            point up to NRE
C          ALEN      Sample interval used to calculate F-number, ft;
C                    greater or equal DIFL and should be multiple DIFL
      DIMENSION HED(20),DEL(1000),ELEV(1000),CELEV(1000),ALENIN(1000),
     1ELEINT(1000),ALENG(1000),DELEV(1000)
      OPEN(5,FILE='DATDIP.TXT')
      OPEN(6,FILE='DIPOUT.TXT')
```

Table B3. (Continued)

```
      OPEN(7,FILE='\GRAPHER\ELEV.DAT')
      OPEN(8,FILE='\GRAPHER\ELEVL.DAT')
      OPEN(9,FILE='\GRAPHER\FNUM.DAT')
      BIAS=0.0
      FL10=0.0
      STD = 0.0
      AMEAN = 0.0
      DDMAX = 0.0
      DCMAX = 0.0
      DEMAX = 0.0
      READ(5,10) (HED(I),I=1,20)
      WRITE(6,12)(HED(I),I=1,20)
   10 FORMAT(20A4)
   12 FORMAT(/,20A4)
      READ(5,15)LOOP,KOPT,NREAD,DIFL,NRE,JOPT,IOPT,ALEN
   15 FORMAT(3I5,F10.2,3I5,F10.2)
      IF(ALEN.LT.DIFL) ALEN=DIFL
      IF(LOOP.EQ.0) WRITE(6,17)
      IF(LOOP.EQ.1) WRITE(6,18)
   17 FORMAT(/,10X,'OPEN LINE')
   18 FORMAT(/,10X,'CLOSED LINE')
      IF(IOPT.EQ.0) WRITE(6,20)
      IF(IOPT.EQ.1) WRITE(6,21)
   20 FORMAT(/,1X,'F-NUMBER CALCULATED FOR FULL LENGTH')
   21 FORMAT(/,1X,'F-NUMBERS CALCULATED FOR HALF LENGTHS')
      WRITE (6,25) NREAD,DIFL,ALEN
   25 FORMAT(/,1X,'NUMBER OF READINGS=',11X,I5,/,1X,'ACTUAL SAMPLE',
     1' INTERVAL =',6X,F10.2,'  FEET',/,1X,'LENGTH INTERVAL FOR ',
     2'F-NUMBER =',F10.2,'  FEET')
      IF(KOPT.EQ.0)WRITE(6,26)
      IF(KOPT.EQ.1)WRITE(6,27)
   26 FORMAT(/,1X,'INPUT DATA ARE ELEVATIONS',/)
   27 FORMAT(/,1X,'INPUT DATA ARE CHANGES IN ELEVATIONS',/)
C     INITIALIZE
      N = NREAD + 1
      DO 30 I = 1,N
      DEL(I) = 0.0
      ELEV(I) = 0.0
      CELEV(I) = 0.0
      DELEV(I) = 0.0
      ALENIN(I) = 0.0
      ALENG(I) = 0.0
      ELEINT(I) = 0.0
   30 CONTINUE
      IF(KOPT.EQ.0)READ(5,40)(ELEV(I),I=2,N)
      IF(KOPT.EQ.1)READ(5,40)(DEL(I), I=2,N)
   40 FORMAT(10F7.3)
   41 FORMAT(//,1X,'UNCORRECTED PROFILOGRAPH READINGS',//,
     11X,'DEPTH,FT     0      1      2      3      4      5      6',
```

Table B3. (Continued)

```
     2'      7      8      9',/)
      IF(JOPT.EQ.1)WRITE(6,41)
      IF(JOPT.EQ.0)GOTO 48
      JJ = N/10 + 1
      AK = 0.0
      J1 = 1
      J2 = 10
      DO 45 I = 1,JJ
      IF(I.EQ.JJ)J2 = N
      IF(KOPT.EQ.0)WRITE(6,47)AK,(ELEV(J),J=J1,J2)
      IF(KOPT.EQ.1)WRITE(6,47)AK,(DEL(J),J=J1,J2)
      AK = AK + 10.*DIFL
      J1 = J1 + 10
      J2 = J2 + 10
   45 CONTINUE
   47 FORMAT(1X,F8.2,10F7.3)
   48 N1 = 2
      N2 = N
      IF(KOPT.EQ.0)CALL STAND (N1,N2,ELEV,STD,AMEAN,0,IOPT)
      IF(KOPT.EQ.1)CALL STAND (N1,N2,DEL,STD,AMEAN,0,IOPT)
      SUM = AMEAN*FLOAT(NREAD)
      WRITE(6,50) SUM, AMEAN, STD
   50 FORMAT(//,4X,'TOTAL  ELEV DIFFERENCE  =', F7.3,'  INCH',/,1X,
     1'MEAN DIFFERENCE/READING =',F10.6,'  INCH',/,1X,'STANDARD',
     2' DEVIATION =',F15.5)
      IF(LOOP.EQ.0) GOTO 60
      IF(KOPT.EQ.1)BIAS = AMEAN
      IF(KOPT.EQ.0)BIAS = (ELEV(N)-ELEV(1))/FLOAT(NREAD)
      WRITE(6,52)BIAS
   52 FORMAT(/,1X,'BIAS =',F10.5,' IN./FT')
      DO 55 I = 2,N
      IF(KOPT.EQ.0)ELEV(I)=ELEV(I)-BIAS*FLOAT(I-1)
      IF(KOPT.EQ.1)DEL(I) = DEL(I) - BIAS
   55 CONTINUE
   60 TOTLEN = FLOAT(NREAD)*DIFL
      WRITE(6,61)TOTLEN
   61 FORMAT(/,1X,'TOTAL LENGTH =',F10.2,'  FEET')
      DO 65 I = 2,N
      ALENG(I) = ALENG(I-1) + DIFL
      IF(KOPT.EQ.0)DEL(I)=ELEV(I)-ELEV(I-1)
      IF(KOPT.EQ.1)ELEV(I) = ELEV(I-1) + DEL(I)
   65 CONTINUE
   66 FORMAT(//,1X,'PROFILOGRAPH ELEVATION DIFFERENCES',//,1X,'DEPTH,FT'
     1,'     0      1      2      3      4      5      6      7      8', 8'
     2'      9',/)
      IF(JOPT.EQ.1)WRITE(6,66)
      IF(JOPT.EQ.0)GOTO 73
      JJ = N/10 + 1
      AK = 0.0
```

Table B3. (Continued)

```
      J1 = 1
      J2 = 10
      DO 70 I = 1,JJ
      IF(I.EQ.JJ)J2 = N
      WRITE(6,72)AK,(DEL(J),J=J1,J2)
      AK = AK + 10.*DIFL
      J1 = J1 + 10
      J2 = J2 + 10
   70 CONTINUE
   72 FORMAT(1X,F8.2,10F7.3)
   73 NUMR = IFIX(TOTLEN/ALEN)
      NO = NUMR + 1
      WRITE(6,67)NUMR
   67 FORMAT(1X,'NUMBER OF DATA POINTS =',I5)
      DO 80 I = 2,NO
      ALENIN(I) = ALENIN(I-1) + ALEN
   80 CONTINUE
      IF(JOPT.EQ.1)WRITE(6,90)
   90 FORMAT(//,3X,'SAMPLE INTERVAL FOR F-NUMBER',12X,'ACTUAL SAMPLE',
     1' INTERVAL',/1X,'DISTANCE (FT)    ELEVATION (IN.)    DISTANCE',
     2' (FT)    ELEVATION (IN.)',/)
      DO 140 I = 2,NO
  110 DO 120 II = 2,N
      IF(ALENIN(I) - ALENG(II)) 130,130,120
  120 CONTINUE
  130 ELEINT(I) = ELEV(II-1) + ((ELEV(II)-ELEV(II-1))/(ALENG(II)-ALENG
     1(II-1)))*(ALENIN(I)-ALENG(II-1))
  140 CONTINUE
      DO 148 I = 1,N
      IF(I.LE.NO.AND.JOPT.EQ.1)WRITE(6,144) ALENIN(I),ELEINT(I),ALENG(I)
     1,ELEV(I)
      WRITE(7,143) ALENG(I),ELEV(I)
      IF(I.LE.NO)WRITE(8,143) ALENIN(I), ELEINT(I)
      IF(I.GT.NO.AND.JOPT.EQ.1)WRITE(6,145)ALENG(I),ELEV(I)
  148 CONTINUE
  143 FORMAT(1X,F10.2,F10.3)
  144 FORMAT(1X,F10.2,6X,F10.3,11X,F10.2,6X,F10.3)
  145 FORMAT(38X,F10.2,6X,F10.3)
  150 CONTINUE
C     ***     CALCULATE STANDARD DEVIATION FOR LEVELNESS/FLATNESS    ***
      DO 155 I = 2,NO
      DEL(I) = ELEINT(I) - ELEINT(I-1)
      CELEV(I) = DEL(I) - DEL(I-1)
      IF(I.GE.11)DELEV(I) = ELEINT(I) - ELEINT(I-10)
  155 CONTINUE
      IJKL=0
 1000 M = 0
      IJKL=IJKL+1
      N1 = 2
```

Table B3. (Continued)

```
      IF(IOPT.EQ.0) N2 = NUMR + 1
      IF(IOPT.GE.1) N2 = NRE +1
      IF(IOPT.EQ.2)SPAN=ALEN*FLOAT(NRE)
      IF(IJKL.EQ.1)WRITE(6,156)N1,N2
  156 FORMAT(/,5X,'STARTING POINT =',I5,5X,'END POINT =',I5)
  160 STDD = 0.0
      STDC = 0.0
      STDE = 0.0
      STDEL = 0.0
      AMEANEL = 0.0
      AMEAND = 0.0
      AMEANC = 0.0
      AMEANE = 0.0
      IF(IOPT.EQ.0)WRITE(6,161)
  161 FORMAT(///,1X,'THIS CALCULATION IS FOR THE FULL LENGTH')
      IF(IOPT.EQ.1.AND.IJKL.EQ.1)WRITE(6,162)NRE
  162 FORMAT(///,1X,'THIS CALCULATION IS FOR',I5,'  FIRST DATA POINTS')
      CALL STAND (N1,N2,DEL,STDD,AMEAND,0,IOPT)
      CALL STAND (N1,N2,CELEV,STDC,AMEANC,0,IOPT)
      IF(IOPT.EQ.0)CALL STAND (N1,N2,DELEV,STDE,AMEANE,1,IOPT)
      CALL STAND (N1,N2,ELEINT,STDEL,AMEANEL,0,IOPT)
C     ***     CALCULATE MAXIMUM CHANGE IN ELEVATION AND CURVATURE    ***
      DDMAX = STDD*3. + ABS(AMEAND)
      DCMAX = STDC*3. + ABS(AMEANC)
      DEMAX = STDE*3. + ABS(AMEANE)
      IF(IJKL.EQ.1)WRITE(6,163) AMEANEL,STDEL
  163 FORMAT(//,1X,'MEAN ELEV =',F10.5,'  INCH     STANDARD DEVIATION ='
     1,F10.5)
      IF(IJKL.EQ.1)WRITE(6,165) ALEN,DDMAX,AMEAND,STDD
  165 FORMAT(//,1X,'MAXIMUM EXPECTED ELEVATION CHANGE FOR 99 PERCENT C',
     1'ONFIDENCE',/,1X,'FOR SAMPLE INTERVAL',F10.2,'  FEET    IS',F10.5,
     2'  INCH',/,1X,'MEAN ELEVATION DIFFERENCE =',14X,F10.5,'  INCH',/,
     31X,'STANDARD DEVIATION =',F10.5)
      IF(IJKL.EQ.1)WRITE(6,170) ALEN,DCMAX,AMEANC,STDC
  170 FORMAT(//,1X,'MAXIMUM EXPECTED CURVATURE (CHANGE IN ELEVATION',
     1' CHANGE)',/,1X,'FOR SAMPLE INTERVAL',F10.2,'  FEET IS',F10.5,
     2'  INCH INCH',/,1X,'MEAN CURVATURE =',22X,F10.5,'  INCH INCH',/,
     31X,'STANDARD DEVIATION =',F10.5)
      IF(IOPT.EQ.0)WRITE(6,172) ALEN,DEMAX,AMEANE,STDE
  172 FORMAT(//,1X,'MAXIMUM EXPECTED ELEVATION CHANGE AT 10 FEET FOR 99'
     1,' PERCENT CONFIDENCE',/,1X,'FOR SAMPLE INTERVAL',F10.2,'  FEET',
     2'    IS'.F10.5,'  INCH',/,1X,'MEAN ELEVATION DIFFERENCE AT 10 FEET
     3',' =',3X,F10.5,'  INCH',/,1X,'STANDARD DEVIATION =',F10.5)
C     ***     CALCULATE FLOOR F-NUMBERS     ***
      ALIN = ALEN*12.
      TEMP = (((ALIN)**2.)*0.007 + 1.)**0.5
      TEMP = TEMP + 0.083*ALIN
      FL = 4.175*ALOG(TEMP)/DDMAX
      AALIN=ALIN*10.
```

Table B3. (Continued)

```
      TEMP = (((AALIN)**2.)*0.007 + 1.)**0.5
      TEMP = TEMP + 0.083*AALIN
      IF(IOPT.EQ.0)FL10 = 4.175*ALOG(TEMP)/DEMAX
      IF(ALIN.GE.15.) GOTO 175
      TEMP = COS(0.105*ALIN) - 1.0
      FF = 6.585*ABS(TEMP)/DCMAX
      GOTO 178
  175 TEMP = 0.088*ALIN
      FF = (ALOG(TEMP) + 0.844)*7.892/DCMAX
  178 WRITE(6,180) ALIN,FL,AALIN,FL10,ALIN,FF
      IF(M.EQ.0)WRITE(9,185)SPAN,FL,FF
C     ***     CALCULATE PROFILE BIAS     ***
      PBIAS = 200.*(FL - FF)/(FL + FF)
      IF(IJKL.EQ.1)WRITE(6,250)PBIAS
  250 FORMAT(/,5X,'PROFILE BIAS (PERCENT) =',F8.2)
      IF(PBIAS)260,270,280
  260 IF(IJKL.EQ.1)WRITE(6,261)
  261 FORMAT(/,1X,'THIS FLOOR IS MORE FLAT THAN IT IS LEVEL')
      GOTO 290
  270 IF(IJKL.EQ.1)WRITE(6,271)
  271 FORMAT(/,1X,'THIS FLOOR HAS NO BIAS')
      GOTO 290
  280 IF(IJKL.EQ.1)WRITE(6,281)
  281 FORMAT(/,1X,'THIS FLOOR IS MORE LEVEL THAN IT IS FLAT')
  290 IF(IOPT.EQ.0) GOTO 300
      M = M+1
      IF(M.GE.2) GOTO 300
      N1 = NRE + 2
      N2 = NUMR + 1
      IF(N1.GE.N2)GOTO 300
      IF(IJKL.EQ.1)WRITE(6,190)
      IF(IJKL.EQ.1)WRITE(6,156)N1,N2
      GOTO 160
  180 FORMAT(//,10X,'FLOOR F-NUMBERS',/,5X,'LEVELNESS:  FL(',F6.2,') ='
     1,F8.2,/,16X,'FL(',F7.2,') =',F8.2,/,5X,' FLATNESS:  FF(',F6.2,
     2') =',F8.2)
  185 FORMAT(3F10.2)
  190 FORMAT(///,1X,'THIS CALCULATION IS FOR THE SECOND HALF LENGTH')
  300 CONTINUE
      IF(IOPT.LT.2)GOTO 2000
      NRE=NRE-1
      IF(NRE.LT.4)GOTO 2000
      GOTO 1000
 2000 CLOSE(5,STATUS='KEEP')
      CLOSE(6,STATUS='KEEP')
      CLOSE(7,STATUS='KEEP')
      CLOSE(8,STATUS='KEEP')
      CLOSE(9,STATUS='KEEP')
      STOP
```

Table B3. (Concluded)

```
      END
C
C
      SUBROUTINE STAND (N1,N2,VAR,STD,AMEAN,J,IOPT)
      DIMENSION VAR(1000)
      NI=N1
      NJ=N2
      IF(J.EQ.1.AND.IOPT.EQ.0)NI=N1+10
      N=NJ-NI
      NN=N-1
      SUM = 0.0
      SUMSQ = 0.0
      DO 10 I = NI,NJ
      SUM = SUM + VAR(I)
      SUMSQ = SUMSQ + VAR(I)*VAR(I)
   10 CONTINUE
      AMEAN = SUM/FLOAT(N)
      STDSQ = (SUMSQ - SUM*SUM/FLOAT(N))/FLOAT(NN)
      STD = ABS(STDSQ)**0.5
      RETURN
      END
```

Table B4. Listing Program ADATG.FOR

```
C  PROGRAM ADATG.FOR: TO CALCULATE ANGULAR DISTORTION AND TILT FROM
C  ELEVATION OR ELEVATION CHANGES
C     NOMENCLATURE
C          LOOP      = 1     Closed loop; Operator bias subtracted from
C                            dipstick readings
C                    = 0     Open loop
C          KOPT      = 0     Elevation readings input
C                    = 1     Elevation change readings input
C          NREAD     Number of readings
C          DIFL      Sample interval of profile data, ft
C          NRE       Maximum readings used in calculation
C          JOPT      = 0  Minimum output listing
C                    = 1  Maximum output listing
C          IOPT      = 0  Data for length to NRE and NRE+1 to NREAD
C                    = 1  Data for readings from 4 to NRE
      DIMENSION HED(20),DEL(1000),ELEV(1000),ALENG(1000),AMP(1000),ALEN(
     11000),ANG(1000)
      OPEN(5,FILE='FTRIN.TXT')
      OPEN(6,FILE='FTROUT.TXT')
      OPEN(8,FILE='\GRAPHER\FTRE.DAT')
      OPEN(9,FILE='\GRAPHER\ANGU1.DAT')
      OPEN(10,FILE='\GRAPHER\ANGU2.DAT')
      OPEN(11,FILE='\GRAPHER\MEAN.DAT')
      OPEN(12,FILE='\GRAPHER\FRACTAL.DAT')
```

Table B4. (Continued)

```
      OPEN(13,FILE='\GRAPHER\ANGU1A.DAT')
      OPEN(14,FILE='\GRAPHER\ANGU2A.DAT')
      OPEN(15,FILE='\GRAPHER\BETA.DAT')
      STD=0.0
      AMEAN=0.0
      BIAS=0.0
      READ(5,10) (HED(I),I=1,20)
      WRITE(6,12)(HED(I),I=1,20)
   10 FORMAT(20A4)
   12 FORMAT(1X,20A4)
      READ(5,15)LOOP,KOPT,NREAD,DIFL,NRE,JOPT,IOPT
   15 FORMAT(3I5,F10.2,3I5)
      IF(LOOP.EQ.0) WRITE(6,17) NRE
      IF(LOOP.EQ.1) WRITE(6,18) NRE
   17 FORMAT(/,10X,'OPEN LINE   LENGTH TO NRE=',I5,'   UNCORRECTED')
   18 FORMAT(/,10X,'CLOSED LINE   LENGTH TO NRE=',I5,'  CORRECTED')
      WRITE (6,25) NREAD,DIFL
   25 FORMAT(/,1X,'NUMBER OF READINGS=',11X,I5,/,1X,'ACTUAL SAMPLE',
     1' INTERVAL =',6X,F10.2,'  FEET',/)
      IF(KOPT.EQ.0)WRITE(6,26)
      IF(KOPT.EQ.1)WRITE(6,27)
   26 FORMAT(/,1X,'INPUT DATA ARE ELEVATIONS',/)
   27 FORMAT(/,1X,'INPUT DATA ARE CHANGES IN ELEVATIONS',/)
C     INITIALIZE
      NN = NREAD + 1
      DO 30 I = 1,NN
      DEL(I)=0.0
      ELEV(I) = 0.0
      ALENG(I) = 0.0
   30 CONTINUE
      READ(5,40)(DEL(I), I=2,NN)
   40 FORMAT(10F7.3)
   41 FORMAT(//,1X,'UNCORRECTED INPUT DATA',//,
     11X,'LENGTH,FT    0      1      2      3     4      5      6',
     2'      7      8      9',/)
      IF(JOPT.EQ.1)WRITE(6,41)
      JJ = NN/10 + 1
      AK = 0.0
      J1 = 1
      J2 = 10
      DO 45 I = 1,JJ
      IF(I.EQ.JJ)J2 = NN
      IF(JOPT.EQ.1)WRITE(6,47)AK,(DEL(J),J=J1,J2)
      AK = AK + 10.*DIFL
      J1 = J1 + 10
      J2 = J2 + 10
   45 CONTINUE
   47 FORMAT(1X,F8.2,10F7.3)
   48 N1 = 2
```

Table B4. (Continued)

```
      N2 = NN
      CALL STAND (N1,N2,DEL,STD,AMEAN)
      SUM = AMEAN*FLOAT(NREAD)
      WRITE(6,50) SUM, AMEAN, STD
   50 FORMAT(//,4X,'SUM  =', F7.3,'INCH',/,1X,
     1'MEAN  =',F10.6,'  INCH',/,1X,'STANDARD',
     2' DEVIATION =',F15.5)
      IF(LOOP.EQ.0) GOTO 60
      IF(KOPT.EQ.0) BIAS=DEL(NN)/FLOAT(NREAD)
      IF(KOPT.EQ.1)BIAS = AMEAN
      DO 55 I = 2,NN
      IF(KOPT.EQ.1)DEL(I) = DEL(I) - BIAS
      IF(KOPT.EQ.0)DEL(I) = DEL(I) - BIAS*FLOAT(I-1)
   55 CONTINUE
   60 TOTLEN = FLOAT(NREAD)*DIFL
      WRITE(6,61)TOTLEN
   61 FORMAT(/,1X,'TOTAL LENGTH =',F10.2,'  FEET')
      DO 65 I = 2,NN
      ALENG(I) = ALENG(I-1) + DIFL
      IF(KOPT.EQ.0)ELEV(I)=DEL(I)
      IF(KOPT.EQ.1)ELEV(I) =  ELEV(I-1) + DEL(I)
   65 CONTINUE
   66 FORMAT(//,1X,'CORRECTED ELEVATION DATA',//,1X,'LENGTH,FT'
     1,'    0      1      2      3      4      5      6      7    8',
     2'      9',/)
      IF(JOPT.EQ.1)WRITE(6,66)
      IF(JOPT.EQ.0)GOTO 73
      JJ = NN/10 + 1
      AK = 0.0
      J1=1
      J2 = 10
   DO 70 I = 1,JJ
      IF(I.EQ.JJ)J2 = NN
      WRITE(6,72)AK,(ELEV(J),J=J1,J2)
      AK=AK+10.*DIFL
      J1=J1+10
      J2 = J2 + 10
   70 CONTINUE
   72 FORMAT(1X,F8.2,10F7.3)
   73 DO 90 I=1,NN
      WRITE(8,95)ALENG(I),ELEV(I)
   90 CONTINUE
   95 FORMAT(2F10.5)
C  DETERMINE ELEVATION AND LOCATION OF PEAKS
      IJK=0
 1000 CONTINUE
      L1=2
      L2=NRE
      IF(IOPT.EQ.0.AND.IJK.EQ.0)WRITE(6,96)
```

Table B4. (Continued)

```
   96 FORMAT(/,1X,'*****   FIRST SET CALCULATIONS   ****')
      IF(IOPT.EQ.0.AND.IJK.EQ.1)WRITE(6,97)
   97 FORMAT(/,1X,'*****   SECOND SET CALCULATIONS   *****')
      IF(IOPT.EQ.0.AND.IJK.EQ.1)L1=NRE+1
      IF(IOPT.EQ.0.AND.IJK.EQ.1)L2=NN
      J=1
      DO 100  I=L1,L2
      IF(ELEV(I).GE.ELEV(I-1).AND.ELEV(I).GT.ELEV(I+1))GOTO 98
      GOTO 100
   98 AMP(J)=ELEV(I)
      ALEN(J)=DIFL*FLOAT(I-1)
      J=J+1
  100 CONTINUE
  105 FORMAT(2F10.3)
      IF(IOPT.EQ.0)WRITE(6,110)J-1
  110 FORMAT(/,1X,'TOTAL NUMBER OF PEAKS =',I5)
C  DETERMINE SPAN, TILT AND ANGULAR DISTORTION OF ADJACENT PEAKS
  115 FORMAT(I5,4F10.3)
      IF(IOPT.EQ.0)WRITE(6,120)
  120 FORMAT(/,1X,'  SPAN,  TILT,  AMPLITUDE, ANGULAR DISTORTION,    LOG
     1       RELATIVE     LENGTH,',/,1X,'   FT   PERCENT    IN.
     2  PERCENT       STIFFNESS  THICKNESS,FT     FT')
      II=0
      BETA=0.0
      BETA2=0.0
      DTOT=0.0
      DRMAX=0.0
      DRMAXLEN=0.0
      SLE=0.0
      AVEINT=0.0
      AVEINT2=0.0
      BMAX=0.0
      AIMAX=0.0
      AVESPAN=0.0
      TTILT2=0.0
      TTILT=0.0
      DO 200 I=2,J-1
      SPAN=(ALEN(I)-ALEN(I-1))
      IF(SPAN.GT.150.OR.SPAN.LT.4.0)GOTO 200
      TILT=(AMP(I)-AMP(I-1))/(SPAN*12.)
      ANGTILT=ATAN(TILT)
      TILT=100.*TILT
      HALFL=ALEN(I-1)+SPAN/2.
      AK=HALFL/DIFL
      K=IFIX(AK)+1
      ELEVH=ELEV(K)+((ELEV(K+1)-ELEV(K))/(ALENG(K+1)-ALENG(K)))*(HALFL-A
     1LENG(K))
C     WRITE(6,115)K,ELEVH,HALFL,ALENG(K),ALENG(K+1)
      HSPAN=SPAN*6.
```

Table B4. (Continued)

```
      BETAL=(AMP(I-1)-ELEVH)/HSPAN
      ANGBETAL=ATAN(BETAL)
      ANGBETAL=ANGBETAL+ANGTILT
      BETAL=TAN(ANGBETAL)*100.
      DELTA=0.0015*HSPAN
      DELEV=TILT*HSPAN/100.
      PAMP=AMP(I-1)-ELEVH+DELEV
      IF(PAMP.LT.0.01)GOTO 200
      AAOAE=DELTA/PAMP
      CALL STIFF(AAOAE,RSL)
      DELEFT=(SPAN*10.**(RSL*0.333))/2.
      BETAR=(AMP(I)-ELEVH)/HSPAN
      ANGBETAR=ATAN(BETAR)
      ANGBETAR=ANGBETAR-ANGTILT
      BETAR=TAN(ANGBETAR)*100.
      FRE=1/SPAN
      IF(BETAL.LT.0.0.OR.BETAR.LT.0.0)GOTO 200
      II=II+1
      T=(BETAL+BETAR)/2.
      DTOT=DTOT+DELEFT
      BETA=BETA+T
      BETA2=BETA2+T*T
      AI=T/SPAN
      AVEINT=AVEINT+AI
      AVEINT2=AVEINT2+AI*AI
      AVESPAN=AVESPAN+SPAN
      TTILT2=TTIL2+TILT*TILT
      TTILT=TTILT+ABS(TILT)
      IF(T.GT.BMAX)BMAX=T
      IF(DELEFT.GT.DRMAX)GOTO 180
      GOTO 190
  180 DRMAX=DELEFT
      DRMAXLEN=ALEN(I)
      SLE=SPAN
  190 IF(AI.GT.AIMAX)AIMAX=AI
      IF(IOPT.EQ.0)WRITE(6,210)SPAN,TILT,PAMP,BETAL,RSL,DELEFT,ALEN(I)
      IF(IOPT.EQ.0.AND.IJK.EQ.0)WRITE(9,210)FRE,BETAL,BETAR,TILT,DELEFT
      IF(IOPT.EQ.0.AND.IJK.EQ.1)WRITE(13,210(FRE,BETAL,BETAR,TILT,DELEFT
  200 CONTINUE
      DRA=DTOT/(FLOAT(L2-L1+1)*DIFL)
      R1BETA=BETA/(FLOAT(L2-L1+1)*DIFL)
  210 FORMAT(3F8.3,2F16.3,2F12.3)
C  DETERMINE SPAN, TILT AND ANGULAR DISTORTION OF NONADJACENT PEAKS
      DO 300 I=2,J-1
      ALEFTL=ALEN(I-1)
      ELEFT=AMP(I-1)
      KL=I-1
      DO 260 K=1,I-1
      JK=I-K
```

Table B4. (Continued)

```
      CLEN=ALEN(I)-ALEN(JK)
      ANG(JK)=((AMP(JK)-AMP(I))/CLEN)*10000.
      IF(K.EQ.1)GOTO 260
      IF(ANG(JK).GT.ANG(KL))ALEFTL=ALEN(JK)
      IF(ANG(JK).GT.ANG(KL))ELEFT=AMP(JK)
      IF(ANG(JK).GT.ANG(KL))KL=JK
  260 CONTINUE
      ARIGHTL=ALEN(I+1)
      ERIGHT=AMP(I+1)
      KL=I+1
      DO 270 K=I+1,J-1
      CLEN=ALEN(K)-ALEN(I)
      ANG(K)=((AMP(K)-AMP(I))/CLEN)*10000.
      IF(K.EQ.I+1)GOTO 270
      IF(ANG(K).GT.ANG(KL))ARIGHTL=ALEN(K)
      IF(ANG(K).GT.ANG(KL))ERIGHT=AMP(K)
      IF(ANG(K).GT.ANG(KL))KL=K
  270 CONTINUE
      SPAN=ARIGHTL-ALEFTL
      IF(SPAN.GT.150..OR.SPAN.LT.4.)GOTO 300
      TILT=(ERIGHT-ELEFT)/(SPAN*12.)
      ANGTILT=ATAN(TILT)
      TILT=100.*TILT
      HALFL=ALEFTL+SPAN/2.
      AK=HALFL/DIFL
      K=IFIX(AK)+1
      ELEVH=ELEV(K)+((ELEV(K+1)-ELEV(K))/(ALENG(K+1)-ALENG(K)))*(HALFL-A
     1LENG(K))
C     WRITE(6,272)ARIGHTL,ALEFTL,ERIGHT,ELEFT,AMP(I),ALEN(I)
  272 FORMAT(6F10.3)
      HSPAN=SPAN*6.
      BETAL=(ELEFT-AMP(I))/HSPAN
      ANGBETAL=ATAN(BETAL)
      ANGBETAL=ANGBETAL+ANGTILT
      BETAL=TAN(ANGBETAL)*100.
      DELTA=0.0015*HSPAN
      DELEV=TILT*(ALEN(I)-ALEFTL)*12./100.
      PAMP=ELEFT-AMP(I)+DELEV
      IF(PAMP.LT.0.01)GOTO 300
      AAOAE=DELTA/PAMP
      CALL STIFF(AAOAE,RSL)
      DELEFT=(SPAN*10.**(RSL*0.333))/2.
      BETAR=(ERIGHT-AMP(I))/HSPAN
      ANGBETAR=ATAN(BETAR)
      ANGBETAR=ANGBETAR-ANGTILT
      BETAR=TAN(ANGBETAR)*100.
      FRE=1/SPAN
      IF(BETAL.LT.0.0.OR.BETAR.LT.0.0)GOTO 300
      II=II+1
```

Table B4. (Continued)

```
      T=(BETAL+BETAR)/2.
      DTOT=DTOT+DELEFT
      AI=T/SPAN
      BETA=BETA+T
      BETA2=BETA2+T*T
      AVESPAN=AVESPAN+SPAN
      AVEINT=AVEINT+AI
      AVEINT2=AVEINT2+AI*AI
      TTILT2=TTILT2+TILT*TILT
      TTILT=TTILT+ABS(TILT)
      IF(T.GT.BMAX)BMAX=T
      IF(DELEFT.GT.DRMAX)GOTO 280
      GOTO 290
  280 DRMAX=DELEFT
      DRMAXLEN=ALEN(I)
      SLE=SPAN
  290 IF(AI.GT.AIMAX)AIMAX=AI
      IF(IOPT.EQ.0)WRITE(6,210)SPAN,TILT,PAMP,BETAL,RSL,DELEFT,ALEN(I)
      IF(IOPT.EQ.0.AND.IJK.EQ.0)WRITE(10,210)FRE,BETAL,BETAR,TILT,DELEFT
      IF(IOPT.EQ.0.AND.IJK.EQ.1)WRITE(14,210)FRE,BETAL,BETAR,TILT,DELEFT
  300 CONTINUE
      DRAT=DTOT/(FLOAT(L2-L1+1)*DIFL)
      RTBETA=BETA/(FLOAT(L2-L1+A)*DIFL)
      IF(II.LE.1)GOTO 320
      AVEBETA=BETA/FLOAT(II)
      AVETILT=TTILT/FLOAT(II)
      AVESPAN=AVESPAN/FLOAT(II)
      AVEINT=AVEINT/FLOAT(II)
      SBETA2=(BETA2-BETA*BETA/FLOAT(II))/FLOAT(II-1)
      SI2=(AVEINT2-AVEINT*AVEINT/FLOAT(II))/FLOAT(II-1)
      STILT2=(TTILT2-TTILT*TTILT/FLOAT(II))/FLOAT(II-1)
      SBETA=ABS(SBETA2)**0.5
      SI=ABS(SI2)**0.5
      STILT=ABS(STILT2)**0.5
      S3BETA=AVEBETA+3*SBETA
      S3I=AVEINT+3*SI
      IF(IOPT.EQ.0)WRITE(6,310)AVEBETA,SBETA,S3BETA,AVEINT,SI,S3I,BMAX,A
     1IMAX,AVETILT,STILT,II
      IF(IOPT.EQ.0)WRITE(6,315)R1BETA,RTBETA,DRA,DRAT,DRMAX,DRMAXLEN,SLE
  310 FORMAT(/,1X,'AVERAGE BETA =',F10.5,'  PERCENT     STANDARD DEVIATI
     1ON =',F10.5,/,1X,'AVE BETA + 3 TIMES DEVIATION =',F10.5,'  PERCENT
     2',/,1X,'AVE INTENSITY =',F10.5,'  PERCENT/FT   STANDARD DEVIATION
     3=',F10.5,/,1X,'AVERAGE INTENSITY + 3 TIMES DEVIATION =',F10.5,/,1X
     4,'MAXIMUM BETA =',F10.5,'  PERCENT     MAXIMUM INTENSITY =',F10.5,
     5/,1X,'AVERAGE TILT =',F10.5,'   PERCENT    STANDARD DEVIATION =',F
     610.5,/,1X,'NUMBER OF READINGS =',I5)
  315 FORMAT(/,1X,'FIRST BETA ROUGHNESS =',F10.5,' PERCENT ANGULAR DISTO
     1RTION/FT',/,1X,'TOTAL BETA ROUGHNESS =',F10.5,' PERCENT ANGULAR DI
     2STORTION/FT',/,1X,'FIRST RELATIVE THICKNESS =',F10.5,' FT/FT',/,1X
```

Table B4. (Continued)

```
     3,'TOTAL RELATIVE THICKNESS =',F10.5,' FT/FT',/,1X,'MAXIMUM RELATIV
     4E THICKNESS =',F10.5,' FT AT',/,10X,'LENGTH',F8.2,' FT AND SPAN',F
     58.2,' FT')
  320 AL=DIFL*FLOAT(L2-L1+1)
      IF(II.LE.1)WRITE(6,330)AL
  330 FORMAT('ONE OR NO PEAKS FOR LENGTH =',F10.5,'  FT')
C           CALCULATE MACRORELIEF INDEX
      XI=0.0
      YI=0.0
      XI2=0.0
      XYI=0.0
      YI2=0.0
      DO 350 I=L1,L2
      IF(IOPT.EQ.0.AND.IJK.EQ.0)ALAB=ALENG(I)
      IF(IOPT.EQ.0.AND.IJK.EQ.1)ALAB=ALENG(I)-ALENG(L1)
      IF(IOPT.EQ.1)ALAB=ALENG(I)
      XI2=XI2+ALAB*ALAB
      XI=XI+ALAB
      XYI=XYI+ELEV(I)*ALAB
      YI=YI+ELEV(I)
      YI2=YI2+ELEV(I)*ELEV(I)
  350 CONTINUE
      NOPE=L2-L1+1
      AN=REAL(NOPE)
      TXY=XYI-XI*YI/AN
      TX=XI2-XI*XI/AN
      TY=YI2-YI*YI/AN
      B=TXY/TX
      A=YI/AN - B*XI/AN
      R2=TXY*TXY/(TX*TY)
      IF(IOPT.EQ.0)WRITE(6,360)A,B,R2
  360 FORMAT(/,1X,'A =',F10.5,'   B =',F10.5,'   R2 =',F10.5)
      AMI=0.0
      DO 400 I=L1,L2
      IF(IOPT.EQ.0.AND.IJK.EQ.0)ALAB=ALENG(I)
      IF(IOPT.EQ.0.AND.IJK.EQ.1)ALAB=ALENG(I)-ALENG(L1)
      IF(IOPT.EQ.1)ALAB=ALENG(I)
      Y=A+B*(ALAB-DIFL/2.)
      T=(ELEV(I-1)+ELEV(I))/2.
      T=T-Y
      AMI=AMI+ABS(T)
  400 CONTINUE
      AMRI=8.33333*AMI*FLOAT(J-1)/(DIFL*AN*AN)
      IF(IOPT.EQ.0)WRITE(6,410)AMRI
  410 FORMAT(/,1X,'MACRORELIEF INDEX =',F10.5,'  PERCENT')
      AL=DIFL*AN
      IF(IOPT.EQ.1.AND.II.GT.1)WRITE(11,40)AL,AVEBETA,AVETILT,AMRI
      IF(IOPT.EQ.1.AND.II.GT.1)WRITE(15,40)AL,R1BETA,RTBETA,DRA,DRAT
  420 NRE=NRE-1
```

Table B4. (Continued)

```
      IF(NRE.LT.3)GOTO 500
      IJK=IJK+1
C   DETERMINE FRACTAL ROUGHNESS
      IF(IJK.NE.1)GOTO 460
      TOTFL=FLOAT(NRE)*DIFL
      DX=DIFL
      NC=NRE+1
      IJ=1
      KLM=0
  445 PE=0.0
      KLM=KLM+1
      KJ=1
      DO 450 I=2,NC
      TEMP=(ELEV(KJ+IJ)-ELEV(KJ))/(DX*12.)
      TEMP=ATAN(TEMP)
      PE=PE+DX/COS(TEMP)
      KJ=KJ+IJ
  450 CONTINUE
      IJ=IJ+1
      PE=PE/TOTFL
      PE=ALOG10(PE)
      DDX=ALOG10(DX)
      WRITE(12,40)DDX,PE
      DX=DX+DIFL
      NC=IFIX(TOTFL/DX)+1
      IF(NC.GT.4)GOTO 445
  460 IF(IOPT.EQ.1)GOTO 1000
      IF(IOPT.EQ.0.AND.IJK.EQ.1)GOTO 1000
  500 CLOSE(5,STATUS='KEEP')
      CLOSE(6,STATUS='KEEP')
      CLOSE(8,STATUS='KEEP')
      CLOSE(9,STATUS='KEEP')
      CLOSE(10,STATUS='KEEP')
      CLOSE(11,STATUS='KEEP')
      CLOSE(12,STATUS='KEEP')
      CLOSE(13,STATUS='KEEP')
      CLOSE(14,STATUS='KEEP')
      CLOSE(15,STATUS='KEEP')
      STOP
      END
C
C
      SUBROUTINE STAND (N1,N2,VAR,STD,AMEAN)
      DIMENSION VAR(1000)
      NI=N1
      NJ=N2
      N=NJ-NI
      NN=N-1
      SUM = 0.0
```

Table B4. (Concluded)

```
      SUMSQ = 0.0
      DO 10 I = NI,NJ
      SUM = SUM + VAR(I)
      SUMSQ = SUMSQ + VAR(I)*VAR(I)
   10 CONTINUE
      AMEAN = SUM/FLOAT(N)
      STDSQ = (SUMSQ - SUM*SUM/FLOAT(N))/FLOAT(NN)
      STD = ABS(STDSQ)**0.5
      RETURN
      END
C
C
      SUBROUTINE STIFF(AAOAE,RS)
      DIMENSION RF(15),RIGID(15)
      DATA RF/1.000,.975,.945,.900,.827,.731,.578,.400,.285,.200,.114
     1,.064,.027,.005,.001/
      DATA RIGID/-9.00,-5.00,-2.00,-1.50,-1.13,-0.84,-0.50,-0.21,.0,.18
     1,.50,.75,1.00,1.50,2.00/
      IF(AAOAE.GT.1.0)AAOAE=1.0
      IF(AAOAE.LT.0.001)AAOAE=0.001
      DO 10 L=2,15
      IF(AAOAE.GT.RF(L))GOTO 20
   10 CONTINUE
   20 RS=RIGID(L)+((RIGID(L)-RIGID(L-1))/(RF(L)-RF(L-1)))*(AAOAE-RF(L))
      RETURN
      END
```

Table B5. Listing Program WAVEI.FOR

```
C     PROGRAM WAVEI.FOR:  ANALYSIS OF FLOOR PROFILE USING F-NUMBERS
C     NOMENCLATURE
C          LOOP      = 1     Closed loop; Operator bias subtracted from
C                            dipstick readings
C                    = 0     Open loop
C          KOPT      = 0     Elevation readings input
C                    = 1     Elevation change readings input
C          NREAD     = Number of readings
C          DIFL      = Sample interval of profile data, ft
C          NRE       = Number of readings used in analysis
C          JOPT      = 0     All data printed
C                    = 1     Omit distance-elevation data
C                    = 2     Omit uncorrected profilograph readings,
C                            and distance-elevation data
C                    = 3     Print only Wave Index
C          IOPT      = 0     Calculate for full length and NRE, then
C                            NRE to NREAD
C                    = 1     Calculate distribution to NRE
      DIMENSION HED(20),DEL(1000),ELEV(1000)
```

Table B5. (Continued)

```
      OPEN(5,FILE='DATDIP.TXT')
      OPEN(6,FILE='DIPOUT.TXT')
      OPEN(7,FILE='\GRAPHER\ELEV.DAT')
      OPEN(8,FILE='\GRAPHER\RWAVE.DAT')
      OPEN(9,FILE='\GRAPHER\WAVE.DAT')
      BIAS=0.0
      FL10=0.0
      STD = 0.0
      AMEAN = 0.0
      READ(5,10) (HED(I),I=1,20)
      WRITE(6,12)(HED(I),I=1,20)
   10 FORMAT(20A4)
   12 FORMAT(1X,20A4)
      READ(5,15)LOOP,KOPT,NREAD,DIFL,NRE,JOPT,IOPT
   15 FORMAT(3I5,F10.2,3I5)
      IF(LOOP.EQ.0) WRITE(6,17)
      IF(LOOP.EQ.1) WRITE(6,18)
   17 FORMAT(/,10X,'OPEN LINE')
   18 FORMAT(/,10X,'CLOSED LINE')
      IF(IOPT.EQ.0)WRITE(6,20)
   20 FORMAT(/,1X,'WAVE SPECTRUM CALCULATED FOR FULL LENGTH')
      WRITE (6,25) NREAD,DIFL
   25 FORMAT(/,1X,'NUMBER OF READINGS=',11X,I5,/,1X,'ACTUAL SAMPLE',
     1' INTERVAL =',6X,F10.2,'  FEET')
      IF(KOPT.EQ.0)WRITE(6,26)
      IF(KOPT.EQ.1)WRITE(6,27)
   26 FORMAT(/,1X,'INPUT DATA ARE ELEVATIONS',/)
   27 FORMAT(/,1X,'INPUT DATA ARE CHANGES IN ELEVATIONS',/)
C     INITIALIZE
      N = NREAD + 1
      DO 30 I = 1,N
      DEL(I) = 0.0
      ELEV(I) = 0.0
   30 CONTINUE
      IF(KOPT.EQ.0)READ(5,40)(ELEV(I),I=2,N)
      IF(KOPT.EQ.1)READ(5,40)(DEL(I), I=2,N)
   40 FORMAT(10F7.3)
   41 FORMAT(//,1X,'UNCORRECTED PROFILOGRAPH READINGS',//,
     11X,'LENGTH,FT    0      1      2      3      4      5      6',
     2'      7      8      9',/)
      IF(JOPT.LE.1)WRITE(6,41)
      IF(JOPT.GE.2)GOTO 48
      JJ = N/10 + 1
      AK = 0.0
      J1 = 1
      J2 = 10
      DO 45 I = 1,JJ
      IF(I.EQ.JJ)J2 = N
      IF(KOPT.EQ.0)WRITE(6,47)AK,(ELEV(J),J=J1,J2)
```

Table B5. (Continued)

```
      IF(KOPT.EQ.1)WRITE(6,47)AK,(DEL(J),J=J1,J2)
      AK = AK + 10.*DIFL
      J1 = J1 + 10
      J2 = J2 + 10
   45 CONTINUE
   47 FORMAT(1X,F8.2,10F7.3)
   48 N1 = 2
      N2 = N
      IF(KOPT.EQ.0)CALL STAND (N1,N2,ELEV,STD,AMEAN)
      IF(KOPT.EQ.1)CALL STAND (N1,N2,DEL,STD,AMEAN)
      SUM = AMEAN*FLOAT(NREAD)
      WRITE(6,50) SUM, AMEAN, STD
   50 FORMAT(//,4X,'TOTAL  =', F7.3,'  INCH',/,1X,
     1'MEAN DIFFERENCE/READING =',F10.6,'  INCH',/,1X,'STANDARD',
     2' DEVIATION =',F15.5)
      IF(LOOP.EQ.0) GOTO 60
      IF(KOPT.EQ.1)BIAS = AMEAN
      IF(KOPT.EQ.0)BIAS = (ELEV(N)-ELEV(1))/FLOAT(NREAD)
      WRITE(6,52)BIAS
   52 FORMAT(/,1X,'BIAS =',F10.5,' IN./FT',/)
      DO 55 I = 2,N
      IF(KOPT.EQ.0)ELEV(I)=ELEV(I)-BIAS*FLOAT(I-1)
      IF(KOPT.EQ.1)DEL(I) = DEL(I) - BIAS
   55 CONTINUE
   60 TOTLEN = FLOAT(NREAD)*DIFL
      WRITE(6,61)TOTLEN    61 FORMAT(/,1X,'TOTAL LENGTH =',F10.2,'  FEET')
      DO 65 I = 2,N
      IF(KOPT.EQ.1)ELEV(I) = ELEV(I-1) + DEL(I)
   65 CONTINUE
   66 FORMAT(//,1X,'CORRECTED PROFILOGRAPH READINGS',//,1X,'LENGTH,FT'
     1,'    0      1      2      3      4      5      6      7      8', 8'
     2'      9',/)
      IF(JOPT.LE.2)WRITE(6,66)
      IF(JOPT.GE.3)GOTO 1000
      JJ = N/10 + 1
      AK = 0.0
      J1 = 1
      J2 = 10
      DO 70 I = 1,JJ
      IF(I.EQ.JJ)J2 = N
      WRITE(6,72)AK (ELEV(J),J=J1,J2)
      AK = AK + 10.*DIFL
      J1 = J1 + 10
      J2 = J2 + 10
   70 CONTINUE
      MM=0
   72 FORMAT(1X,F8.2,10F7.3)
      NO=1
 1000 N=NRE-MM
```

Table B5. (Continued)

```
      IF(IOPT.EQ.0.AND.MM.EQ.0)N=NREAD
      IF(IOPT.EQ.0.AND.MM.EQ.2)N=NREAD
      IF(IOPT.EQ.0.AND.MM.EQ.1)N=NRE
      IF(IOPT.EQ.0.AND.MM.EQ.2)NO=NRE+1
      NOT=N-(NO-1)
   73 WRITE(6,67)NOT
   67 FORMAT(1X,'NUMBER OF DATA POINTS =',I5)
      ALEN=0.0
      DO 85 I=NO,N
      ALEN=ALEN+DIFL
      IF(MM.EQ.0)WRITE(7,86) ALEN,ELEV(I)
   85 CONTINUE
   86 FORMAT(1X,F10.2,F10.3)
      WINDEX = 0.0
      IF(JOPT.LE.2.AND.MM.EQ.0)WRITE(6,87)
   87 FORMAT(/,1X,'LENGTH, FT     ROOT MEAN SQUARE AMPLITUDE, INCH')
      DELX=0.0
      DO 100 J = 1,50
      J9 = N-2*J-NO
      IF(J9.LT.1) GOTO 105
      DELX = DELX + DIFL
      SUM = 0.0
      DO 90 I = NO,N-2*J
      A=ELEV(I+J)-(ELEV(I)+ELEV(I+2*J))/2.
      SUM=SUM + A*A
   90 CONTINUE
      IN=I-NO+1
      SUM=SUM/(2.*FLOAT(IN))
      ARMS = ((SUM)**0.5)
      IF(JOPT.EQ.2.AND.MM.EQ.0)WRITE(6,110)DELX,ARMS
      IF(MM.EQ.0)WRITE(9,120)DELX,ARMS
      WINDEX=WINDEX + ARMS*ARMS
  100 CONTINUE
  105 CONTINUE
  110 FORMAT(5X,F7.2,10X,F10.5)
  120 FORMAT(2F10.5)
      WAVEIND=(WINDEX/FLOAT(50))**0.5
      WRITE(6,150)ALEN,WAVEIND
  150 FORMAT(1X,'LENGTH = ',F10.2,'  FT    WAVE INDEX =',F10.5,/)
      WRITE(8,120)ALEN,WAVEIND
      MM=MM+1
      IF(N.LT.10)GOTO 170
      IF(IOPT.EQ.0.AND.MM.GE.3)GOTO 170
      GOTO 1000
  170 CONTINUE
      CLOSE(5,STATUS='KEEP')
      CLOSE(6,STATUS='KEEP')
      CLOSE(7,STATUS='KEEP')
      CLOSE(8,STATUS='KEEP')
```

Table B5. (Concluded)

```
      CLOSE(9,STATUS='KEEP')
      STOP
      END
C
C
      SUBROUTINE STAND (N1,N2,VAR,STD,AMEAN)
      DIMENSION VAR(1000)
      NI=N1
      NJ=N2
      N=NJ-NI
      NN=N-1
      SUM = 0.0
      SUMSQ = 0.0
      DO 10 I = NI,NJ
      SUM = SUM + VAR(I)
      SUMSQ = SUMSQ + VAR(I)*VAR(I)
   10 CONTINUE
      AMEAN = SUM/FLOAT(N)
      STDSQ = (SUMSQ - SUM*SUM/FLOAT(N))/FLOAT(NN)
      STD = ABS(STDSQ)**0.5
      RETURN
      END
```

Table B6. Input File FTRIN.TXT (or DATDIP.TXT)

a. Organization

Line	Parameters	Format
1	HED(I),I=1,20	20A4
2	LOOP KOPT NREAD DIFL NRE JOPT IOPT*	3I5,F10.2,3I5,F10.5
3	(If KOPT = 1) DEL(I), I=2,NREAD + 1	10F7.3
	(If KOPT = 0) ELEV(I), I=2,NREAD + 1	10F7.3

*For Program FTROPT, replace "IOPT" with "NO PEAKA"
For Program FNUMR, replace "IOPT" with "IOPT ALEN"

b. Description

Line	Item	Description
1	HED(I)	Description or name or problem to be analyzed
2	LOOP	= 1 Closed loop; operator bias subtracted from dipstick readings
		= 0 Open loop (no closure to original point)
	KOPT	= 1 Elevation change readings input, in.
		= 0 Elevation readings input, in.

Table B6. (Concluded)

	NREAD	Number of readings taken with profiler or dipstick device
	DIFL	Sample length interval of profile data, ft
	NRE	Number of readings used in analysis
	JOPT	(Not used in Program FTRC) = 0 Minimum output in file FTROUT.TXT (or DIPOUT.TXT) = 1 Maximum output in file FTROUT.TXT
	Following not used in Program FTRC and FTROPT	
		Program FNUMR:
	IOPT	= 0 Calculate F-numbers for full length = 1 Calculate F-numbers for readings up to NRE, then from NRE to full length = 2 Calculate F-numbers at increments of 1 up to NRE
		Program ADATG:
	IOPT	= 0 Calculate for given NRE and NRE+1 to NREAD+1 = 1 Calculate for readings 4 to NRE
		Program WAVEI:
	IOPT	= 0 Calculate WAVEI for given NREAD, NRE and NRE+1 to NREAD+1 = 1 Calculate WAVEI in increments up to NRE
	Following used only in Program FTROPT	
	NO	Number of Fourier runs at decrement = 2
	PEAKA	Limiting peak amplitude used to calculate resonant frequency, in.
	Following used only in Program FNUMR	
	ALEN	Sample increment length used to calculate F-number, ft; ≥ DIFL and should be multiple of DIFL
3	DEL(I)	Elevation change, in.
	ELEV(I)	Elevation, in.

Table B7. Transform of a Sine Wave

a. Input Data, File FTRIN.TXT

```
SINE WAVE A= 1.00 INCH, L= 32 FT  SLOPE = 0.00 IN/FT

   0    0  300      1.00   64
 0.195  0.383  0.556  0.707  0.831  0.924  0.981  1.000  0.981  0.924
 0.831  0.707  0.556  0.383  0.195  0.000 -0.195 -0.383 -0.556 -0.707
-0.831 -0.924 -0.981 -1.000 -0.981 -0.924 -0.831 -0.707 -0.556 -0.383
-0.195  0.000  0.195  0.383  0.556  0.707  0.831  0.924  0.981  1.000
 0.981  0.924  0.831  0.707  0.556  0.383  0.195  0.000 -0.195 -0.383
-0.556 -0.707 -0.831 -0.924 -0.981 -1.000 -0.981 -0.924 -0.831 -0.707
-0.556 -0.383 -0.195  0.000  0.195  0.383  0.556  0.707  0.831  0.924
 0.981  1.000  0.981  0.924  0.831  0.707  0.556  0.383  0.195  0.000
-0.195 -0.383 -0.556 -0.707 -0.831 -0.924 -0.981 -1.000 -0.981 -0.924
-0.831 -0.707 -0.556 -0.383 -0.195  0.000  0.195  0.383  0.556  0.707
 0.831  0.924  0.981  1.000  0.981  0.924  0.831  0.707  0.556  0.383
```

Table B7. (Continued)

0.195	0.000	-0.195	-0.383	-0.556	-0.707	-0.831	-0.924	-0.981	-1.000
-0.981	-0.924	-0.831	-0.707	-0.556	-0.383	-0.195	0.000	0.195	0.383
0.556	0.707	0.831	0.924	0.981	1.000	0.981	0.924	0.831	0.707
0.556	0.383	0.195	0.000	-0.195	-0.383	-0.556	-0.707	-0.831	-0.924
-0.981	-1.000	-0.981	-0.924	-0.831	-0.707	-0.556	-0.383	-0.195	0.000
0.195	0.383	0.556	0.707	0.831	0.924	0.981	1.000	0.981	0.924
0.831	0.707	0.556	0.383	0.195	0.000	-0.195	-0.383	-0.556	-0.707
-0.831	-0.924	-0.981	-1.000	-0.981	-0.924	-0.831	-0.707	-0.556	-0.383
-0.195	0.000	0.195	0.383	0.556	0.707	0.831	0.924	0.981	1.000
0.981	0.924	0.831	0.707	0.556	0.383	0.195	0.000	-0.195	-0.383
-0.556	-0.707	-0.831	-0.924	-0.981	-1.000	-0.981	-0.924	-0.831	-0.707
-0.556	-0.383	-0.195	0.000	0.195	0.383	0.556	0.707	0.831	0.924
0.981	1.000	0.981	0.924	0.831	0.707	0.556	0.383	0.195	0.000
-0.195	-0.383	-0.556	-0.707	-0.831	-0.924	-0.981	-1.000	-0.981	-0.924
-0.831	-0.707	-0.556	-0.383	-0.195	0.000	0.195	0.383	0.556	0.707
0.831	0.924	0.981	1.000	0.981	0.924	0.831	0.707	0.556	0.383
0.195	0.000	-0.195	-0.383	-0.556	-0.707	-0.831	-0.924	-0.981	-1.000
-0.981	-0.924	-0.831	-0.707	-0.556	-0.383	-0.195	0.000	0.195	0.383
0.556	0.707	0.831	0.924	0.981	1.000	0.981	0.924	0.831	0.707

b. Output of program FTRC, File FTROUT.TXT

```
SINE WAVE A= 1.00 INCH, L= 32 FT  SLOPE = 0.00 IN/FT

         OPEN LINE    UNCORRECTED READINGS

NUMBER OF READINGS=              300
ACTUAL SAMPLE INTERVAL =            1.00  FEET
READINGS USED =   64

INPUT DATA ARE ELEVATIONS

UNCORRECTED INPUT DATA
```

LENGTH,FT	0	1	2	3	4	5	6	7	8	9
0.00	0.000	0.195	0.383	0.556	0.707	0.831	0.924	0.981	1.000	0.981
10.00	0.924	0.831	0.707	0.556	0.383	0.195	0.000	-0.195	-0.383	-0.556
20.00	-0.707	-0.831	-0.924	-0.981	-1.000	-0.981	-0.924	-0.831	-0.707	-0.556
30.00	-0.383	-0.195	0.000	0.195	0.383	0.556	0.707	0.831	0.924	0.981
40.00	1.000	0.981	0.924	0.831	0.707	0.556	0.383	0.195	0.000	-0.195
50.00	-0.383	-0.556	-0.707	-0.831	-0.924	-0.981	-1.000	-0.981	-0.924	-0.831
60.00	-0.707	-0.556	-0.383	-0.195	0.000	0.195	0.383	0.556	0.707	0.831
70.00	0.924	0.981	1.000	0.981	0.924	0.831	0.707	0.556	0.383	0.195
80.00	0.000	-0.195	-0.383	-0.556	-0.707	-0.831	-0.924	-0.981	-1.000	-0.981
90.00	-0.924	-0.831	-0.707	-0.556	-0.383	-0.195	0.000	0.195	0.383	0.556
100.00	0.707	0.831	0.924	0.981	1.000	0.981	0.924	0.831	0.707	0.556
110.00	0.383	0.195	0.000	-0.195	-0.383	-0.556	-0.707	-0.831	-0.924	-0.981

Table B7. (Concluded)

120.00	-1.000	-0.981	-0.924	-0.831	-0.707	-0.556	-0.383	-0.195	0.000	0.195
130.00	0.383	0.556	0.707	0.831	0.924	0.981	1.000	0.981	0.924	0.831
140.00	0.707	0.556	0.383	0.195	0.000	-0.195	-0.383	-0.556	-0.707	-0.831
150.00	-0.924	-0.981	-1.000	-0.981	-0.924	-0.831	-0.707	-0.556	-0.383	-0.195
160.00	0.000	0.195	0.383	0.556	0.707	0.831	0.924	0.981	1.000	0.981
170.00	0.924	0.831	0.707	0.556	0.383	0.195	0.000	-0.195	-0.383	-0.556
180.00	-0.707	-0.831	-0.924	-0.981	-1.000	-0.981	-0.924	-0.831	-0.707	-0.556
190.00	-0.383	-0.195	0.000	0.195	0.383	0.556	0.707	0.831	0.924	0.981
200.00	1.000	0.981	0.924	0.831	0.707	0.556	0.383	0.195	0.000	-0.195
210.00	-0.383	-0.556	-0.707	-0.831	-0.924	-0.981	-1.000	-0.981	-0.924	-0.831
220.00	-0.707	-0.556	-0.383	-0.195	0.000	0.195	0.383	0.556	0.707	0.831
230.00	0.924	0.981	1.000	0.981	0.924	0.831	0.707	0.556	0.383	0.195
240.00	0.000	-0.195	-0.383	-0.556	-0.707	-0.831	-0.924	-0.981	-1.000	-0.981
250.00	-0.924	-0.831	-0.707	-0.556	-0.383	-0.195	0.000	0.195	0.383	0.556
260.00	0.707	0.831	0.924	0.981	1.000	0.981	0.924	0.831	0.707	0.556
270.00	0.383	0.195	0.000	-0.195	-0.383	-0.556	-0.707	-0.831	-0.924	-0.981
280.00	-1.000	-0.981	-0.924	-0.831	-0.707	-0.556	-0.383	-0.195	0.000	0.195
290.00	0.383	0.556	0.707	0.831	0.924	0.981	1.000	0.981	0.924	0.831
300.00	0.707									

TOTAL READINGS = 0.000INCH
MEAN = 0.000000 INCH
STANDARD DEVIATION = 0.00000

TOTAL LENGTH = 300.00 FEET
READINGS USED FOR FOURIER TRANSFORM= 64

NUMBER	FREQUENCY	REAL	IMAGINARY	AMPLITUDE	PHASE SHIFT, DEG
1	0.00000	0.00000	0.00000	0.00000	0.00000
2	0.01562	0.00000	0.00000	0.00000	16.28700
3	0.03125	-0.00001	32.00158	0.50002	-89.99998
4	0.04687	0.00000	0.00000	0.00000	-75.89912
5	0.06250	0.00000	0.00000	0.00000	-84.14005
6	0.07812	0.00000	0.00000	0.00000	-89.45983
7	0.09375	0.00000	0.00218	0.00003	89.98723
8	0.10937	0.00000	0.00000	0.00000	-88.17467
9	0.12500	0.00000	0.00000	0.00000	-86.93304
10	0.14062	0.00000	0.00000	0.00000	60.06903
11	0.15625	0.00000	0.00729	0.00011	-89.99947
12	0.17187	0.00000	-0.00001	0.00000	-89.30286
13	0.18750	0.00000	0.00001	0.00000	-88.30740
14	0.20312	0.00000	0.00000	0.00000	-87.39510
15	0.21875	0.00000	-0.00352	0.00006	89.99906
16	0.23437	0.00000	0.00000	0.00000	87.43274

AMPLITUDE ROUGHNESS OF TRANSFORM IS 0.06253 IN.
BETA ROUGHNESS OF TRANSFORM IS 0.06525
ELEVATION ROUGHNESS IS 0.63310 IN.

Table B8. Listing Program SINEW.FOR

```
C  PROGRAM SINEW.FOR: TO CALCULATE ELEVATION PROFILE OF MULTIPLE SINE WAVES
C     NOMENCLATURE
C          LOOP      = 1     Closed loop; Operator bias subtracted from
C                            dipstick readings
C                    = 0     Open loop
C          KOPT      = 0     Elevation readings input
C                    = 1     Elevation change readings input
C          NREAD     Number of readings
C          DIFL      Sample interval of profile data, ft
C          NRE       Number of readings used in Fourier Transform
C          N         Number of waves in calculation
C          SLOPE     Slope or change in height per sample interval DIFL
C          A(I)      Amplitude of each wave for I=1,N
C          ALEN(I)   Wavelength of each wave for I=1,N
       DIMENSION HED(20),A(10),ALEN(10),Y(1000)
       OPEN(5,FILE='WAVEIN.TXT')
       OPEN(6,FILE='WAVEOUT.TXT')
       READ(5,10) (HED(I),I=1,20)
       REWIND 6
       WRITE(6,10)(HED(I),I=1,20)
    10 FORMAT(20A4)
       READ(5,15)LOOP,KOPT,NREAD,DIFL,NRE,N,SLOPE
       WRITE(6,16)LOOP,KOPT,NREAD,DIFL,NRE
    15 FORMAT(3I5,F10.2,2I5,F10.2)
    16 FORMAT(1X,3I5,F10.2,2I5)
       READ(5,20) (A(I),I=1,N)
       READ(5,20) (ALEN(I),I=1,N)
    20 FORMAT(10F7.3)
C      INITIALIZE
       P=3.14159265*2.
       DELX=0.0
       DO 200 J=1,NREAD
       DELX=DELX+DIFL
       Y(J)=0.0
       DO 100 I=1,N
       ARG=P*DELX/ALEN(I)
       T=A(I)*SIN(ARG)
       Y(J)=Y(J)+T
   100 CONTINUE
       Y(J)=Y(J)+SLOPE*FLOAT(J)
   200 CONTINUE
       WRITE(6,250)(Y(J),J=1,NREAD)
   250 FORMAT(1X,10F7.3)
       CLOSE(5,STATUS='KEEP')
       CLOSE(6,STATUS='KEEP')
       STOP
       END
C
```

APPENDIX C: ELEVATION PROFILOMETER SURVEYS

Table C1. Red River Army Depot, May 1987 (Elevation Changes)

a. Survey Line 3, Building 333

FROM K-13 TO AGV TRACK, N TO S, K.5-26 THEN RETURN, BLDG 333

1 1 649 1.00 311 0 0

-0.131	-0.134	0.036	-0.055	-0.045	-0.063	-0.072	0.031	0.015	-0.012
0.065	0.055	-0.028	-0.081	0.074	0.068	0.029	0.047	-0.005	-0.007
0.082	0.116	0.005	-0.039	0.010	-0.101	0.002	-0.033	-0.104	0.038
-0.034	0.020	-0.018	0.003	-0.023	-0.019	-0.093	-0.041	-0.023	-0.002
-0.036	0.074	-0.061	-0.053	0.091	0.012	0.058	-0.081	0.026	0.018
-0.075	-0.044	0.024	0.021	0.044	-0.019	0.059	-0.017	-0.025	0.001
-0.034	-0.071	-0.020	-0.007	0.007	0.018	0.034	-0.010	-0.013	-0.063
-0.013	-0.001	0.003	0.017	-0.006	-0.053	0.007	-0.044	0.019	0.050
0.036	-0.012	-0.013	-0.003	-0.021	0.018	0.004	0.010	0.024	0.016
0.017	-0.017	0.010	0.038	-0.007	-0.026	-0.075	-0.036	0.020	-0.092
-0.073	0.025	0.006	-0.018	-0.024	0.009	-0.100	0.006	0.022	-0.008
-0.061	-0.016	0.023	-0.017	0.058	0.042	0.076	0.040	0.086	0.060
0.066	0.000	0.033	0.013	-0.022	-0.076	-0.085	-0.070	-0.091	0.114
0.068	0.005	0.058	0.092	0.023	0.009	-0.062	-0.124	-0.121	-0.033
0.010	0.056	0.015	0.065	0.083	0.017	0.034	-0.034	-0.073	-0.041
-0.023	-0.113	-0.041	-0.053	0.061	0.028	0.075	0.010	0.044	-0.029
0.031	0.034	0.073	0.003	-0.026	-0.062	-0.061	-0.047	-0.024	-0.042
-0.081	-0.057	0.051	0.009	0.023	-0.072	-0.083	-0.113	-0.103	-0.016
0.009	0.073	-0.032	-0.060	-0.088	-0.167	0.269	0.055	0.115	0.025
-0.023	-0.119	0.005	0.052	0.027	0.030	0.012	0.019	0.024	0.041
0.000	0.016	0.019	-0.193	0.082	0.201	0.047	-0.010	0.013	0.067
0.002	-0.022	-0.005	0.004	-0.054	0.113	0.051	0.163	-0.139	-0.007
-0.011	0.085	0.086	0.024	-0.036	0.014	-0.093	-0.089	0.102	-0.001
0.043	0.030	0.045	-0.030	0.034	0.052	0.065	0.026	0.067	0.070
0.089	-0.037	0.046	0.063	0.035	0.075	0.004	0.043	0.030	-0.039
-0.061	-0.165	-0.109	-0.230	0.054	0.069	0.056	-0.057	0.035	-0.110
-0.070	0.014	0.017	-0.030	0.028	0.064	0.021	0.015	0.125	0.142
0.029	0.046	0.119	0.028	0.086	0.041	-0.034	-0.056	-0.046	-0.076
-0.005	0.044	0.014	-0.037	-0.016	-0.011	-0.147	0.072	-0.013	-0.025
-0.059	-0.039	-0.016	-0.010	0.031	-0.017	0.054	0.040	0.045	-0.027
-0.081	-0.099	-0.038	-0.096	0.157	0.079	0.329	0.309	-0.068	0.130
0.040	-0.126	0.070	-0.294	-0.284	-0.145	-0.036	0.075	0.021	0.065
0.119	0.032	0.000	-0.045	-0.034	-0.005	-0.017	0.030	0.011	-0.010
0.040	0.018	0.045	-0.055	0.049	0.019	0.042	0.042	-0.035	-0.027
0.004	0.128	0.045	0.066	-0.002	-0.005	-0.024	-0.079	-0.085	-0.070
-0.078	-0.135	-0.146	-0.032	-0.049	-0.043	0.011	-0.063	0.041	0.012
0.050	0.010	0.033	-0.025	-0.009	-0.047	0.070	0.056	0.059	0.263
0.075	0.044	0.012	0.003	0.049	-0.025	0.027	-0.112	-0.043	-0.087
-0.131	0.025	0.010	0.027	-0.051	-0.084	-0.073	-0.019	0.042	-0.093
-0.077	0.001	0.003	0.047	0.128	0.027	-0.035	-0.027	0.039	-0.064
-0.060	0.083	0.044	-0.254	-0.077	0.061	-0.043	0.045	-0.012	-0.085
-0.041	-0.010	-0.046	-0.085	-0.072	-0.073	0.017	0.149	-0.001	-0.026
-0.059	-0.040	0.030	0.000	-0.082	-0.006	-0.032	0.040	0.079	0.023

Table C1 (Continued)

-0.075	-0.037	-0.169	-0.123	0.045	0.001	0.036	-0.006	-0.059	-0.095
0.026	-0.016	0.001	-0.037	0.086	0.017	0.018	-0.003	-0.012	-0.027
0.109	-0.026	0.118	0.062	-0.126	-0.119	0.024	0.072	0.099	0.066
0.042	0.024	0.007	-0.037	-0.056	-0.090	-0.002	0.087	0.107	0.051
0.090	0.062	-0.013	-0.045	-0.110	0.028	0.052	0.002	-0.001	0.010
0.046	0.063	0.065	0.339	-0.339	-0.066	-0.052	-0.036	-0.014	-0.003
0.000	-0.045	0.127	0.099	-0.056	0.007	0.134	-0.022	0.007	0.058
0.112	0.004	-0.092	0.156	0.089	0.003	-0.016	-0.099	-0.054	-0.059
-0.028	0.019	-0.013	0.012	0.078	0.025	-0.057	-0.039	0.011	-0.014
0.012	0.002	-0.035	0.050	0.078	0.032	0.045	0.084	0.031	-0.007
-0.050	-0.070	-0.108	-0.050	-0.050	-0.007	-0.035	-0.028	0.009	0.040
-0.028	-0.002	0.043	0.068	0.088	0.047	0.022	-0.046	0.125	-0.061
0.019	0.030	0.009	0.058	0.054	0.062	0.018	-0.002	-0.068	-0.052
0.005	-0.012	-0.037	-0.036	0.009	-0.006	-0.005	0.050	-0.068	-0.061
0.063	0.033	-0.017	0.058	0.090	0.046	0.045	-0.057	-0.042	0.061
0.003	0.015	0.053	0.035	-0.066	-0.073	-0.107	-0.069	0.056	0.040
0.070	-0.027	0.006	0.013	0.030	-0.011	-0.001	0.001	-0.059	0.017
0.038	0.004	-0.014	0.006	0.007	0.028	-0.095	0.047	-0.052	0.015
0.144	-0.054	0.020	-0.049	0.050	0.017	0.046	0.003	0.029	0.067
-0.099	0.057	0.033	0.100	0.035	0.004	0.020	0.035	0.071	-0.006
-0.028	-0.052	-0.003	-0.012	-0.042	-0.056	0.022	-0.036	-0.028	-0.028
0.035	-0.003	-0.061	-0.109	0.031	0.101	-0.068	0.165	-0.094	

b. Survey Line 4, Building 312

LINE 4: E TO W LOOP BETWEEN RACKS 48 & 49, BLDG 312									
1	1	353	1.00	176	0	0			
0.001	0.012	-0.002	0.004	-0.005	0.005	-0.015	0.003	-0.036	-0.031
-0.082	-0.004	0.069	0.050	0.020	0.023	0.024	0.000	0.001	-0.007
-0.019	-0.023	-0.021	-0.025	-0.019	-0.028	0.030	0.042	-0.033	0.034
0.021	0.076	-0.023	-0.099	-0.037	-0.078	0.019	0.070	-0.029	0.051
0.062	0.006	-0.014	-0.002	0.036	0.024	0.040	-0.048	-0.031	0.012
0.072	-0.012	-0.012	0.004	-0.002	0.003	-0.062	-0.024	0.021	-0.008
-0.025	-0.070	0.038	0.044	0.038	-0.030	0.015	-0.033	-0.040	-0.048
0.002	-0.023	-0.009	-0.024	0.042	0.053	0.029	-0.022	0.022	0.031
0.007	0.047	0.001	-0.003	0.010	-0.098	0.024	0.058	-0.020	-0.032
0.0000	0.001	0.014	-0.011	-0.019	0.006	0.010	0.023	0.000	0.003
0.008	0.001	0.014	0.024	-0.022	-0.052	0.032	0.037	-0.019	-0.070
0.004	0.121	0.013	0.085	0.031	0.032	-0.050	-0.009	-0.006	-0.010
0.038	0.005	-0.022	0.022	0.038	0.024	0.000	0.045	0.026	0.026
0.050	-0.066	-0.129	-0.063	-0.070	-0.120	0.097	0.017	0.045	0.041
0.037	0.060	-0.050	-0.033	-0.009	-0.037	-0.013	-0.008	0.025	0.058
-0.009	0.075	0.049	0.008	0.008	-0.028	0.013	0.048	0.014	-0.054
-0.095	0.170	0.072	0.034	0.019	0.064	-0.004	0.019	-0.001	-0.049
-0.059	-0.012	0.017	-0.026	-0.058	0 003	-0.050	0.000	-0.051	-0.008
0.014	0.019	0.046	0.049	-0.021	0.068	-0.061	0.115	-0.143	-0.122
-0.110	0.124	0.092	-0.035	0.040	-0.047	0.026	-0.019	-0.048	-0.028
-0.028	-0.071	-0.072	-0.029	-0.043	0.024	0.072	0.064	0.010	0.004

Table C1 (Continued)

```
 0.048 -0.018 -0.037 -0.058 -0.005 -0.105  0.106  0.071  0.129  0.010
 0.049  0.065 -0.030 -0.018 -0.057 -0.023 -0.005 -0.010 -0.014  0.020
 0.018 -0.016 -0.006 -0.011  0.035 -0.013 -0.049 -0.053 -0.044 -0.037
-0.188  0.031  0.085  0.010  0.024 -0.017  0.036 -0.020  0.016  0.026
-0.055  0.012 -0.033  0.032 -0.014 -0.062  0.051 -0.015  0.043  0.046
 0.022 -0.032 -0.010  0.019 -0.021  0.038  0.028  0.016  0.041 -0.038
-0.073  0.066 -0.013 -0.047 -0.055  0.041 -0.034 -0.043  0.039 -0.023
 0.004  0.045  0.021  0.058  0.058  0.008  0.003 -0.021 -0.035 -0.068
-0.060  0.151 -0.017  0.040  0.024  0.053  0.033 -0.089 -0.012  0.078
-0.010 -0.030 -0.030  0.033 -0.002 -0.029  0.092 -0.005 -0.048 -0.006
-0.030 -0.024 -0.016 -0.014 -0.010 -0.017  0.055 -0.005  0.024  0.110
 0.042 -0.057 -0.068  0.025 -0.004 -0.042 -0.001  0.020  0.009 -0.044
 0.076  0.047  0.004  0.018  0.060  0.004 -0.039 -0.021 -0.008 -0.038
-0.080  0.032  0.097  0.025  0.016  0.031 -0.008 -0.021 -0.025 -0.055
-0.018  0.029  0.043
```

c. Survey Line 5, Building 312

```
LINE 5: E TO W LOOP BETWEEN RACKS 24 & 25, BLDG 312
   1     1  372       1.00  186     0     0
-0.009  0.031  0.046  0.015 -0.024 -0.059 -0.019  0.026 -0.076 -0.005
 0.007  0.038  0.082 -0.026  0.023 -0.012 -0.014  0.016 -0.078  0.035
-0.021 -0.007 -0.026 -0.015  0.003  0.022 -0.049  0.007 -0.022  0.012
-0.014  0.000  0.023  0.030  0.000  0.032  0.030 -0.028  0.085  0.054
-0.036  0.050  0.028 -0.022 -0.035 -0.041 -0.019  0.000 -0.045 -0.025
 0.049  0.047  0.020 -0.028 -0.047  0.012  0.041 -0.030 -0.029 -0.022
-0.028 -0.067 -0.022 -0.012  0.034  0.015  0.035  0.029 -0.013 -0.021
 0.035 -0.027 -0.013  0.005  0.026  0.043  0.044  0.056  0.037  0.059
 0.032  0.025  0.023  0.020  0.037  0.013 -0.146 -0.040 -0.011  0.032
 0.020 -0.006 -0.002 -0.026 -0.040 -0.011 -0.047 -0.029  0.047  0.010
-0.022  0.014  0.012  0.014  0.038  0.027  0.004 -0.006  0.000  0.011
-0.047  0.086 -0.053  0.008  0.014  0.008  0.013 -0.009  0.000  0.007
 0.014  0.039  0.030  0.003 -0.049  0.020 -0.073 -0.034 -0.011  0.002
 0.000  0.019 -0.021  0.000 -0.003  0.004 -0.106 -0.064  0.070 -0.029
 0.004  0.004 -0.007  0.001  0.028 -0.009  0.022  0.033  0.061 -0.025
-0.017  0.013 -0.043  0.035  0.060  0.025  0.078  0.020 -0.024  0.017
-0.014  0.027 -0.031 -0.016  0.019  0.049  0.030 -0.013 -0.014  0.002
-0.044 -0.080 -0.004 -0.004 -0.019  0.010 -0.025  0.039 -0.012  0.050
-0.019  0.015 -0.001 -0.060 -0.028 -0.023  0.023  0.015  0.009  0.033
 0.009  0.009 -0.044 -0.016  0.000 -0.023 -0.017  0.055  0.018  0.039
 0.061  0.039  0.021  0.004 -0.030 -0.023  0.005 -0.042 -0.023  0.035
 0.048  0.001 -0.021  0.016 -0.028 -0.005 -0.013 -0.048 -0.012  0.021
-0.014  0.019 -0.033 -0.029 -0.046 -0.043  0.020  0.030  0.059 -0.016
 0.013 -0.004 -0.035 -0.109  0.015  0.229 -0.016  0.020  0.020 -0.014
 0.014  0.029  0.024  0.010 -0.027 -0.019 -0.026 -0.008 -0.032  0.063
 0.074 -0.016  0.041 -0.023 -0.020  0.030 -0.039 -0.035  0.017  0.003
-0.087 -0.005  0.032  0.028  0.010  0.019  0.000 -0.017 -0.036 -0.016
-0.003  0.000  0.000  0.024  0.034  0.058  0.027 -0.014  0.004 -0.019
```

Table C1 (Continued)

```
 0.077 -0.041 -0.052  0.022  0.025  0.135  0.013 -0.003 -0.018 -0.054
 0.017 -0.027 -0.030 -0.054 -0.004 -0.090 -0.075  0.021  0.007 -0.025
 0.034 -0.014  0.005 -0.044 -0.030 -0.035  0.000 -0.006 -0.060 -0.114
 0.111 -0.026  0.033  0.014  0.021  0.003  0.000  0.013  0.036 -0.020
 0.000 -0.009  0.011  0.039  0.029  0.023 -0.037  0.057  0.020  0.018
 0.031 -0.014 -0.109 -0.057 -0.016 -0.021 -0.045 -0.020 -0.004 -0.016
-0.004  0.012  0.083 -0.016 -0.007 -0.022  0.010  0.022  0.030  0.012
 0.020  0.038  0.035  0.017  0.004 -0.012 -0.016 -0.030  0.002  0.018
-0.050 -0.013  0.048  0.016 -0.002  0.033  0.037  0.014 -0.025 -0.042
 0.027  0.010
```

d. Survey Line 6, Building 312

```
LINE 6: E TO W LOOP BETWEEN RACKS 37 & 38, BLDG 312
   1     1  372       1.00  184     0     0
 0.028  0.009  0.016 -0.020 -0.062 -0.037  0.027 -0.009 -0.020  0.000
-0.036 -0.007  0.041 -0.044  0.046 -0.017 -0.039 -0.020  0.006 -0.007
 0.001 -0.041 -0.067 -0.060 -0.005  0.074 -0.006  0.005  0.022  0.029
 0.003  0.016  0.042 -0.017 -0.023 -0.028  0.014  0.099  0.100  0.076
 0.009  0.020  0.045 -0.004 -0.015 -0.017 -0.025 -0.028  0.006  0.037
-0.021  0.054  0.083  0.033 -0.012 -0.041 -0.031 -0.003 -0.061 -0.093
-0.098 -0.037  0.008  0.086  0.098  0.039  0.040 -0.021 -0.041 -0.059
-0.028 -0.018 -0.025 -0.025  0.038  0.032  0.000  0.015  0.029  0.022
-0.055 -0.019  0.063 -0.090 -0.072 -0.043 -0.041  0.022 -0.003  0.000
 0.003 -0.031 -0.004 -0.027 -0.027  0.000 -0.002  0.030  0.008 -0.032
 0.018  0.007  0.037 -0.006  0.037 -0.014  0.008  0.015 -0.068 -0.077
-0.015  0.108  0.130  0.064  0.055  0.062  0.095  0.041  0.036  0.026
 0.012 -0.042 -0.012 -0.027  0.033  0.081  0.089  0.009 -0.013  0.038
-0.036 -0.061 -0.035 -0.155 -0.109 -0.035 -0.056  0.012  0.053  0.010
 0.001  0.029 -0.019 -0.044  0.042 -0.041  0.004  0.003 -0.051  0.031
 0.053  0.054  0.029  0.000  0.005  0.003 -0.020  0.011 -0.025 -0.026
-0.013 -0.026  0.014  0.087  0.021  0.041  0.013  0.015 -0.007 -0.050
-0.024 -0.073  0.032  0.044 -0.016  0.110  0.029  0.022  0.031  0.044
 0.020 -0.064 -0.028 -0.019  0.036  0.134  0.026  0.043 -0.006 -0.101
 0.095 -0.061  0.014  0.024 -0.072 -0.136 -0.066 -0.076 -0.017  0.046
 0.040  0.041 -0.010 -0.039 -0.016 -0.003 -0.012 -0.015 -0.024 -0.094
-0.014  0.012  0.059  0.042 -0.005  0.037  0.024 -0.028  0.013  0.001
-0.017 -0.048 -0.035  0.013 -0.053 -0.018  0.075  0.076  0.036  0.017
 0.035 -0.035 -0.068 -0.011 -0.029  0.113  0.079  0.097  0.068  0.080
-0.018  0.029 -0.033 -0.020 -0.006  0.007 -0.032 -0.034  0.060  0.054
-0.011 -0.008 -0.029 -0.085 -0.029 -0.036 -0.055 -0.073 -0.052 -0.054
-0.173  0.048  0.021  0.083 -0.003  0.029 -0.020 -0.053  0.006 -0.025
-0.054 -0.048  0.018  0.007  0.036  0.033  0.015  0.022  0.011  0.000
 0.070 -0.009 -0.027  0.009 -0.095  0.002 -0.050  0.041  0.060  0.029
-0.008  0.017  0.017 -0.050  0.052 -0.057 -0.027 -0.015  0.030  0.042
 0.068  0.115 -0.018  0.032  0.022 -0.084  0.094 -0.135 -0.155 -0.025
 0.103  0.063  0.074  0.037  0.009  0.022  0.059 -0.004 -0.031  0.011
-0.020 -0.016 -0.018  0.043  0.012  0.022  0.040 -0.001  0.011 -0.073
```

Table C1 (Continued)

```
-0.017 -0.080 -0.078 -0.130  0.037 -0.037 -0.005  0.005  0.027 -0.034
-0.035 -0.040 -0.066  0.031  0.021  0.004  0.018 -0.065  0.056  0.072
 0.030  0.021 -0.021 -0.006  0.050  0.038  0.007 -0.067  0.041 -0.029
 0.006  0.057  0.054  0.007 -0.066 -0.061  0.026  0.009  0.044  0.087
-0.043  0.002
```

e. Survey Line 7, Building 312

```
 LINE 7: E TO W LOOP BETWEEN RACKS 20 & 21, BLDG 312
   1    1  516       1.00  258    0    0
 0.034 -0.038  0.001  0.008 -0.047 -0.026  0.035 -0.004 -0.097  0.110
-0.023  0.006 -0.043  0.002  0.002  0.066 -0.034 -0.047 -0.112 -0.038
-0.022  0.001  0.030  0.074  0.108 -0.002 -0.069  0.018 -0.010 -0.070
 0.023  0.085  0.073 -0.054  0.000  0.047  0.112  0.044  0.062 -0.075
-0.007  0.029 -0.014 -0.008 -0.029 -0.030  0.010  0.021  0.069 -0.003
 0.021  0.024  0.002  0.071 -0.008  0.014  0.003 -0.006  0.064  0.013
 0.001 -0.007  0.038 -0.023 -0.023 -0.018 -0.060  0.011 -0.053 -0.005
 0.050  0.060 -0.108 -0.068  0.040  0.007  0.022  0.048 -0.040 -0.035
 0.028  0.007 -0.001 -0.132  0.029  0.107  0.060  0.013 -0.036 -0.041
-0.022  0.002 -0.043 -0.012 -0.013 -0.016  0.072  0.090  0.123  0.013
 0.000  0.005  0.024 -0.016  0.042 -0.012  0.000  0.001  0.082 -0.033
 0.003  0.013  0.006  0.015 -0.034  0.015  0.042  0.003 -0.036 -0.055
 0.028  0.092 -0.049  0.000  0.050 -0.012  0.010 -0.017 -0.057 -0.079
 0.048  0.053 -0.074 -0.011  0.032 -0.004  0.022  0.038 -0.007 -0.009
-0.065 -0.026 -0.002  0.025  0.003 -0.078  0.003  0.015 -0.024  0.013
 0.048  0.046  0.009  0.001  0.004 -0.002 -0.039  0.013  0.041  0.074
 0.020  0.050 -0.041 -0.011 -0.050 -0.040 -0.012 -0.001  0.064 -0.015
 0.022  0.054  0.014 -0.020  0.047  0.047  0.013  0.059  0.052  0.016
-0.011 -0.032 -0.046 -0.029 -0.100  0.095  0.014  0.008 -0.062  0.007
 0.079 -0.026  0.005  0.056 -0 052  0.034  0.023  0.035 -0.004  0.043
 0.002  0.001  0.007  0.018  0.026 -0.055 -0.094 -0.102 -0.044  0.102
-0.015  0.031 -0.058  0.040  0.036  0.000 -0.026 -0.007 -0.057 -0.057
-0.012  0.006  0.085  0.134  0.086  0.055  0.043  0.015  0.045  0.006
 0.013 -0.005 -0.043 -0.054  0.024 -0.052 -0.002 -0.124  0.130  0.022
 0.005  0.033  0.033  0.047 -0.018  0.011  0.019  0.062 -0.052 -0.041
 0.047  0.070  0.016 -0.020  0.057  0.108  0.147 -0.034 -0.137 -0.162
 0.047 -0.013  0.038  0.016 -0.104 -0.052  0.021 -0.017  0.008  0.013
-0.022 -0.002 -0.043 -0.017  0.021 -0.037  0.007 -0.015  0.003  0.024
 0.004 -0.012  0.100  0.059 -0.023  0.051  0.012 -0.065 -0.060 -0.060
-0.038 -0.030 -0.082 -0.096 -0.061  0.095 -0.026  0.006  0.017  0.060
 0.022  0.002 -0.054 -0.010  0.043  0.014 -0.044  0.001  0.076  0.104
 0.034  0.050  0.035  0.008  0.023 -0.056 -0.101 -0.080  0.013 -0.030
-0.050  0.003  0.023  0.037 -0.003 -0.060  0.014  0.095  0.003  0.023
-0.004 -0.054  0.099  0.036  0.034  0.095  0.010 -0.057 -0.025 -0.010
-0.002 -0.044 -0.033  0.008 -0.045  0.002 -0.013  0.001 -0.041 -0.016
 0.041  0.035  0.058  0.018 -0.034 -0.026 -0.051 -0.032 -0.011 -0.009
-0.004 -0.006 -0.010  0.007  0.015 -0.015  0.013 -0.027 -0.076 -0.070
 0.088  0.042 -0.016  0.008  0.029  0.130  0.029 -0.033 -0.051 -0.014
```

Table C1 (Continued)

-0.047	0.002	0.030	-0.002	0.040	0.013	0.074	-0.001	0.060	0.038
0.004	-0.011	-0.025	-0.046	-0.044	-0.034	0.052	0.029	-0.010	0.043
0.005	-0.008	-0.015	0.000	-0.002	-0.060	-0.022	0.021	-0.019	0.025
0.026	-0.046	0.000	0.015	0.039	-0.020	0.044	-0.156	-0.143	-0.025
0.003	0.060	0.027	-0.014	0.027	-0.009	0.066	0.028	0.031	-0.072
-0.094	0.049	0.050	0.003	-0.003	0.019	0.020	0.010	-0.033	0.001
-0.037	0.046	0.044	0.008	-0.040	0.039	-0.024	0.020	0.037	-0.036
0.011	0.045	-0.018	-0.012	0.004	0.018	0.073	-0.034	-0.023	-0.002
0.017	0.000	-0.044	0.019	0.018	0.005	-0.023	0.011	-0.056	-0.011
0.023	0.023	-0.006	-0.028	-0.040	0.001	0.075	0.015	-0.063	-0.062
-0.041	0.029	0.063	-0.075	-0.084	0.018	0.041	0.026	0.021	-0.044
-0.022	-0.052	-0.061	-0.046	0.026	0.058	0.068	0.068	-0.010	-0.006
0.007	0.038	0.016	0.033	0.020	0.017	-0.066	0.062	-0.029	0.005
0.003	0.063	-0.009	-0.002	0.062	-0.018				

f. Survey Line 10, Building 312

LINE 10: E TO W LOOP BETWEEN RACKS 12 & 13, BLDG 312

1	1	515	1.00	257	0	0			
-0.002	0.074	-0.062	-0.064	0.002	-0.021	0.023	-0.018	0.002	0.000
0.007	-0.002	-0.026	0.019	-0.034	0.013	-0.049	0.016	-0.003	-0.071
-0.010	0.000	0.020	0.052	0.046	0.019	0.039	0.000	0.005	0.035
0.017	0.047	-0.017	-0.140	0.136	0.043	0.071	0.000	-0.001	-0.013
-0.010	-0.009	-0.007	-0.024	-0.034	-0.026	-0.012	0.027	0.019	0.008
0.007	-0.015	-0.049	-0.053	-0.019	0.000	-0.033	-0.060	0.066	0.114
0.017	0.021	0.049	-0.022	-0.016	-0.007	-0.018	-0.070	-0.010	0.012
0.039	-0.001	0.053	-0.001	0.013	0.047	0.006	-0.058	-0.052	0.000
0.007	-0.058	0.000	-0.013	0.016	0.033	0.018	0.058	-0.005	0.006
-0.010	0.022	-0.048	-0.036	0.015	0.008	0.090	0.040	0.066	0.015
0.048	0.000	-0.036	0.058	0.028	0.003	0.010	0.030	-0.011	0.036
-0.015	-0.040	0.017	0.025	-0.033	-0.022	-0.046	0.005	-0.015	0.046
0.050	-0.109	-0.015	0.014	0.020	-0.039	-0.001	-0.072	0.095	0.016
-0.015	0.017	-0.038	0.046	0.076	0.020	0.024	0.005	-0.014	0.024
0.032	0.070	-0.007	0.039	-0.002	0.006	0.045	0.029	0.004	-0.026
-0.001	0.022	-0.002	-0.010	-0.008	-0.099	-0.055	0.003	0.003	0.117
-0.002	0.011	-0.006	-0.049	0.019	0.014	0.072	0.020	-0.029	0.009
0.047	0.039	0.021	-0.017	0.016	0.016	0.054	-0.001	-0.037	0.000
0.009	0.012	0.016	-0.036	-0.017	-0.017	0.032	0.006	0.024	-0.002
0.031	0.006	-0.062	-0.036	-0.095	-0.047	-0.019	-0.001	0.142	0.049
-0.036	-0.021	0.022	0.030	0.040	-0.003	-0.017	-0.041	-0.054	0.069
0.000	-0.013	-0.025	-0.089	-0.007	0.016	0.067	-0.112	-0.098	-0.035
0.031	-0.011	0.026	0.077	0.108	-0.008	0.020	-0.022	0.025	0.044
0.112	0.045	-0.136	-0.125	0.123	0.028	0.023	0.028	0.018	0.016
0.007	0.013	0.016	0.038	-0.007	-0.032	0.020	0.012	-0.009	0.030
0.047	0.016	0.042	0.032	0.010	0.059	0.008	-0.027	-0.063	0.010
0.026	0.012	-0.061	-0.090	0.082	-0.018	-0.047	0.019	-0.016	0.003
-0.078	0.038	-0.062	0.019	-0.063	-0.003	0.029	-0.038	-0.051	0.040
0.034	-0.049	0.029	0.043	0.029	0.047	-0.025	-0.030	-0.059	-0.046

Table C1 (Continued)

```
-0.122  0.075 -0.036  0.017 -0.106 -0.007  0.053  0.119  0.073 -0.057
-0.010 -0.002  0.171  0.038  0.000  0.002 -0.067 -0.002  0.012  0.004
 0.009 -0.011 -0.024 -0.005 -0.012 -0.032  0.058 -0.075  0.009 -0.019
 0.000  0.081  0.068  0.112  0.077  0.012  0.045 -0.076 -0.048 -0.031
 0.040 -0.008  0.006  0.014 -0.002 -0.013  0.037 -0.031 -0.038 -0.016
-0.010  0.002 -0.006 -0.030 -0.008 -0.041 -0.018 -0.031 -0.026  0.008
-0.004  0.043  0.018 -0.033  0.009 -0.116 -0.004  0.082  0.076  0.038
-0.030 -0.001  0.003  0.040  0.002  0.007 -0.026 -0.007 -0.023 -0.025
-0.021 -0.012  0.004  0.002 -0.058  0.009 -0.085 -0.019  0.020  0.013
 0.004 -0.092  0.030  0.103  0.010 -0.012 -0.051  0.018 -0.054 -0.046
 0.120  0.004  0.154  0.126 -0.140  0.000 -0.050  0.001  0.219 -0.028
-0.067  0.073  0.055  0.010 -0.016 -0.005  0.009 -0.058 -0.053 -0.018
-0.021 -0.017  0.018  0.027  0.042 -0.012 -0.037 -0.077 -0.063  0.000
 0.031 -0.012  0.043 -0.034  0.012  0.034 -0.025 -0.062  0.044 -0.020
 0.016 -0.022  0.011  0.058 -0.007  0.012 -0.032  0.067  0.008 -0.016
-0.006  0.006  0.073 -0.043 -0.009 -0.021  0.027 -0.038  0.039  0.033
-0.005 -0.003 -0.035 -0.025  0.003  0.013 -0.042  0.037  0.015  0.032
-0.007  0.025  0.069  0.049  0.050 -0.004 -0.047 -0.056  0.068  0.057
 0.008 -0.014  0.008 -0.010  0.015  0.063  0.035 -0.018 -0.055  0.002
-0.030  0.041  0.005 -0.027 -0.039 -0.009 -0.020 -0.033 -0.029 -0.037
-0.073 -0.005  0.050 -0.033 -0.015  0.095  0.050  0.015 -0.035 -0.042
-0.007  0.062  0.039  0.026  0.025 -0.105 -0.080  0.072  0.008  0.056
 0.013 -0.013 -0.044 -0.030  0.013
```

g. Survey Line 11, Building 312

```
LINE 11: E TO W LOOP BETWEEN RACKS 3 & 4, BLDG 312
  1    1  517       1.00  258    0    0
-0.055 -0.031 -0.065 -0.008 -0.007 -0.084 -0.082 -0.105 -0.059  0.062
-0.044  0.022 -0.016 -0.011  0.010 -0.007 -0.025  0.013 -0.094 -0.051
 0.006  0.010  0.007 -0.072  0.035  0.071  0.044  0.047  0.008  0.084
-0.087 -0.024  0.050  0.023  0.037  0.027  0.005 -0.004  0.007 -0.013
-0.015 -0.004 -0.010 -0.053 -0.014 -0.023 -0.010  0.006  0.003  0.037
 0.037 -0.007 -0.013  0.002 -0.012  0.006  0.031  0.007  0.046  0.054
 0.073  0.025  0.023 -0.030 -0.043 -0.004  0.003  0.005 -0.016 -0.027
-0.013  0.014  0.044 -0.016  0.003 -0.026 -0.027 -0.006 -0.054 -0.028
-0.026  0.022  0.021 -0.065  0.047  0.089  0.053  0.036  0.019  0.007
-0.006  0.007 -0.025 -0.035  0.016 -0.009  0.010  0.071  0.015 -0.006
-0.002 -0.010  0.010  0.015 -0.018 -0.030 -0.023 -0.022  0.016  0.020
 0.001  0.035  0.049  0.014  0.019 -0.006 -0.013 -0.039 -0.047 -0.009
-0.043 -0.056  0.073  0.091  0.001  0.042 -0.004 -0.031  0.126 -0.037
 0.007  0.047  0.158  0.001  0.008  0.011  0.020 -0.023 -0.030 -0.022
-0.031  0.034 -0.037 -0.002 -0.044 -0.052 -0.029  0.006  0.046 -0.012
-0.017  0.048  0.010  0.014  0.027  0.020  0.049 -0.112  0.033  0.117
 0.006  0.012  0.051  0.058 -0.013 -0.040 -0.037 -0.007  0.006 -0.073
 0.029 -0.005 -0.003  0.042  0.073  0.005 -0.003  0.026  0.049  0.090
-0.031  0.035 -0.004 -0.019 -0.078 -0.071 -0.018  0.024 -0.075 -0.051
 0.004 -0.103 -0.047 -0.058  0.077  0.019  0.006  0.030  0.031  0.041
```

Table C1 (Continued)

```
 0.054  0.035  0.049 -0.026  0.083  0.029 -0.024 -0.006 -0.093 -0.039
 0.051 -0.032 -0.031  0.052 -0.031 -0.044 -0.006  0.006 -0.022 -0.084
 0.022  0.087  0.076 -0.004  0.073 -0.027  0.028  0.054  0.071  0.100
 0.043 -0.101  0.001  0.020 -0.043  0.022  0.031  0.020 -0.009 -0.004
 0.016  0.032  0.000  0.037 -0.019  0.040  0.010  0.014 -0.002 -0.009
 0.042  0.057  0.007  0.090  0.000  0.012  0.083  0.000 -0.008 -0.021
-0.018 -0.049 -0.030 -0.037 -0.024 -0.032 -0.031 -0.008  0.002  0.014
-0.046 -0.022 -0.020  0.019  0.011 -0.003  0.001 -0.021 -0.018  0.009
-0.013 -0.017 -0.102  0.108  0.107 -0.007  0.019 -0.032 -0.046 -0.091
-0.093 -0.032 -0.025 -0.005 -0.035 -0.055 -0.016 -0.058 -0.046  0.018
 0.057 -0.116  0.021  0.022  0.011  0.031  0.024 -0.018  0.068  0.046
 0.076 -0.026 -0.083  0.026 -0.013 -0.052 -0.060 -0.030 -0.017 -0.051
 0.070  0.085 -0.111 -0.101  0.041  0.062  0.060  0.080  0.062 -0.022
 0.004  0.045  0.008  0.103  0.014 -0.007 -0.030 -0.032  0.019 -0.043
-0.060  0.017 -0.012 -0.035 -0.075  0.007  0.010 -0.025  0.079 -0.025
 0.038  0.035  0.013  0.018  0.002  0.014 -0.034 -0.049 -0.068 -0.004
 0.084  0.020 -0.105  0.036 -0.005 -0.046 -0.012 -0.023  0.016  0.022
 0.031  0.060  0.052  0.034  0.010  0.025  0.018  0.047  0.064  0.025
 0.040 -0.004 -0.052 -0.063  0.108  0.000 -0.008 -0.047 -0.032  0.012
 0.023 -0.014 -0.014 -0.079 -0.082  0.036  0.056  0.049  0.033  0.014
 0.028  0.007  0.010  0.004 -0.077  0.000 -0.039 -0.021  0.003  0.033
 0.056  0.003  0.017  0.002 -0.006  0.023 -0.031 -0.030 -0.045 -0.059
-0.007  0.002  0.055  0.056 -0.020 -0.004 -0.008 -0.040 -0.039 -0.019
-0.031 -0.017  0.073  0.023 -0.014 -0.003  0.018  0.037  0.031  0.022
-0.010  0.004  0.008  0.017 -0.002  0.011  0.059 -0.015  0.012 -0.002
-0.007  0.025  0.027 -0.011 -0.010 -0.050 -0.024 -0.053 -0.007  0.018
-0.062 -0.021  0.008  0.030  0.025 -0.022 -0.054  0.011 -0.002  0.006
 0.042  0.002 -0.050  0.076  0.008  0.012  0.028  0.005  0.058 -0.066
 0.032 -0.035 -0.029  0.083 -0.027 -0.024  0.032 -0.047 -0.012 -0.017
-0.053 -0.070 -0.082  0.159 -0.009 -0.042 -0.031  0.047  0.091  0.069
 0.059 -0.004  0.009  0.021 -0.025  0.001 -0.027  0.024 -0.029  0.059
 0.091  0.059  0.077  0.008  0.045  0.071  0.044
```

h. Survey Line 12, Building 312

```
LINE 12    E TO W LOOP BETWEEN RACKS 39 & 40 IN BLDG 312
  1    1  371      1.00  185    0    0
-0.019 -0.072  0.006 -0.029 -0.032 -0.017 -0.007  0.045  0.017 -0.011
-0.006 -0.034  0.066  0.078  0.055 -0.001 -0.083  0.074 -0.034  0.005
-0.034 -0.101 -0.054 -0.093 -0.041  0.091  0.056 -0.037  0.021  0.077
 0.070  0.029 -0.012 -0.099 -0.077 -0.002 -0.058  0.009  0.123  0.118
 0.101  0.067  0.089 -0.018 -0.023  0.000 -0.059 -0.048  0.037  0.036
 0.015  0.038  0.030 -0.079  0.041  0.062  0.051 -0.010 -0.026 -0.085
-0.054 -0.097 -0.010  0.077  0.063 -0.013 -0.014  0.059 -0.021 -0.045
-0.038 -0.106 -0.027  0.021  0.007  0.044  0.012  0.046  0.010 -0.010
 0.007 -0.007 -0.036 -0.077  0.018  0.019  0.069  0.024  0.065  0.023
 0.024  0.008 -0.022 -0.062 -0.070 -0.013 -0.098  0.000  0.029  0.025
 0.072  0.073  0.010 -0.024  0.069  0.028 -0.019 -0.031 -0.038 -0.016
```

Table C1 (Continued)

-0.024	0.102	0.070	0.085	0.056	0.080	0.026	-0.023	-0.051	-0.076
-0.022	-0.023	-0.043	-0.047	0.004	0.027	0.106	-0.018	-0.026	0.012
0.051	-0.086	0.025	0.010	-0.055	-0.028	-0.062	-0.023	0.074	0.006
0.063	0.077	-0.004	-0.002	-0.035	-0.077	-0.050	-0.026	-0.015	-0.043
0.008	-0.020	-0.022	-0.086	0.005	-0.013	-0.001	-0.042	-0.014	-0.018
-0.029	-0.072	0.057	0.100	0.091	0.053	0.066	0.051	-0.033	0.067
0.020	-0.048	-0.056	0.003	0.180	0.115	0.093	0.131	0.053	0.000
-0.018	0.001	-0.065	0.039	0.017	0.037	-0.010	0.026	0.004	-0.005
-0.032	-0.088	-0.106	-0.135	-0.140	-0.059	-0.016	0.033	0.048	-0.004
-0.003	-0.030	-0.008	-0.037	-0.038	-0.040	-0.027	-0.115	0.026	0.042
0.006	0.021	0.005	0.007	0.002	0.017	-0.060	0.082	0.023	-0.013
0.007	0.040	0.021	0.067	0.023	0.044	-0.022	-0.055	0.044	-0.026
-0.009	-0.074	0.005	0.007	0.082	0.019	0.118	-0.032	0.039	0.007
0.020	0.010	-0.010	-0.007	-0.014	0.017	-0.020	-0.046	0.022	0.023
0.085	0.059	-0.016	0.004	0.021	-0.046	-0.077	-0.075	-0.071	-0.103
0.074	0.008	0.024	0.039	-0.004	-0.030	-0.021	0.007	-0.004	-0.050
-0.081	-0.047	-0.014	0.015	0.040	0.084	0.060	-0.013	0.062	0.004
0.031	-0.002	-0.091	0.015	0.056	0.042	0.041	-0.002	-0.057	-0.021
-0.003	0.042	-0.003	0.015	0.028	-0.042	-0.030	0.000	-0.024	0.072
0.030	0.018	0.018	0.013	0.000	-0.004	-0.029	-0.076	0.023	0.043
0.086	0.093	0.013	0.033	-0.021	-0.076	-0.015	0.026	-0.022	-0.004
-0.069	-0.023	-0.018	-0.005	-0.011	0.050	0.033	0.000	-0.059	-0.074
-0.114	-0.096	-0.131	0.033	0.028	0.007	0.093	0.099	0.032	-0.023
-0.044	-0.051	-0.116	-0.023	-0.029	0.081	0.048	0.030	0.108	0.096
-0.003	-0.021	0.043	0.089	0.043	0.014	-0.041	-0.044	-0.057	0.020
0.065	0.025	0.031	-0.101	0.026	0.088	-0.010	0.004	0.010	0.022
0.013									

i. Survey Line 13, Building 312

LINE 13: E TO W LOOP BETWEEN RACKS 37 & 38, BLDG 312									
1	1	372	1.00	186	0	0			
0.022	0.011	0.019	-0.025	-0.065	-0.031	0.019	-0.004	-0.013	-0.002
-0.039	0.009	0.025	-0.045	0.045	-0.014	-0.046	-0.012	0.006	0.001
-0.007	-0.042	-0.075	-0.063	0.000	0.071	-0.008	0.061	0.020	0.036
0.000	0.018	0.035	-0.008	-0.025	-0.033	0.000	0.123	0.097	0.073
0.011	0.022	0.038	0.005	-0.019	-0.021	-0.022	-0.031	0.016	0.035
-0.023	0.057	0.067	0.073	-0.028	-0.034	-0.034	-0.007	-0.070	-0.091
-0.109	-0.042	0.028	0.093	0.118	0.042	0.009	-0.018	-0.031	-0.055
-0.041	-0.010	-0.032	-0.024	0.050	0.028	-0.004	0.017	0.023	0.031
-0.067	-0.020	0.047	-0.086	-0.066	-0.039	-0.041	0.049	-0.014	-0.004
-0.003	-0.025	-0.014	-0.028	-0.039	0.020	-0.003	0.035	-0.002	-0.024
0.012	0.007	0.034	-0.007	0.044	0.002	0.004	0.002	-0.053	-0.083
-0.023	0.109	0.145	0.062	0.063	0.067	0.080	0.054	0.039	0.021
0.012	-0.039	-0.022	-0.017	0.036	0.086	0.095	0.000	-0.021	0.040
-0.027	-0.059	-0.035	-0.156	-0.109	-0.029	-0.042	0.005	0.048	0.016
-0.002	0.027	-0.019	-0.042	-0.048	-0.036	0.006	0.006	-0.053	0.038
0.050	0.054	0.025	0.000	0.003	0.009	-0.028	0.016	-0.021	-0.028

Table C1 (Continued)

-0.015	-0.028	0.023	0.082	0.021	0.038	0.013	0.023	-0.017	-0.055
-0.024	-0.070	0.035	0.047	-0.027	0.128	0.010	0.016	0.055	0.030
0.017	-0.051	-0.035	-0.018	0.016	0.139	0.040	-0.015	-0.042	0.053
0.070	-0.048	0.046	-0.017	-0.081	-0.134	-0.069	-0.072	-0.029	0.042
0.054	0.030	-0.018	-0.039	-0.009	0.003	-0.015	-0.007	-0.012	-0.118
-0.002	0.005	0.062	0.035	0.006	0.037	0.019	-0.021	0.016	0.002
-0.019	-0.048	-0.039	0.011	-0.054	-0.015	0.077	0.072	0.033	0.023
0.036	-0.034	-0.065	-0.009	-0.033	0.103	0.079	0.103	0.088	0.079
-0.019	0.034	-0.034	-0.023	-0.004	0.010	-0.035	-0.031	0.060	0.055
-0.015	-0.008	-0.035	-0.083	-0.030	-0.037	-0.036	-0.066	-0.051	-0.063
-0.180	0.055	0.023	0.080	0.007	0.029	-0.020	-0.050	0.006	-0.026
-0.059	-0.042	0.006	0.030	0.032	0.041	0.017	0.019	0.012	0.014
0.056	-0.008	-0.023	0.004	0.106	-0.003	-0.046	0.039	0.054	0.025
-0.003	0.018	0.012	-0.045	0.039	-0.044	-0.026	-0.010	0.031	0.050
0.069	0.116	-0.022	0.031	0.020	-0.085	0.092	-0.138	-0.151	-0.015
0.100	0.065	0.073	0.041	0.011	0.034	0.050	-0.001	-0.038	0.003
-0.020	-0.009	-0.021	0.043	0.016	0.026	0.038	-0.002	0.010	-0.068
-0.018	-0.081	-0.082	-0.122	0.043	-0.025	-0.005	0.006	0.022	-0.031
-0.038	-0.037	-0.067	0.040	0.011	0.010	0.016	-0.064	0.058	0.075
0.029	0.025	-0.024	0.000	0.053	0.040	-0.001	-0.057	0.045	-0.033
0.007	0.058	0.059	0.006	-0.065	-0.059	0.020	0.014	0.038	0.090
-0.048	-0.010								

j. Survey Line 14, Building 312

LINE 14	E TO W LOOP BETWEEN RACKS 28 & 29 IN BLDG 312								
1	1	372	1.00	186	0	0			
-0.081	-0.029	-0.029	-0.004	-0.021	-0.108	-0.062	0.007	-0.048	0.000
-0.033	0.017	0.002	0.042	0.003	0.000	-0.025	0.010	-0.008	-0.003
-0.038	-0.060	0.087	-0.002	-0.002	-0.001	0.033	0.046	0.002	0.028
-0.037	0.000	-0.057	-0.013	-0.027	0.006	0.057	0.065	0.023	0.038
0.021	-0.043	0.020	0.007	0.022	0.022	0.012	0.014	0.021	-0.048
0.035	0.028	0.001	-0.018	0.008	0.011	-0.036	-0.003	-0.024	-0.023
-0.008	-0.063	0.011	0.038	0.030	0.025	-0.044	-0.021	0.000	0.026
-0.005	-0.035	0.001	-0.028	0.012	0.010	0.052	0.051	0.018	0.019
0.015	-0.012	-0.007	-0.003	-0.031	0.029	-0.070	-0.036	-0.045	-0.026
0.004	0.030	0.025	-0.003	-0.002	-0.044	0.004	-0.048	0.031	0.001
-0.101	0.055	0.032	-0.002	0.004	0.060	0.037	-0.019	-0.100	-0.021
-0.039	0.018	0.110	0.042	0.052	0.055	0.040	-0.014	-0.019	0.026
0.032	0.016	-0.030	0.022	0.014	0.022	0.002	-0.010	0.003	-0.004
-0.021	0.021	-0.007	0.019	-0.039	-0.064	-0.187	-0.026	0.103	0.047
-0.034	-0.023	-0.024	-0.008	-0.019	-0.032	-0.035	-0.095	0.051	0.018
0.024	0.011	-0.030	-0.028	0.043	0.011	-0.011	0.011	-0.006	-0.035
-0.028	-0.111	0.143	0.144	0.053	0.047	-0.004	0.036	-0.018	0.022
-0.066	-0.072	0.093	0.019	0.057	0.066	0.047	0.038	0.035	-0.023
0.035	0.026	0.007	-0.022	-0.016	0.009	0.018	-0.010	-0.020	0.007
-0.021	-0.013	-0.007	-0.013	-0.006	0.004	-0.035	-0.073	-0.033	-0.024
-0.029	-0.009	0.003	0.007	-0.002	-0.024	-0.015	-0.051	-0.147	-0.079

Table C1 (Continued)

0.040	0.081	0.054	0.002	0.010	-0.036	-0.084	0.026	0.086	-0.003
-0.002	-0.038	-0.082	0.077	0.078	0.041	0.018	0.087	-0.003	0.024
0.010	-0.006	0.054	-0.038	0.046	0.122	0.045	0.072	0.004	-0.012
0.016	0.012	0.033	0.020	0.000	0.005	-0.011	-0.026	0.010	0.067
-0.014	-0.031	-0.018	0.003	0.051	-0.022	-0.022	-0.031	-0.047	-0.210
-0.060	0.108	0.116	0.048	0.040	0.000	-0.020	-0.030	-0.070	0.076
-0.040	0.005	0.008	0.003	0.034	0.021	-0.022	0.002	-0.002	0.011
0.020	-0.004	-0.020	-0.012	0.033	0.108	0.055	0.024	-0.012	-0.027
0.023	-0.020	-0.008	0.025	-0.011	-0.069	0.013	-0.033	0.027	0.006
0.008	0.017	0.029	0.005	0.002	-0.030	-0.043	0.000	0.003	0.002
-0.058	0.036	0.085	0.000	-0.015	0.022	0.018	0.020	0.009	0.040
0.002	-0.023	0.015	0.012	-0.030	0.001	-0.011	-0.003	-0.002	-0.006
-0.032	-0.028	-0.002	-0.011	-0.074	-0.040	-0.010	0.005	0.071	-0.018
0.069	0.004	0.011	-0.042	-0.007	-0.001	0.006	-0.025	-0.071	0.000
0.061	-0.037	0.020	0.016	-0.021	-0.004	0.027	-0.008	-0.010	0.002
0.015	0.023	0.074	0.107	0.063	0.029	0.064	0.058	-0.021	-0.036
0.052	-0.059								

k. Survey Line 15, Building 312

LINE 15: E TO W LOOP BETWEEN RACKS 54 & 55, BLDG 312									
1	1	353	1.00	176	0	0			
-0.025	-0.026	0.023	0.018	0.015	0.005	-0.002	-0.020	0.014	-0.047
-0.070	-0.091	0.034	0.067	0.056	0.048	0.029	-0.071	-0.080	-0.075
-0.089	0.022	0.007	0.038	0.031	0.057	0.067	-0.002	-0.038	-0.062
-0.115	-0.073	-0.035	-0.035	-0.056	-0.092	0.044	0.072	0.121	0.105
0.103	0.061	0.004	-0.035	-0.026	0.030	0.054	-0.057	-0.020	0.002
0.047	-0.005	0.044	0.050	-0.036	-0.076	0.089	0.055	-0.014	-0.039
-0.061	-0.045	0.006	0.098	0.063	0.087	-0.016	0.009	-0.029	-0.029
-0.045	-0.025	-0.063	-0.002	-0.003	0.035	0.000	0.103	0.014	0.049
0.082	0.086	0.017	-0.017	-0.099	-0.085	-0.047	-0.005	-0.002	0.022
-0.005	0.020	-0.022	-0.040	-0.006	0.025	0.002	-0.005	-0.003	0.021
0.064	0.091	-0.074	-0.015	0.036	0.038	0.048	0.074	-0.032	-0.071
-0.047	0.032	0.087	0.025	0.019	0.042	-0.043	-0.071	0.001	0.034
0.008	0.005	0.016	-0.025	0.013	0.031	0.007	0.030	-0.051	-0.066
0.007	0.010	0.009	-0.113	-0.102	-0.077	-0.104	0.129	0.060	-0.020
0.012	-0.009	-0.017	0.012	-0.029	0.009	-0.034	0.018	-0.024	0.024
-0.023	0.023	-0.006	0.027	0.078	0.124	0.050	-0.020	-0.095	-0.024
-0.011	-0.028	0.016	0.061	0.047	0.053	0.034	0.003	-0.061	-0.011
-0.064	-0.026	0.098	-0.086	0.112	0.003	-0.077	-0.038	-0.031	0.027
0.003	0.026	-0.044	0.086	0.053	0.022	-0.080	-0.056	0.103	-0.038
-0.103	-0.012	0.052	0.076	0.050	0.050	0.014	-0.046	-0.053	-0.074
-0.068	-0.001	-0.032	-0.039	0.004	0.042	0.009	0.047	0.053	-0.054
-0.074	0.073	0.100	-0.067	0.011	-0.018	-0.058	0.101	0.062	0.064
0.022	0.053	-0.037	0.036	0.063	0.007	-0.034	-0.003	-0.031	0.028
0.020	0.005	-0.036	0.002	-0.042	0.018	0.044	0.022	-0.015	-0.024
-0.055	-0.107	0.037	0.067	0.018	-0.012	0.002	-0.061	-0.016	0.013
0.025	-0.036	-0.009	-0.009	0.024	0.023	-0.008	-0.049	-0.097	0.005

Table C1 (Continued)

```
 0.120  0.111 -0.015  0.033 -0.035 -0.043  0.013  0.036  0.034  0.064
 0.048  0.004 -0.023 -0.222 -0.023  0.071 -0.044 -0.066 -0.051 -0.030
 0.018  0.068  0.075  0.053 -0.001  0.039  0.006  0.000 -0.070 -0.016
-0.102 -0.105  0.116  0.048  0.044  0.034  0.023  0.013  0.003 -0.027
-0.028  0.008 -0.106 -0.015  0.019 -0.086  0.020 -0.021 -0.036 -0.014
 0.060  0.042  0.016 -0.134 -0.144 -0.004 -0.061  0.010  0.072  0.039
 0.032  0.126  0.003  0.125  0.092 -0.002  0.023 -0.041 -0.046 -0.005
 0.035  0.011  0.032  0.079  0.082  0.055  0.042 -0.021 -0.042 -0.030
-0.096  0.028  0.110  0.063 -0.018 -0.018  0.017  0.053  0.006 -0.008
-0.013 -0.060 -0.011
```

1. Survey Line 16, Building 312

```
 LINE 16: E TO W LOOP BETWEEN RACKS 48 & 49, BLDG 312
   1    1  354       1.00  177    0    0
 0.009  0.011 -0.003  0.006 -0.002 -0.007 -0.014  0.004 -0.035 -0.036
-0.082  0.008  0.075  0.044  0.025  0.024  0.021 -0.005 -0.003 -0.003
-0.024 -0.019 -0.017 -0.032 -0.015 -0.029  0.034  0.051 -0.044  0.030
 0.030  0.075 -0.020 -0.099 -0.027 -0.060  0.016  0.055 -0.022 -0.059
 0.048  0.004 -0.015 -0.007  0.039  0.018  0.043 -0.044 -0.027  0.014
 0.070 -0.010 -0.014 -0.003  0.004 -0.013 -0.061 -0.022  0.024 -0.007
-0.027 -0.062  0.041  0.045  0.040 -0.027  0.010 -0.036 -0.041 -0.053
 0.005 -0.024 -0.003 -0.025  0.040  0.055  0.025 -0.029  0.028  0.029
 0.009  0.054  0.002 -0.006  0 005  0.006 -0.116  0.056  0.050 -0.027
-0.029 -0.037 -0.002  0.017 -0.018 -0.014  0.008  0.011  0.020  0.004
 0.004  0.010 -0.002  0.021  0.017 -0.030 -0.042  0.037  0.028 -0.024
-0.074  0.017  0.119  0.008  0.096  0.029  0.026 -0.057  0.003 -0.013
-0.005  0.047 -0.007 -0.018  0.042  0.034  0.024 -0.004  0.046  0.034
 0.035  0.027 -0.073 -0.122 -0.063 -0.080 -0.103  0.077  0.029  0.042
 0.034 -0.032  0.064 -0.057 -0.042 -0.003 -0.032 -0.015 -0.008  0.032
 0.045  0.004  0.082  0.033  0.026  0.000 -0.028  0.016  0.057  0.008
-0.067 -0.082  0.173  0.068  0.033  0.025  0.058 -0.005  0.021 -0.006
-0.048 -0.063 -0.001 -0.001 -0.006 -0.048 -0.003 -0.038  0.000 -0.058
-0.006  0.013  0.015  0.044  0.068 -0.016  0.051 -0.041  0.081 -0.099
-0.130 -0.139  0.119  0.099 -0.016  0.036 -0.046  0.038 -0.038 -0.043
-0.022 -0.020 -0.066 -0.070 -0.032 -0.041  0.016  0.059  0.079  0.012
-0.012  0.061 -0.018 -0.030 -0.066 -0.011 -0.105  0.105  0.047  0.143
 0.006  0.061  0.057 -0.016 -0.020 -0.052 -0.034 -0.002  0.007 -0.020
 0.019  0.034  0.032 -0.026 -0.010  0.026  0.005 -0.038 -0.044 -0.046
-0.041 -0.167 -0.024  0.099  0.021  0.025 -0.033  0.040 -0.016 -0.003
 0.045 -0.048  0.009 -0.020  0.016  0.002  0.068  0.035 -0.009  0.049
 0.047  0.008 -0.002 -0.038  0.032 -0.014 -0.018  0.083 -0.023  0.055
-0.004 -0.111  0.052 -0.007 -0.030 -0.060  0.036 -0.004 -0.054  0.041
-0.017 -0.006  0.047  0.016  0.049  0.058  0.017  0.017 -0.018 -0.015
-0.081 -0.107  0.144  0.011  0.021  0.030  0.054  0.034 -0.080 -0.017
 0.054  0.013 -0.013 -0.048  0.017  0.019 -0.029  0.087  0.007  0.038
-0.007 -0.027 -0.029 -0.009 -0.022 -0.004 -0.035  0.074 -0.011  0.013
 0.095  0.074 -0.059 -0.075  0.012  0.052 -0.079 -0.010  0.025  0.007
```

Table C1 (Continued)

```
-0.036  0.049  0.039  0.036 -0.009  0.075  0.010 -0.028 -0.034 -0.002
-0.043 -0.038 -0.021  0.080  0.016  0.032  0.028  0.020  0.018  0.013
 0.034 -0.024  0.033  0.021
```

m. Survey Line 17, Building 312

```
 LINE 17  E TO W LOOP BETWEEN RACKS 46 & 47 IN BLDG 312
   1    1  372       1.00  186    0    0
 0.051 -0.076  0.025 -0.003 -0.016 -0.025 -0.058 -0.027 -0.018 -0.029
-0.083 -0.017  0.091  0.011  0.042 -0.022 -0.019  0.004  0.067 -0.019
-0.051 -0.072 -0.021 -0.022 -0.035  0.067  0.140  0.032  0.073 -0.006
-0.036  0.023 -0.006 -0.098 -0.147 -0.105  0.003  0.063  0.118  0.073
 0.069  0.002 -0.010 -0.018 -0.028  0.008 -0.028  0.037 -0.040  0.034
 0.038  0.055  0.031  0.070  0.049  0.019 -0.059 -0.065 -0.071 -0.063
-0.026 -0.093 -0.002  0.023  0.089  0.079  0.011 -0.034 -0.250 -0.009
-0.034 -0.066 -0.048 -0.039  0.011  0.071  0.066  0.066 -0.004  0.041
-0.021  0.040 -0.014  0.012 -0.010 -0.036 -0.245 -0.139 -0.017  0.023
 0.064  0.052 -0.005  0.028 -0.009  0.014  0.010 -0.063  0.013 -0.012
 0.046  0.045 -0.031 -0.005 -0.055  0.087  0.063 -0.013 -0.031 -0.022
 0.000  0.036  0.076  0.027  0.118  0.079  0.068  0.030  0.011 -0.019
-0.103 -0.022  0.010  0.083 -0.004  0.004  0.070  0.005 -0.006  0.026
 0.004 -0.003  0.008  0.062 -0.038 -0.022 -0.093 -0.022  0.101  0.065
 0.050 -0.026 -0.045 -0.096  0.002 -0.076 -0.071  0.000  0.012 -0.003
 0.012  0.087  0.030  0.033 -0.029 -0.096 -0.051 -0.035 -0.006 -0.031
-0.014  0.000  0.009  0.034  0.078  0.030  0.018  0.034 -0.025 -0.013
-0.023 -0.010  0.003  0.010  0.061  0.062  0.013  0.080  0.047  0.033
-0.029 -0.021 -0.021 -0.038  0.003  0.055  0.018  0.018 -0.057 -0.031
-0.030  0.031 -0.079  0.010 -0.049 -0.010 -0.025 -0.008  0.028 -0.009
 0.009  0.003 -0.022  0.005 -0.003  0.029  0.009 -0.041 -0.040  0.043
 0.001 -0.037  0.063 -0.073 -0.007  0.216  0.072 -0.006 -0.008 -0.043
-0.076  0.001 -0.029  0.013  0.005  0.057  0.064  0.007  0.105  0.023
 0.012 -0.018 -0.063 -0.036 -0.056  0.057  0.058  0.075 -0.024  0.001
 0.011 -0.019 -0.004 -0.003 -0.009 -0.034  0.002 -0.034 -0.048 -0.012
-0.001  0.126 -0.028  0.001 -0.048 -0.036 -0.095 -0.132 -0.039 -0.063
-0.002  0.010  0.042  0.056  0.024 -0.108 -0.058  0.066  0.013  0.031
-0.010 -0.045 -0.021 -0.020  0.004  0.036 -0.029  0.037 -0.006 -0.021
-0.015 -0.005 -0.069  0.030  0.096  0.195  0.103  0.040  0.012  0.021
 0.005 -0.015 -0.030 -0.028 -0.100  0.076 -0.169  0.055  0.043  0.023
 0.047  0.049  0.052  0.000  0.026  0.006 -0.042 -0.062 -0.041  0.003
 0.016  0.017  0.081  0.113  0.022  0.036  0.057 -0.043 -0.055 -0.025
-0.046 -0.012 -0.064  0.038  0.002  0.016  0.006  0.011  0.026 -0.001
-0.078 -0.029 -0.049 -0.137 -0.018 -0.086  0.036  0.080  0.089  0.070
 0.010  0.007 -0.004 -0.025 -0.109  0.013 -0.067  0.034  0.016  0.035
 0.052  0.029 -0.016 -0.018 -0.050  0.020  0.116 -0.144 -0.022 -0.044
 0.062  0.045  0.022  0.093  0.071  0.105  0.003  0.020  0.003 -0.051
 0.026  0.028
```

Table C2. Automated Technology Center

a. Survey Line ATC1

```
RUN ATC1.ELV   12/12/89
   1    0  497       1.00  497    0    0
-0.067 -0.063 -0.170 -0.174 -0.160 -0.106 -0.096 -0.041  0.100 -0.007
-0.004  0.008 -0.153  0.014  0.121  0.099  0.120  0.160  0.152  0.176
 0.144  0.105  0.094  0.067  0.034 -0.018 -0.074 -0.083 -0.002  0.007
-0.016  0.005 -0.004 -0.019 -0.059 -0.119 -0.191 -0.252 -0.307 -0.273
-0.096  0.121  0.232  0.285  0.401  0.397  0.399  0.289  0.233  0.142
 0.010 -0.177 -0.157 -0.037 -0.145 -0.026  0.098 -0.082 -0.053  0.011
-0.126 -0.337 -0.456 -0.446 -0.533 -0.588 -0.629 -0.535 -0.439 -0.371
-0.230 -0.173  0.182  0.276  0.261  0.226  0.177  0.180  0.135  0.135
 0.082  0.072  0.017  0.024  0.053 -0.168  0.019  0.006  0.024  0.029
 0.079  0.110  0.088  0.123  0.158  0.211  0.155  0.152 -0.016  0.094
 0.112  0.102  0.204  0.237  0.133  0.086  0.076  0.087 -0.001  0.072
 0.081  0.142  0.173  0.130  0.134  0.199  0.162  0.211  0.222  0.230
 0.192  0.241  0.304  0.255  0.242  0.161  0.011 -0.103 -0.018 -0.008
-0.057 -0.037 -0.014  0.003 -0.064  0.082  0.035 -0.066 -0.034 -0.018
-0.018 -0.034 -0.061 -0.079 -0.035  0.006  0.099  0.218  0.205  0.152
 0.212  0.215  0.352  0.383  0.526  0.582  0.533  0.611  0.599  0.655
 0.629  0.367  0.242  0.109  0.099  0.169  0.176  0.277  0.261  0.242
 0.302  0.390  0.428  0.562  0.504  0.530  0.515  0.558  0.664  0.663
 0.709  0.566  0.650  0.707  0.578  0.712  0.613  0.575  0.663  0.721
 0.631  0.545  0.496  0.380  0.298  0.289  0.289  0.360  0.412  0.410
 0.473  0.545  0.492  0.493  0.335  0.287  0.293  0.337  0.290  0.316
 0.247  0.328  0.319  0.321  0.315  0.366  0.273  0.131  0.090 -0.036
-0.056 -0.045 -0.052 -0.013 -0.008  0.214  0.159  0.181  0.196  0.054
 0.155  0.171  0.191  0.230  0.270  0.228  0.237  0.325  0.430  0.563
 0.507  0.565  0.658  0.785  1.034  1.049  1.016  1.124  1.098  0.924
 0.901  0.844  0.717  0.659  0.629  0.510  0.451  0.377  0.355  0.383
 0.334  0.337  0.332  0.295  0.229  0.435  0.379  0.426  0.426  0.259
 0.259  0.229  0.248  0.236  0.236  0.397  0.484  0.677  0.852  0.822
 0.865  0.937  0.913  0.893  0.947  0.922  0.952  0.950  0.986  0.974
 1.169  1.189  1.249  1.188  1.137  1.193  1.139  1.096  1.097  1.163
 1.216  1.361  1.441  1.536  1.667  1.684  1.613  1.642  1.701  1.674
 1.758  1.792  1.660  1.816  1.806  1.864  1.782  1.729  1.747  1.754
 1.782  1.704  1.674  1.615  1.626  1.616  1.566  1.609  1.563  1.616
 1.511  1.604  1.795  1.946  2.154  2.154  2.179  2.074  2.138  2.167
 2.032  1.901  1.914  1.831  1.768  1.849  1.947  1.922  1.769  1.736
 1.730  1.707  1.760  1.872  1.851  1.851  1.896  1.886  2.027  1.972
 1.914  1.981  1.924  1.930  1.920  1.983  1.861  1.889  2.003  2.121
 2.190  2.259  2.265  2.203  2.191  2.218  2.213  2.208  2.176  2.189
 2.159  2.221  2.244  2.199  2.163  2.176  2.148  2.210  2.228  2.243
 2.326  2.342  2.370  2.280  2.329  2.257  2.257  2.419  2.421  2.445
 2.435  2.423  2.412  2.410  2.361  2.375  2.389  2.363  2.343  2.221
 2.456  2.459  2.485  2.514  2.561  2.613  2.634  2.700  2.724  2.771
 2.819  2.835  2.710  2.402  2.361  2.251  2.202  2.123  2.045  2.033
 2.089  2.228  2.318  2.380  2.579  2.722  2.669  2.636  2.836  2.728
 2.612  2.748  2.617  2.629  2.834  2.927  3.064  3.099  3.241  3.251
```

Table C2. (Continued)

3.286	3.177	3.153	3.013	2.822	2.586	2.572	2.612	2.659	2.794
2.822	2.868	2.896	2.902	2.914	2.930	2.941	2.881	2.880	2.951
3.003	3.033	3.085	3.097	3.133	3.189	3.171	3.182	3.141	3.118
3.111	3.041	2.886	3.023	2.993	2.904	2.941	2.895	2.884	2.925
2.916	2.920	2.851	2.999	2.927	2.929	3.020			

b. Survey Line ATC2

RUN ATC2.ELV 12/12/89

1	0	99	1.00	99	0	0			
0.049	0.042	0.136	0.073	0.051	0.154	-0.001	0.144	0.091	0.042
0.081	-0.009	0.031	0.091	-0.032	0.138	0.129	0.041	0.008	0.110
0.050	0.009	0.110	0.175	0.094	0.121	0.162	0.159	0.120	0.096
0.244	0.336	0.305	0.267	0.173	0.217	0.224	0.337	0.333	0.210
0.332	0.410	0.447	0.514	0.481	0.487	0.458	0.505	0.468	0.473
0.520	0.550	0.556	0.517	0.530	0.469	0.496	0.466	0.242	0.371
0.407	0.305	0.298	0.318	0.412	0.379	0.459	0.301	0.244	0.240
0.281	0.322	0.278	0.293	0.363	0.253	0.191	0.238	0.267	0.273
0.249	0.285	0.265	0.245	0.364	0.262	0.282	0.381	0.325	0.393
0.456	0.404	0.471	0.424	0.493	0.531	0.436	0.495	0.487	

c. Survey Line ATC3

RUN ATC.ELV 12/12/89

1	0	102	1.00	102	0	0			
-0.095	-0.219	-0.254	-0.347	-0.485	-0.491	-0.570	-0.559	-0.476	-0.387
-0.387	-0.364	-0.305	-0.242	-0.220	-0.293	-0.258	-0.208	-0.103	-0.105
-0.067	-0.096	-0.115	-0.095	-0.152	-0.209	-0.230	-0.221	-0.212	-0.180
-0.153	-0.192	-0.147	-0.180	-0.165	-0.149	-0.143	-0.092	0.013	0.012
-0.007	-0.074	-0.184	-0.141	-0.167	-0.184	-0.146	-0.151	-0.151	-0.122
-0.070	-0.140	-0.095	-0.056	-0.074	-0.045	-0.082	-0.128	-0.072	-0.024
0.000	0.091	0.017	-0.038	-0.050	-0.064	-0.098	-0.040	-0.071	-0.093
-0.173	-0.148	-0.174	-0.183	-0.146	-0.054	0.039	0.072	0.073	0.105
0.042	0.025	-0.065	-0.074	-0.107	-0.033	-0.067	-0.120	-0.158	-0.199
-0.209	-0.316	-0.403	-0.428	-0.303	-0.273	-0.153	-0.002	0.042	0.133
0.203	0.202								

d. Survey Line ATC4

RUN ATC4.ELV 12/12/89

1	0	102	1.00	102	0	0			
-0.134	-0.004	-0.030	-0.186	-0.273	-0.199	-0.253	-0.180	-0.175	-0.193
-0.266	-0.308	-0.455	-0.400	-0.342	-0.378	-0.363	-0.355	-0.217	-0.021
-0.028	-0.010	0.003	-0.049	-0.059	-0.043	-0.153	0.026	-0.087	0.024
0.029	0.004	-0.094	-0.123	-0.101	0.054	-0.048	-0.014	0.004	-0.088
0.014	0.032	0.078	0.010	-0.091	-0.066	0.007	-0.015	-0.103	-0.010

Table C2. (Continued)

0.004	0.019	0.080	0.060	0.005	0.001	0.107	0.084	0.026	0.061
-0.065	-0.053	0.014	0.058	0.100	0.098	0.111	0.074	0.080	0.037
0.169	0.091	0.185	0.082	0.153	0.128	0.130	0.207	0.203	0.199
0.096	-0.019	-0.135	-0.247	-0.193	-0.146	-0.150	-0.241	-0.140	-0.002
0.030	0.157	0.098	0.070	0.097	0.005	0.096	0.247	0.413	0.284
0.420	0.414								

e. Survey Line ATC5

RUN ATC5.ELV 12/12/89

1	0	102	1.00	102	0	0			
-0.011	-0.007	0.029	0.036	0.131	0.350	0.256	0.364	0.390	0.371
0.399	0.383	0.377	0.450	0.459	0.346	0.293	0.251	0.194	0.218
0.255	0.339	0.425	0.606	0.690	0.752	0.573	0.477	0.413	0.377
0.394	0.410	0.440	0.551	0.567	0.629	0.767	0.839	0.750	0.815
0.843	0.835	0.858	0.766	0.692	0.680	0.625	0.616	0.668	0.761
0.706	0.647	0.608	0.598	0.624	0.617	0.607	0.676	0.690	0.776
0.734	0.702	0.796	0.763	0.687	0.676	0.642	0.526	0.492	0.459
0.434	0.487	0.552	0.623	0.766	0.756	0.681	0.501	0.374	0.264
0.242	0.187	0.213	0.262	0.342	0.476	0.492	0.444	0.432	0.467
0.513	0.497	0.525	0.425	0.483	0.324	0.199	0.268	0.276	0.171
0.265	0.212								

f. Survey Line ATC6

RUN ATC6.ELV 12/12/89

1	0	206	1.00	206	0	0			
0.000	-0.081	-0.069	-0.031	0.063	0.155	0.044	0.078	0.107	0.129
0.172	0.133	0.142	0.077	0.055	0.171	0.294	0.376	0.372	0.444
0.532	0.404	0.366	0.398	0.515	0.470	0.437	0.330	0.245	0.312
0.312	0.328	0.214	0.182	0.149	0.298	0.354	0.450	0.424	0.476
0.502	0.493	0.515	0.556	0.595	0.593	0.611	0.511	0.474	0.448
0.392	0.408	0.479	0.556	0.487	0.430	0.437	0.506	0.447	0.475
0.515	0.671	0.614	0.638	0.565	0.597	0.743	0.832	0.835	0.839
0.662	0.573	0.546	0.621	0.752	0.752	0.710	0.689	0.670	0.682
0.701	0.714	0.728	0.790	0.913	0.874	0.916	0.848	0.846	0.923
1.117	1.031	0.980	0.862	0.986	0.950	0.776	0.728	0.856	0.864
0.847	0.836	0.911	0.965	0.944	0.952	0.971	0.963	0.905	1.052
1.228	1.084	1.145	1.262	1.321	1.216	1.154	1.154	1.234	1.213
1.252	1.215	1.099	1.122	1.114	1.116	1.132	1.159	1.187	1.203
1.310	1.192	1.128	1.166	1.236	1.428	1.479	1.434	1.441	1.193
1.185	1.296	1.297	1.353	1.282	1.262	1.280	1.353	1.301	1.290
1.348	1.405	1.372	1.330	1.321	1.385	1.457	1.481	1.628	1.611
1.607	1.591	1.573	1.561	1.594	1.613	1.571	1.636	1.571	1.537
1.419	1.477	1.521	1.633	1.635	1.656	1.598	1.707	1.814	1.830
1.916	1.814	1.807	1.881	1.989	1.921	1.888	1.881	1.780	1.730

Table C2. (Continued)

```
 1.621  1.725  1.767  1.833  1.839  1.845  1.774  1.800  1.841  1.982
 1.932  1.804  1.822  1.748  1.831  1.905
```

g. Survey Line ATC7

```
RUN ATC7.ELV   12/12/89
   1     0  190       1.00  190     0     0
-0.029  0.001  0.001  0.061  0.168  0.138  0.267  0.134  0.177  0.253
 0.176  0.257  0.577  0.674  0.711  0.657  0.589  0.717  0.658  0.696
 0.669  0.642  0.636  0.613  0.651  0.527  0.554  0.528  0.549  0.485
 0.578  0.413  0.597  0.838  0.956  1.038  1.080  1.122  1.193  1.193
 1.159  1.123  1.166  1.265  1.221  1.229  1.177  1.179  1.212  1.234
 1.210  1.150  1.004  0.928  0.956  0.988  1.050  1.006  0.937  0.857
 0.807  0.850  0.861  0.839  0.805  0.824  0.827  0.934  0.899  0.880
 0.915  0.766  0.743  0.730  0.710  0.751  0.797  0.921  0.983  1.050
 1.022  1.030  1.006  0.864  0.809  0.809  0.804  0.954  0.925  0.946
 0.952  0.953  0.896  1.038  1.016  0.941  0.942  0.981  0.953  0.924
 0.896  0.863  0.886  0.920  1.080  1.056  1.170  1.201  1.107  1.058
 1.021  1.029  1.013  0.958  0.976  0.960  0.974  1.120  1.114  1.135
 1.160  1.049  1.046  1.068  1.110  1.080  1.079  1.099  1.193  1.219
 1.438  1.356  1.279  1.276  1.274  1.403  1.503  1.530  1.525  1.541
 1.506  1.460  1.514  1.563  1.618  1.541  1.487  1.617  1.624  1.655
 1.552  1.565  1.511  1.455  1.321  1.079  0.995  1.105  1.008  0.978
 1.066  1.039  1.008  1.104  1.136  1.228  1.254  1.259  1.281  1.271
 1.257  1.235  1.264  1.391  1.352  1.276  0.878  0.884  0.859  0.872
 0.827  0.835  0.789  0.858  0.764  0.656  0.661  0.640  0.642  0.691
```

h. Survey Line ATC8

```
RUN ATC8.ELV   12/12/89
   1     0  205       1.00  205     0     0
-0.006  0.069  0.020 -0.037 -0.045 -0.098 -0.191 -0.314 -0.382 -0.332
-0.344 -0.388 -0.411 -0.409 -0.389 -0.391 -0.260 -0.353 -0.323 -0.349
-0.260 -0.202 -0.269 -0.220 -0.216 -0.200 -0.130  0.055  0.057 -0.005
-0.010  0.044  0.080  0.142  0.178  0.147  0.159  0.079 -0.031 -0.048
-0.086 -0.069 -0.039  0.030  0.139  0.170  0.192  0.245  0.248  0.218
 0.172  0.186  0.202  0.125  0.127  0.272  0.369  0.460  0.536  0.464
 0.369  0.298  0.385  0.389  0.463  0.572  0.617  0.597  0.508  0.460
 0.408  0.431  0.488  0.544  0.558  0.645  0.668  0.714  0.819  0.847
 0.852  0.866  0.846  0.846  0.849  0.764  0.760  0.479  0.292  0.195
 0.192  0.204  0.298  0.464  0.581  0.675  0.563  0.618  0.650  0.631
 0.660  0.819  0.892  0.776  0.760  0.802  0.816  0.860  0.836  0.837
 0.719  0.555  0.506  0.456  0.487  0.599  0.799  1.041  1.038  1.116
 1.171  1.235  1.205  1.215  1.237  1.258  1.192  1.180  1.139  1.114
 1.138  1.104  1.065  1.104  1.159  1.228  1.325  1.371  1.371  1.257
 1.233  1.272  1.165  1.255  1.324  1.400  1.373  1.360  1.185  1.120
 1.137  1.202  1.218  1.270  1.343  1.379  1.435  1.390  1.365  1.354
```

Table C2. (Continued)

1.195	1.164	1.194	1.152	1.204	1.296	1.463	1.547	1.573	1.621
1.534	1.524	1.460	1.471	1.513	1.537	1.470	1.410	1.414	1.399
1.411	1.499	1.473	1.433	1.434	1.417	1.476	1.527	1.424	1.502
1.477	1.513	1.552	1.639	1.618	1.647	1.790	1.980	1.979	1.992
2.029	2.042	2.072	2.027	2.174					

i. Survey Line ATC9

RUN 9 12/12/89

1	0	215	1.00	215	0	0			
0.069	0.189	0.253	0.304	0.224	0.210	0.088	-0.117	-0.295	-0.370
-0.313	-0.264	-0.212	-0.127	-0.110	-0.204	-0.159	-0.176	-0.182	-0.180
-0.212	-0.198	-0.151	-0.097	-0.008	0.115	0.072	0.092	0.096	0.033
0.078	0.093	0.088	0.155	0.275	0.359	0.302	0.204	0.116	0.136
0.104	0.189	0.218	0.337	0.304	0.187	0.151	0.213	0.262	0.261
0.299	0.314	0.269	0.238	0.186	0.255	0.323	0.374	0.500	0.804
0.750	0.751	0.748	0.775	0.693	0.568	0.496	0.494	0.598	0.736
0.740	0.721	0.718	0.577	0.560	0.610	0.534	0.542	0.582	0.588
0.636	0.672	0.655	0.693	0.627	0.605	0.528	0.445	0.365	0.388
0.373	0.420	0.487	0.527	0.654	0.689	0.663	0.802	0.862	0.744
0.640	0.579	0.563	0.571	0.590	0.656	0.611	0.677	0.736	0.694
0.704	0.711	0.774	0.718	0.801	1.037	0.902	0.773	0.712	0.706
0.732	0.745	0.661	0.660	0.652	0.677	0.731	0.792	0.858	0.937
0.889	0.893	0.946	0.916	0.916	0.878	0.948	0.990	0.977	0.976
1.035	1.142	1.164	1.232	1.179	1.061	0.992	1.007	1.098	1.227
1.330	1.307	1.339	1.464	1.372	1.214	1.141	1.126	1.023	1.019
1.056	1.101	1.148	1.152	1.108	1.104	1.082	1.082	1.164	1.215
1.222	1.128	1.115	1.081	1.126	1.126	1.189	1.364	1.416	1.251
1.225	1.236	1.202	1.175	1.164	1.178	1.219	1.258	1.209	1.146
1.090	1.093	1.034	1.083	1.127	1.113	1.123	1.141	1.145	1.215
1.160	1.186	1.118	1.052	1.094	1.284	1.529	1.725	1.725	1.853
1.829	1.762	1.710	1.674	1.666					

j. Survey Line ATC10A

RUN ATC10A.ELV 12/13/89

1	0	236	1.00	236	0	0			
-0.008	0.016	0.064	0.018	-0.044	-0.029	-0.004	-0.079	-0.199	-0.148
-0.116	-0.052	0.041	0.019	-0.065	-0.109	-0.127	-0.221	-0.243	-0.244
-0.188	-0.182	-0.219	-0.124	-0.071	-0.044	-0.110	-0.079	0.026	-0.024
-0.057	-0.005	0.004	-0.054	0.035	-0.034	0.025	0.045	0.000	-0.009
0.048	0.042	-0.013	0.114	0.182	0.129	0.089	0.119	0.003	-0.148
-0.235	-0.263	-0.198	-0.142	-0.058	-0.095	-0.083	0.000	-0.074	-0.097
-0.171	-0.099	-0.046	0.037	0.005	-0.051	-0.083	-0.176	-0.238	-0.253
-0.279	-0.220	-0.151	-0.148	-0.162	-0.264	-0.294	-0.214	-0.073	0.012
0.025	0.053	-0.051	-0.188	-0.237	-0.187	-0.120	0.015	0.075	0.014
0.084	0.061	-0.086	-0.069	0.027	0.142	0.090	-0.029	0.089	0.060

Table C2 (Continued)

```
 0.057  0.038  0.082  0.046  0.091  0.183  0.171  0.218  0.241  0.286
 0.367  0.303  0.292  0.343  0.283  0.330  0.458  0.489  0.397  0.293
 0.350  0.281  0.326  0.390  0.299  0.227  0.225  0.163  0.173  0.090
 0.033  0.057  0.032  0.061  0.047  0.085 -0.045  0.044  0.044 -0.070
-0.116 -0.078 -0.057 -0.053  0.009  0.077  0.008 -0.111 -0.182 -0.217
-0.142 -0.001  0.012 -0.055 -0.147 -0.204 -0.260 -0.278 -0.244 -0.244
-0.275 -0.289 -0.295 -0.331 -0.375 -0.235 -0.196 -0.086 -0.133 -0.038
-0.037  0.009 -0.050 -0.096 -0.105 -0.119 -0.109 -0.075 -0.164 -0.200
-0.190 -0.187 -0.202 -0.165 -0.148 -0.035  0.053  0.092  0.080  0.093
 0.087  0.051  0.003 -0.035 -0.023 -0.010  0.021 -0.006 -0.066 -0.055
-0.056  0.067  0.059  0.008  0.047  0.019 -0.042 -0.094 -0.088 -0.158
-0.158 -0.164 -0.200 -0.230 -0.278 -0.295 -0.233 -0.203 -0.168 -0.089
-0.012 -0.023 -0.142 -0.165 -0.226 -0.273 -0.222 -0.176 -0.133 -0.065
-0.029  0.034 -0.003 -0.116 -0.089 -0.062
```

j. Survey Line ATC11

```
RUN ATC11.ELV   12/13/89
   1    0  168       1.00  168    0    0
 0.005  0.020  0.098  0.144  0.239  0.257  0.217  0.181  0.185  0.147
 0.187  0.256  0.233  0.101  0.146  0.217  0.279  0.165  0.082  0.049
 0.122  0.156  0.128  0.159  0.185  0.256  0.337  0.347  0.276  0.303
 0.331  0.312  0.325  0.387  0.497  0.429  0.394  0.397  0.344  0.276
 0.338  0.347  0.343  0.333  0.328  0.319  0.329  0.412  0.445  0.448
 0.517  0.667  0.614  0.640  0.581  0.559  0.582  0.430  0.357  0.372
 0.452  0.449  0.154  0.033  0.013  0.277  0.444  0.611  0.727  0.516
 0.454  0.542  0.531  0.558  0.381  0.271  0.346  0.210  0.120  0.070
 0.093  0.103  0.270  0.318  0.224  0.179  0.208  0.215  0.268  0.408
 0.276  0.438  0.681  0.821  0.708  0.471  0.626  0.614  0.611  0.572
 0.431  0.148  0.120  0.399  0.559  0.477  0.391  0.435  0.526  0.684
 0.758  0.685  0.601  0.589  0.679  0.762  0.725  0.772  0.682  0.652
 0.662  0.654  0.604  0.574  0.562  0.529  0.474  0.513  0.568  0.598
 0.563  0.685  0.666  0.629  0.635  0.598  0.635  0.550  0.655  0.552
 0.486  0.445  0.443  0.367  0.395  0.374  0.331  0.310  0.408  0.476
 0.485  0.389  0.342  0.459  0.466  0.417  0.431  0.451  0.462  0.518
 0.546  0.556  0.502  0.401  0.329  0.340  0.315  0.326
```

k. Survey Line ATC1.ELV

```
RUN ATC1.ELV   02/21/90
   1    0  495       1.00  495    0    0
-0.010 -0.061 -0.181 -0.170 -0.084 -0.090 -0.027  0.042  0.081  0.046
 0.032  0.070 -0.062  0.078  0.267  0.193  0.269  0.293  0.272  0.310
 0.299  0.279  0.292  0.221  0.161  0.142  0.080  0.086  0.181  0.206
 0.171  0.196  0.196  0.167  0.111  0.029 -0.002 -0.025 -0.076 -0.018
 0.118  0.342  0.433  0.525  0.630  0.641  0.645  0.563  0.427  0.379
 0.236  0.033  0.076  0.152  0.117  0.162  0.261  0.204  0.271  0.218
```

Table C2. (Concluded)

0.086	0.057	-0.069	-0.193	-0.307	-0.307	-0.282	-0.206	-0.120	-0.057
0.033	0.118	0.448	0.536	0.542	0.563	0.457	0.451	0.448	0.394
0.381	0.385	0.325	0.361	0.277	0.117	0.312	0.373	0.368	0.363
0.410	0.427	0.474	0.510	0.517	0.547	0.565	0.525	0.411	0.484
0.392	0.400	0.433	0.488	0.441	0.400	0.369	0.371	0.334	0.303
0.363	0.418	0.487	0.422	0.424	0.479	0.489	0.466	0.470	0.448
0.488	0.440	0.533	0.424	0.381	0.290	0.192	0.235	0.306	0.292
0.358	0.377	0.457	0.503	0.431	0.441	0.351	0.332	0.308	0.309
0.329	0.335	0.277	0.275	0.324	0.378	0.496	0.661	0.607	0.527
0.656	0.688	0.782	0.773	0.852	0.875	0.822	0.841	0.750	0.731
0.758	0.625	0.537	0.493	0.494	0.680	0.549	0.428	0.496	0.534
0.482	0.559	0.558	0.681	0.649	0.660	0.630	0.620	0.808	0.683
0.746	0.647	0.811	0.846	0.777	0.828	0.901	0.923	0.922	0.993
0.918	0.808	0.788	0.645	0.616	0.580	0.583	0.591	0.691	0.754
0.696	0.755	0.770	0.706	0.542	0.501	0.466	0.467	0.386	0.349
0.288	0.285	0.320	0.323	0.313	0.396	0.219	0.184	0.200	0.052
0.167	0.002	-0.090	-0.117	-0.071	0.127	0.178	0.219	0.209	0.148
0.228	0.248	0.346	0.341	0.325	0.333	0.414	0.533	0.661	0.729
0.830	0.984	1.108	1.104	1.199	1.104	1.275	1.228	1.215	1.242
1.226	1.082	0.971	0.979	0.798	0.753	0.703	0.598	0.606	0.644
0.616	0.527	0.499	0.486	0.571	0.532	0.550	0.427	0.280	0.354
0.400	0.494	0.485	0.518	0.669	0.693	0.832	0.869	0.902	0.931
0.836	0.890	0.878	0.996	1.047	1.110	1.151	1.195	1.306	1.484
1.556	1.531	1.511	1.512	1.501	1.488	1.499	1.508	1.519	1.615
1.783	1.786	1.938	1.923	1.899	1.865	1.848	1.846	1.797	1.870
1.774	1.660	1.762	1.919	1.881	1.846	1.886	1.872	1.804	1.909
1.733	1.758	1.775	1.840	1.755	1.761	1.853	1.947	1.953	1.930
1.981	2.003	2.116	2.134	2.165	2.237	2.240	2.273	2.261	2.257
2.228	2.207	2.154	2.162	2.240	2.291	2.147	2.018	1.992	1.975
1.973	2.072	2.069	2.059	2.069	2.109	2.147	2.262	2.259	2.331
2.335	2.236	2.217	2.209	2.216	2.093	2.095	2.174	2.290	2.322
2.427	2.363	2.381	2.394	2.445	2.446	2.480	2.457	2.441	2.434
2.476	2.422	2.386	2.383	2.425	2.429	2.455	2.483	2.517	2.600
2.569	2.532	2.481	2.508	2.614	2.688	2.742	2.752	2.730	2.726
2.740	2.694	2.664	2.640	2.640	2.669	2.650	2.518	2.534	2.670
2.706	2.717	2.750	2.760	2.792	2.839	2.839	2.919	2.966	3.002
2.959	2.697	2.536	2.462	2.440	2.340	2.262	2.238	2.264	2.329
2.409	2.572	2.635	2.630	2.873	2.721	2.788	2.794	2.803	2.719
2.751	2.739	2.820	3.000	3.001	3.205	3.314	3.371	3.307	3.357
3.263	3.182	3.079	2.866	2.744	2.782	2.795	2.866	2.955	2.980
3.024	2.993	3.036	3.033	3.042	3.030	2.976	3.033	3.073	3.136
3.181	3.230	3.244	3.292	3.313	3.278	3.304	3.278	3.225	3.307
3.095	3.037	3.117	3.088	3.134	3.182	3.143	3.102	3.068	3.020
2.975	2.997	3.113	3.149	3.172					

Table C3. Coastal Engineering Research Center

a. Survey Line CERC1

```
RUN CERC1   07/20/89
   1    0  330       1.00  330    0    0
-0.011 -0.037 -0.055 -0.021 -0.044 -0.054 -0.079  0.002 -0.017 -0.004
 0.004  0.011 -0.024 -0.033 -0.006  0.086  0.078  0.027 -0.054 -0.047
 0.055  0.125  0.129  0.186  0.266  0.171  0.112  0.185  0.192  0.171
 0.186  0.164  0.204  0.203  0.082 -0.046 -0.171 -0.197 -0.148 -0.060
-0.023  0.009  0.069  0.101  0.126  0.121  0.051  0.029  0.045  0.071
 0.075  0.079  0.180  0.199  0.099 -0.003  0.047  0.090  0.112  0.032
 0.016  0.013  0.024  0.096  0.191  0.209  0.234  0.257  0.306  0.360
 0.280  0.262  0.282  0.224  0.172  0.163  0.142 -0.040  0.019 -0.029
-0.220 -0.293 -0.189 -0.068 -0.011 -0.032 -0.068 -0.008 -0.108 -0.150
-0.168 -0.170 -0.128 -0.105 -0.066 -0.093 -0.176 -0.149 -0.182 -0.188
-0.303 -0.351 -0.381 -0.258 -0.192 -0.109 -0.046 -0.186 -0.184 -0.158
-0.140 -0.129 -0.145 -0.217 -0.175 -0.165 -0.213 -0.168 -0.217 -0.316
-0.270 -0.317 -0.317 -0.345 -0.392 -0.365 -0.399 -0.257 -0.225 -0.212
-0.221 -0.347 -0.324 -0.309 -0.335 -0.430 -0.541 -0.591 -0.538 -0.479
-0.409 -0.345 -0.307 -0.414 -0.444 -0.440 -0.480 -0.465 -0.429 -0.318
-0.325 -0.459 -0.536 -0.484 -0.464 -0.430 -0.457 -0.403 -0.378 -0.377
-0.397 -0.360 -0.275 -0.290 -0.312 -0.388 -0.389 -0.394 -0.445 -0.472
-0.467 -0.455 -0.494 -0.496 -0.473 -0.369 -0.329 -0.411 -0.442 -0.478
-0.439 -0.440 -0.436 -0.392 -0.380 -0.422 -0.472 -0.534 -0.575 -0.559
-0.495 -0.396 -0.344 -0.386 -0.465 -0.353 -0.262 -0.317 -0.411 -0.459
-0.438 -0.453 -0.422 -0.298 -0.312 -0.354 -0.375 -0.268 -0.220 -0.263
-0.292 -0.307 -0.303 -0.215 -0.166 -0.123 -0.193 -0.197 -0.234 -0.228
-0.222 -0.239 -0.304 -0.341 -0.277 -0.286 -0.233 -0.237 -0.132 -0.177
-0.134 -0.128 -0.152 -0.075 -0.093 -0.111 -0.156 -0.154 -0.102 -0.134
-0.143 -0.116 -0.141 -0.186 -0.281 -0.270 -0.263 -0.247 -0.173 -0.023
 0.138  0.199  0.266  0.319  0.278  0.304  0.326  0.246  0.179  0.163
 0.181  0.214  0.072  0.012 -0.027 -0.041  0.014  0.052  0.085  0.044
 0.002  0.054  0.148  0.193  0.080  0.117  0.113  0.095  0.044  0.151
 0.188  0.119  0.085  0.085  0.076 -0.035 -0.007  0.005 -0.055 -0.194
-0.168 -0.012  0.117  0.084  0.109  0.184  0.188  0.141  0.169  0.085
 0.107  0.202  0.129  0.077  0.070  0.064  0.023 -0.087 -0.068 -0.033
 0.022 -0.072 -0.083 -0.105 -0.103 -0.103 -0.117 -0.105 -0.144 -0.140
-0.112 -0.055 -0.062 -0.071 -0.059 -0.046 -0.072 -0.062  0.026  0.027
```

b. Survey Line CERC2

```
RUN CERC2   07/20/89
   1    0  202       1.00  202    0    0
 0.056  0.112  0.088  0.003 -0.099 -0.090 -0.124 -0.128 -0.161 -0.341
-0.489 -0.547 -0.602 -0.551 -0.554 -0.581 -0.570 -0.476 -0.465 -0.310
-0.429 -0.606 -0.753 -0.705 -0.581 -0.524 -0.510 -0.425 -0.418 -0.430
-0.445 -0.501 -0.482 -0.356 -0.335 -0.273 -0.252 -0.250 -0.223 -0.310
-0.390 -0.478 -0.544 -0.489 -0.520 -0.517 -0.460 -0.400 -0.469 -0.521
-0.573 -0.592 -0.581 -0.590 -0.602 -0.551 -0.569 -0.664 -0.597 -0.489
```

Table C3. (Continued)

```
-0.585 -0.625 -0.661 -0.713 -0.724 -0.694 -0.730 -0.651 -0.689 -0.690
-0.544 -0.555 -0.579 -0.601 -0.573 -0.544 -0.478 -0.447 -0.384 -0.240
-0.274 -0.402 -0.367 -0.364 -0.356 -0.377 -0.394 -0.470 -0.478 -0.490
-0.500 -0.554 -0.624 -0.661 -0.633 -0.578 -0.482 -0.481 -0.423 -0.537
-0.454 -0.495 -0.500 -0.571 -0.694 -0.747 -0.734 -0.698 -0.609 -0.575
-0.562 -0.520 -0.505 -0.537 -0.527 -0.548 -0.516 -0.539 -0.557 -0.489
-0.382 -0.244 -0.181 -0.264 -0.387 -0.462 -0.430 -0.549 -0.545 -0.550
-0.510 -0.529 -0.621 -0.515 -0.461 -0.419 -0.406 -0.375 -0.368 -0.362
-0.483 -0.613 -0.678 -0.682 -0.640 -0.586 -0.626 -0.627 -0.602 -0.590
-0.565 -0.562 -0.603 -0.614 -0.514 -0.619 -0.727 -0.682 -0.512 -0.363
-0.191 -0.261 -0.340 -0.332 -0.305 -0.304 -0.374 -0.356 -0.396 -0.385
-0.475 -0.448 -0.514 -0.501 -0.579 -0.548 -0.604 -0.517 -0.244 -0.218
-0.399 -0.499 -0.523 -0.485 -0.412 -0.397 -0.491 -0.506 -0.457 -0.328
-0.103 -0.079 -0.076 -0.052 -0.122 -0.098 -0.058  0.036  0.062  0.125
 0.081  0.141
```

c. Survey Line CERC3

```
RUN CERC3   07/20/89
   1    0  431      1.00  431    0    0
-0.002 -0.169 -0.144 -0.117 -0.178 -0.240 -0.269 -0.309 -0.322 -0.346
-0.454 -0.523 -0.619 -0.694 -0.667 -0.612 -0.402 -0.450 -0.487 -0.380
-0.336 -0.341 -0.285 -0.075 -0.083 -0.118 -0.263 -0.278 -0.278 -0.301
-0.347 -0.376 -0.433 -0.411 -0.320 -0.543 -0.536 -0.457 -0.472 -0.427
-0.491 -0.503 -0.498 -0.565 -0.558 -0.565 -0.504 -0.478 -0.413 -0.415
-0.398 -0.443 -0.412 -0.349 -0.381 -0.340 -0.330 -0.327 -0.297 -0.313
-0.342 -0.352 -0.308 -0.343 -0.338 -0.379 -0.374 -0.394 -0.420 -0.405
-0.373 -0.393 -0.359 -0.346 -0.409 -0.275 -0.275 -0.345 -0.408 -0.405
-0.393 -0.401 -0.380 -0.338 -0.386 -0.388 -0.372 -0.392 -0.432 -0.453
-0.453 -0.456 -0.484 -0.501 -0.530 -0.552 -0.532 -0.462 -0.286 -0.159
-0.137 -0.156 -0.232 -0.235 -0.268 -0.269 -0.299 -0.309 -0.309 -0.283
-0.247 -0.211 -0.160 -0.154 -0.175 -0.218 -0.242 -0.205 -0.141 -0.061
-0.029 -0.117 -0.160 -0.154 -0.143 -0.115 -0.108 -0.129 -0.146 -0.147
-0.139 -0.090 -0.127 -0.109 -0.132 -0.169 -0.213 -0.191 -0.202 -0.233
-0.340 -0.334 -0.331 -0.281 -0.307 -0.314 -0.325 -0.361 -0.343 -0.301
-0.289 -0.281 -0.288 -0.323 -0.331 -0.309 -0.288 -0.271 -0.282 -0.269
-0.243 -0.203 -0.190 -0.231 -0.222 -0.216 -0.186 -0.124 -0.168 -0.188
-0.168 -0.170 -0.210 -0.235 -0.265 -0.258 -0.241 -0.222 -0.151 -0.077
-0.084 -0.132 -0.157 -0.189 -0.201 -0.214 -0.230 -0.272 -0.280 -0.315
-0.323 -0.336 -0.317 -0.313 -0.353 -0.399 -0.447 -0.417 -0.428 -0.445
-0.390 -0.293 -0.317 -0.391 -0.367 -0.358 -0.374 -0.393 -0.414 -0.425
-0.442 -0.523 -0.611 -0.700 -0.670 -0.707 -0.735 -0.646 -0.558 -0.478
-0.462 -0.451 -0.429 -0.408 -0.391 -0.399 -0.422 -0.348 -0.320 -0.419
-0.475 -0.459 -0.447 -0.473 -0.430 -0.383 -0.341 -0.342 -0.365 -0.351
-0.346 -0.312 -0.301 -0.261 -0.246 -0.229 -0.221 -0.190 -0.161 -0.108
-0.109 -0.181 -0.250 -0.271 -0.286 -0.283 -0.281 -0.255 -0.216 -0.216
-0.238 -0.221 -0.177 -0.233 -0.268 -0.274 -0.281 -0.242 -0.257 -0.290
-0.315 -0.330 -0.324 -0.334 -0.358 -0.379 -0.369 -0.332 -0.326 -0.335
```

Table C3. (Continued)

```
-0.342 -0.383 -0.399 -0.365 -0.354 -0.350 -0.321 -0.371 -0.372 -0.380
-0.274 -0.243 -0.228 -0.247 -0.201 -0.162 -0.139 -0.155 -0.120 -0.166
-0.174 -0.172 -0.155 -0.126 -0.129 -0.139 -0.162 -0.177 -0.156 -0.048
-0.082 -0.159 -0.223 -0.257 -0.233 -0.191 -0.167 -0.173 -0.226 -0.260
-0.296 -0.319 -0.319 -0.306 -0.276 -0.274 -0.241 -0.233 -0.154 -0.138
-0.164 -0.290 -0.464 -0.531 -0.550 -0.523 -0.496 -0.482 -0.453 -0.444
-0.444 -0.424 -0.385 -0.366 -0.381 -0.382 -0.341 -0.379 -0.402 -0.391
-0.402 -0.404 -0.340 -0.270 -0.270 -0.405 -0.344 -0.357 -0.392 -0.369
-0.328 -0.343 -0.315 -0.297 -0.300 -0.258 -0.264 -0.228 -0.184 -0.176
-0.146 -0.127 -0.164 -0.167 -0.175 -0.214 -0.179 -0.244 -0.269 -0.227
-0.247 -0.244 -0.309 -0.333 -0.395 -0.386 -0.391 -0.325 -0.327 -0.318
-0.249 -0.296 -0.282 -0.360 -0.365 -0.145 -0.225 -0.255 -0.193 -0.167
-0.115 -0.095 -0.095 -0.080  0.068  0.105  0.105 -0.100 -0.153 -0.149
-0.195 -0.297 -0.257 -0.211 -0.425 -0.475 -0.497 -0.424 -0.330 -0.263
-0.152 -0.134 -0.118 -0.077 -0.043  0.023  0.086  0.058  0.027  0.199
 0.203
```

d. Survey Line CERC4

```
RUN CERC4   07/20/89
   1    0  145       1.00   73    0    0
-0.001 -0.018  0.001  0.024  0.012 -0.016 -0.048 -0.125 -0.185 -0.210
-0.180 -0.186 -0.223 -0.298 -0.162 -0.140 -0.135 -0.098 -0.135 -0.150
-0.159 -0.136 -0.103 -0.030  0.026  0.049 -0.010 -0.021  0.029  0.028
-0.014  0.035  0.078  0.045 -0.009  0.042  0.002 -0.054 -0.105 -0.201
-0.224 -0.190 -0.202 -0.301 -0.347 -0.360 -0.373 -0.393 -0.370 -0.287
-0.305 -0.158 -0.152 -0.192 -0.202 -0.167 -0.154 -0.207 -0.186 -0.196
-0.233 -0.307 -0.385 -0.456 -0.520 -0.566 -0.474 -0.558 -0.684 -0.824
-0.856 -0.893 -0.939 -0.882 -0.853 -0.711 -0.586 -0.502 -0.407 -0.361
-0.297 -0.227 -0.145 -0.073 -0.035 -0.026 -0.046  0.010 -0.007 -0.030
-0.031  0.011  0.008 -0.139 -0.119 -0.200 -0.220 -0.200 -0.184 -0.175
-0.130 -0.032 -0.018 -0.050 -0.028  0.065  0.120  0.178  0.219  0.169
 0.223  0.255  0.213  0.165  0.210  0.207  0.161  0.173  0.235  0.209
 0.158  0.083  0.051  0.033  0.042  0.064  0.092  0.059  0.054  0.034
-0.102 -0.032  0.010  0.018 -0.011  0.011  0.074  0.151  0.180  0.207
 0.219  0.198  0.180  0.194  0.195
```

e. Survey Line CERC5

```
RUN CERC5   07/20/89
   1    0  139       1.00  139    0    0
-0.007 -0.051 -0.069 -0.069 -0.106 -0.119 -0.129 -0.158 -0.234 -0.217
-0.187 -0.207 -0.238 -0.263 -0.202 -0.156 -0.221 -0.142 -0.205 -0.295
-0.342 -0.364 -0.405 -0.430 -0.437 -0.448 -0.432 -0.369 -0.361 -0.386
-0.401 -0.408 -0.415 -0.447 -0.480 -0.483 -0.458 -0.459 -0.428 -0.346
-0.318 -0.350 -0.350 -0.368 -0.376 -0.362 -0.323 -0.295 -0.268 -0.338
-0.300 -0.267 -0.246 -0.294 -0.213 -0.223 -0.279 -0.386 -0.395 -0.504
```

Table C3. (Continued)

```
-0.547 -0.666 -0.777 -0.855 -0.944 -0.968 -1.103 -1.141 -1.084 -1.229
-1.291 -1.239 -1.115 -1.089 -0.996 -0.917 -0.803 -0.688 -0.640 -0.533
-0.522 -0.411 -0.361 -0.349 -0.432 -0.390 -0.403 -0.438 -0.474 -0.404
-0.428 -0.457 -0.498 -0.510 -0.507 -0.485 -0.485 -0.451 -0.482 -0.561
-0.590 -0.590 -0.614 -0.612 -0.576 -0.548 -0.544 -0.535 -0.521 -0.497
-0.505 -0.567 -0.581 -0.569 -0.566 -0.536 -0.495 -0.473 -0.425 -0.335
-0.271 -0.351 -0.287 -0.333 -0.394 -0.368 -0.339 -0.315 -0.349 -0.364
-0.289 -0.256 -0.249 -0.234 -0.197 -0.195 -0.176 -0.132 -0.128
```

f. Survey Line CERC6

```
RUN CERC6   07/20/89
   1    0  207       1.00  207    0    0
 0.035 -0.005  0.092  0.165  0.146  0.233  0.229  0.220  0.160  0.114
 0.058  0.007  0.074  0.051 -0.004  0.113  0.169  0.131  0.151  0.124
 0.104  0.114  0.168  0.009  0.068  0.084  0.005  0.010  0.069  0.113
 0.044  0.019 -0.044 -0.031  0.051  0.040  0.067  0.113  0.126  0.091
 0.062  0.054 -0.051  0.133  0.221  0.205  0.231  0.269  0.238  0.203
 0.121  0.096  0.024 -0.006 -0.019 -0.009 -0.043 -0.023  0.093  0.155
 0.116  0.239  0.252  0.298  0.399  0.480  0.523  0.525  0.584  0.441
 0.330  0.486  0.371  0.354  0.333  0.268  0.139  0.044  0.017  0.089
 0.172  0.223  0.175  0.143  0.153  0.152  0.153  0.170  0.150  0.164
 0.064  0.036  0.036  0.048  0.074  0.064  0.059  0.153  0.185  0.176
 0.146  0.165  0.211  0.234  0.188  0.168  0.215  0.206  0.192  0.096
 0.086  0.117  0.091  0.074  0.076  0.101  0.194  0.188  0.213  0.191
 0.192  0.198  0.185  0.218  0.270  0.221  0.145  0.062  0.082  0.177
 0.317  0.371  0.398  0.429  0.536  0.389  0.483  0.619  0.577  0.558
 0.538  0.448  0.356  0.302  0.295  0.158  0.196  0.150  0.033  0.001
 0.042  0.034  0.046  0.075  0.147  0.170  0.246  0.288  0.313  0.289
 0.254  0.266  0.200  0.008  0.091  0.122  0.140  0.173  0.173  0.114
 0.098  0.109  0.022  0.020  0.071  0.102  0.170  0.131  0.067  0.071
 0.153  0.119  0.069  0.224  0.173  0.161  0.182  0.195  0.188  0.234
 0.179  0.041  0.108  0.131  0.060  0.113  0.164  0.207  0.270  0.281
 0.289  0.206  0.211  0.147  0.045  0.095  0.056
```

g. Survey Line CERC7

```
RUN CERC7   07/20/89
   1    0   65       1.00   65    0    0
-0.029  0.040  0.111  0.083  0.018  0.003  0.065  0.069  0.054  0.034
 0.072  0.059  0.100  0.138  0.239  0.170  0.138  0.218 -0.060  0.053
 0.071  0.061  0.208  0.158  0.100  0.080 -0.014 -0.105 -0.167 -0.221
-0.342 -0.470 -0.370 -0.239 -0.113 -0.064 -0.004  0.087  0.178  0.207
 0.254  0.313  0.165  0.180  0.163  0.051  0.332  0.255  0.283  0.354
 0.253  0.215  0.173  0.180  0.143  0.166  0.183  0.176  0.114  0.130
 0.197  0.222  0.154  0.082  0.114
```

Table C3. (Continued)

h. Survey Line CERC8

```
RUN CERC8   07/20/89
   1    0  401      1.00  401    0    0
-0.143 -0.327 -0.391 -0.487 -0.620 -0.867 -0.964 -1.177 -1.310 -1.500
-1.716 -1.889 -1.950 -2.172 -2.326 -2.475 -2.653 -2.844 -2.986 -3.175
-3.388 -3.640 -3.845 -4.038 -4.230 -4.472 -4.674 -4.818 -4.923 -5.043
-5.257 -5.516 -5.632 -5.738 -5.919 -6.067 -6.290 -6.322 -6.407 -6.526
-6.708 -6.985 -7.198 -7.355 -7.445 -7.590 -7.733 -7.806 -7.963 -8.161
-8.413 -8.600 -8.824 -8.993 -9.192 -9.316 -9.417 -9.579 -9.716 -9.804
-9.973-10.362-10.577-10.905-11.070-11.185-11.402-11.566-11.285-11.355
-11.584-11.796-12.019-12.221-12.335-12.471-12.650-12.783-12.983-13.237
-13.429-13.651-13.875-13.569-13.758-14.026-14.115-14.212-14.298-14.329
-14.303-14.314-14.279-14.218-14.089-14.033-14.134-13.987-13.977-13.856
-13.657-13.508-13.532-13.412-13.284-13.152-12.986-12.859-12.811-12.883
-12.733-12.627-12.535-12.384-12.342-12.205-12.067-11.941-11.835-11.696
-11.460-11.477-11.343-11.246-11.243-11.166-11.113-10.998-10.887-10.855
-10.763-10.671-10.644-10.445-10.271-10.199-10.153-10.075-10.034 -9.997
 -9.906 -9.803 -9.681 -9.554 -9.481 -9.405 -9.384 -9.297 -9.189 -9.084
 -9.015 -8.997 -8.983 -8.932 -8.868 -8.711 -8.543 -8.510 -8.472 -8.435
 -8.357 -8.350 -8.244 -8.212 -8.043 -7.993 -8.029 -7.953 -7.840 -7.801
 -7.722 -7.667 -7.498 -7.381 -7.227 -7.190 -7.148 -7.092 -6.994 -6.839
 -6.778 -6.707 -6.522 -6.426 -6.352 -6.302 -6.283 -6.281 -6.257 -6.070
 -6.042 -5.951 -5.866 -5.804 -5.772 -5.713 -5.701 -5.679 -5.559 -5.586
 -5.551 -5.493 -5.580 -5.587 -5.607 -5.680 -5.691 -5.736 -5.814 -5.900
 -5.952 -6.005 -6.057 -6.094 -6.108 -6.159 -6.213 -6.332 -6.529 -6.607
 -6.731 -6.866 -6.970 -6.963 -6.947 -6.992 -7.115 -7.215 -7.358 -7.364
 -7.484 -7.598 -7.686 -7.770 -7.755 -7.784 -7.979 -7.984 -8.085 -8.101
 -8.194 -8.230 -8.222 -8.307 -8.432 -8.586 -8.730 -8.781 -8.793 -8.857
 -8.885 -8.926 -8.998 -9.061 -9.166 -9.328 -9.410 -9.478 -9.617 -9.738
 -9.765 -9.869 -9.877 -9.953-10.066-10.117-10.342-10.562-10.552-10.655
-10.749-10.790-10.913-11.031-11.075-11.157-11.142-11.253-11.418-11.591
-11.641-11.762-11.915-12.062-12.203-12.353-12.407-12.516-12.651-12.748
-12.859-12.799-12.880-12.995-13.162-13.308-13.458-13.559-13.475-13.609
-13.757-13.839-13.826-13.924-13.844-13.931-14.027-14.054-14.173-14.185
-14.119-14.115-13.961-13.872-13.767-13.557-13.352-13.129-12.912-12.730
-12.464-12.272-12.077-11.963-11.762-11.582-11.459-11.275-11.054-10.803
-10.604-10.519-10.410-10.229-10.026 -9.925 -9.685 -9.315 -9.070 -8.800
 -8.593 -8.450 -8.323 -8.168 -8.119 -8.024 -7.828 -7.615 -7.375 -7.153
 -6.823 -6.634 -6.516 -6.473 -6.317 -6.170 -5.997 -5.849 -5.702 -5.458
 -5.282 -5.211 -5.139 -5.032 -4.869 -4.744 -4.591 -4.485 -4.356 -4.106
 -3.878 -3.791 -3.698 -3.513 -3.292 -3.088 -2.885 -2.667 -2.480 -2.197
 -1.985 -1.828 -1.706 -1.520 -1.318 -1.171 -0.984 -0.756 -0.697 -0.530
 -0.342 -0.172 -0.061  0.160  0.217  0.498  0.602  0.707  0.777  0.930
  0.679
```

Table C3. (Continued)

i. Survey Line CERC9

```
RUN CERC9   08/10/89
   1    0  151       1.00  151    0    0
-0.266 -0.331 -0.430 -0.495 -0.546 -0.543 -0.676 -0.588 -0.689 -0.749
-0.756 -0.858 -0.985 -0.921 -0.795 -0.869 -0.861 -0.925 -0.992 -0.917
-0.942 -0.911 -0.845 -0.770 -0.714 -0.748 -0.879 -0.980 -0.994 -0.937
-0.873 -0.962 -0.946 -0.848 -0.850 -0.913 -0.983 -0.969 -0.860 -0.643
-0.680 -0.795 -0.798 -0.825 -0.942 -0.866 -0.727 -0.700 -0.700 -0.630
-0.559 -0.565 -0.649 -0.607 -0.532 -0.330 -0.318 -0.378 -0.448 -0.472
-0.438 -0.438 -0.389 -0.508 -0.509 -0.451 -0.428 -0.345 -0.220 -0.130
-0.094 -0.017  0.099  0.271  0.431  0.074  0.046 -0.043 -0.199 -0.259
-0.295 -0.361 -0.406 -0.437 -0.460 -0.505 -0.502 -0.378 -0.430 -0.434
-0.443 -0.419 -0.343 -0.253 -0.287 -0.483 -0.581 -0.642 -0.570 -0.537
-0.623 -0.662 -0.641 -0.692 -0.848 -0.920 -0.833 -0.784 -0.790 -0.668
-0.600 -0.840 -0.955 -0.987 -0.885 -0.829 -0.787 -0.855 -0.928 -0.844
-0.807 -0.899 -0.969 -0.816 -0.759 -0.637 -0.752 -0.756 -0.924 -0.912
-0.920 -0.981 -0.934 -0.849 -0.860 -0.781 -0.882 -0.943 -0.823 -0.724
-0.677 -0.590 -0.494 -0.552 -0.436 -0.444 -0.344 -0.243 -0.132 -0.013
 0.159
```

j. Survey Line CERC10

```
RUN CERC10   08/10/89
   1    0  434       1.00  434    0    0
 0.063 -0.067 -0.075 -0.041  0.114  0.178  0.051 -0.111  0.161  0.548
 0.943  1.176  1.535  1.664  1.515  1.277  1.115  1.007  0.999  0.954
 0.954  0.998  1.063  1.203  1.174  1.346  1.639  1.737  1.677  1.599
 1.796  1.921  2.047  2.375  2.323  2.186  2.078  2.075  2.232  2.373
 2.410  2.410  2.418  2.517  2.612  2.701  2.691  2.720  2.949  2.857
 2.923  2.985  2.868  2.925  3.000  3.018  3.103  3.115  3.267  3.162
 3.249  3.322  3.259  3.343  3.312  3.318  3.298  3.200  3.245  3.331
 3.370  3.494  3.427  3.519  3.505  3.677  3.780  3.745  3.881  3.891
 3.886  3.846  3.916  3.960  3.912  3.984  4.092  4.161  4.226  4.232
 4.348  4.409  4.416  4.648  4.994  5.221  5.088  5.191  5.184  4.912
 4.777  4.728  4.635  4.624  4.647  4.696  4.703  4.633  4.622  4.639
 4.439  4.444  4.415  4.410  4.245  4.196  4.196  4.087  4.243  4.172
 4.138  4.071  4.178  4.279  4.393  4.305  4.293  4.206  3.957  3.796
 3.710  3.680  3.738  3.883  3.822  3.930  3.994  3.867  3.900  3.863
 3.737  3.679  3.514  3.555  3.585  3.592  3.556  3.323  3.433  3.450
 3.345  3.196  3.063  3.033  2.992  2.911  2.836  2.745  2.650  2.645
 2.680  2.527  2.500  2.519  2.504  2.566  2.507  2.516  2.574  2.446
 2.481  2.427  2.414  2.498  2.559  2.545  2.471  2.529  2.483  2.464
 2.446  2.384  2.474  2.476  2.386  2.248  2.221  2.205  2.336  2.313
 2.319  2.379  2.264  2.434  2.267  2.312  2.266  2.271  2.424  2.467
 2.440  2.314  2.328  2.254  2.406  2.199  1.946  1.796  1.669  1.752
 1.649  1.675  1.654  1.739  1.968  2.233  1.984  1.759  1.574  1.467
 1.636  1.560  1.567  1.620  1.602  1.706  1.860  2.057  2.017  2.034
```

Table C3. (Concluded)

2.071	2.185	2.152	2.008	1.909	1.899	1.974	1.935	2.045	1.828
1.897	1.822	1.828	1.779	1.743	1.732	1.767	1.880	1.968	1.904
1.768	1.723	1.730	1.713	1.763	1.788	1.812	1.752	1.668	1.557
1.560	1.709	1.765	1.966	1.931	1.897	1.912	1.940	1.915	1.771
1.800	2.044	2.061	2.088	2.165	2.313	2.440	2.542	2.563	2.525
2.545	2.657	2.882	2.889	2.893	2.926	2.969	2.939	3.077	3.122
3.322	3.441	3.459	3.547	3.492	3.625	3.513	3.432	3.453	3.399
3.434	3.518	3.515	3.639	3.744	3.760	3.697	3.592	3.431	3.511
3.599	3.598	3.575	3.668	3.746	3.839	3.787	3.794	3.985	3.946
4.012	4.051	3.990	4.000	4.038	4.065	4.124	4.075	4.090	4.070
4.103	4.165	4.347	4.456	4.569	4.643	4.714	4.546	4.221	4.133
4.142	4.209	4.001	4.006	3.935	3.935	3.878	3.735	3.756	3.686
3.655	3.657	3.628	3.535	3.471	3.541	3.563	3.432	3.416	3.385
3.461	3.374	3.135	3.105	3.060	3.082	3.074	3.052	2.970	3.041
3.074	2.932	2.840	2.860	2.852	2.838	2.813	2.742	2.698	2.667
2.645	2.707	2.693	2.746	2.736	2.711	2.785	2.567	2.481	2.400
2.412	2.481	2.293	2.141	1.981	1.989	2.149	2.172	2.131	2.031
1.866	1.827	1.736	1.785	1.872	1.825	1.510	1.340	1.402	1.235
1.066	0.984	0.957	1.051	0.988	1.042	1.141	1.319	1.328	1.272
0.998	0.786	0.490	0.249	0.294	0.398	0.476	0.264	0.095	0.072
0.051	-0.073	0.187	0.401						

Table C4. Fort Sam Houston, Texas

a. Survey Line PMF1, Pest Management Facility

RUN PMF1.ELV		02/01/90							
1	0 116		1.00 116		0	0			
0.194	0.291	0.549	0.870	1.165	1.442	1.726	2.023	2.265	2.529
2.722	2.932	3.095	3.290	3.542	3.826	4.102	4.295	4.463	4.636
4.792	4.929	5.007	5.111	5.196	5.293	5.464	5.490	5.369	5.316
5.308	5.344	5.350	5.265	5.203	5.109	5.067	5.032	4.926	4.732
4.574	4.573	4.489	4.468	4.431	4.392	4.327	4.237	4.256	4.300
4.301	4.284	4.206	4.121	4.038	3.997	3.968	3.915	3.953	4.090
4.147	4.209	4.289	4.319	4.315	4.263	4.261	4.346	4.401	4.448
4.505	4.510	4.593	4.597	4.736	4.936	5.055	5.089	5.134	5.249
5.296	5.345	5.373	5.358	5.382	5.417	5.536	5.492	5.334	5.258
5.208	5.073	4.996	4.891	4.757	4.541	4.355	4.180	3.885	3.600
3.337	3.152	3.002	2.779	2.605	2.331	2.081	1.784	1.505	1.223
0.932	0.615	0.362	0.288	0.118	0.103				

b. Survey Line PMF2, Pest Management Facility

RUN PMF2.ELV		02/01/90							
1	0 167		1.00 167		0	0			
-0.058	-0.123	-0.239	-0.282	-0.338	-0.424	-0.290	-0.218	-0.207	-0.232

Table C4. (Continued)

-0.269	-0.250	-0.192	0.212	0.960	1.658	2.301	2.876	3.389	3.735
3.757	3.675	3.626	3.547	3.545	3.452	3.319	3.457	3.564	3.586
3.495	3.574	3.645	3.721	3.769	3.882	3.949	3.948	3.938	3.922
3.943	3.943	3.931	3.893	3.835	3.791	3.729	3.725	3.756	3.777
3.840	3.866	3.835	3.785	3.683	3.608	3.632	3.588	3.438	3.363
3.343	3.350	3.252	3.199	3.233	3.264	3.230	3.224	3.314	3.311
3.298	3.232	3.101	2.987	3.002	2.998	2.976	2.888	2.813	2.749
2.712	2.708	2.588	2.549	2.696	2.733	2.774	2.822	2.883	2.958
2.955	3.000	3.020	3.103	3.223	3.285	3.340	3.365	3.283	3.275
3.311	3.352	3.285	3.339	3.399	3.423	3.443	3.525	3.590	3.628
3.623	3.673	3.810	3.838	3.874	3.923	3.814	3.802	3.854	3.781
3.830	3.831	3.939	3.927	3.927	3.911	3.897	3.920	3.951	3.952
3.898	3.834	3.701	3.635	3.579	3.493	3.608	3.574	3.502	3.439
3.501	3.559	3.608	3.660	3.757	3.848	3.789	3.557	3.062	2.529
1.892	1.186	0.503	-0.073	-0.252	-0.262	-0.246	-0.183	-0.132	-0.168
-0.327	-0.331	-0.270	-0.264	-0.162	-0.092	-0.031			

c. Survey Line TMC3, Troop Medical Clinic

RUN TMC3.ELV 02/01/90									
1	0 316		1.00 316		0	0			
-0.001	-0.014	-0.082	-0.080	-0.138	-0.158	-0.214	-0.218	-0.255	-0.251
-0.283	-0.184	-0.129	-0.098	-0.050	0.064	0.101	0.203	0.273	0.422
0.507	0.549	0.575	0.680	0.714	0.716	0.679	0.677	0.650	0.714
0.730	0.746	0.696	0.683	0.643	0.660	0.668	0.692	0.671	0.689
0.650	0.674	0.662	0.564	0.468	0.511	0.524	0.482	0.456	0.544
0.523	0.479	0.454	0.450	0.419	0.456	0.390	0.391	0.299	0.283
0.239	0.184	0.184	0.238	0.196	0.258	0.226	0.165	0.145	0.187
0.180	0.095	0.167	0.249	0.238	0.318	0.260	0.258	0.176	0.251
0.259	0.236	0.265	0.377	0.516	0.636	0.540	0.507	0.440	0.366
0.285	0.310	0.333	0.421	0.418	0.523	0.567	0.695	0.716	0.744
0.762	0.843	0.806	0.730	0.682	0.806	0.828	0.833	0.809	0.793
0.796	0.777	0.724	0.726	0.643	0.610	0.599	0.594	0.530	0.523
0.517	0.577	0.587	0.674	0.721	0.672	0.657	0.731	0.789	0.828
0.838	0.910	0.938	0.966	1.000	1.123	1.191	1.139	1.077	1.058
1.049	1.093	1.063	1.088	1.078	1.055	1.032	1.033	1.023	1.057
1.081	1.126	1.099	1.114	1.107	1.083	1.145	1.157	1.073	1.078
1.040	1.092	1.077	1.088	1.047	1.064	1.055	1.082	1.076	1.144
1.116	1.093	1.083	1.049	1.037	1.120	1.122	1.224	1.143	1.057
0.967	0.981	0.930	0.875	0.862	0.841	0.759	0.721	0.689	0.724
0.697	0.633	0.539	0.542	0.530	0.586	0.636	0.643	0.629	0.673
0.715	0.760	0.785	0.827	0.781	0.801	0.826	0.800	0.771	0.681
0.701	0.744	0.761	0.765	0.678	0.671	0.592	0.479	0.367	0.295
0.282	0.329	0.265	0.250	0.289	0.414	0.466	0.493	0.510	0.568
0.469	0.385	0.238	0.214	0.154	0.087	0.075	0.128	0.093	0.117
0.120	0.046	0.022	0.011	0.052	0.013	-0.013	0.109	0.137	0.165
0.127	0.077	0.076	0.136	0.160	0.258	0.285	0.323	0.347	0.371
0.364	0.385	0.429	0.471	0.477	0.439	0.453	0.430	0.544	0.499

Table C4. (Continued)

```
 0.551  0.684  0.666  0.641  0.649  0.688  0.669  0.677  0.648  0.654
 0.647  0.697  0.698  0.719  0.659  0.605  0.628  0.659  0.694  0.703
 0.626  0.567  0.506  0.521  0.398  0.318  0.192  0.102  0.030 -0.058
-0.126 -0.207 -0.256 -0.279 -0.320 -0.292 -0.316 -0.264 -0.264 -0.224
-0.222 -0.192 -0.172 -0.131 -0.181 -0.049
```

d. Survey Line TMC4, Troop Medical Clinic

```
RUN TMC4.ELV   02/01/90
   1    0  192       1.00  192    0    0
-0.005  0.038 -0.009  0.081  0.178  0.188  0.193  0.223  0.238  0.253
 0.314  0.417  0.320  0.339  0.384  0.262  0.160  0.125  0.102  0.121
 0.105  0.123  0.108  0.115  0.151  0.100  0.079  0.094  0.034  0.037
 0.031  0.020  0.063  0.035  0.069  0.078  0.058  0.087  0.116  0.096
 0.074  0.087  0.083  0.064  0.087  0.107  0.078  0.160  0.180  0.159
 0.119  0.119  0.130  0.180  0.151  0.152  0.082  0.075  0.000 -0.020
-0.010  0.044  0.033  0.129  0.177  0.259  0.295  0.297  0.242  0.225
 0.240  0.262  0.210  0.231  0.261  0.239  0.151  0.161  0.205  0.239
 0.197  0.231  0.169  0.092  0.011 -0.065 -0.139 -0.111 -0.102 -0.098
-0.089 -0.039 -0.039 -0.022 -0.103 -0.042  0.004 -0.038 -0.054 -0.028
-0.029 -0.039 -0.071 -0.088 -0.072 -0.020  0.017  0.080  0.128  0.129
 0.104  0.144  0.126  0.153  0.191  0.235  0.207  0.225  0.236  0.247
 0.273  0.327  0.270  0.279  0.202  0.248  0.123 -0.012 -0.090 -0.145
-0.219 -0.115 -0.092 -0.044 -0.003  0.060  0.031  0.040  0.053  0.081
 0.100  0.104  0.103  0.132  0.063  0.064  0.037  0.078  0.047  0.101
 0.060  0.077  0.073  0.119  0.083  0.080  0.015  0.036  0.025  0.025
-0.011  0.054  0.095  0.135  0.105  0.108  0.065  0.081  0.077  0.075
 0.053  0.131  0.177  0.176  0.207  0.262  0.283  0.282  0.319  0.325
 0.304  0.265  0.228  0.216  0.143  0.137  0.071 -0.002 -0.005 -0.041
-0.048  0.006
```

e. Survey Line TMC5, Troop Medical Clinic

```
RUN TMC5.ELV   02/01/90
   1    0  309       1.00  309    0    0
 0.067  0.231  0.334  0.370  0.411  0.464  0.544  0.714  0.719  0.754
 0.769  0.852  0.933  1.050  1.160  1.238  1.243  1.267  1.244  1.263
 1.220  1.264  1.218  1.207  1.145  1.139  1.139  1.136  1.125  1.160
 1.081  1.109  1.165  1.235  1.244  1.276  1.322  1.389  1.375  1.413
 1.451  1.426  1.351  1.343  1.246  1.223  1.244  1.194  1.115  1.133
 1.127  1.096  1.092  1.104  1.019  1.009  1.055  1.089  1.075  1.109
 1.101  1.057  1.028  0.984  0.971  1.049  1.164  1.155  1.091  1.085
 1.076  1.048  0.974  1.034  1.049  1.044  1.062  1.019  0.973  0.967
 0.968  0.919  0.963  0.987  0.914  0.927  0.978  0.989  0.915  0.892
 0.800  0.758  0.790  0.824  0.811  0.823  0.857  0.837  0.744  0.719
 0.769  0.824  0.834  0.829  0.833  0.877  0.965  1.118  0.965  0.750
 0.658  0.702  0.640  0.723  0.741  0.781  0.861  0.913  0.908  1.093
```

Table C4. (Continued)

1.144	1.105	1.101	1.075	1.080	1.145	1.149	1.127	1.106	1.175
1.147	1.105	1.020	0.991	0.905	0.756	0.520	0.492	0.424	0.456
0.346	0.299	0.186	0.117	0.059	0.043	0.004	-0.012	-0.143	-0.223
-0.250	-0.289	-0.301	-0.305	-0.410	-0.404	-0.297	-0.252	-0.253	-0.203
-0.205	-0.092	0.037	0.069	0.113	0.124	0.092	0.174	0.242	0.319
0.365	0.408	0.429	0.576	0.753	0.897	0.946	1.026	1.055	1.099
1.073	1.067	1.096	1.161	1.088	1.066	1.044	1.102	1.079	1.145
1.069	0.896	0.909	0.888	0.780	0.712	0.610	0.582	0.678	0.717
0.734	1.015	1.093	1.161	1.164	1.201	1.207	1.243	1.268	1.332
1.258	1.181	1.172	1.214	1.199	1.198	1.226	1.264	1.208	1.146
1.140	1.107	1.080	1.157	1.131	1.085	1.076	1.126	1.089	1.094
1.110	1.226	1.189	1.214	1.177	1.153	1.186	1.262	1.235	1.251
1.321	1.350	1.260	1.255	1.231	1.298	1.293	1.325	1.298	1.322
1.287	1.267	1.175	1.171	1.242	1.263	1.237	1.266	1.252	1.231
1.299	1.358	1.331	1.370	1.444	1.463	1.527	1.594	1.530	1.492
1.524	1.517	1.431	1.413	1.404	1.345	1.278	1.199	1.269	1.278
1.278	1.295	1.298	1.302	1.329	1.360	1.370	1.339	1.338	1.346
1.359	1.340	1.349	1.296	1.219	1.127	1.060	0.954	0.913	0.902
0.872	0.753	0.621	0.608	0.525	0.491	0.433	0.285	0.149	

f. Survey Line TDC6, Troop Dental Clinic

RUN TDC6.ELV 02/01/90

1 0 268 1.00 268 0 0

-0.001	0.015	-0.041	-0.456	-0.475	-0.492	-0.431	-0.443	-0.448	-0.503
-0.531	-0.494	-0.469	-0.506	-0.510	-0.416	-0.360	-0.311	-0.276	-0.240
-0.261	-0.260	-0.214	-0.167	-0.086	-0.117	-0.189	-0.244	-0.311	-0.495
-0.631	-0.600	-0.684	-0.691	-0.558	-0.588	-0.600	-0.557	-0.564	-0.496
-0.388	-0.277	-0.196	-0.196	-0.195	-0.169	-0.177	-0.149	-0.079	-0.043
-0.079	-0.166	-0.287	-0.360	-0.409	-0.393	-0.425	-0.487	-0.519	-0.566
-0.578	-0.689	-0.741	-0.696	-0.597	-0.478	-0.473	-0.430	-0.348	-0.277
-0.316	-0.311	-0.306	-0.287	-0.315	-0.331	-0.350	-0.323	-0.399	-0.382
-0.351	-0.349	-0.363	-0.380	-0.368	-0.397	-0.456	-0.474	-0.511	-0.533
-0.536	-0.513	-0.408	-0.388	-0.392	-0.380	-0.412	-0.436	-0.421	-0.511
-0.526	-0.566	-0.575	-0.529	-0.472	-0.420	-0.258	-0.260	-0.302	-0.253
-0.203	-0.209	-0.209	-0.240	-0.306	-0.348	-0.438	-0.473	-0.396	-0.483
-0.564	-0.529	-0.541	-0.603	-0.667	-0.700	-0.693	-0.706	-0.644	-0.414
-0.522	-0.477	-0.270	-0.251	-0.394	-0.546	-0.456	-0.636	-0.698	-0.708
-0.703	-0.680	-0.622	-0.546	-0.509	-0.557	-0.504	-0.403	-0.450	-0.432
-0.352	-0.302	-0.256	-0.202	-0.194	-0.195	-0.201	-0.252	-0.269	-0.218
-0.359	-0.440	-0.483	-0.557	-0.554	-0.526	-0.509	-0.405	-0.426	-0.398
-0.358	-0.379	-0.347	-0.357	-0.469	-0.513	-0.512	-0.486	-0.447	-0.416
-0.366	-0.337	-0.337	-0.331	-0.303	-0.290	-0.342	-0.388	-0.330	-0.314
-0.309	-0.277	-0.256	-0.254	-0.259	-0.282	-0.257	-0.298	-0.372	-0.439
-0.454	-0.505	-0.628	-0.691	-0.695	-0.586	-0.496	-0.475	-0.435	-0.361
-0.345	-0.340	-0.293	-0.248	-0.136	-0.050	0.007	-0.008	-0.057	-0.106
-0.107	-0.100	-0.130	-0.123	-0.186	-0.294	-0.389	-0.474	-0.491	-0.528
-0.517	-0.510	-0.615	-0.650	-0.566	-0.543	-0.456	-0.271	-0.178	-0.144

Table C4. (Continued)

```
-0.059 -0.030 -0.068 -0.123 -0.154 -0.168 -0.152 -0.150 -0.204 -0.257
-0.321 -0.385 -0.431 -0.386 -0.380 -0.440 -0.422 -0.369 -0.340 -0.351
-0.376 -0.388 -0.355  0.039  0.110  0.125  0.078  0.089
```

g. Survey Line TDC7, Troop Dental Clinic

```
RUN TDC7.ELV   02/01/90
   1    0  268       1.00  268    0    0
-0.005 -0.267 -0.295 -0.329 -0.320 -0.162 -0.177 -0.252 -0.296 -0.275
-0.158 -0.099 -0.050 -0.010  0.015  0.092  0.156  0.236  0.324  0.350
 0.387  0.293  0.143  0.074  0.023  0.075  0.066  0.048  0.045  0.072
 0.068  0.057  0.066  0.105  0.186  0.226  0.164  0.115  0.009  0.003
 0.017  0.000  0.097  0.204  0.350  0.468  0.574  0.661  0.680  0.840
 0.964  0.983  0.954  1.004  1.072  0.886  0.852  0.900  0.865  0.742
 0.585  0.497  0.433  0.393  0.350  0.292  0.234  0.214  0.194  0.129
 0.145  0.145  0.003 -0.040 -0.016 -0.002  0.049  0.063  0.096  0.120
 0.188  0.212  0.209  0.126  0.033 -0.057  0.011  0.044  0.074  0.077
 0.063  0.002 -0.102 -0.233 -0.252 -0.292 -0.330 -0.342 -0.318 -0.400
-0.295 -0.246 -0.225 -0.138 -0.083 -0.104 -0.114 -0.105 -0.077 -0.110
-0.082 -0.033 -0.010  0.015  0.095  0.157  0.121  0.031 -0.067 -0.124
-0.163 -0.263 -0.294 -0.335 -0.335 -0.374 -0.464 -0.501 -0.508 -0.392
-0.348 -0.266 -0.501 -0.271 -0.221 -0.375 -0.370 -0.541 -0.496 -0.478
-0.378 -0.318 -0.334 -0.284 -0.254 -0.151 -0.110 -0.058  0.056  0.142
 0.177  0.130  0.048  0.017 -0.002 -0.033 -0.078 -0.053 -0.081 -0.087
-0.068 -0.075 -0.107 -0.167 -0.220 -0.246 -0.354 -0.284 -0.305 -0.298
-0.264 -0.234 -0.189 -0.074  0.011  0.085  0.128  0.124  0.091  0.088
-0.006  0.066  0.147  0.256  0.272  0.250  0.181  0.163  0.118  0.121
 0.043  0.056  0.013  0.037  0.180  0.212  0.187  0.251  0.269  0.297
 0.338  0.390  0.457  0.476  0.557  0.640  0.767  0.917  0.951  0.920
 0.935  1.104  1.102  1.032  1.050  1.051  0.942  0.778  0.734  0.669
 0.562  0.449  0.324  0.178  0.086  0.116  0.076  0.086  0.176  0.231
 0.300  0.287  0.210  0.161  0.136  0.157  0.158  0.128  0.147  0.136
 0.176  0.113  0.134  0.207  0.352  0.464  0.441  0.420  0.355  0.262
 0.206  0.124  0.091  0.073  0.009 -0.059 -0.167 -0.207 -0.174 -0.109
-0.047 -0.232 -0.297 -0.169 -0.225 -0.069  0.062  0.021
```

h. Survey Line TDC8, Troop Dental Clinic

```
RUN TDC8.ELV   02/01/90
   1    0  136       1.00  136    0    0
-0.014  0.044  0.119  0.167  0.157  0.150  0.138  0.117  0.075  0.028
 0.026  0.030  0.049  0.132  0.146  0.093 -0.013 -0.138 -0.312 -0.390
-0.313 -0.349 -0.313 -0.308 -0.207 -0.099  0.044  0.190  0.171  0.007
-0.024 -0.008  0.033  0.010  0.002  0.013  0.064  0.069  0.115  0.141
 0.162  0.139  0.053 -0.004  0.045 -0.042 -0.219 -0.370 -0.477 -0.517
-0.544 -0.636 -0.447 -0.182 -0.069  0.052  0.176  0.270  0.315  0.392
 0.435  0.450  0.410  0.382  0.343  0.402  0.471  0.505  0.423  0.413
```

Table C4. (Continued)

```
 0.457  0.500  0.481  0.457  0.403  0.318  0.268  0.169  0.044 -0.075
-0.201 -0.462 -0.657 -0.532 -0.521 -0.477 -0.360 -0.208 -0.042  0.047
 0.004  0.055  0.142  0.171  0.136  0.089  0.077  0.065  0.036  0.023
 0.026  0.054  0.013  0.008  0.057  0.207  0.222  0.077 -0.057 -0.175
-0.266 -0.273 -0.322 -0.292 -0.354 -0.281 -0.108  0.024  0.121  0.181
 0.168  0.073  0.067  0.063  0.073  0.104  0.146  0.180  0.113  0.138
 0.220  0.206  0.133  0.046  0.009  0.042
```

i. Survey Line MB9, Maintenance Building

```
RUN MB9.ELV   02/01/90
   1    0  417       1.00  417    0    0
-0.195 -0.241 -0.227 -0.219 -0.175 -0.109 -0.104 -0.063 -0.070 -0.083
-0.025  0.010 -0.031 -0.035 -0.076 -0.154 -0.114 -0.082 -0.081 -0.087
-0.131 -0.192 -0.044 -0.008  0.001  0.023 -0.021  0.206  0.156  0.120
 0.067  0.054 -0.014 -0.091 -0.171 -0.187 -0.291 -0.329 -0.415 -0.377
-0.352 -0.303 -0.296 -0.268 -0.225 -0.273 -0.291 -0.287 -0.275 -0.300
-0.254 -0.151 -0.081 -0.061  0.000  0.034  0.051  0.104  0.135  0.038
 0.025  0.022 -0.001 -0.009 -0.022 -0.057 -0.082 -0.171 -0.201 -0.183
-0.170 -0.080  0.012  0.048  0.021  0.020  0.008  0.008  0.117  0.188
 0.186  0.306  0.303  0.334  0.319  0.388  0.375  0.388  0.381  0.380
 0.339  0.398  0.356 -0.135 -0.784 -0.902 -0.915 -0.866 -0.777 -0.786
-0.766 -0.740 -0.680 -0.541 -0.448 -0.379 -0.343 -0.217 -0.105  0.000
 0.047  0.041  0.103  0.075  0.072  0.011 -0.035 -0.067 -0.016  0.040
 0.036 -0.096  0.016  0.002  0.026  0.246  0.190  0.140  0.083  0.015
-0.179 -0.073 -0.045 -0.077 -0.189 -0.278 -0.228 -0.168 -0.166 -0.131
-0.045  0.076  0.128  0.159  0.181  0.231  0.205  0.139  0.089  0.050
-0.078 -0.079 -0.102 -0.151  0.171  0.356  0.365  0.272  0.274  0.176
 0.210  0.214  0.221  0.160  0.199  0.181  0.216  0.232  0.236  0.252
 0.271  0.283  0.248  0.105 -0.053 -0.145 -0.183 -0.139 -0.179 -0.162
-0.163 -0.227 -0.260 -0.305 -0.330 -0.313 -0.338 -0.330 -0.344 -0.284
-0.226 -0.161 -0.087 -0.032 -0.007  0.006 -0.034  0.067  0.085  0.051
 0.015 -0.011 -0.089 -0.137 -0.179 -0.176 -0.161 -0.140 -0.053 -0.164
-0.168 -0.220 -0.156 -0.103 -0.053  0.005  0.046  0.046  0.055  0.031
 0.051 -0.015  0.016 -0.035 -0.125 -0.189 -0.172 -0.240 -0.208 -0.244
-0.245 -0.253 -0.161 -0.086 -0.068 -0.059 -0.091 -0.073 -0.050 -0.082
-0.114 -0.022  0.137  0.341  0.343  0.346  0.316  0.310  0.270  0.269
 0.202  0.231  0.229  0.268  0.281  0.302  0.306  0.374  0.407  0.423
 0.417  0.293 -0.006  0.097  0.062  0.167  0.196  0.253  0.284  0.321
 0.370  0.307  0.284  0.192  0.141  0.037 -0.039 -0.087 -0.099 -0.146
-0.130 -0.069  0.038  0.247  0.236  0.172  0.254  0.288  0.299  0.308
 0.359  0.181  0.105  0.135  0.045  0.100  0.101  0.048  0.016  0.137
 0.186  0.205  0.115  0.090  0.045  0.033  0.024  0.011 -0.194 -0.358
-0.477 -0.512 -0.554 -0.604 -0.666 -0.705 -0.786 -0.832 -0.859 -0.888
-0.953 -0.590  0.174  0.547  0.564  0.500  0.523  0.507  0.521  0.499
 0.494  0.469  0.499  0.486  0.443  0.347  0.322  0.256  0.221  0.210
 0.230  0.249  0.193  0.194  0.160  0.021  0.042  0.061  0.059  0.096
 0.166  0.198  0.185  0.208  0.246  0.284  0.316  0.311  0.290  0.236
```

Table C4. (Concluded)

```
 0.185  0.139  0.095  0.044 -0.021 -0.080 -0.059  0.000 -0.002 -0.007
-0.007  0.002 -0.055 -0.096 -0.105 -0.087 -0.122 -0.151 -0.100 -0.034
 0.018  0.008  0.052  0.198  0.259  0.288  0.320  0.433  0.372  0.264
 0.217  0.216  0.193  0.129  0.055  0.110  0.115  0.145  0.126  0.065
 0.131  0.170  0.198  0.234  0.231  0.178  0.167  0.170  0.158  0.131
 0.104  0.059  0.021 -0.039 -0.101 -0.027  0.225
```

j. Survey Line MB10M, Maintenance Building

```
RUN MB10M.ELV   02/01/90
   1    0  141       1.00  141    0    0
 0.250  0.492  0.511  0.441  0.414  0.404  0.341  0.371  0.368  0.395
 0.457  0.618  0.788  0.799  0.858  0.918  1.021  1.053  1.082  1.322
 1.513  1.579  1.775  1.978  1.978  2.070  2.179  2.287  2.313  2.355
 2.575  2.627  2.765  2.883  3.008  3.142  3.003  2.839  2.737  2.600
 2.466  2.336  2.203  2.040  1.929  1.812  1.759  1.422  1.222  1.069
 0.997  0.991  0.895  0.786  0.765  0.764  0.636  0.547  0.544  0.571
 0.597  0.685  0.708  0.706  0.661  0.568  0.444  0.383  0.465  0.355
 0.400  0.243  0.426  0.371  0.143  0.150  0.033  0.375  0.506  0.579
 0.658  0.765  0.789  0.897  1.026  1.100  1.132  1.241  1.462  1.459
 1.499  1.653  1.821  2.122  2.338  2.461  2.577  2.716  2.873  2.998
 3.076  3.228  3.330  3.398  3.486  3.478  3.331  3.242  3.095  2.988
 2.798  2.751  2.699  2.644  2.549  2.442  2.449  2.258  2.082  2.003
 1.833  1.607  1.541  1.515  1.400  1.343  1.302  1.268  1.116  0.952
 0.892  0.858  0.850  0.832  0.886  0.928  0.971  1.037  1.092  0.906
 0.638
```

Table C5. Red River Army Depot, Old Facilities

a. Survey Line HDQ1.ELV, Headquarters Building

```
HDQ1    04/26/90
   1    0  275       1.00  275    0    0
-0.396 -0.840 -1.249 -1.535 -1.615 -1.942 -1.901 -2.255 -2.210 -2.212
-2.336 -2.375 -2.444 -2.505 -2.474 -2.436 -2.423 -2.324 -2.287 -2.354
-2.324 -2.378 -2.554 -2.350 -2.306 -2.254 -2.217 -2.216 -2.229 -2.212
-2.208 -2.136 -2.041 -1.969 -1.931 -1.872 -1.880 -1.903 -1.896 -1.937
-1.940 -1.919 -1.875 -1.881 -1.845 -1.706 -1.622 -1.541 -1.552 -1.583
-1.620 -1.565 -1.531 -1.510 -1.501 -1.482 -1.352 -1.332 -1.360 -1.443
-1.462 -1.548 -1.559 -1.620 -1.604 -1.556 -1.546 -1.536 -1.513 -1.571
-1.557 -1.416 -1.390 -1.429 -1.448 -1.488 -1.486 -1.541 -1.616 -1.669
-1.746 -1.731 -1.708 -1.614 -1.596 -1.523 -1.633 -1.634 -1.573 -1.541
-1.449 -1.392 -1.410 -1.437 -1.466 -1.429 -1.421 -1.356 -1.435 -1.381
-1.262 -0.710 -0.240  0.354  1.013  1.601  2.024  2.422  2.749  3.160
 3.422  3.649  3.965  4.252  4.418  4.475  4.719  4.933  5.127  5.382
 5.657  5.766  5.949  6.143  6.381  6.605  6.784  6.824  7.018  7.124
 6.990  6.784  6.609  6.489  6.280  6.145  5.968  6.143  6.323  6.437
```

Table C5. (Continued)

```
 6.615  6.765  6.943  7.106  7.144  7.041  6.979  6.998  6.675  6.567
 6.343  6.136  6.016  5.758  5.566  5.424  5.190  5.001  4.814  4.600
 4.336  4.156  3.796  3.580  3.263  2.881  2.508  2.151  1.659  1.169
 0.585  0.050 -0.436 -0.837 -1.063 -1.161 -1.161 -1.163 -1.206 -1.195
-1.156 -1.159 -1.214 -1.173 -1.229 -1.276 -1.292 -1.247 -1.208 -1.249
-1.336 -1.441 -1.445 -1.395 -1.289 -1.252 -1.204 -1.194 -1.153 -1.155
-1.154 -1.191 -1.181 -1.232 -1.230 -1.206 -1.221 -1.186 -1.185 -1.237
-1.177 -1.157 -1.156 -1.129 -1.068 -0.955 -0.920 -0.945 -1.001 -1.008
-1.003 -1.052 -1.164 -1.250 -1.232 -1.280 -1.266 -1.280 -1.371 -1.483
-1.513 -1.518 -1.527 -1.540 -1.561 -1.536 -1.555 -1.584 -1.568 -1.586
-1.621 -1.640 -1.651 -1.645 -1.675 -1.701 -1.757 -1.725 -1.750 -1.784
-1.784 -1.914 -1.798 -1.793 -1.798 -1.738 -1.771 -1.803 -1.840 -1.824
-1.831 -1.844 -1.759 -1.679 -1.675 -1.761 -1.554 -1.352 -1.442 -1.029
-0.877 -0.544 -0.100  0.286  0.752
```

b. Survey Line HDQ2.ELV, Headquarters Building

```
HDQ2    04/26/90
   1     0  176       1.00  176    0     0
 0.076  0.148  0.209  0.267  0.411  0.636  0.822  1.073  1.299  1.645
 1.925  2.214  2.385  2.792  3.258  3.697  4.109  4.551  4.774  4.855
 4.798  4.782  4.733  4.746  4.784  4.719  4.628  4.617  4.486  4.325
 4.424  4.300  4.213  4.115  4.052  3.880  3.512  3.339  3.277  3.341
 3.314  3.114  2.881  2.738  2.621  2.536  2.320  2.131  1.909  1.389
 1.241  1.147  1.186  0.954  0.853  0.737  0.613  0.475  0.484  0.353
 0.118 -0.022 -0.140 -0.116 -0.364 -0.502 -0.694 -1.041 -1.530 -1.886
-2.159 -2.290 -2.437 -2.637 -2.434 -2.279 -2.262 -2.206 -2.126 -1.986
-1.897 -1.869 -1.847 -1.819 -1.793 -1.673 -1.513 -1.487 -1.599 -1.696
-1.791 -1.868 -1.932 -1.916 -1.983 -2.099 -2.227 -2.258 -2.319 -2.392
-2.510 -2.672 -2.858 -3.027 -3.211 -3.444 -3.863 -4.307 -4.599 -4.818
-4.913 -5.106 -5.252 -5.409 -5.460 -5.757 -5.913 -5.953 -6.095 -6.170
-6.340 -6.517 -6.626 -6.694 -6.932 -7.197 -7.482 -7.642 -7.824 -8.042
-8.212 -8.388 -8.528 -8.750 -8.970 -9.041 -9.144 -9.238 -9.511 -9.746
-9.859 -9.911-10.064-10.212-10.361-10.432-10.601-10.698-10.732-10.810
-10.732-10.767-10.732-10.714-10.709-10.701-10.547-10.213 -9.888 -9.448
-9.202 -8.817 -8.448 -8.101 -7.789 -7.460 -7.270 -7.008 -6.700 -6.545
-6.349 -6.233 -6.157 -6.133 -6.098 -6.038
```

c. Survey Line HDQ3.ELV, Headquarters Building

```
HDQ3    04/26/90
   1     0  276       1.00  276    0     0
 0.238  0.395  0.530  0.689  0.871  1.047  1.137  1.192  1.137  1.144
 1.056  0.686  0.597  0.408  0.253  0.101 -0.124 -0.328 -0.493 -0.696
-0.904 -1.148 -1.402 -1.737 -1.866 -2.160 -2.446 -2.758 -3.106 -3.486
-3.885 -4.359 -4.846 -5.453 -5.951 -6.364 -6.726 -6.945 -7.058 -7.080
-7.027 -7.092 -7.054 -7.042 -7.028 -7.051 -7.078 -7.125 -7.155 -7.155
```

Table C5. (Continued)

```
-7.107 -7.097 -7.140 -7.247 -7.322 -7.331 -7.263 -7.167 -7.116 -7.082
-7.071 -7.029 -7.027 -7.014 -7.052 -7.028 -7.106 -7.081 -7.058 -7.083
-7.042 -7.060 -7.122 -7.054 -7.045 -7.024 -7.021 -6.872 -6.787 -6.805
-6.798 -6.875 -6.877 -6.902 -6.941 -7.091 -7.110 -7.093 -7.121 -7.086
-7.129 -7.253 -7.349 -7.357 -7.376 -7.382 -7.403 -7.388 -7.370 -7.373
-7.380 -7.382 -7.436 -7.443 -7.460 -7.510 -7.486 -7.608 -7.606 -7.603
-7.620 -7.658 -7.643 -7.746 -7.793 -7.625 -7.680 -7.706 -7.573 -7.623
-7.672 -7.716 -7.743 -7.777 -7.709 -7.647 -7.573 -7.559 -7.595 -7.331
-7.219 -7.356 -6.959 -6.740 -6.415 -5.987 -5.577 -5.212 -5.466 -5.795
-6.205 -6.577 -6.804 -7.043 -7.190 -7.215 -7.471 -7.433 -7.482 -7.588
-7.657 -7.751 -7.752 -7.735 -7.698 -7.677 -7.583 -7.566 -7.603 -7.585
-7.636 -7.719 -7.576 -7.562 -7.478 -7.478 -7.457 -7.475 -7.469 -7.463
-7.370 -7.263 -7.214 -7.187 -7.127 -7.145 -7.160 -7.175 -7.209 -7.209
-7.179 -7.152 -7.143 -7.113 -6.950 -6.872 -6.833 -6.823 -6.855 -6.885
-6.818 -6.778 -6.757 -6.750 -6.722 -6.601 -6.573 -6.632 -6.751 -6.740
-6.822 -6.825 -6.896 -6.858 -6.818 -6.816 -6.790 -6.792 -6.846 -6.815
-6.667 -6.665 -6.671 -6.683 -6.738 -6.726 -6.777 -6.860 -6.911 -6.958
-6.956 -6.928 -6.842 -6.812 -6.775 -6.846 -6.831 -6.781 -6.740 -6.655
-6.615 -6.610 -6.650 -6.667 -6.642 -6.643 -6.590 -6.620 -6.551 -6.482
-5.922 -5.449 -4.857 -4.162 -3.641 -4.031 -4.364 -4.779 -5.042 -5.262
-5.574 -5.869 -6.047 -6.093 -6.316 -6.540 -6.732 -6.975 -7.236 -7.328
-7.508 -7.739 -8.049 -8.162 -8.417 -8.534 -8.695 -8.800 -8.670 -8.436
-8.259 -8.155 -8.099 -7.873 -7.794 -7.575
```

d. Survey Line DYNA4.ELV, Dynamometer Facility

```
DYNA4    04/26/90
   1     0  455       1.00  455     0     0
-0.028 -0.140 -0.148 -0.141 -0.126 -0.152 -0.194 -0.145 -0.071 -0.018
 0.079  0.131  0.148  0.076  0.076 -0.011 -0.165 -0.214 -0.212 -0.181
-0.219 -0.216 -0.199 -0.181 -0.216 -0.165 -0.084 -0.024  0.058  0.058
 0.091  0.131  0.184  0.205  0.164  0.159  0.165  0.164  0.193  0.126
 0.075 -0.018 -0.032  0.001 -0.120 -0.210 -0.373 -0.478 -0.557 -0.610
-0.624 -0.695 -0.715 -0.731 -0.798 -0.838 -0.865 -0.838 -0.818 -0.805
-0.718 -0.693 -0.538 -0.391 -0.337 -0.285 -0.257 -0.191 -0.159 -0.131
-0.048 -0.041  0.064  0.078  0.091  0.228  0.355  0.366  0.366  0.284
 0.252  0.279  0.271  0.227  0.232  0.263  0.351  0.402  0.369  0.497
 0.640  0.810  0.790  0.873  0.935  0.889  0.871  0.846  0.843  0.772
 0.783  0.668  0.634  0.628  0.634  0.458  0.457  0.496  0.514  0.590
 0.625  0.625  0.601  0.669  0.765  0.750  0.747  0.851  0.897  0.971
 0.995  0.967  0.956  0.997  0.983  0.944  0.964  1.063  1.130  1.102
 1.123  0.979  0.896  0.914  0.980  0.922  0.943  0.926  0.817  0.774
 0.816  0.918  0.990  1.020  1.041  1.013  1.033  1.165  1.163  1.230
 1.195  1.261  1.332  1.333  1.378  1.376  1.327  1.267  1.159  1.221
 1.313  1.382  1.503  1.512  1.543  1.530  1.553  1.553  1.607  1.624
 1.701  1.765  1.773  1.731  1.638  1.611  1.654  1.507  1.575  1.614
 1.629  1.603  1.507  1.465  1.419  1.345  1.362  1.360  1.355  1.353
 1.331  1.308  1.397  1.479  1.496  1.435  1.398  1.381  1.343  1.249
```

Table C5. (Continued)

```
 1.294  1.421  1.568  1.598  1.569  1.547  1.589  1.611  1.594  1.550
 1.465  1.347  1.362  1.266  1.296  1.175  1.202  1.167  1.219  1.299
 1.161  1.152  1.206  1.191  1.126  1.034  1.018  1.090  1.172  1.201
 1.194  1.288  1.270  1.220  1.211  1.200  1.185  1.242  1.250  1.324
 1.352  1.433  1.509  1.548  1.599  1.564  1.522  1.522  1.552  1.542
 1.392  1.264  1.216  1.290  1.333  1.368  1.390  1.451  1.442  1.354
 1.259  1.283  1.304  1.307  1.330  1.362  1.326  1.345  1.393  1.444
 1.453  1.595  1.596  1.530  1.481  1.551  1.518  1.543  1.619  1.587
 1.610  1.615  1.571  1.518  1.503  1.428  1.409  1.447  1.475  1.452
 1.361  1.224  1.142  1.004  1.083  1.227  1.254  1.254  1.204  1.211
 1.144  1.114  1.160  1.219  1.144  0.952  0.949  0.985  0.921  0.912
 0.847  0.771  0.698  0.761  0.853  0.822  0.817  0.788  0.750  0.771
 0.808  0.907  0.947  0.964  0.913  0.863  0.810  0.804  0.865  0.816
 0.768  0.825  0.898  0.786  0.730  0.638  0.618  0.583  0.547  0.414
 0.469  0.467  0.388  0.269  0.208  0.248  0.276  0.441  0.413  0.392
 0.457  0.558  0.552  0.656  0.736  0.684  0.715  0.784  0.656  0.600
 0.578  0.447  0.333  0.170  0.179  0.117  0.111  0.125  0.071  0.011
 0.041  0.055  0.044  0.094  0.109  0.135 -0.002 -0.085 -0.232 -0.158
-0.260 -0.334 -0.464 -0.512 -0.542 -0.540 -0.571 -0.647 -0.744 -0.838
-0.953 -1.008 -1.095 -1.107 -1.125 -1.166 -1.147 -1.118 -1.049 -1.006
-0.994 -1.001 -1.079 -1.088 -1.148 -1.212 -1.321 -1.490 -1.576 -1.715
-1.688 -1.694 -1.775 -1.862 -1.926 -1.890 -1.900 -1.915 -1.901 -1.961
-1.940 -1.870 -1.839 -1.805 -1.788 -1.737 -1.671 -1.617 -1.529 -1.574
-1.566 -1.550 -1.527 -1.578 -1.558 -1.550 -1.592 -1.706 -1.829 -1.832
-1.890 -1.895 -1.838 -1.764 -1.710 -1.649 -1.588 -1.628 -1.660 -1.651
-1.631 -1.656 -1.742 -1.795 -1.805
```

e. Survey Line DYNA5.ELV, Dynamometer Facility

```
DYNA5   04/26/90
   1    0  158       1.00  158    0    0
-0.018 -0.240 -0.302 -0.245 -0.347 -0.362 -0.333 -0.307 -0.292 -0.255
-0.315 -0.350 -0.379 -0.476 -0.476 -0.523 -0.591 -0.651 -0.642 -0.652
-0.724 -0.708 -0.755 -0.741 -0.719 -0.840 -0.916 -1.054 -1.163 -1.216
-1.368 -1.469 -1.479 -1.455 -1.467 -1.494 -1.558 -1.563 -1.565 -1.615
-1.696 -1.723 -1.669 -1.585 -1.585 -1.516 -1.583 -1.600 -1.631 -1.711
-1.764 -1.869 -1.883 -1.900 -1.958 -1.973 -2.033 -2.056 -2.057 -2.133
-2.145 -2.093 -2.067 -2.155 -2.138 -2.095 -2.176 -2.226 -2.260 -2.319
-2.405 -2.479 -2.474 -2.412 -2.509 -2.558 -2.708 -2.759 -2.774 -2.686
-2.573 -2.504 -2.457 -2.419 -2.526 -2.478 -2.441 -2.395 -2.340 -2.213
-2.262 -2.193 -2.196 -2.154 -2.111 -2.090 -2.112 -2.059 -2.056 -2.047
-1.984 -1.926 -1.923 -1.856 -1.829 -1.783 -1.719 -1.671 -1.606 -1.526
-1.443 -1.431 -1.451 -1.478 -1.457 -1.522 -1.566 -1.505 -1.467 -1.416
-1.372 -1.337 -1.298 -1.262 -1.243 -1.179 -1.118 -1.056 -1.060 -0.933
-0.805 -0.726 -0.688 -0.611 -0.655 -0.643 -0.614 -0.601 -0.688 -0.627
-0.603 -0.640 -0.602 -0.565 -0.451 -0.343 -0.323 -0.261 -0.358 -0.352
-0.403 -0.397 -0.329 -0.247 -0.188 -0.174 -0.037  0.080
```

Table C5. (Continued)

f. Survey Line DYNA6.ELV, Dynamometer Facility

```
DYNA6    04/26/90
   1     0  454        1.00  454    0     0
 0.049   0.090   0.205   0.298   0.340   0.452   0.662   0.817   0.690   0.597
 0.563   0.635   0.490   0.442   0.469   0.469   0.766   1.082   1.249   1.398
 1.476   1.508   1.513   1.603   1.744   2.104   2.278   2.488   2.610   2.731
 3.021   3.096   3.233   3.333   3.433   3.503   3.572   3.522   3.519   3.572
 3.574   3.547   3.534   3.466   3.466   3.349   3.275   3.341   3.231   3.015
 2.816   2.788   2.703   2.602   2.676   2.537   2.530   2.543   2.451   2.356
 2.205   2.040   1.996   1.952   2.008   1.959   2.085   2.060   1.963   1.942
 1.854   1.771   1.714   1.620   1.524   1.527   1.574   1.773   1.852   1.781
 1.672   1.543   1.494   1.278   1.087   0.856   0.710   0.376   0.192   0.101
-0.074  -0.295  -0.401  -0.333  -0.489  -0.498  -0.535  -0.623  -0.837  -0.850
-0.721  -0.889  -0.853  -0.927  -1.107  -1.016  -0.946  -0.978  -0.994  -0.962
-0.948  -1.019  -1.137  -1.163  -1.109  -1.137  -1.185  -1.269  -1.284  -1.208
-1.195  -1.221  -1.225  -1.214  -1.118  -1.078  -0.979  -0.908  -0.783  -0.710
-0.624  -0.481  -0.424  -0.335  -0.322  -0.239  -0.139  -0.209  -0.166  -0.020
-0.081  -0.129  -0.143  -0.219  -0.303  -0.334  -0.428  -0.494  -0.481  -0.588
 0.939   1.141   1.222   1.382   1.444   1.541   1.569   1.626   1.710   1.750
 1.785   1.793   1.732   1.739   1.831   1.817   1.694   1.776   1.756   1.692
 1.569   1.488   1.429   1.326   1.319   1.191   1.090   0.956   0.845   0.707
 0.650   0.683   0.790   0.829   0.785   0.860   0.877   0.928   0.949   0.876
 0.790   0.749   0.686   0.697   0.767   0.833   0.890   0.981   0.992   1.027
 1.107   1.222   1.348   1.529   1.661   1.827   1.998   1.992   1.860   1.780
 1.718   1.639   1.673   1.617   1.628   1.633   1.637   1.700   1.810   1.859
 1.964   2.073   2.142   2.183   2.296   2.282   2.212   2.301   2.268   2.203
 2.071   1.945   1.875   1.832   1.741   1.662   1.708   1.729   1.737   1.805
 1.810   1.790   1.804   1.920   2.030   1.988   1.764   1.605   1.464   1.352
 1.231   1.089   1.090   1.102   1.128   1.049   1.072   1.038   1.002   0.943
 1.008   1.016   1.043   1.128   1.187   1.121   1.099   1.108   1.141   1.200
 1.161   1.236   1.235   1.295   1.416   1.487   1.580   1.686   1.901   1.934
 1.942   2.007   2.122   2.128   2.025   2.058   2.158   2.027   1.877   1.996
 2.092   2.012   1.972   1.888   1.769   1.654   1.578   1.526   1.565   1.401
 1.326   1.204   1.043   1.005   1.009   0.955   0.919   0.861   0.812   0.784
 0.755   0.567   0.659   0.691   0.742   0.786   0.978   0.948   1.008   1.088
 1.175   1.231   1.306   1.344   1.448   1.535   1.529   1.566   1.579   1.606
 1.497   1.581   1.595   1.562   1.487   1.445   1.483   1.551   1.470   1.311
 1.379   1.317   1.379   1.359   1.461   1.460   1.575   1.364   1.390   1.328
 1.198   1.200   1.219   1.107   1.016   0.939   0.855   0.755   0.797   0.702
 0.564   0.367   0.309   0.178  -0.096  -0.226  -0.479  -0.739  -0.786  -0.952
-0.990  -1.133  -1.202  -1.229  -1.107  -1.081  -1.123  -1.229  -1.316  -1.407
-1.512  -1.628  -1.526  -1.538  -1.564  -1.559  -1.666  -1.695  -1.730  -1.760
-1.860  -2.052  -2.130  -2.234  -2.176  -2.172  -2.244  -2.213  -2.168  -2.206
-2.228  -2.336  -2.396  -2.538  -2.516  -2.651  -2.731  -2.772  -2.852  -2.964
-3.018  -3.000  -2.918  -2.996  -3.062  -2.946  -2.846  -2.761  -2.707  -2.511
-2.396  -2.223  -2.184  -2.035  -1.919  -1.831  -1.460  -1.314  -1.176  -1.295
-1.168  -1.040  -1.057  -0.843  -0.529  -0.441  -0.238  -0.267  -0.276  -0.473
```

Table C5. (Concluded)

```
-0.382 -0.421 -0.542 -0.681 -0.582 -0.409 -0.287 -0.204 -0.126 -0.038
-0.008  0.095  0.227  0.126
```

g. Survey Line DYNA7.ELV, Dynamometer Facility

```
DYNA7    04/26/90
   1     0   93       1.00   93    0     0
 0.570  1.078  1.700  2.243  2.669  3.176  3.657  4.135  4.625  4.913
 4.771  4.751  4.683  4.587  4.453  4.280  4.152  3.908  3.639  3.462
 3.361  3.147  3.036  2.912  2.839  2.821  2.763  2.613  2.529  2.391
 2.227  1.988  1.766  1.576  1.537  1.602  1.757  1.726  1.658  1.565
 1.150  0.605  0.374  0.245  0.025 -0.317 -0.368 -0.053  0.246  0.387
 0.657  1.173  1.564  1.661  1.759  1.865  1.842  1.891  1.957  2.177
 2.273  2.424  2.627  2.854  2.830  2.890  2.944  2.962  3.030  3.140
 3.257  3.420  3.540  3.696  3.987  4.175  4.291  4.457  4.614  4.725
 4.778  4.807  5.003  4.619  4.176  3.700  3.227  2.723  2.323  1.738
 1.086  0.602  0.032
```

h. Survey Line DYNA8.ELV, Dynamometer Facility

```
DYNA8    04/26/90
   1     0   39       1.00   39    0     0
 0.171  0.201  0.275  0.308  0.425  0.541  0.650  0.755  0.807  0.888
 0.964  1.002  1.024  1.057  1.010  0.966  0.981  0.895  0.913  0.884
 0.830  0.932  0.982  0.999  1.063  1.009  0.987  0.960  0.876  0.792
 0.717  0.642  0.560  0.420  0.317  0.174  0.163  0.128  0.039
```

i. Survey Line WHS1.ELV, Warehouse A

```
WHS1     04/27/90
   1     0  373       1.00  373    0     0
 0.038  0.009  0.062  0.092  0.063 -0.028 -0.065 -0.102 -0.143 -0.174
-0.241 -0.184 -0.217 -0.273 -0.238 -0.260 -0.276 -0.307 -0.302 -0.308
-0.286 -0.347 -0.349 -0.378 -0.372 -0.400 -0.432 -0.500 -0.429 -0.457
-0.517 -0.670 -0.707 -0.720 -0.734 -0.793 -0.862 -0.887 -0.835 -0.909
-0.906 -0.948 -0.931 -0.998 -1.050 -1.103 -1.150 -1.220 -1.230 -1.278
-1.256 -1.240 -1.281 -1.320 -1.311 -1.341 -1.378 -1.399 -1.341 -1.378
-1.407 -1.443 -1.456 -1.527 -1.501 -1.589 -1.548 -1.582 -1.590 -1.600
-1.668 -1.673 -1.717 -1.685 -1.688 -1.729 -1.770 -1.769 -1.796 -1.796
-1.813 -1.812 -1.797 -1.756 -1.769 -1.803 -1.852 -1.961 -1.927 -1.953
-1.955 -1.936 -1.974 -1.974 -2.030 -2.029 -2.126 -2.220 -2.276 -2.271
-2.341 -2.351 -2.307 -2.159 -2.261 -2.253 -2.276 -2.324 -2.394 -2.402
-2.373 -2.438 -2.438 -2.418 -2.364 -2.305 -2.281 -2.241 -2.232 -2.203
-2.167 -2.167 -2.090 -2.081 -2.020 -2.017 -1.988 -1.927 -1.797 -1.690
-1.654 -1.632 -1.505 -1.369 -1.285 -1.174 -1.060 -0.899 -0.824 -0.651
-0.496 -0.278 -0.115  0.131  0.326  0.603  0.835  1.022  1.283  1.564
```

Table C5. (Continued)

```
 1.757  2.010  2.274  2.426  2.591  2.769  2.883  3.015  3.165  3.219
 3.315  3.389  3.428  3.472  3.478  3.525  3.572  3.572  3.648  3.682
 3.674  3.712  3.712  3.666  3.682  3.695  3.703  3.757  3.755  3.762
 3.740  3.701  3.727  3.746  3.688  3.788  3.615  3.669  3.718  3.737
 3.730  3.745  3.781  3.761  3.765  3.772  3.758  3.748  3.658  3.784
 3.714  3.688  3.693  3.657  3.638  3.613  3.579  3.490  3.488  3.440
 3.416  3.371  3.267  3.201  3.082  2.964  2.876  2.712  2.510  2.316
 2.124  1.865  1.660  1.395  1.210  0.905  0.692  0.461  0.273  0.031
-0.127 -0.340 -0.520 -0.703 -0.762 -0.939 -1.023 -1.143 -1.241 -1.351
-1.480 -1.533 -1.543 -1.648 -1.753 -1.821 -1.865 -1.896 -1.943 -1.945
-2.012 -2.033 -2.073 -2.093 -2.102 -2.122 -2.168 -2.234 -2.264 -2.271
-2.276 -2.231 -2.234 -2.239 -2.178 -2.131 -2.084 -2.111 -2.012 -2.153
-2.181 -2.171 -2.108 -2.129 -2.052 -1.969 -1.878 -1.857 -1.793 -1.810
-1.764 -1.752 -1.788 -1.776 -1.782 -1.679 -1.637 -1.602 -1.611 -1.611
-1.629 -1.661 -1.621 -1.645 -1.584 -1.599 -1.558 -1.524 -1.502 -1.507
-1.459 -1.463 -1.376 -1.398 -1.353 -1.352 -1.357 -1.306 -1.314 -1.269
-1.221 -1.166 -1.138 -1.133 -1.190 -1.136 -1.102 -1.085 -1.095 -1.060
-1.003 -1.031 -1.037 -1.004 -0.991 -0.984 -0.889 -0.851 -0.788 -0.706
-0.684 -0.680 -0.687 -0.606 -0.635 -0.627 -0.550 -0.493 -0.475 -0.474
-0.420 -0.280 -0.218 -0.208 -0.268 -0.212 -0.167 -0.128 -0.128 -0.089
-0.094 -0.041 -0.057 -0.042 -0.049 -0.022 -0.001  0.030  0.004  0.041
 0.089  0.027  0.111  0.135  0.190  0.208  0.251  0.337  0.377  0.342
 0.294  0.323  0.296
```

j. Survey Line WHS2.ELV, Warehouse A

```
WHS2     04/27/90
   1     0  358       1.00  358    0     0     .02000
 0.088  0.191  0.213  0.243  0.195  0.239  0.282  0.212  0.215  0.127
 0.096  0.082  0.116  0.106  0.051 -0.046 -0.091 -0.104 -0.112 -0.045
-0.075 -0.107 -0.120 -0.136 -0.078 -0.108 -0.125 -0.128 -0.099 -0.187
-0.222 -0.188 -0.196 -0.337 -0.375 -0.337 -0.349 -0.426 -0.455 -0.330
-0.391 -0.515 -0.548 -0.611 -0.651 -0.664 -0.768 -0.768 -0.756 -0.781
-0.736 -0.713 -0.778 -0.745 -0.815 -0.780 -0.830 -0.950 -0.981 -0.985
-1.026 -1.126 -1.273 -1.312 -1.312 -1.348 -1.388 -1.422 -1.407 -1.396
-1.386 -1.452 -1.468 -1.478 -1.491 -1.546 -1.501 -1.511 -1.539 -1.580
-1.637 -1.618 -1.577 -1.510 -1.442 -1.466 -1.512 -1.558 -1.534 -1.520
-1.490 -1.502 -1.538 -1.573 -1.631 -1.698 -1.802 -1.840 -1.926 -2.044
-2.120 -2.077 -2.049 -1.984 -2.158 -2.053 -2.050 -2.006 -2.088 -2.086
-2.051 -2.056 -2.057 -2.010 -2.000 -2.003 -2.061 -1.962 -2.042 -1.977
-1.934 -1.832 -1.849 -1.827 -1.843 -1.808 -1.691 -1.604 -1.561 -1.407
-1.326 -1.268 -1.120 -0.964 -0.927 -0.786 -0.639 -0.552 -0.455 -0.288
-0.026  0.260  0.567  0.872  1.228  1.517  1.667  1.896  2.099  2.308
 2.545  2.681  2.885  3.090  3.129  3.247  3.358  3.522  3.600  3.695
 3.718  3.796  3.906  3.965  4.046  4.045  3.940  3.899  3.829  3.860
 3.869  3.936  3.980  4.014  4.054  4.108  4.123  4.180  4.169  4.301
 4.242  4.157  4.124  4.080  4.049  4.029  3.963  3.900  3.890  3.866
 3.806  3.770  3.895  3.913  3.827  3.836  3.681  3.617  3.599  3.491
```

Table C5. (Continued)

```
 3.403  3.277  3.151  3.038  2.970  2.846  2.637  2.520  2.252  2.079
 1.859  1.645  1.478  1.248  0.844  0.546  0.275  0.003 -0.260 -0.467
-0.568 -0.657 -0.814 -0.983 -1.014 -1.170 -1.306 -1.374 -1.484 -1.570
-1.631 -1.693 -1.832 -1.871 -1.852 -1.885 -1.894 -1.910 -1.961 -2.068
-2.032 -2.012 -2.059 -2.072 -2.056 -2.072 -2.089 -2.053 -2.123 -2.097
-2.034 -2.031 -2.070 -2.124 -2.038 -2.060 -2.098 -2.132 -2.066 -1.971
-1.885 -1.795 -1.733 -1.653 -1.590 -1.531 -1.535 -1.444 -1.520 -1.500
-1.535 -1.496 -1.482 -1.401 -1.496 -1.497 -1.574 -1.590 -1.556 -1.497
-1.491 -1.448 -1.503 -1.517 -1.492 -1.465 -1.420 -1.412 -1.433 -1.432
-1.451 -1.370 -1.351 -1.339 -1.312 -1.150 -1.089 -0.987 -1.003 -0.950
-0.866 -0.783 -0.795 -0.755 -0.746 -0.676 -0.671 -0.694 -0.710 -0.674
-0.682 -0.621 -0.621 -0.614 -0.555 -0.452 -0.452 -0.330 -0.451 -0.425
-0.324 -0.308 -0.356 -0.379 -0.200 -0.152 -0.214 -0.198 -0.110 -0.091
-0.119 -0.043 -0.029 -0.046 -0.091 -0.053 -0.035  0.020 -0.030 -0.099
-0.033 -0.014  0.101  0.148  0.223  0.144  0.157  0.213  0.274  0.281
 0.301  0.300  0.267  0.308  0.282  0.318  0.248  0.116
```

k. Survey Line WHS3.ELV, Warehouse A

```
WHS3   04/27/90
   1    0  423       1.00  423    0    0
-0.025 -0.098 -0.181 -0.205 -0.228 -0.147 -0.036 -0.042  0.020 -0.096
-0.150 -0.191 -0.175 -0.218 -0.225 -0.280 -0.282 -0.368 -0.484 -0.549
-0.530 -0.455 -0.418 -0.438 -0.635 -0.707 -0.749 -0.774 -0.811 -0.822
-0.795 -0.730 -0.704 -0.914 -1.022 -1.071 -1.124 -1.163 -1.138 -1.057
-0.944 -0.843 -0.994 -0.961 -0.979 -1.061 -1.136 -1.119 -1.138 -1.101
-1.018 -1.021 -0.978 -0.985 -0.932 -0.788 -0.800 -0.796 -0.815 -0.858
-0.849 -0.883 -0.896 -0.986 -0.992 -1.114 -1.189 -1.195 -1.256 -1.213
-1.169 -1.084 -1.017 -0.972 -0.988 -1.013 -1.043 -1.061 -1.115 -1.157
-1.157 -1.051 -0.965 -0.896 -0.821 -0.804 -0.694 -0.635 -0.613 -0.567
-0.516 -0.377 -0.375 -0.514 -0.628 -0.772 -0.763 -0.699 -0.642 -0.588
-0.540 -0.507 -0.436 -0.390 -0.312 -0.207 -0.149 -0.103 -0.038 -0.008
-0.086 -0.125 -0.059 -0.015  0.096  0.134  0.182  0.190  0.164  0.090
 0.006  0.029  0.083  0.118  0.147  0.174  0.199  0.170  0.160  0.135
 0.089  0.043  0.044  0.138  0.125  0.212  0.263  0.239  0.249  0.243
 0.236  0.198  0.163  0.067  0.080  0.027  0.024  0.037  0.045  0.059
 0.111  0.169  0.178  0.192  0.134  0.161  0.112  0.162  0.187  0.183
 0.175  0.124  0.124  0.171  0.148  0.106  0.089  0.100  0.046 -0.022
-0.040 -0.040 -0.035 -0.039 -0.063 -0.133 -0.189 -0.163 -0.234 -0.226
-0.227 -0.303 -0.326 -0.334 -0.333 -0.391 -0.427 -0.426 -0.403 -0.416
-0.437 -0.507 -0.556 -0.617 -0.622 -0.657 -0.583 -0.623 -0.687 -0.775
-0.724 -0.836 -0.820 -0.807 -0.778 -0.753 -0.794 -0.796 -0.762 -0.672
-0.696 -0.694 -0.744 -0.806 -0.828 -0.821 -0.800 -0.835 -0.869 -0.884
-0.915 -0.816 -0.842 -0.746 -0.652 -0.629 -0.710 -0.681 -0.665 -0.605
-0.541 -0.495 -0.492 -0.465 -0.421 -0.384 -0.325 -0.336 -0.344 -0.323
-0.300 -0.223 -0.237 -0.231 -0.200 -0.200 -0.182 -0.103 -0.082 -0.111
-0.099 -0.130 -0.070  0.027  0.100  0.118  0.148  0.148  0.185  0.142
 0.097  0.060  0.106  0.107  0.090  0.057  0.103  0.075  0.118  0.111
```

Table C5. (Continued)

0.111	0.004	-0.014	-0.057	-0.039	-0.082	-0.074	-0.025	-0.024	0.025
0.084	0.136	0.131	0.132	0.149	0.155	0.112	0.029	0.023	-0.024
-0.043	-0.101	-0.101	-0.107	-0.117	-0.086	-0.062	-0.040	-0.005	0.022
0.039	-0.027	-0.092	-0.141	-0.124	-0.092	-0.026	0.078	0.127	0.174
0.184	0.091	0.150	0.227	0.315	0.354	0.438	0.510	0.551	0.603
0.669	0.694	0.763	0.777	0.888	0.850	0.722	0.621	0.490	0.485
0.617	0.683	0.734	0.777	0.838	0.900	0.945	1.007	1.089	1.180
1.293	1.298	1.259	1.192	1.192	1.166	1.162	1.126	1.194	1.216
1.317	1.342	1.404	1.348	1.336	1.253	1.110	1.045	1.090	1.186
1.230	1.228	1.228	1.243	1.281	1.245	1.268	1.155	1.112	1.094
1.057	1.024	0.994	0.991	0.978	1.042	1.152	1.155	1.125	1.125
1.185	1.152	1.097	1.063	0.987	1.003	1.062	1.143	1.289	1.472
1.436	1.368	1.398	1.385	1.443	1.435	1.470	1.520	1.757	1.716
1.687	1.614	1.626	1.712	1.820	1.850	1.852	1.922	1.935	1.992
1.959	1.978	2.107	2.187	2.150	2.136	2.019	1.932	1.959	1.964
2.082	2.134	2.168							

1. Survey Line WHS4.ELV

WHS4	04/27/90								
1	0	513	1.00	513	0	0			
0.044	0.078	0.122	0.190	0.300	0.405	0.477	0.504	0.546	0.589
0.753	0.810	0.907	0.976	1.035	1.173	1.312	1.441	1.601	1.765
1.935	2.134	2.334	2.470	2.448	2.460	2.567	2.667	2.655	2.712
2.805	2.888	2.981	2.933	2.923	2.865	2.771	2.724	2.692	2.623
2.599	2.604	2.600	2.590	2.617	2.579	2.700	2.768	2.817	2.935
2.956	3.010	3.083	3.229	3.260	3.866	4.001	4.046	4.019	4.088
4.186	4.318	4.395	4.457	4.563	4.603	4.590	4.598	4.632	4.571
4.590	4.586	4.576	4.464	4.496	4.493	4.608	4.564	4.612	4.701
4.794	4.874	4.888	5.001	5.060	5.055	5.034	4.995	4.967	5.069
5.207	5.276	5.316	5.363	5.315	5.324	5.269	5.235	5.189	5.156
5.099	5.011	4.927	4.893	4.865	4.853	4.755	4.694	4.663	4.576
4.483	4.409	4.392	4.341	4.341	4.337	4.298	4.351	4.333	4.303
4.351	4.338	4.319	4.414	4.421	4.496	4.517	4.568	4.578	4.608
4.660	4.671	4.666	4.677	4.718	4.849	4.898	4.942	5.011	5.057
5.117	5.089	5.085	5.092	5.150	5.100	5.201	5.297	5.347	5.360
5.437	5.469	5.530	5.538	5.497	5.640	5.601	5.702	5.784	5.913
6.012	6.029	6.070	6.131	6.152	6.107	6.064	6.088	6.123	6.108
6.148	6.276	6.242	6.264	6.246	6.387	6.330	6.395	6.435	6.438
6.454	6.463	6.478	6.455	6.416	6.386	6.396	6.345	6.271	6.260
6.288	6.264	6.242	6.191	6.118	6.208	6.084	6.064	6.015	6.049
6.044	6.069	6.037	6.013	5.935	5.933	5.890	5.850	5.839	5.820
5.842	5.809	5.827	5.796	5.683	5.789	5.728	5.729	5.709	5.661
5.644	5.577	5.513	5.466	5.429	5.375	5.343	5.384	5.376	5.345
5.364	5.393	5.391	5.385	5.377	5.445	5.409	5.304	5.279	5.204
5.196	5.182	5.185	5.209	5.277	5.305	5.288	5.247	5.234	5.270
5.262	5.234	5.270	5.329	5.403	5.590	5.373	5.304	5.218	5.211
5.198	5.210	5.207	5.224	5.265	5.291	5.267	5.192	5.173	5.165

Table C5. (Continued)

5.149	5.180	5.265	5.296	5.377	5.372	5.342	5.343	5.343	5.330
5.310	5.310	5.315	5.323	5.293	5.329	5.388	5.430	5.454	5.507
5.574	5.582	5.645	5.650	5.682	5.672	5.651	5.720	5.719	5.732
5.740	5.734	5.754	5.773	5.819	5.873	5.874	5.931	5.955	5.969
5.939	5.949	5.913	5.952	5.990	6.066	6.086	6.077	6.149	6.152
6.217	6.173	6.171	6.200	6.266	6.260	6.258	6.303	6.315	6.311
6.297	6.272	6.272	6.216	6.167	6.118	6.113	6.101	6.116	6.102
5.994	5.946	5.983	5.914	5.926	5.947	5.976	5.954	5.885	5.839
5.808	5.677	5.556	5.491	5.433	5.429	5.280	5.333	5.319	5.238
5.221	5.173	5.128	5.072	4.975	4.901	4.888	4.872	4.838	4.860
4.872	4.817	4.762	4.707	4.676	4.578	4.509	4.464	4.447	4.456
4.408	4.365	4.343	4.349	4.289	4.279	4.210	4.188	4.101	4.086
4.096	4.070	4.097	4.104	4.076	4.108	4.098	4.100	4.154	4.143
4.250	4.349	4.413	4.445	4.525	4.592	4.620	4.647	4.689	4.760
4.861	4.925	4.937	4.986	5.033	5.082	5.071	5.085	5.044	4.975
4.893	4.636	4.693	4.711	4.746	4.738	4.740	4.683	4.613	4.573
4.487	4.357	4.278	4.243	4.256	4.404	4.172	4.170	4.242	4.310
4.288	4.286	4.284	4.272	4.267	4.298	4.193	4.078	4.060	3.959
3.826	3.760	3.683	3.573	3.533	3.416	2.806	2.760	2.619	2.547
2.480	2.396	2.307	2.228	2.089	2.053	2.072	2.077	2.137	2.167
2.128	2.145	2.089	2.111	2.084	2.044	1.954	1.880	1.897	1.852
1.900	1.909	1.943	2.036	2.065	2.177	2.277	2.285	2.284	2.419
2.596	2.788	2.959	3.135	3.292	3.426	3.556	3.694	3.743	3.803
3.913	3.975	4.138	4.197	4.258	4.319	4.383	4.460	4.570	4.608
4.652	4.671	4.741							

m. Survey Line WHS5.ELV

WHS5	04/27/90								
1	0 333		1.00	333	0	0			
-0.006	0.086	0.094	0.132	0.139	0.183	0.253	0.348	0.416	0.460
0.523	0.566	0.577	0.627	0.665	0.584	0.641	0.669	0.700	0.746
0.654	0.655	0.603	0.561	0.550	0.586	0.571	0.532	0.614	0.743
0.772	0.756	0.676	0.780	0.751	0.787	0.778	0.815	0.870	0.925
0.921	0.954	0.881	0.817	0.754	0.747	0.784	0.860	0.853	0.923
0.976	0.968	0.985	0.967	0.954	0.908	0.899	0.937	0.881	0.801
0.761	0.738	0.667	0.608	0.443	0.326	0.266	0.276	0.184	0.148
0.099	0.008	-0.056	-0.079	-0.136	-0.161	-0.132	-0.250	-0.394	-0.412
-0.504	-0.494	-0.538	-0.611	-0.670	-0.730	-0.812	-0.840	-0.928	-0.958
-0.918	-0.941	-1.008	-1.010	-1.083	-1.096	-1.112	-1.145	-1.152	-1.136
-1.170	-1.182	-1.214	-1.238	-1.248	-1.268	-1.333	-1.297	-1.281	-1.362
-1.414	-1.451	-1.452	-1.526	-1.543	-1.630	-1.706	-1.652	-1.645	-1.684
-1.741	-1.785	-1.794	-1.853	-2.016	-1.914	-1.912	-1.929	-1.848	-1.699
-1.500	-1.459	-1.487	-1.473	-1.323	-1.224	-1.100	-1.005	-0.935	-0.853
-0.826	-0.727	-0.675	-0.628	-0.490	-0.227	0.050	0.254	0.431	0.543
0.846	1.029	1.228	1.424	1.573	1.578	1.702	1.767	1.811	1.723
1.691	1.631	1.577	1.546	1.483	1.418	1.371	1.485	1.524	1.550
1.615	1.675	1.761	1.833	1.850	1.758	1.701	1.623	1.540	1.362

Table C5. (Concluded)

1.155	0.984	0.707	0.524	0.406	0.241	-0.031	-0.323	-0.503	-0.609
-0.617	-0.723	-0.790	-0.868	-0.907	-1.023	-1.095	-1.234	-1.407	-1.452
-1.467	-1.424	-1.573	-1.741	-1.878	-1.886	-1.860	-1.914	-1.836	-1.779
-1.741	-1.710	-1.664	-1.639	-1.596	-1.634	-1.622	-1.531	-1.494	-1.445
-1.405	-1.407	-1.348	-1.273	-1.255	-1.274	-1.254	-1.189	-1.203	-1.186
-1.155	-1.120	-1.103	-1.088	-1.093	-1.067	-1.030	-1.023	-0.968	-0.916
-0.873	-0.828	-0.863	-0.865	-0.790	-0.753	-0.680	-0.606	-0.555	-0.419
-0.431	-0.385	-0.372	-0.293	-0.195	-0.063	-0.077	-0.035	0.010	0.022
0.047	0.139	0.239	0.255	0.359	0.394	0.380	0.485	0.620	0.741
0.801	0.841	0.865	0.944	0.993	0.990	1.002	1.037	1.062	1.094
1.070	1.054	1.105	0.978	1.006	0.941	0.893	0.888	0.930	1.001
1.088	1.087	1.067	1.054	0.994	0.935	0.908	0.905	0.937	0.904
0.873	0.911	0.896	0.907	0.739	0.749	0.766	0.739	0.736	0.752
0.845	0.855	0.961	0.885	0.881	0.807	0.762	0.765	0.764	0.732
0.724	0.728	0.661	0.587	0.557	0.470	0.439	0.306	0.331	0.330
0.270	0.271	0.289							